POLSKI ZWIĄZEK INŻYNIERÓW
I TECHNIKÓW BUDOWNICTWA

STRUCTURAL FAILURES

VADEMECUM

2022

awarie.zut.edu.pl

Edited by **Jarosław Błyszko**

STRUCTURAL FAILURES 2022

VADEMECUM

AWARIE BUDOWLANE 2022

MONOGRAPH
prevention
diagnostics
repairs
reconstructions

Edited by
Jarosław Błyszko

Wydanie publikacji dofinansowane przez
Ministerstwo Nauki i Szkolnictwa Wyższego
w ramach programu „Doskonała Nauka II – Wsparcie monografii naukowych”

Doskonała Nauka

PROGRAMY NAUKA

Ministry of Science and Higher Education
Republic of Poland

Zachodniopomorski Uniwersytet Technologiczny w Szczecinie

Wydział
Budownictwa
i Inżynierii Środowiska

Editor-in-Chief
Redaktor naukowy
dr inż. Jarosław Błyszko

Editorial proofreading and typesetting
Korekta edytorska i skład
dr inż. Mateusz Techman

Review
Recenzja
prof. dr hab. inż. Elżbieta Horszczaruk

ISBN: 978-83-951719-7-0

Publisher: Zarząd Główny PZITB
Warszawa, May 2024

The texts of individual chapters selected for presentation in this monograph have been reviewed by a scientific committee consisting of outstanding specialists in their field under the chairmanship of Professor Kazimierz Flaga..

REVIEWERS

prof. dr hab. inż. KAZIMIERZ FLAGA
prof. dr hab. inż. WŁODZIMIERZ KIERNOŻYCKI
prof. dr inż. BENOIT BISSONNETTE
prof. dr hab. inż. ANDRZEJ M. BRANDT †
prof. dr inż. LESŁAW BRUNARSKI
prof. dr hab. inż. JOANNA BZÓWKA
prof. dr hab. inż. LECH CZARNECKI
prof. dr hab. inż. JAN DEJA
prof. dr hab. inż. KAZIMIERZ FURTAK
prof. dr hab. inż. ANDRZEJ GARBACZ
prof. dr hab. inż. MARIAN GIŻEJOWSKI
prof. dr hab. inż. BARBARA GOSZCZYŃSKA
prof. dr hab. inż. ANNA HALICKA
prof. dr hab. inż. JERZY HOŁA
prof. dr hab. inż. ZBIGNIEW JANOWSKI
prof. dr hab. inż. MARIA KASZYŃSKA
prof. ZUT dr hab. inż. JERZY KASZYŃSKI
prof. dr hab. inż. JANUSZ KAWECKI
prof. dr hab. inż. ZBIGNIEW KLEDYŃSKI
prof. dr hab. inż. RYSZARD KOWALCZYK
prof. dr hab. inż. ALEKSANDER KOZŁOWSKI
prof. dr hab. inż. Jan KUBICA
prof. dr hab. inż. ZBIGNIEW LECHOWICZ
prof. dr hab. inż. WOJCIECH LORENC
prof. dr hab. inż. CEZARY MADRYAS
prof. dr hab. inż. JAKUB MARCINOWSKI
prof. dr hab. inż. ZYGMUNT MEYER
prof. dr inż. RADOSŁAW MICHAŁOWSKI
prof. dr hab. inż. ZBIGNIEW MIELCZAREK †
prof. dr hab. inż. ZBIGNIEW MŁYNAREK
prof. dr. inż. PIOTR MONCARZ
prof. dr hab. inż. KRYSTYNA NAGRODZKA-GODYCKA
prof. dr hab. inż. PIOTR NOAKOWSKI
prof. dr inż. ANDRZEJ S. NOWAK
prof. dr hab. inż. ADAM PODHORECKI
prof. dr hab. inż. WOJCIECH RADOMSKI
prof. dr hab. inż. ANNA SIEMIŃSKA-LEWANDOWSKA
prof. dr hab. inż. TOMASZ SIWOWSKI
prof. dr hab. inż. ANDRZEJ SZARATA
prof. dr hab. inż. ANTONI SZYDŁO
prof. dr hab. inż. JACEK ŚLIWIŃSKI
prof. dr hab. inż. MARIAN TRACZ
prof. dr hab. inż. WIESŁAW TRĄMPCZYŃSKI
prof. dr hab. inż. TADEUSZ URBAN
prof. dr hab. inż. JOOST C. WALRAVEN
prof. dr hab. inż. KRZYSZTOF WILDE

Scientific Secretary: dr inż. Jarosław Błyszko

TABLE OF CONTENT

INTRODUCTION

This book introduces the reader to the issues surrounding building failures. Damage to buildings can have both trivial and complex, non-obvious causes. They all share a common denominator – the costs of remediation are typically very high and often encompass not just financial aspects, but also social ones. The occurrence of a failure usually initiates a long journey for the investor to restore the building to its pre-failure state. Additionally, the investor must contend with numerous legal and formal difficulties, professional liability of the participants in the construction process, and often, insurance and financial responsibility. It is only when we pay for mistakes that we realize their true cost.

The monograph presents over 40 examples discussing the latest cases of diagnostics and prevention of building failures. The book was published on the occasion of the 30th edition of the Building Failures Conference, which has been organized for almost 50 years by the Szczecin center, formerly the Szczecin University of Technology, and now ZUT in Szczecin, with the participation of the Polish scientific community. The co-organizer is the Polish Association of Civil Engineers and Technicians with the support of KILiW PAN and ITB.

Building failures have various causes. They are most often the result of a combination of many adverse factors and neglect. While their effects are well visible, determining the causes is often very difficult in many situations. Due to the significant costs of construction, proper diagnosis of the causes can save future repair costs and provide the opportunity to properly direct claims for coverage.

The book is divided into seven sections, depending on the dominant topic. These are:

- Material aspects of failures, damage, and repairs,
- Diagnostics, repairs, and reconstructions of building elements and structures,
- Failures of general construction buildings,
- Diagnostics in the assessment of structural safety,
- Geotechnical causes of building failures,
- Failures of metal structures,
- Failures of reinforced concrete structures,
- Failures of bridge and road structures.

In the coming years, large infrastructure investments are planned. These projects will include road and bridge structures, as well as new power plants, airports, wind farms, and many others. Many engineers will likely find employment in the reconstruction of war damage in neighboring Ukraine. Therefore, up-to-date knowledge of diagnostics, repairs, and prevention of building failures will be very important. Books that comprehensively discuss the issues of repairs and strengthening of structures appear relatively rarely in the Polish publishing market. Notable examples include works by B. Bukowski, J. Thierry and S. Zalewski, and E. Masłowski and D. Spiżewska. Despite the passage of time and changing construction and design technology, these works remain canonical regarding post-failure repairs. Newer works often treat building failure issues more specifically, narrowing the application area to particular types of structures or repair methods. In the dynamically changing world of the latest technologies, it is worth and necessary to use the latest solutions.

Over the past few decades, building failure problems have changed, as have technology, workmanship quality, the prevalence of materials, or the trend towards specific solutions. This monograph is a collection of problems submitted for discussion at the Building Failures Conference in 2022. Besides current problems and proposed solutions, the reader will find contact details of the best Polish engineers from across the country, who are currently dealing with the issues of building repairs and diagnostics. I hope that the mentioned names, combined with the interestingly presented failure cases, will allow for quicker and more accurate actions regarding the selection of experts and solutions in case of a problem.

The current construction market in Poland is a global market. The reach of companies often extends beyond the country's borders and the European Union. The professional contacts of Polish engineers are increasingly international. We commonly use foreign technology and export our solutions to other countries. I hope that this monograph will contribute to the popularization of Polish engineering thought and will, in many cases, spark discussions about the need and method of conducting engineering work.

Presenting several dozen failure cases will allow the reader to begin searching for their own solutions to problems they encounter in their engineering career. Conference materials from previous years, available on the website www.awarie.zut.edu.pl, can be helpful in this regard. The materials collected in this work, in an extended Polish-language version, are also available on the conference website.

The discussed issues have been reviewed by a group of professors, specialists, and construction experts, ensuring an appropriate level of substantive content.

In my work as a construction expert, I often encounter situations where participants in the construction process expect a quick and unambiguous declaration from the appointed expert on who is to blame for the failure. It is rather the rule that a failure has many causes, and only their synergy causes the problem to manifest. "He who asks questions cannot be wrong." Let us ask questions, study the cases presented by other engineer colleagues, and draw conclusions and lessons for ourselves. I hope that this monograph will find a prominent place in your engineering library and help in avoiding many problems or allow to find effective resolution

SECTION I
MATERIAL ASPECTS OF FAILURE, DAMAGE, AND REPAIRS

CORROSION OF STEEL STRUCTURES LOCATED IN THE COASTAL BELT – CONTRIBUTION TO THE DISCUSSION ON METHODS OF DETERMINING THE CORROSIVITY CATEGORY OF THE ATMOSPHERE

JAROSŁAW BŁYSZKO[1], *blyszko@zut.edu.pl*
TOMASZ WRÓBLEWSKI[1]

[1]Zachodniopomorski Uniwersytet Technologiczny w Szczecinie, Wydział Budownictwa i Inżynierii Środowiska, al. Piastów 50a, 70-311 Szczecin

Abstract: Elements of small architecture placed in public areas, such as seaside promenades, are required to have an extraordinary and impeccable appearance. If an element is made of steel and located in the immediate vicinity of a saline water body, corrosion problems are only a matter of time. This time can be very short if the category of atmospheric corrosivity is incorrectly determined, resulting in a poorly chosen system for protecting the structure against corrosion.

Keywords: metal corrosion, chloride deposition, atmospheric corrosivity category

1. Introduction

Steel structures constructed in seaside promenade areas are primarily intended to serve decorative and representational purposes. Examples of such structures include lighting masts, lamps, shade structures, light rings, and other small architectural objects - see Fig. 1. The aesthetic appearance of these structures is required throughout the entire period of their use.

Fig. 1. Steel structures discussed in the article. [source: Internet]

Improperly applied anti-corrosion protection for structures can lead to the first signs of corrosion appearing very shortly after the construction is completed. Such a situation occurred in Świnoujście, where the steel structural elements decorating the promenade showed signs of corrosion despite being recently constructed. The first reports of corrosion problems with these steel elements emerged just a few months after the construction was completed. This indicates both poor quality of the anti-corrosion protections and the high aggressiveness of the environment - see Fig. 2.

The investment in question was carried out at a short distance from the shoreline, and correctly determining the category of atmospheric corrosivity was essential for adopting the appropriate method of protecting the steel structures against corrosion.

The article presents an analysis of the current knowledge on the impact of the marine atmosphere on the corrosion of steel elements, an analysis of the environment at the investment site, and the final determination of the category of atmospheric corrosivity. Correctly determining the category of atmospheric corrosivity is crucial for adopting the appropriate protection methods and for potential warranty claims.

Fig. 2. Corrosion of steel elements at the investment site [Source: https://iswinoujscie.pl/artykuly/60923/]

2. The impact of the marine atmosphere on metal corrosion in light of literature data

Atmospheric corrosion causes the greatest economic losses among all known types of corrosion. It is estimated that the costs of protection against atmospheric corrosion account for about 70% of the expenditures incurred on all types of anti-corrosion measures [4]. Atmospheric corrosion is electrochemical in nature. It occurs with the involvement of water from sources such as precipitation or condensed water vapor and with unlimited access to oxygen. During atmospheric corrosion, two processes occur simultaneously on the metal surface: anodic and cathodic.

In the anodic process, the metal undergoes oxidation, meaning it transitions from a metallic state to an ionic state. The cathodic process occurs in two forms, depending on the pH of the environment. In an acidic environment, cathodic reduction of hydrogen ions occurs, releasing hydrogen. In neutral and alkaline environments, cathodic reduction of oxygen in the aqueous solution takes place, forming hydroxide ions. Corrosion products on the metal surface are formed at the boundary of the anodic and cathodic areas as a result of subsequent chemical reactions.

The basic environmental and atmospheric factors responsible for the occurrence of atmospheric corrosion include [5]:

- the action of water in all its forms,
- high relative humidity of the air,
- presence of chlorides in the air,
- the action of temperature and its changes,
- the action of UV radiation,
- the presence of gaseous substances in the air, mainly SO_2, NO_x, H_2S, CO_2, etc.,
- the presence of volatile aromatic and aliphatic hydrocarbons in the air,
- the presence of dust in the air resulting from the combustion of coal fuels.

Many studies worldwide have been conducted on the impact of the marine atmosphere on metal corrosion. Many of these studies highlight the fact that the concentration of chloride ions (Cl^-), and consequently the corrosion loss of steel, largely depends on the distance of the structure from the shoreline.

Alcantara and others [7] demonstrated through extensive experimental research conducted on the coast of Spain that the deposition of chloride ions (Cl–), measured in milligrams per square meter per day, strongly depends on the distance from the shoreline. This is due to the high concentration of chloride ions originating from marine aerosols, which consist of dispersed sea water droplets and particles formed from the evaporation of sea water under the influence of wind. Very high chloride deposition, and consequently a high degree of corrosion measured in micrometers per year, is maintained even at distances up to 1000 meters from the shoreline.

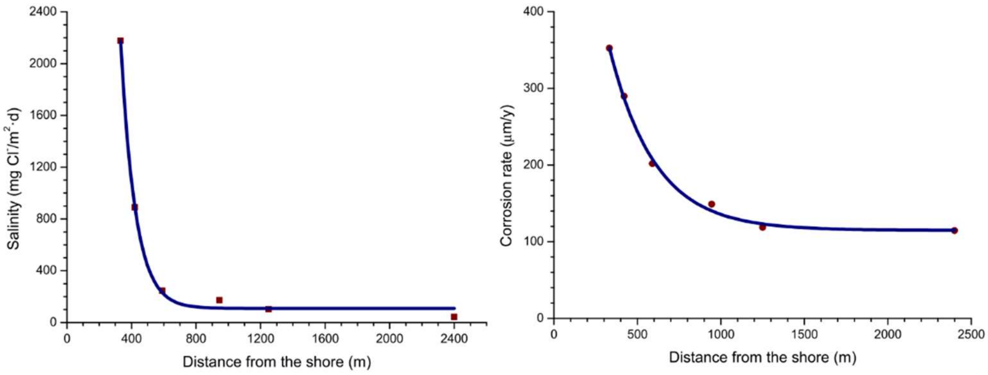

Fig. 3. Chloride deposition and thickness loss as a function of distance from the sea according to [7]

Gustafsson reached similar conclusions in his studies conducted on the southwestern coast of Sweden [8]. He demonstrated that the dry deposition of sea salt strongly depends on the distance from the sea. A sharp increase in deposition can be observed for distances less than 400 meters from the shoreline. Haberecht also utilized the results of his work in his doctoral dissertation [9].

Similar research results, demonstrating that both the concentration of chloride ions in the air and, consequently, the extent of their dry deposition leading to corrosion loss, have been reached by other researchers from various countries. These include Hernández (Cuba) [10], Corvo (Cuba) [11], Somay (Turkey) [12], and Meira (Brazil) [13]. Therefore, it is evident that this relationship occurs regardless of the region or the salinity of the body of water.

An example of domestic research also showing a clear relationship between the distance from the Baltic Sea shoreline and the amount of chloride ion (Cl^-) deposition, as well as the resulting corrosion rate, are the studies conducted by Dr. Eng. Marian Głuszko presented in [4-6]. During these extensive studies, which included nine measurement sites across the country, research was conducted in various environments: coastal, industrial, urban-industrial, urban, and rural (in conventionally clean air). These studies were carried out in 1997-1998 [6]. The research focused on the corrosion rates of four basic structural metals and the deposition levels of SO2 and chloride ions (Cl^-).

The analysis of the collected data identified two locations that stood out in terms of the amount of chloride ion (Cl^-) deposition:

- The village of Dunowo, in the Koszalin County, located approximately 17 km from the Baltic Sea coast,
- The village of Żarnowiec, in the Puck County, located approximately 5 km from the Baltic Sea coast.

In both of these locations, a significantly higher chloride deposition was observed compared to the other seven locations across the country. In the village of Żarnowiec, due to its closer proximity to the shoreline, the deposition is 17% higher than in Dunowo. The corrosion loss measurements recorded during the studies allowed both locations to be classified into the atmospheric corrosivity category C3 according to [14]. The atmosphere in these locations was described as coastal with low salinity.

The studies presented in the works of Głuszko [4-6] clearly indicate the strong influence of the marine atmosphere and the marine aerosols it contains on the amount of chloride ion (Cl^-) deposition, which is one of the main factors causing steel corrosion. It is important to note that even locations several (Żarnowiec) or several dozen (Dunowo) kilometers away from the shoreline remain under the strong influence of the marine atmosphere.

As demonstrated in numerous studies mentioned above, the amount of chloride ion (Cl^-) deposition significantly increases as one approaches the shoreline, where it can reach values of several hundred or even several thousand milligrams per square meter per day. This amount strongly depends on various factors, including wind direction and speed. Comparing the deposition rate a few hundred meters from the shore with the rate a few kilometers away, one can observe a several-fold or even a dozen-fold increase in deposition, which in turn translates to a multiple increase in corrosion loss caused by steel corrosion.

Table 1. Corrosivity of atmospheric environments in Poland according to [6]

Lp.	Miejsce badania		Szybkość korozji			Wielkość depozycji SO_2	Wielkość depozycji Cl^-
			$g\ m^{-2}\ m\text{-}c^{-1}$	$g\ m^{-2}\ rok^{-1}$	$\mu m\ rok^{-1}$	$mg\ m^{-2}\ doba^{-1}$	$mg\ m^{-2}\ doba^{-1}$
1	ŁAGISZA	M-1	1.61	18.12	2.03	151.3	10.2
		A-1	0.44	5.09	1.88		
		Zn	3.28	38.21	5.35		
		St3S	54.06	633.8	80.64		
2	TARNÓW	M-1	1.02	9.69	1.09	44.6	6.2
		A-1	0.34	3.08	1.14		
		Zn	1.98	18.03	2.52		
		St3S	29.28	289.3	36.81		
3	SOLINA	M-1	0.35	3.41	0.38	12.3	0.13
		A-1	0.26	2.48	0.92		
		Zn	0.81	7.51	1.05		
		St3S	16.63	154	19.59		
4	PUŁAWY	M-1	1.79	20.27	2.27	160.5	11.2
		A-1	0.45	5.21	1.93		
		Zn	3.39	39.92	5.59		
		St3S	58.8	689.4	87.71		
5	DUNOWO	M-1	0.42	3.84	0.43	17.5	24.6
		A-1	0.27	2.51	0.93		
		Zn	1.63	15.66	2.19		
		St3S	28.73	264.5	33.65		
6	ŻARNOWIEC	M-1	0.48	4.72	0.53	18.5	28.7
		A-1	0.29	2.89	1.07		
		Zn	1.8	17.11	2.4		
		St3S	27.77	267.8	34.07		
7	HUTA GŁOGÓW	M-1	2.05	23.74	2.66	176.8	15.9
		A-1	0.49	5.16	1.91		
		Zn	3.87	45.21	6.55		
		St3S	66.1	784.3	99.78		
8	TURÓW	M-1	1.69	19.44	2.18	162.1	11.4
		A-1	0.48	5.76	2.13		
		Zn	3.41	38.83	5.44		
		St3S	56.34	659.6	83.92		
9	WROCŁAW	M-1	1.58	16.54	1.85	86.3	4.7
		A-1	0.39	4.08	1.51		
		Zn	2.16	20.11	2.83		
		St3S	49.6	433.8	67.91		

3. Atmospheric Corrosivity According to different Standards

PN-EN ISO 12944-2 [14]

According to the standard [14], atmospheric corrosion is a process that occurs in the moisture layer on the surface of the metal. This moisture layer can be so thin that it is invisible to the naked eye. The rate of corrosion is increased by the following factors:

- Increase in relative humidity;
- Occurrence of condensation (when the surface temperature equals or is lower than the dew point);
- Increase in atmospheric pollutants (corrosive pollutants can react with steel and form deposits on the surface).

Experience indicates that significant corrosion typically occurs when the relative humidity is above 80% and the temperature is above 0°C. However, if contaminants and/or hygroscopic salts are present, corrosion can occur at much lower humidity levels.

According to section 5.1.1 of the standard [14], atmospheric environments are classified into six corrosivity categories, as presented in the ISO 9223 standard [15].

According to Section 5.1.2 of the standard [14], it is strongly recommended to expose standard samples to determine the corrosivity category. Table 1 of the standard [14] defines the corrosivity categories based on the mass loss or thickness loss of these standard samples made of low-carbon steel and/or zinc after the first year of exposure. Details regarding the standard samples, their treatment before and after exposure, are provided in ISO 9226.

If it is not possible to expose standard samples in the actual environment of interest, the corrosivity categories can be estimated based on typical environment examples given in Table 1. However, special attention should be paid, as the specified examples and environment descriptions in the standard are solely for informational purposes and may occasionally be misleading. Only the actual measurement of mass loss or thickness loss provides accurate classification. In cases of doubt, such as when the mass losses of steel and zinc indicate different corrosivity categories, the higher category should be assumed.

PN-EN ISO 9223 [15]

According to ISO 9223, atmospheric corrosivity should be classified by determining the corrosivity based on the measurement of corrosion losses of standard metal samples as specified in ISO 9226, or if this is not possible, by assessing the corrosivity based on environmental information, that is, through the calculation of corrosion losses. Both methods of assessing corrosivity represent generalized approaches and are characterized by various uncertainties and limitations.

The corrosivity category determined based on corrosion losses after the first year of exposure reflects the specific environmental conditions during the year of exposure. The corrosivity category assessed using the dose-response equation reflects the statistical uncertainty of this function. The corrosivity category assessed using an informational description based on comparing local environmental conditions with the description of typical atmospheric conditions may lead to misinterpretation. This approach should be used only when experimental data is not available.

The dose-response equations for carbon steel are provided in [15] as follows: $r_{corr} = 1{,}77 \cdot P_d^{0{,}52} \cdot \exp(0{,}020 \cdot \mathrm{RH} + f_{St}) + 0{,}102 \cdot S_d^{0{,}62} \cdot \exp(0{,}033 \cdot \mathrm{RH} + 0{,}040 \cdot T)$ (1)

$$f_{St} = 0{,}150(T - 10)\ gdy\ T \leq 10^{o}C \quad (2)$$

where:

r_{corr} – corrosion loss after the first year [mm/year]
T – average annual temperature [°C]
RH – average annual relative humidity [%]
P_d – average annual SO_2 deposition, [mg/(m^2·d)]
S_d – average annual Cl^- deposition[mg/(m^2·d)]

PN-EN 1993-1-4 [16, 17]

The standard PN-EN 1993-1-4 [16] and its amendment introduced in 2015 [17] specify the principles for selecting the appropriate grade of stainless steel depending on the operating environment of structural elements. The selection of the steel grade is preceded by an environmental assessment performed using the Corrosion Resistance Factor (CRF), which is the sum of three components:

$$CRF = F_1 + F_2 + F_3 \quad (3)$$

F_1 – risk of exposure to chlorides from salty water or road salt [mm/year]
F_2 – risk of exposure to sulfur dioxide [°C]
F_3 – requirements for periodic cleaning or natural washing by rain [%]

The most significant factor in determining the CRF value is the coefficient F1, which defines the risk of exposure to chlorides (Cl^-) from salty water. For example, the value of this coefficient for all coastal areas of the Baltic Sea, assuming the distance from the shoreline is less than 250 meters, is F1 = -10, indicating a very high risk of chloride exposure to the structure. This means that even assuming no exposure to sulfur dioxide (F2 = 0) and assuming natural washing by rain (not containing chloride ions) (F3 = 0), the CRF would be -10. This necessitates the use of stainless steel with a corrosion resistance class of CRC = III on a five-point scale.

4. Location and Climate – Basis for Assessing Atmospheric Corrosivity

In engineering practice, the selection of an atmospheric corrosivity category is an arbitrary decision made by the designer and is often associated with the need to optimize the overall investment costs. Choosing a lower atmospheric corrosivity class clearly reduces the total costs of implementing protective coating systems. Therefore, contractors will aim to adopt the minimal corrosivity class. The problem lies in unequivocally determining the atmospheric corrosivity class in accordance with normative regulations, which would settle discussions between the Investor and the Contractor. The proximity to the seashore inherently implies high atmospheric corrosivity, which must be substantiated with appropriate normative references or experimental research results.

As demonstrated, several standards [15-18] exist, presenting challenges for an average designer in precisely determining the atmospheric corrosivity category, particularly in the absence of relevant climatic data for the investment site.

Location

The Promenada Zdrowia, where most of the corroding steel structures are located, is situated in Świnoujście approximately 200 meters from the shoreline.

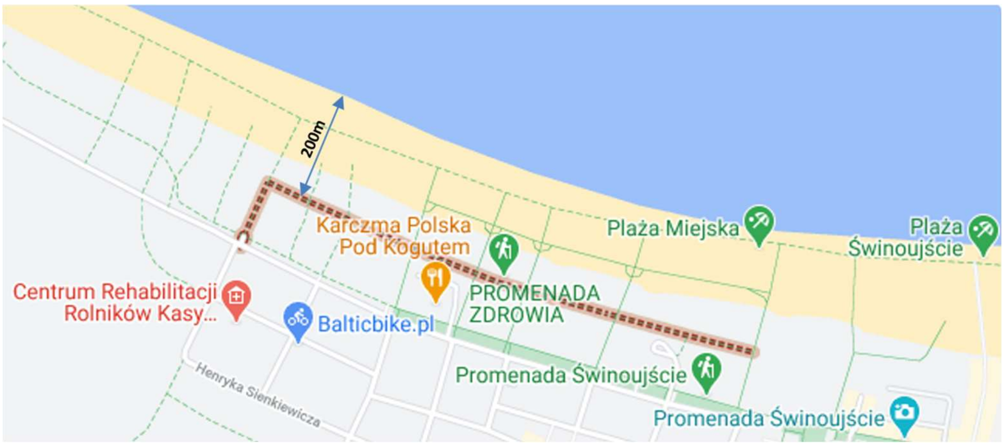

Fig. 4. Location of the investment

Climate and atmospheric conditions

In the city of Świnoujście, a maritime climate [1] prevails. It is characterized by a lower annual temperature amplitude compared to other parts of the country. Winters are milder and less frosty. The average annual air temperature is around 9°C. Variations in wind strength and direction are quite significant. The average annual wind speed is about 4 m/s. Strong westerly and southwesterly winds predominate. The climate is characterized by high air humidity due to the presence of sea water particles in the air [1]. The average annual air humidity is close to 80%. The total number of rainy days in a year is about 170. The total annual precipitation amount is close to 600 mm. It is worth noting that the precipitation entering the area of Świnoujście records the highest concentration of chlorides in the country – see Fig. 5.

Data concerning high concentrations of chloride anions Cl^- in atmospheric precipitation can also be found in the report on the state of geoecosystems in Poland [2], prepared annually by the Chief Inspectorate of Environmental Protection as part of the Integrated Programme for Monitoring the Natural Environment. Research within this programme is conducted, among others, at the Environmental Monitoring Station of the Adam Mickiewicz University in Biała Góra, located on the island of Wolin, in the commune of Międzyzdroje, within the area of the Wolin National Park, designated by the symbol 11ZM.

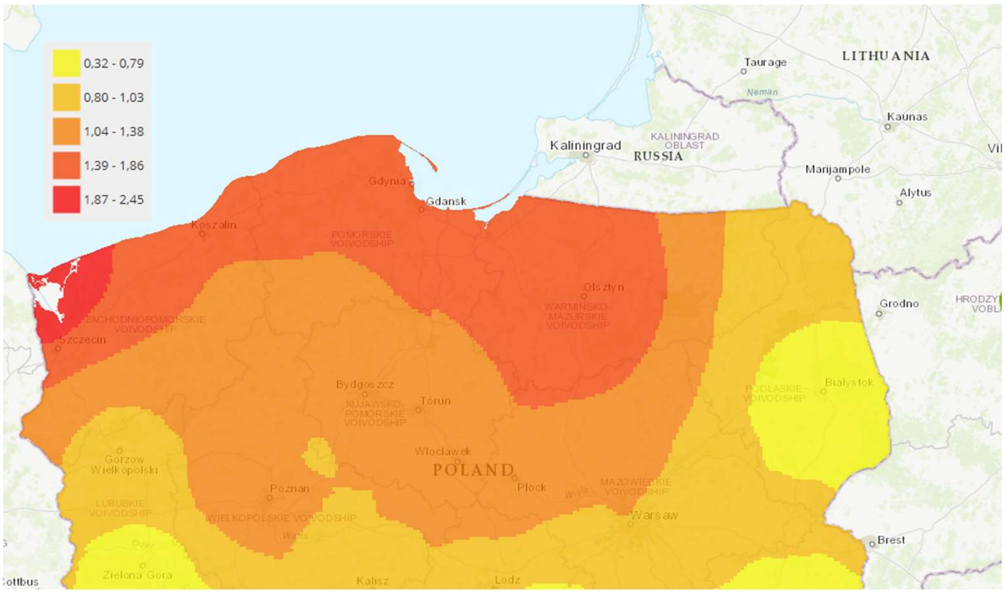

Fig. 5. Average annual concentration of chlorides in atmospheric precipitation [mg/dm3]
[Source: air.gios.gov.pl, 2016]

It is worth noting that station 11ZM in Biała Góra is located at a short distance from Świnoujście, approximately 14 km away. The distance from the monitoring station to the coastline is slightly above 300 meters, which is very close to the distance between the coastline and the Promenade Zdrowia in Świnoujście. Therefore, the measurement results at the station practically correspond to the conditions present at the investment site discussed in this paper. In the section regarding atmospheric deposition in the [2] report, it can be read that the average annual concentration of chlorides in atmospheric precipitation at the Biała Góra station (Wolin Island) is 3.12 mg/dm^3. This value has been classified as elevated. The significant level of chloride ion concentration in atmospheric precipitation is a consequence of the station's location in the direct vicinity of the Baltic Sea. The high concentration of chloride and sodium ions in atmospheric precipitation is associated with marine-origin aerosols.

Air pollution from sulfur dioxide (SO_2) in the city of Świnoujście is not high. According to the [3] report, the daily concentration of sulfur dioxide, and consequently, the average annual concentration in the northern regions of the West Pomeranian Voivodeship, does not exceed 5 $\mu g/m^3$.

5. Determination of the forecasted corrosion loss

In earlier chapters of the paper, the problem of atmospheric corrosion of steel was generally characterized, normative guidelines were presented, and literature data regarding the assessment of atmospheric corrosion were analyzed.

According to norm [15], the magnitude of forecasted corrosion losses can be determined using the dose-response equation. It was decided to estimate the forecasted corrosion losses using the data established during the assessment of climatic conditions on the investment site and literature data, especially national research results presented in [5]. The following assumptions were adopted during the calculations:

$T = 9^oC$ – average annual temperature [°C]
RH = 80% – average annual relative humidity [%]
$P_d = 4\ \frac{mg}{m^2 d}$ – average annual SO_2 deposition, [mg/(m²·d)]
$S_d = 144\ \frac{mg}{m^2 d}$ – average annual Cl^- deposition[mg/(m²·d)]

- Values for sulfur dioxide (SO_2) determined by the deposition method P_d and the volumetric method P_c are equivalent in the case of norm [15]. Relationships between measurements made using both methods can be approximately expressed as $P_d = 0{,}8 \cdot P_c$, where P_d is expressed in [mg/(m^2·d)] and P_c in [µg/m^3].
- • Values for chloride ion deposition strongly depend on the distance from the seashore, as demonstrated in many previously mentioned studies. Values within a few hundred meters from the shore may be several times greater than those determined at distances of a few kilometers. The Promenada Zdrowia is located just 200 meters from the seashore. For calculations, a fivefold increase in chloride (Cl^-) deposition was adopted, determined for the town of Żarnowiec located approximately 5 km from the seashore, i.e., 5 x 28.7 = 144 mg/(m^2·d).

The dose-response equations for carbon steel:

$$f_{St} = 0{,}150(T - 10) = 0{,}150(9 - 10) = -0{,}15 \tag{4}$$

$$r_{corr} = 1{,}77 \cdot P_d^{0{,}52} \cdot \exp(0{,}020 \cdot \mathrm{RH} + f_{St}) + 0{,}102 \cdot S_d^{0{,}62} \cdot \exp(0{,}033 \cdot \mathrm{RH} + 0{,}040 \cdot T) \tag{5}$$

$$r_{corr} = 1{,}77 \cdot 4^{0{,}52} \cdot \exp(0{,}020 \cdot 80 - 0{,}15) + 0{,}102 \cdot 144^{0{,}62} \cdot \exp(0{,}033 \cdot 80 + 0{,}040 \cdot 9) \tag{6}$$

$$\boldsymbol{r_{corr} = 60,1\frac{\mu m}{a} = 480\frac{g}{m^2 a}} \quad (7)$$

It should be noted that the magnitude of the corrosion loss strongly depends on the amount of chloride ion deposition. Assuming S_dg as ten times the deposition in Żarnowiec, which is approximately 287 mg/(m^2·d), results in an increase in the predicted loss to the level of:

$$\boldsymbol{r_{corr} = 84\frac{\mu m}{a} = 672\frac{g}{m^2 a}} \quad (7)$$

6. Determining the atmospheric corrosivity category

The predicted corrosion loss r_{corr} values determined in the previous section should be compared with the threshold values specified in standards [14] and [15].

Table 2. Determining the atmospheric corrosivity category based on r_{corr}

Corrosivity Categories	Mass loss per unit area/thickness loss (after the first year of exposure)				Examples of typical environments (for information)	
	Low-carbon steel		Zinc		outsiede	inside
	g/m²	µm	g/m²	µm		
C4 High	400 – 650	50 – 80	15 – 30	2,1 - 4,2	Industrial and coastal areas with moderately salty atmosphere	Zakłady chemiczne, baseny kąpielowe, statki żeglugi przybrzeżnej itp.
C5 Very high	650-1500	80 – 200	30 – 60	4,2 - 8,4	Industrial areas with high air humidity and highly aggressive corrosive pollutants Coastal areas with a highly salty atmosphere	Buildings and areas with condensation and high atmospheric contamination

Assuming the chloride deposition level as five times the measured value in Żarnowiec, the annual corrosion loss is r_{corr} = 480 g/m², which falls within the range of 400 to 650 g/m². This means that the atmospheric corrosivity category for the investment site located approximately 200 meters from the shore is:

C4 – High corrosivity

However, it should be noted that the chloride deposition level determined in this way may be significantly underestimated considering the proximity to the shoreline. Assuming ten times the deposition measured in Żarnowiec, resulting in r_{corr} with a value of 672 g/m² per year, the atmospheric corrosivity category is:

C5 – Very high corrosivity

Precise determination of the corrosion loss values r_{corr} would be possible after conducting tests on standard metal samples (carbon steel, zinc, copper, aluminum) according to the provisions of Chapter Seven of the standard [15].

Precise determination of the S_d value, i.e., chloride ion deposition, would be possible experimentally using the wet candle method described in ISO 9225 standard. Clarifying this value would allow for a more accurate determination of the predicted corrosion losses r_{corr}.

7. Summary

The analysis presented in the paper allows us to draw the following conclusions:

- The atmosphere at the investment site should be classified as a typical marine atmosphere, characterized by high humidity as well as a high concentration of chloride ions (Cl^-) originating from marine aerosol.
- The atmosphere at the investment site is highly aggressive, as evidenced by the fact that the first signs of corrosion appeared on the structure just a few months (possibly a few weeks) after its construction.
- The designed structure primarily serves aesthetic and representational functions. In addition to safety, it is required to maintain an impeccable appearance to meet the provisions of the ultimate limit state specified in PN-EN 1990.
- Literature studies, environmental data analysis, and calculations unequivocally indicate that a corrosion resistance category of C4 or C5, i.e., high or very high corrosivity, should have been adopted for the anti-corrosion protection of the structure. Precise determination of the corrosion resistance category would be possible after conducting additional studies to determine the chloride ion deposition on the investment site (see ISO 9225) or based on the measurement of corrosion losses on standard metal samples (see ISO 9226).

- Similar conclusions regarding the assessment of atmospheric corrosivity can be drawn based on the provisions of the standard for designing structures with stainless steel [16, 17], according to which structures located within 250 meters from the Baltic Sea shoreline are exposed to very high risks of chloride exposure from seawater, therefore they should be designed with stainless steel of at least corrosion resistance class CRC III.
- Adopting a too low corrosion resistance class may lead to accelerated corrosion and consequently shorten the intended service life of the structure. As a result, financial costs for maintaining the proper technical condition, especially the appearance of the structure, will increase.

References

1. Program Ochrony Środowiska dla Miasta Świnoujście na lata 2016-2019 z perspektywą na lata 2020-2023. Greenkey Rozwiązania dla środowiska. Styczeń, 2017 r.
2. Raport o stanie geoekosystemów Polski w roku 2009. Zintegrowany Monitoring Środowiska Przyrodniczego. Główny Inspektorat Ochrony Środowiska, https://www.gios.gov.pl
3. Roczna ocena jakości powietrza w województwie zachodniopomorskim. Raport wojewódzki za rok 2019. Główny Inspektorat Ochrony Środowiska. Departament Monitoringu Środowiska. Regionalny Wydział Monitoringu Środowiska w Szczecinie. Szczecin 2020 r.
4. Głuszko M.: Zagadnienia ochrony antykorozyjnej konstrukcji stalowych oraz urządzeń elektroenergetycznych eksploatowanych w warunkach atmosferycznych. Sieć Badawcza Łukasiewicz - Prace Instytutu Elektrotechniki, Zeszyt 235, 2008.
5. Głuszko M.: Korozja Atmosferyczna Konstrukcji Stalowych i Stalowych ocynkowanych w Otoczeniu Elektrowni Węglowych. Metody ochrony. IV Seminarium Naukowo-Techniczne Zakopane, s. 20, 18-20 czerwca 1997.
6. Głuszko M.: Ocena narażeń środowiskowych i ocena uszkodzeń konstrukcji stalowych i stalowych ocynkowanych. Polskie Sieci Elektroenergetyczne S.A., Dokumentacja Techniczna Nr RB/DP/46/96, Warszawa, 1997.
7. Alcantara J., de la Fuente D., Chico B., Simancas J., Diaz I. and Morcillo M.: Marine Atmospheric Corrosion of Carbon Steel: A Review. Materials 2017, 10, 406; doi:10.3390/ma10040406
8. Gustafsson M. E. R., Franzen L. G.: Dry deposition and concentration of marine aerosols in a coastal area, SW Sweden. Atmospheric Environment Vol. 30, No. 6, pp. 977-989, 1996.
9. Haberecht P. W.: Pollution Deposition Rates on Insulator (HV) Surfaces for use in Atmospheric Corrosivity Estimation. Thesis, Doctor of Philosophy, The University of Newcastle, September 2008.
10. Hernández A.: Impact of environmental pollution in the historical buildings of Havana, Cuba. Effect of future climate change. Revista Ingeniería de Construcción RIC Vol 33 Nº3 2018.
11. Corvo F., Perez T., Dzib L.R., Martin Y., Castaneda A., Gonzalez E., Perez J.: Outdoor–indoor corrosion of metals in tropical coastal atmospheres. Corrosion Science 50 (2008) 220–230
12. Somay A. M., Gemici U., Filiz S.: Hydrogeochemical investigation of Kucuk Menderes River coastal wetland, Selcuk–Izmir, Turkey. Environmental Geology, July 2007
13. Meira G.R., Andrade C., Alonso C., Padaratz I.J., Borba J.C.: Modelling sea-salt transport and deposition in marine atmosphere zone – A tool for corrosion studies. Corrosion Science 50 (2008) 2724–2731
14. PN-EN ISO 12944-2 Farby i lakiery. Ochrona przed korozją konstrukcji stalowych za pomocą ochronnych systemów malarskich. Część 2: Klasyfikacja środowisk.
15. PN-EN ISO 9223 Korozja metali i stopów. Korozyjność atmosfer. Klasyfikacja, określenie i ocena.
16. PN-EN 1993-1-4 Eurokod 3: Projektowanie konstrukcji stalowych – Część 1-4: Reguły ogólne – Reguły uzupełniające dla konstrukcji ze stali nierdzewnych.
17. Zmiana do Polskiej Normy PN-EN 1993-1-4:2007/A1:2015-08 Eurokod 3: Projektowanie konstrukcji stalowych – Część 1-4: Reguły ogólne – Reguły uzupełniające dla konstrukcji ze stali nierdzewnych.

CARBONATION OF CONCRETE COVER OF REINFORCEMENT AS A CAUSE OF LOSS OF DURABILITY OF STRUCTURES

KAJA KŁOS[1], *kaja.klos@tpaqi.com*
GRZEGORZ ADAMCZEWSKI[2], *g.adamczewski@il.pw.edu.pl*
PIOTR WOYCIECHOWSKI[2], *p.woyciechowski@il.pw.edu.pl*
PAWEŁ ŁUKOWSKI[2], *p.lukowski@il.pw.edu.pl*

[1]TPA Sp. z o.o.
[2]Politechnika Warszawska, Wydział Inżynierii Lądowej

Abstract: The phenomenon of concrete carbonation is related to the physical and chemical processes occurring in concrete under the influence of carbon dioxide. Carbonation of concrete of reinforcement cover is one of the main causes of reduction of durability of reinforced concrete structures. The article discusses the physical and chemical mechanisms of the carbonation phenomenon itself as well as points out the synergistic effect of frost destruction and concrete carbonation on reinforced concrete elements. The examples of structural damage from engineering practice in the field of diagnosis of reinforced concrete structures are presented.

Keywords: Carbonation of concrete, frost resistance of concrete, corrosion of concrete, durability of concrete, cover of reinforcement, synergistic effect of frost destruction and carbonation of concrete.

1. Durability of concrete

According to EN 1990: “structures shall be so designed that changes occurring during their design life, taking into account environmental effects and the anticipated level of maintenance, do not reduce the performance of the structure below the intended level” [1]. Durability should therefore be understood as the period during which the level of performance of a structure is maintained above a critical value for a given period of its use.

According to EN 1990:2004, "a structure shall be designed and constructed in such a way that during its intended life, with adequate reliability and without excessive costs: it shall take up all influences and impacts which may be expected to arise during its construction and use; it shall remain fit for its intended use; the structure shall be designed so that its load-bearing capacity, serviceability, and durability are adequate" [1].

Eurocode [1] therefore requires structures to satisfy three fundamental requirements over their intended lifetime: absorption of influences and actions, fitness for use, and adequate durability.

The corrosion process is a phenomenon that progresses over time and is not linear. During the initiation period, symptoms are usually hardly noticeable because they develop locally in the microstructure. During laboratory tests, an initial strengthening of the concrete can often be seen due to the filling of the pores with corrosion products. It is only at a later stage, when the limit stresses resulting from further growth of corrosion products in the pores are exceeded, that cracks, fractures, and localized detachments develop. The further corrosion process is usually faster. In view of these conditions, the earlier the repair is started, the smaller the scope of repair and the higher its efficiency. Moreover, the basis of effective repair is the correct identification of the cause and selection of remedial measures adequate to the identified corrosion mechanism. Conducting the repair "blindly," based on identifying only the symptoms and not the causes, significantly limits the effectiveness of the repair. In extreme cases, neglect at the diagnostic stage may cause rapid deterioration of the structure, e.g., due to the closure of the corrosive environment under the repair layer. In the repair of concrete structures, the same principle applies as in medicine: treat the causes and not the symptoms. The tools for proper handling of concrete protection are contained in the PN-EN 1504 family of standards [2]. A necessary step is to conduct a comprehensive diagnostic study.

The design stage is always key in shaping the durability of concrete. It determines the choice of materials, the geometry of elements, and surface protection methods. Determination of the construction class according to EC0, EC1, and EC2, taking into account the specific requirements for concrete exposure classes related to carbonation (XC), allows the selection of the minimum concrete cover of a specific strength class ensuring the required durability of the element [1,3,9]. The aim of this paper is to highlight the risks associated with synergistic effects of the environment despite the adoption of correct solutions in light of current technical knowledge.

2. Carbonation phenomenon

Carbonation is a set of physicochemical transformations of concrete under the influence of long-term exposure to carbon dioxide on the concrete surface, which is constantly present in the surrounding atmospheric air and in the atmosphere inside building structures. The concentration of CO_2 varies between 0.03% and 0.3%, depending on the location of the concrete structure [5].

Steel reinforcement placed in concrete is protected against corrosion if the concrete is not contaminated with aggressive substances and its pH is high enough to ensure the durability of the passive layer on the surface of the reinforcement. The corrosion of the reinforcement, initiated by the process of cover carbonation, gradually leads to its destruction. The first stage of carbonation has no significant negative effects on the structure. When the pH in the reinforcement environment decreases to approximately 11, the passivation state is lost, and electrochemical corrosion of the reinforcement starts. The appearance of cracks in the cover, through which aggressive substances can easily penetrate, intensifies carbonation. In the third stage, gradual chipping and spalling of the cover occur, so that the reinforcement is exposed, leading to a significant reduction in the durability of the concrete structure [5].

Carbonation significantly decreases the durability of reinforcement in reinforced concrete structures, mainly due to a decrease in the pH of the concrete. However, positive effects are observed with respect to concrete. The number and size of pores in the carbonated zone are reduced, resulting in a tightening of the concrete microstructure. Additionally, increased surface hardness and strength of the near-surface layer of carbonated concrete is observed [5,6,7].

Many external and internal factors influence the intensity and rate of carbonation. Decisive factors include the type of concrete, the amount of cement, the w/c ratio, the method of concrete compaction, and the care of the concrete. The climatic and environmental conditions under which the concrete structure is subsequently placed are also crucial. Regarding external factors, the most important are CO_2 concentration, humidity, and air temperature. Among the most important internal factors, the tightness of the concrete, indirectly dependent on the w/c ratio, as well as the type and quantity of the bond, are the main determinants [8].

Concrete cover protects steel reinforcement against corrosion, provides fire resistance, and ensures cooperation of reinforcement with concrete, provided that the structure is properly designed and constructed.

3. Synergistic effect of corrosion interactions

Environmental and climatic conditions have a significant impact on the condition and durability of unprotected reinforced concrete elements. The most common cause of damage to concrete structures is the lack of frost resistance. Carbonation of concrete leads to the loss of protective properties of the concrete cover concerning reinforcing steel (CO_2 penetrates the concrete and reacts with water-soluble components of the hardened cement grout). The combination of these two phenomena (a synergistic effect that is not considered in traditional design methods) can lead to a significant reduction in the durability of concrete structures.

Frost corrosion in temperate climates, where concrete is subjected to cyclic freezing and thawing, often in the presence of de-icing salts, is a very common phenomenon. Frost corrosion occurs by increasing the volume of water as it freezes, and with interacting high stresses, cracks and fissures are noticed in the concrete. As the outside temperature decreases, the remaining water will freeze, resulting in damage (bursting) to the top surface of the concrete [4].

It is worth mentioning the synergy of influences that contribute to the deterioration of the durability of the structure. The environment in which concrete "lives" includes the atmosphere, water, and soil. The prevailing climate in Poland is characterized by a large variability of weather. Winters can be cold or mild, and summers can be hot or rainy. In Poland, for more than 9 months of the year, the relative air humidity is higher than 75%, and quite high but constant pollution in the form of CO_2 emissions is observed.

4. Summary

The issue of the durability of reinforced concrete structures and the simultaneous maintenance of safety during the service life of a given object requires appropriate consideration and analysis of the combination of physical, physicochemical, chemical, and electrochemical phenomena in the expected operating conditions of concrete. The examples of corrosion of concrete and reinforcement elements indicate that synergistic environmental interactions can intensify the destruction of elements. The presented considerations prove that the method of selecting the reinforcement cover due to the threat of carbonation, as imposed by EC2 [3], does not take into account the synergistic effect, which may determine the real resistance of the system to environmental interactions. Durability design based on the concepts of carbonation resistance, frost resistance, and mutual synergy [10] are the basis of the projected new edition of the Eurocodes, in which not only exposure classes but also classes of resistance of structures to these risks will appear.

References

1. PN-EN 1990:2004 Eurokod, Podstawy projektowania konstrukcji.
2. PN-EN 1504 Wyroby i systemy do ochrony i napraw konstrukcji betonowych – Definicje, wymagania, sterowanie jakością i ocena zgodności.
3. PN-EN 1992-1-1 Eurokod 2, Projektowanie konstrukcji z betonu, Część 1-1: Reguły ogólne i reguły dla budynków.
4. Czarnecki L., Emmons P.H.: Naprawa i ochrona konstrukcji betonowych, Polski Cement, Kraków 2002.
5. Woyciechowski P.: Model karbonatyzacji betonu, Oficyna Wydawnicza Politechniki Warszawskiej, Warszawa 2013.
6. Czarnecki L., Woyciechowski P.: Modelling of concrete carbonation; is it a process unlimited in time and restricted in space?; PAN; Bulletin of the Polish Academy of Sciences Technical Sciences 2015.
7. Kurdowski W.: Chemia cementu i betonu, Wydawnictwo Naukowe PWN, Warszawa 2010.
8. Praca zbiorowa: Beton, technologie i metody badań; Stowarzyszenie Producentów Cementu, Kraków 2020.
9. PN-EN 1991-1-1 Eurokod 1: Oddziaływania na konstrukcje, Część 1-1: Odziaływania ogólne, ciężar objętościowy, ciężar własny, obciążenia użytkowe w budynkach.
10. Korycka-Kowalska J., Woyciechowski P.: Analiza stanu wiedzy o współzależności pomiędzy destrukcją mrozową i karbonatyzacją betonu, Materiały Budowlane, 12/2015.

ASSESSMENT OF CORROSION DAMAGE IN REINFORCED CONCRETE COLUMNS

JACEK KORENTZ[1], *j.korentz@ib.uz.zgora.pl*

[1]University of Zielona Góra

Keywords: reinforced concrete column, concrete corrosion, reinforcement corrosion, eccentric compression, ultimate load capacity

1. Intoduction

Every building and construction object is subject to degradation as a result of the environment in which it is used. Damage to reinforced concrete structures resulting from operating conditions is caused by physical and chemical factors acting separately or simultaneously. The result is damage to the surface of the concrete and the concrete cover of the reinforcement, followed by corrosion of the reinforcement. These deterioration processes may reduce the serviceability of components and materials to such an extent that the structure of the building will no longer be able to meet the basic requirements regarding its load-bearing capacity and serviceability by the end of its design lifetime. For these reasons, in some cases, reinforced concrete structures require frequent maintenance and costly repairs.

The paper presents the causes and consequences of corrosion in reinforced concrete structures and the results of an analysis of the load-bearing capacity of eccentrically compressed reinforced concrete columns, in which corrosion damage of varying intensity to the concrete and reinforcement bars has occurred. The aim of the analyses is to assess the consequences of damage to reinforced concrete.

2. Causes and effects of corrosion of concrete and rebar

The classification and subdivision of the most common causes of damage to the surface of concrete and the concrete cover of reinforcement caused by service conditions, as well as corrosion of reinforcement, are given in the standard [1]. They are in accordance with the exposure classes of concrete related to environmental impacts according to [2]. However, corrosive actions affecting the characteristics of concrete and reinforcement are not considered as loads. According to [3,4], it is necessary to design structures considering their durability. This means that the durability of structures is considered one of the three equal elements of structural reliability, alongside safety and serviceability. Adequate durability of reinforced concrete structures can be guaranteed by, among other things, appropriate thickness of the cover and strength class of concrete [5].

a) b) c) d)

Fig. 1. Corrosion damage to reinforced concrete columns

Source: a) https://www.wesavestructures.info/corrosion-evaluation (31.01.2022r), b) https://www.fprimec.com/structural-effects-corrosion/ (31.01.2022r.), c) https://www.theengineeringcommunity.org/types-and-causes-of-concrete-deterioration/ (31.01.2022r.), d) https://www.techdry.com.au/how-to-avoid-salt-water-corrosion-within-reinforced-concrete/ (31.01.2022r.)

Figure 1 shows examples of observed corrosion damage in reinforced concrete columns. The photographs in this figure illustrate the already advanced state of degradation of reinforced concrete columns. In these images, one can distinguish: (a) local cover detachment and reinforcement corrosion, (b) cover detachment and reinforcement corrosion on one of the column's lateral surfaces, (c) cover detachment and reinforcement corrosion along the entire column perimeter, and (d) concrete loss inside the section core and reinforcement corrosion. In all cases presented, the columns did not collapse.

A measure of corrosion damage in concrete is the reduction in cross-sectional dimensions resulting from crushing and spalling of the cover and sometimes the core of the section. The measure of corrosion damage in reinforcement bars is their weight loss, expressed by the weight loss coefficient γ or the reduced diameter d_o.

3. Load capacity analysis of eccentrically compressed columns

We consider columns with a square cross-section in which longitudinal reinforcement of steel bars with a yield strength of f_{yd} = 400MPa is used (Fig. 2). The location of the reinforcement in the section is determined by the parameter a_1/d = 0,10. The total degree of longitudinal tension and compression reinforcement is ρ = 1,50%.. For concrete with a design compressive strength f_{cd}=30 MPa, a parabolic-rectangular stress-strain diagram is adopted. For steel members, an elastic-plastic model without reinforcement was adopted.

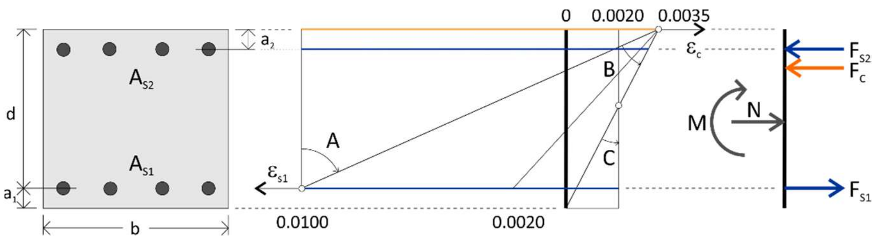

Fig. 2. Strain and sectional forces at ultimate limit state.

Figure 2 shows the distribution of limit deformations in the analyzed eccentrically compressed reinforced section, illustrating the section strains from axial tension to axial compression. The strains in the tensile bars are limited to ε_{s1} = 0,01. The limit strains of the concrete in extreme compression are limited to ε_{cu} = 0,0035, while they cannot be greater than 0.002 for axial compression [5]. In the same range, the deformations in the compression bars change.

Five sections with the same dimensions and the same degree of reinforcement are subjected to analysis (Fig. 3): cross-section RC-0 without corrosion damage, cross-section C4 with the cover separated along the whole perimeter, cross-section C1-S19 with the cover separated on one edge and mass reinforcement corrosion ratio γ=0,19 cross-section C2-S19 with the cover separated on two edges and mass reinforcement corrosion degree γ=0,19; and cross-section C4-S/36 with the cover separated on four edges and mass reinforcement corrosion ratio γ=0,36.

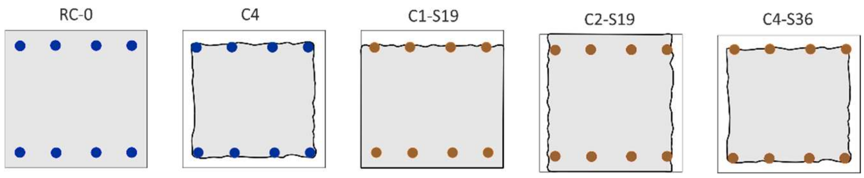

Fig. 3. Analysed column cross-section.

The bending moment - axial force interaction curves for the sections under consideration were obtained on the basis of FEM analyses performed with the XTRACT application from Imbsen Software Systems. Fig. 4 shows the interaction curves between the dimensionless bending moment m and the dimensionless longitudinal force n for sections without damage and sections with different extent of corrosion damage. The lines of the three eccentricities of the longitudinal force e normalised with respect to the useful section height d are also plotted in this figure. The line of the relative eccentricity e/d = 0,6 passes through the so called "balance" point lying on the interaction curve for the section without damage RC-0.

The bending moment-axial force interaction curves for the sections under consideration were obtained based on FEM analyses performed with the XTRACT application from Imbsen Software Systems. Figure 4 shows the interaction curves between the dimensionless bending moment m and the dimensionless longitudinal force n for sections without damage and sections with different extents of corrosion damage. The lines of the three eccentricities of the longitudinal force *e* normalized with respect to the useful section height *d* are also plotted in this figure. The line of the relative eccentricity $e/d = 0.6$ passes through the so-called "balance" point lying on the interaction curve for the section without damage (RC-0).

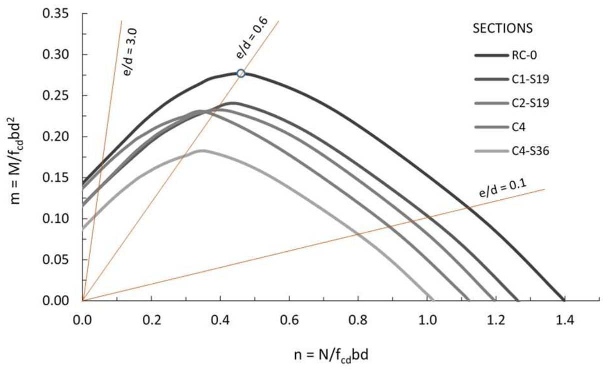

Fig. 4. Interaction curves non-dimensional bending moment m - non-dimensional axial force n.

For the longitudinal force eccentricity $e/d < 0.6$, the concrete in the compression zone determines the section capacity, whereas for the longitudinal force eccentricity $e/d > 0.6$, the tension reinforcement determines the section capacity. Additionally, the eccentricity lines $e/d = 0.1$, corresponding to the case of small eccentricity, and $e/d = 3.0$, corresponding to the case of large eccentricity, are shown.

Figure 5 shows bar diagrams of the non-dimensional longitudinal forces *n* acting on the three eccentricities $e/d = 0.1$, 0.6, and 3.0. These forces have been normalized with respect to the longitudinal force $n_{CR\text{-}0}$ transmitted through the section without damage (RC-0). The greatest loss of load capacity is seen in cross-section C4-S38, i.e., the cross-section without the cover around the whole perimeter and with a 38% loss of reinforcement mass; depending on the longitudinal force eccentricity *e/d*, the loss of load capacity varies from 29% to 36%.

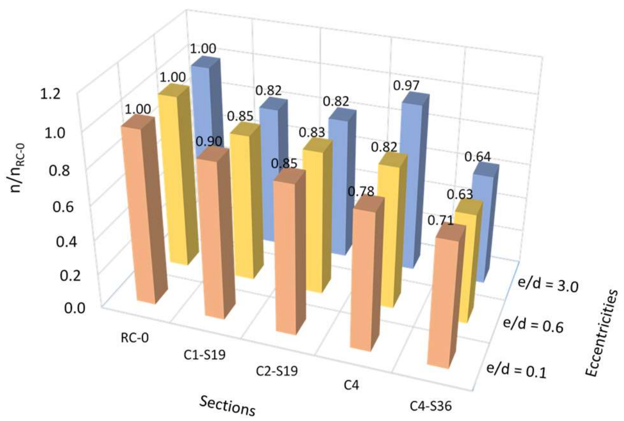

Fig.5. Effect of the longitudinal force eccentricity and corrosion damage on the load carrying capacity of the sections

The smallest reduction in load-bearing capacity is shown in section C4, without cover around the whole perimeter but without corrosion of the longitudinal reinforcement, for the eccentricity of the longitudinal force $e/d = 3.0$; it is only 3%. In the other cases of corrosion damage, the load capacity decreases vary from 10% to 22%.

4. Summary

When corrosion damage occurs to reinforced concrete structures, it is necessary to use appropriate methods to assess their current load-bearing capacity. For reinforced concrete columns, this involves using interaction curves between bending moment and axial force. This method makes it possible to assess the behavior of reinforced concrete columns over the entire load range.

Analyses of the load capacity of eccentrically compressed sections of reinforced concrete columns with corrosion damage to the concrete and reinforcing bars, which are most frequently encountered in practice, have shown that the decreases in load capacity are not so great. The residual bearing capacity is not less than 2/3 of the original load capacity.

References

1. PN-EN 1504-9:2010. Wyroby i systemy do ochrony i napraw konstrukcji betonowych. Definicje, wymagania, sterowanie jakością i ocena zgodności. Część 9: Ogólne zasady dotyczące stosowania wyrobów i systemów.
2. PN-EN 206:2014-04. Beton - Wymagania, właściwości, produkcja i zgodność
3. Ajdukiewicz A., 2014, Prenorma konstrukcji betonowych - fib Model Code 2010, Polski Cement, Kraków.
4. PN-EN 1990:2004/A1:2008. Eurokod 0. Podstawy projektowania konstrukcji.
5. PN-EN 1992-1-1:2008, Eurokod 2, Projektowanie konstrukcji z betonu, Część 1-1: Reguły ogólne i reguły dla budynków.

EVALUATION OF THE EFFECTS OF FROZEN CONCRETE IN THE SLAB – PROBLEMS OF ELECTROHEATING

KAMILA OWCZARSKA[1], *kamila.owczarska@gmail.com*
ELŻBIETA SZMIGIERA[1]
PIOTR WOYCIECHOWSKI[1]

[1]Politechnika Warszawska, Instytut Inżynierii Budowlanej, Aleja Armii Ludowej 16, 00-637 Warszawa, Polska

Abstract: In Poland, the period of lower temperatures occurs on average from November 15 to March 15, which accounts for an entire quarter of the year. To continuously carry out construction activities during this time, it is required and necessary to apply measures aimed at protecting concrete against the adverse effects of frost. Many methods are known, but their combinations are the most common. One such method is the use of electrofusion heating of concrete, also known as electroheating. However, it should be remembered that curing concrete using the electroheating method is a complex issue and depends on many parameters that may change over time. Therefore, the entire heat treatment process should be properly designed and carried out under the control of competent persons. Practice shows, however, that in many cases there are no procedures setting standards for the design of the electroheating installation and the conduct and control of the process itself. The importance of implementing an appropriate control system is demonstrated in this paper through the example of a floor slab of a residential building structure that has been frozen.

Keywords: frozen concrete, concrete heat treatment, electrofusion, lowered temperatures, maintenance in low temperature conditions

1. Introduction

The ambient temperature that ensures the best development of the compressive strength of concrete ranges from +15 °C to +20 °C. At lower temperatures, the setting of the cement slows down, which is especially noticeable below 10 °C. However, when the temperature drops below 0 °C, the hydration process is practically stopped. Therefore, in accordance with [1], the period in which the average daily ambient temperature is lower than 10 °C is considered the period of lowered temperatures.

When analyzing the meteorological yearbooks, it is assumed that this period in Poland falls from November 15 to March 15. To continuously carry out construction activities without skipping an entire quarter of the year, it is required and necessary to apply measures aimed at protecting concrete against the adverse effects of low temperatures. One such measure may be the use of the electrofusion method of heating concrete, also known as electroheating. However, it should be remembered that curing concrete using the electroheating method is a complex issue, and its effectiveness depends on many parameters that may change over time. Therefore, the entire heat treatment process should be properly designed and carried out under the control of competent personnel.

Practice shows, however, that in many cases there are no procedures setting standards for the design of the electroheating installation and the conduct and control of the process itself. The importance of implementing an appropriate control system is demonstrated in this paper through the example of a floor slab of a residential building structure that has been frozen due to errors in the care process using electroheat.

2. Classification and characteristics of methods enabling concrete maturation in conditions of low temperature

To precisely define the type of changes occurring in concrete during exposure to lowered temperatures, three critical periods of early concrete maturation were distinguished (according to B. Bukowski [2], [3]). This is because the most dangerous time for a reinforced concrete element is freezing after the commencement of bonding but before achieving a strength value defined in the literature as safe strength. The manual [1] states that the safe strength (referred to as the critical strength in the latest version of the manual) ranges from 3.5 MPa to 8 MPa, and that the concrete should achieve at least 20% of its design 28-day compressive strength before the first freezing.

The following activities allow for the performance of reinforced concrete works in low-temperature conditions [10]:

- Enabling the maturation of concrete without supplying heat from the outside,
- Supplying heat from the outside,
- A combination of the above variants.

The issue of the influence of electroheating treatment on the properties of concrete in the structure was presented by the authors in [7].

To determine the effectiveness of the applied method of concrete protection against the influence of low temperature, it is necessary to monitor changes over time in two factors influencing its effectiveness: concrete surface temperature and concrete compressive strength [8], [11]. According to the Polish standard [6], "the temperature of the concrete surface may not drop below 0 °C until the safe strength is achieved." The guidelines [4] define exactly which measurements should be taken.

3. Assessment of the effects of freezing the ceiling on the example of the completed structure of a residential building

Construction works during the implementation of the investment in a multi-family residential building were carried out in low-temperature conditions. The concrete mix used was C30/37 S3, made with the so-called "winter recipe," compliant with the standard [19]. Due to technology and cost considerations, the optimal procedure was to use the method of electrofusion heating of concrete (electroheating) in combination with covering the concrete surface with materials such as bubble foil. Electroheating, although difficult to implement due to the multitude of factors that must be taken into account when designing and implementing this process, is the most commonly used method of thermal concrete curing under winter work conditions at construction sites. The structural element described in this paper is the working section of the floor slab of a repeating storey with beams and balcony slabs.

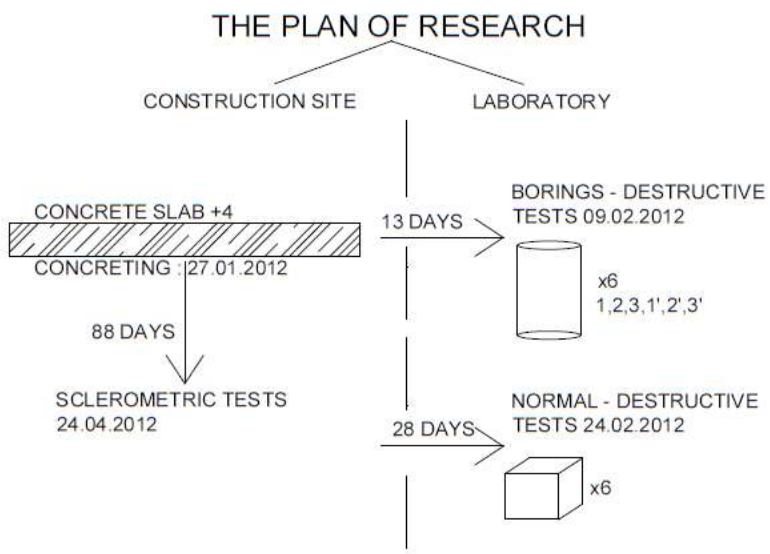

Fig. 1. Test plan of the frozen floor element of the structure

Concreting of the element started around 10:00, and the air temperature was -9 °C. The temperature of the delivered mixture ranged from 9 °C to 12 °C. The weather conditions were very difficult during concreting due to heavy and intense snowfall. Additionally, there was a lack of continuity in concrete supplies. Due to these difficulties, concreting lasted until late at night and was completed around midnight, at an air temperature of -12.9 °C. The effect of the frost was intensified by the wind in the exposed, elevated space and snowfall. After concreting was completed, the electroheating process was started. It should be emphasized that concreting lasted about 14 hours, and during this entire time, the freshly laid concrete was not protected against the effects of low temperatures. According to the authors, this is one of the most unfavorable aspects of using the electroheating system.

When trying to start the system, it was discovered that many heaters had burned out, resulting in the system not working at all. This meant that the freshly laid concrete was left exposed to low temperature conditions without any additional protection measures. The outside temperature continued to drop over the following days, reaching an extreme value of -18.7 °C on the seventh day. Due to these problems, the construction management decided to discontinue any further construction activities. The break lasted about two weeks. During this time, an analysis of the quality of the concrete in the concreted floor slab was commissioned. The test plan is presented in Figure 1.

After inspecting the boreholes (Fig. 2), the presence of a frozen upper layer of concrete, 1.5 to 2 cm thick, was found. Importantly, the top reinforcement bars were below the frozen zone. Visual inspection of the boreholes revealed that the upper zone contained microdefects (microcracks, surface roughness) due to frost damage. Such defects were not found in the lower part of the cores, confirming that the concrete did not freeze from the lower surface of the ceiling. Before laying the mix in the formwork, it was additionally heated from the bottom for about 4 hours to remove the residual snow and maintain the formwork temperature above 0°C. This limited the temperature gradient effect at the interface between the concrete mix and the formwork, contributing to the prevention of freezing of the lower, tensioned surface of the ceiling and reduction of unfavorable thermal stresses. After stripping the ceiling and visually inspecting it, no signs of freezing of the lower surface of the concrete, usually identifiable by the naked eye, were found.

The samples from the wells marked 1, 2, and 3 were taken from the upper part of the cores, while the samples 1', 2', and 3' (Table 1) were taken from the lower part. The tests were carried out in accordance with the standards [13] and [15], and the test results are presented in Table 1. The standards referred to in the paper were valid at the time of construction, tests, and analyses. These standards have since been replaced by others, but as a rule, the basic assumptions and requirements have not changed significantly, which would necessitate a correction of the obtained test results.

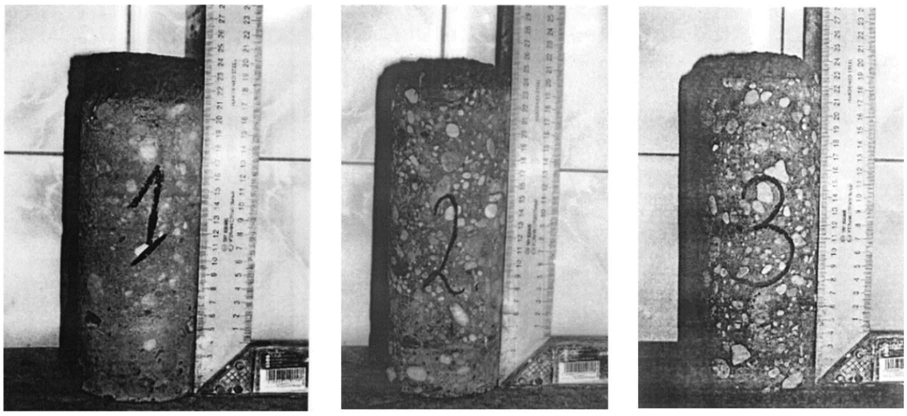

a) b) c)

Fig. 2. Core boreholes taken from the structure

Table 1. Results of destructive testing of cores taken from the structure

No.	Sample determination	Maximum load in the event of destruction [kN]	height of the samples [mm]	f_c [MPa]	f_{cSR} [MPa]
1	1	193	92	28,4	28,5
2	2	197	92	29,0	
3	3	218	92	32,1	
4	1’	184	88	27,1	
5	2’	189	89	27,8	
6	3’	180	93	26,5	

Following the standard procedure of concrete quality control during the execution of reinforced concrete works, samples for destructive tests were also taken ([16], [17]). Based on these tests, it can be concluded that the mixture used meets the requirement for the design class C30/37. The study of wells in the structure shows that the concrete, at the age of 16 days, achieved the strength corresponding to the C20/25 class. This value is for concrete without the frozen layer, which has been removed. To supplement the above results, the construction site was tested using the non-destructive sclerometric method ([14], [18]).

Table 2. Results of non-destructive tests using the sclerometric method of the frozen floor slab

Lp	L_i 1	2	3	4	5	6	7	8	9	L_i	±ΔL	L_i	(L_i -L')	(L_i -L')^2
1	26	22	25	24	27	26	25	25	25	25,0	3,1	28,1	-0,2	0,0400
2	23	26	27	26	25	27	27	28	25	26,0	3,0	29,0	0,7	0,4900
3	23	25	25	24	27	25	25	25	25	24,9	3,1	28,0	-0,3	0,0900
4	23	25	25	24	24	26	25	25	27	24,9	3,1	28,0	-0,3	0,0900
5	25	25	27	27	25	26	26	25	25	25,7	3,0	28,7	0,4	0,1600
6	25	24	25	25	25	26	26	26	24	25,1	3,0	28,1	-0,2	0,0400
Concrete age = 88 days										∑=		169,9	0,1	0,9100

Summarizing the sclerometric analysis, the results indicated a concrete strength class of C20/25. Based on the analysis carried out by the constructor of the object (from design calculations and low component strain indices), it was determined that the actual class C20/25 was sufficient to meet the limit state of the floor. Additionally, it was found that the bottom surface of the element did not freeze. Consequently, no additional repairs and safeguards were necessary, apart from removing the frozen layer at the connection with the vertical elements.

4. Summary

When working in low-temperature conditions, it is necessary to take measures to protect the fresh concrete. Many methods are available, but in practice, the most common combination is electroheating in conjunction with covering the surface of the element. In the case described in the paper, as in many similar situations, electroheating was used alongside surface covering. Regardless of the undeniable effectiveness of this method, in the described case, due to the accumulation of several unfavorable circumstances [12], the effects of concrete protection against freezing were not fully achieved. These factors, related to the concreting process and insufficient control of the electroheating installation, rendered the heat treatment ineffective. Nevertheless, no repairs and additional protection were necessary due to the calculated reserve of the load-bearing capacity resulting from the thickness of the ceiling, which was adopted mainly due to architectural requirements.

Ten years have passed since the described case. The authors' subsequent experiences show that in currently designed structures, such a situation would be unlikely because the thickness of the floor slab is now determined solely by constructional considerations. The example presented in the paper demonstrates the importance of properly planning and preparing for work in low-temperature conditions. However, practice shows that there are often no procedures setting standards for the design of the electroheating installation and the conduct and control of the process itself.

There are many devices and systems for continuous temperature recording available on the market, along with software for determining the increase in concrete strength, e.g., using the maturity curve method [9]. Such systems are usually offered by companies specializing in temperature control services inside concrete, mainly in massive structures and strength development control. In practice, for many investments, complicated measurements carried out by specialized companies may not work well in the conditions of a construction site, and they also generate increased costs. This makes it all the more important to develop simple standards for heat treatment at the construction site that can be used by any construction supervisor. The presented example also shows how the accumulation of unfavorable events, each of which individually would not be a threat, can synergistically lead to serious implementation problems.

References

1. Wykonywanie robót budowlanych w okresie obniżonej temperatury, Instrukcja Instytutu Techniki Budowlanej, nr 282/2020,
2. Bukowski B., „Technologia betonu. Budownictwo betonowe – tom I, część 1, Spoiwo, kruszywa, woda", Arkady, Warszawa 1963 r,
3. Woyciechowski P., Jackiewicz-Rek W., Pielęgnacja betonu. Metody i zasady, XXXIII Ogólnopolskie Warsztaty Pracy Projektanta Konstrukcji / Jasiński R. (red.), PZITB, Szczyrk 2018, t. 3 s. 141-200,
4. ACI 306R-16, „Guide to cold weather concreting",
5. Jamroży Z., „Beton i jego technologie",Warszawa 2005 r,
6. PN-EN 13670:2011 „Wykonywanie konstrukcji z betonu",

7. Owczarska K., Szmigiera E. „Wpływ elektronagrzewu na właściwości betonu w konstrukcji, Dni Betonu 2014, str. 1107-1116,
8. Wrochna S., „Materiały budowlane i technologia betonów, część III: Technologia betonów i zapraw", Wojskowa Akademia Techniczna, Warszawa 1984 r,
9. A. Mariak, K.Wilde, Wyznaczanie wytrzymałości betonu na podstawie funkcji dojrzałości wg amerykańskiej normy ASTM C1074-11,
10. Roboty budowlane w warunkach zimowych, Budownictwo i Architektura , Warszawa 1955 r,
11. Bajorek. G., „Pielęgnacja betonu w okresie dojrzewania", Stowarzyszenie producentów Cementu, Kraków 2017,
12. K. Owczarska, E. Szmigiera, P.Woyciechowski "Błędy wykonawcze związane ze stosowaniem elektronagrzewu betonu" , Monografia Awarie Budowlane 2017, s.923-934,
13. PN-EN 12504-1:2009, „Badania betonu w konstrukcjach - Część 1: Odwierty rdzeniowe -Wycinanie, ocena i badanie wytrzymałości na ściskanie",
14. PN-EN 12504-2: 2002, „Badania betonu w konstrukcjach - Część 2: Badanie nieniszczące -- Oznaczanie liczby odbicia",
15. PN-EN 12390-3:2009, „Badania betonu - Część 3: Wytrzymałość na ściskanie próbek do badań",
16. PN-EN 12390-2:2011, „Badania betonu - Część 2: Wykonywanie i pielęgnacja próbek do badań wytrzymałościowych",
17. PN-EN 12350-1:2011, „Badania mieszanki betonowej - Część 1: Pobieranie próbek",
18. Instrukcja ITB nr 210 (1977): Instrukcja stosowania młotków Schmidta do nieniszczącej kontroli jakości betonu w konstrukcji. Warszawa, ITB,
19. PN-EN 206-1:2003, „Beton - Część 1: Wymagania, właściwości, produkcja i zgodność".

ESTIMATING THE AGE OF CONCRETE ON THE BASIS OF CARBONATION DEPTH MEASUREMENT

Piotr Woyciechowski[1], *p.woyciechowski@il.pw.edu.pl*
Grzegorz Adamczewski[1]

[1]Politechnika Warszawska, Wydział Inżynierii Lądowej, Zakład Inżynierii Materiałów Budowlanych

Keywords: concrete carbonation, in situ concrete testing, acid-base indicators, concrete age assessment

1. Introduction

In the expert activities of the authors, the issue of disputes between parties to legal proceedings, where determining the age of a concrete element was of key importance, has arisen several times. Building documentation should be the basic source of knowledge in this regard. However, in many cases, particularly for items made using economic methods, such documentation is not available.

In litigation concerning, inter alia, property rights, determining when a given structure was actually completed can be of significant importance. For example, the authors of this article have been asked several times to resolve disputes over the age of concrete elements in real estate fences on adjacent plots. Determining the date of erection of such an element can be decisive in the context of awarding the so-called real estate acquisitive prescription. Prescription of real estate is a method of acquiring ownership rights by an unauthorized owner as a result of the actual exercise of these rights over a period specified by law. According to the Polish Civil Code, for real estate to be settled by acquisitive prescription, the following conditions must be met: spontaneous possession, continuity of ownership, and the expiry of the specified period. The decisive factor in determining acquisitive prescription is the length of the period of unauthorized possession. The minimum period is 20 consecutive years for good faith or 30 consecutive years for bad faith. Thus, determining whether an item is more or less than 20 or 30 years old may, in the absence of other evidence, form a relatively objective basis for the final decision on prescription.

In the opinion of the authors of this article, if such an element is made of concrete not covered on the surface with other materials, then a rough estimation of the age of the element could be done using measurements of the depth of concrete carbonation. The subject of this article is to present a procedure that allows for estimating the age of concrete based on measuring the depth of concrete carbonation in situ along with the assessment of other necessary characteristics of this concrete. The possible accuracy of estimation and its adequacy to the assumed goal were considered. Examples of estimates based on the experts' practice of the authors are presented.

2. The method of estimating the age of concrete based on the depth of carbonation

Scope of the investigation: The scope of the necessary tests includes: estimated determination of the concrete strength class, e.g., based on drilled cores; determination of the type of cement in concrete, visually or by instrumental methods; selection of carbonation depth test sites considering exposure conditions; and carbonation depth testing in situ on fresh forgings or sample breaks.

Testing Methods: The best method to estimate the strength class of concrete, for which no technical documentation is available, is to take drill cores from the structure. The procedure is governed by the provisions of PN-EN 13791: 2019-12.

Determining the type of cement (binder) in concrete is important for using nomograms to estimate the depth of carbonation (carbonation progresses faster in concretes with a significant proportion of non-clinker binder components). For a rough estimate, macro- and microscopic observations, including those related to the color of concrete, can be used. The skilled eye of an expert is often a sufficient tool to distinguish.

Measurement of the depth of concrete carbonation is usually performed using phenolphthalein, a colorless solution that turns purple at the limit of pH = 8.3. The measurement procedure is detailed in the PN-EN 14630: 2007 standard. An important element of the test is the selection of the measurement sites. The following rules should be followed: during the period of use, the concrete at the measurement site was not covered with any other material impeding the access of carbon dioxide (e.g., paint coating, plaster, etc.); the tested concrete surface was not constantly or periodically submerged in water; the tested concrete surface was not covered with soil; the measurement is performed on the freshly forged (immediately before testing) concrete surface; it is not allowed to perform the measurement on the side of the well taken from the structure; it is permissible to perform the measurement at the fracture of a newly split well; the measurement of the carbonation depth should be repeated in a few selected places of the element.

Principle of Estimating the Age of Concrete

Information obtained in accordance with the procedure described on the strength class, type of cement used, and the average depth of carbonation allows the use of nomograms (e.g., such as in Figure 1).

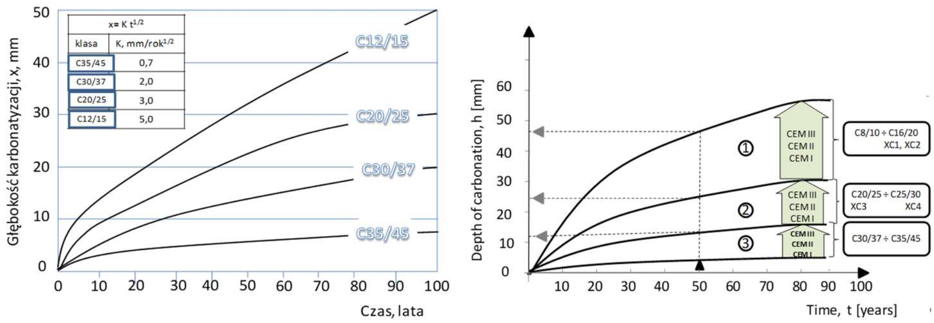

Fig. 1. Nomograms showing the relationship of carbonation depth, strength class and age of concrete

The following part of the article presents an example of using the method to estimate the age of a fence foundation during court proceedings for the prescription of a part of a construction plot. The result of the estimation is illustrated in Figure 2, which presents possible variants for estimating the age of the concrete for the measured carbonation depth of 15-20 mm, depending on the strength class.

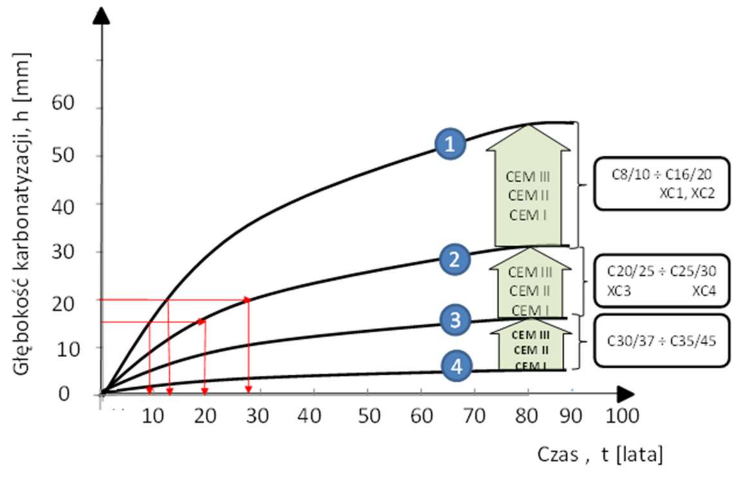

Fig. 2 Concrete age estimation - arrows indicate the estimation range depending on the concrete strength class

Limitations and uncertainty in applying the method

The authors of the idea emphasize that the presented tool should only be considered auxiliary in legal—not technical—contexts, and the obtained results should be treated as burdened with a significant margin of error. However, as indicated at the beginning of the article, the aim is often to determine whether the age of the concrete exceeds the limits of 20-30 years. The practice of using this method shows that it can be primarily employed to demonstrate that the concrete is younger than indicated by oral information. The low carbonation depth of low or average strength concrete clearly indicates that it is relatively "young" concrete. The proposed procedure allows, with high probability, for this presumption to be converted into an experimentally supported numerical value.

3. Conclusions

The authors of the article themselves approach the concept with considerable caution, acknowledging its imperfections, limitations, and high inaccuracy of estimation. However, it is difficult to deny the existence of a close relationship between the actual extent of carbonation in concrete and its age. Thus, despite the method's shortcomings and in the absence of any other means to determine the age of concrete, the authors see some potential in applying the proposed estimation scheme.

From a scientific reliability standpoint, it should also be mentioned that the method is based on infinite carbonation models, as these are the indicators and nomograms available in the literature. This stands in contradiction to the (apparent) theory of finite (limited) carbonation, which has been published many times by the authors. According to this theory, carbonation follows a hyperbolic function of time, suggesting it has a finite range in concrete (model asymptote) but is achieved over infinite time. The apparent contradiction arises because analyses are conducted over a limited time range (i.e., 20-40 years). During this period, under natural carbonation conditions, the hyperbolic and parabolic models are not divergent enough to significantly affect the concrete age estimation result.

References

1. Ustawa z dnia 23 kwietnia 1964 r. - Kodeks cywilny, Dz.U. 1964 nr 16 poz. 93
2. Woyciechowski P.: Model karbonatyzacji betonu, Prace Naukowe Politechniki Warszawskiej. Budownictwo, nr 157, 2013, Warszawa, Oficyna Wydawnicza Politechniki Warszawskiej, 178 s., ISBN 978-83-7814-103-7
3. Czarnecki L., Woyciechowski P., Adamczewski G.: Risk of concrete carbonation with mineral industrial by-products, KSCE Journal of Civil Engineering, 2018, vol. 22, nr 2, s.755-764. DOI:10.1007/s12205-017-1623-5
4. Czarnecki L., Woyciechowski P.,: Concrete Carbonation as a Limited Process and its Relevance to Concrete Cover Thickness, ACI Materials Journal, 2012, vol. 109, nr 3, s.275-282
5. Czarnecki L., Woyciechowski P.: Modelling of concrete carbonation; is it a process unlimited in time and restricted in space?, Bulletin of the Polish Academy of Sciences, Technical Sciences, 2015, vol. 63, nr 1, s.43-54. DOI:10.1515/bpasts-2015-0006
6. Woyciechowski P., Dominika S., Kuziak J., [i in.]: Experimental verification of carbonation models used for estimation of reinforced concrete structures durability, Bulletin of the Polish Academy of Sciences, Technical Sciences, 2020, vol. 68, nr 5, s.1159-1166. DOI:10.24425/bpasts.2020.134652
7. Czarnecki L., Emmons P.: Naprawa i ochrona konstrukcji betonowych, Polski Cement, Kraków 2002
8. Czarnecki L., Woyciechowski P.: Durability of concrete according to the european standard EN 206, ICDC 2012, International Congress on Durability of Concrete 18-21 June 2012, Trondheim, Norway, Norwegian Concrete Association
9. Bajorek G., Gruszczyński M.: Nowe podejście do oceny wytrzymałości betonu w konstrukcji istniejącej wg PN-EN 13791:2019-12, BTA kwiecień – czerwiec 2020, str. 62-67

COMMON DAMAGES IN THE BUILDINGS OF THE CITY CENTER LODZ, THAT WAS BUILT IN THE YEARS 1890-1920

BARTŁOMIEJ ZGORZELSKI[1],
JACEK SZER[1], *jacek.szer@p.lodz.pl*

[1]Politechnika Łódzka, Katedra Fizyki Materiałów i Budownictwa Zrównoważonego

Keywords: Technical conditions, risk, renovation, maintenance, downtown development

1. Introduction.

The data collected on a sample of 116 tested buildings was analyzed in the years 2019-2020 in Łódź. As many as 76 of them (approximately 65%) are tenement houses built before 1920, during the period of the fastest development of the so-called Łódź Fabrykancka—one of the fastest-growing industrial cities in Europe in the second half of the 19th century. At the time of their creation, both the functional layout and dimensions of these facilities were commonly used in Łódź and constituted the basic type of development for the city, which was built from scratch.

In addition, the buildings erected during the aforementioned period are an important element of cultural heritage and constitute a rich and generally accessible display of exceptional architectural details. These buildings have unquestionable historic and historical value. The vast majority of them are located in areas protected for their heritage significance or designated as Cultural Parks or historical monuments [9]. The value of the development in the very center of the city, based on these historical buildings, is also important. This is discussed in more detail in the publications "City in the Face of Challenges - How to Find the Desire to Live in the City" [10] and "A Benevolent City: How to Shape the City with Care for Everyone" [11] additionally supported by documents from state and local authorities regarding the strategic implementation of this direction [9,12].

The analysis of this set of buildings allows for the drawing of conclusions that are relevant to a large group of the remaining existing and functioning buildings in the center of Łódź.

2. Description of the structure and functional arrangement

The buildings analyzed, due to historical ownership conditions and technical limitations available at the time of their construction, have relatively uniform and repeatable construction solutions, which were only slightly modified in some cases. An example of compact development with the analyzed buildings is presented in Fig. 1.

3. Methodology of assessing the technical condition of the buildings in question

The analysis of the archival materials and the data included in the copy of the master map allowed for the preparation of base materials for the execution of the site visit and the assessment of the technical condition. As part of the site visit and interview with the owner or manager, the material and technology used for a given facility were finally determined, allowing for the assessment of individual groups of structural elements. The following possible technical states were assumed: Good, Satisfactory, Average, Bad, Emergency.

4. Results

For the tested set of objects, the following results were obtained:

- Satisfactory condition with local exceptions: 11 items, i.e. approx. 14.5% of all objects meeting the adopted age criteria
- Medium condition with local deviations from this status: 48 items, i.e. approx. 63.2% of all objects meeting the adopted age criteria, including 3 objects with elements in an emergency state
- Bad condition with local exceptions: 17 items, i.e. approx. 22.4% of all objects meeting the adopted age criteria, including 7 objects with elements in an emergency state.

The total number of objects with elements in a emergency condition is 10, i.e. 13.2% of all objects meeting the adopted age criteria.

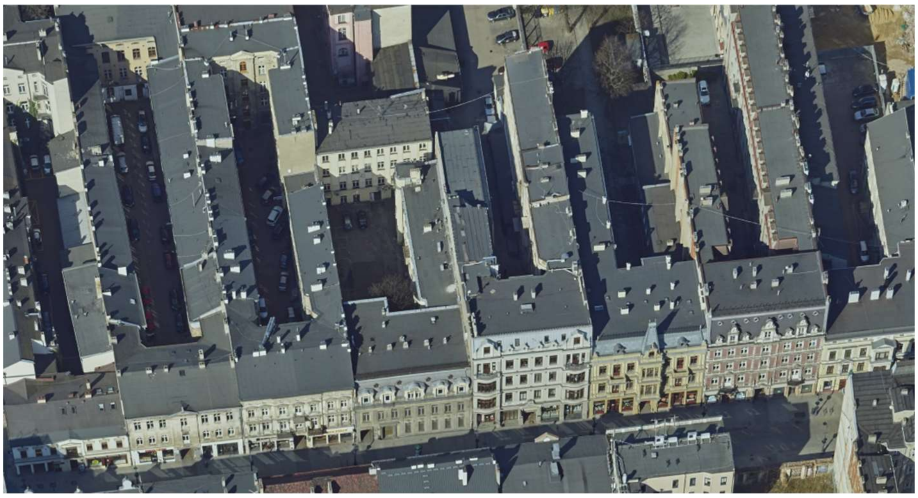

Fig. 1: Orthophotomap, view of the layout of the buildings under study

Source: Mapa.lodz.pl/ortofoto.log.lodz.pl

5. Analysis of the technical conditions of selected structural elements

Based on the assessments of the technical condition, the results were analyzed in groups of structural elements: roof structure, load-bearing walls of a repeating storey, ceilings, stairs, balconies, basement ceilings, and cellar walls. The statistics of the percentage share of individual technical conditions for each tested element are presented in tabular form below. Out of the 76 examined objects, 38 had balconies and 48 had cellars. The aforementioned results refer to these 38 and 48 objects, respectively.

Damage types

For the previously described technical conditions of individual structural elements, an analysis of the causes of damage was carried out and classified into five separate types. It should be emphasized that the examined facilities are mostly over 100 years old. These housing resources, due to historical changes in management, have been subjected to various forms of supervision—ranging from care for their current use value to various levels of "respect" by the residents who use them.

Types of damage accepted:

- TYPE 1 - no ongoing maintenance
- TYPE 2 - incorrect implementation as part of modernization, renovation and reconstruction
- TYPE 3 - insufficient installation and insulation solutions, guiding
- to the occurrence of unfavorable phenomena in the field of building physics.
- TYPE 4 - actions intentionally destructive

Table 1 - Percentage share of elements in a given technical condition.

	Assessment of the tech. condition of the element as:				
structural elements	Good	Satisfactory	Average	Bad	Emergency
Roof construction	3.95	22.37	52.63	15.79	5.26
Load-bearing walls	0	10.53	68.42	15.79	5.26
Ceilings	0	17.11	68.42	9.21	5.26
Stairs	7.89	27.63	52.63	10.53	1.32
Balconies	0	52.63	31.58	5.26	10.53
Ceilings ab. the basement	0	18.75	50.00	16.67	14.58
Basement walls	0	4.17	62.50	33.33	0
Foundations	0	3.95	93.42	2.60	0

6. Conclusions

- The general technical condition of most of the examined objects is average. For the studied sample, treated as representative of buildings of similar construction erected in the analyzed period, this applies to approximately 63% of buildings. This state of affairs is mainly influenced by the lack of adequate financial resources and maintenance of the facilities. This is due to the lack of awareness among the owners regarding their legal obligations [2] for periodic inspections and the recommendations indicated therein. Proper implementation of these recommendations allows buildings to be maintained in satisfactory technical condition on an ongoing basis.
- Approximately 13% of the examined objects require immediate action, with the indicator rising to 15% among objects with cellars. These activities should focus on halting the causes of degradation of the facility's structural integrity and providing conditions for safe repairs.
- According to the research statistics, more than 85% of the objects (63% in average condition, 22% in poor condition) require improvements in their technical condition in the short term to ensure their long-term usability. In each case, it is necessary to prepare individual technical documentation. The conducted assessments and analyses indicate that focusing in the first phase on the effective enforcement of proper ongoing maintenance from the owners will help eliminate the most serious risks deteriorating the technical condition and functional properties of the facilities.
- Construction work on such facilities requires special attention to the sequence of tasks and does not allow for the simultaneous opening of all work fronts. Identifying the scope of work requires an inventory of the facility and an assessment of its technical condition. The owners' obligations in the field of facility documentation, as indicated in the work [2], are also excellent starting materials for planning renovation or modernization investments. These materials allow for the determination of the geometric and physical parameters of the building, which are crucial at the stage of cost estimation and planning necessary financial flows over time.
- The current situation regarding access to building materials and the analyses such as LCA (Life Cycle Analysis) or CBA (Cost-Benefit Analysis), resulting from climatic conditions and the assumptions of implementing circular economy policies [13], significantly impact interest in the described buildings constituting the housing stock. The tested objects have enormous potential for creating attractive living spaces with everyday contact with the cultural heritage and values of the city center [8], [9], [10], [11], [12]. Daily contact with this heritage undoubtedly influences the development of cognitive competences among inhabitants and society.

References

1. Materials from site visits, technical expertise, technical condition assessments carried out by BZB Projekt.
2. Jacek Szer, Bartłomiej Zgorzelski, „Stan techniczny budynku a obowiązek przechowywania dokumentacji obiektu budowlanego", Materiały budowlane 3/2021 (nr 583), marzec 2021r.
3. Construction and executive designs for the reconstruction of buildings, with constructional features analogous to the buildings subject to the study, made by BZB Projekt in 2016-2021.
4. Jacek Szer „Katastrofy budowlane", Wydawnictwo Naukowe PWN S.A., 2018 r.
5. Jacek Szer, Jan Jeruzal, Iwona Szer, Piotr Filipowicz „Kontrole okresowe budynków – zalecenia, wymagania, problemy", Wydawnictwo Politechniki Łódzkiej, 2020 r.
6. Leonard Runkiewicz „Podstawy prawne realizacji napraw, wzmacniania i rozbiórek konstrukcji budowlanych", Przegląd Budowlany 10/2007.
7. Leonard Runkiewicz, Jan Sieczkowski „Najważniejsze problemy poprawy projektowania elementów i obiektów budowlanych", Builder, maj 2021.
8. Maria Dąbrowska „Łódzki detal", Wydawnictwo Regio, 2017r.
9. Regulation of the President of the Republic of Poland of February 16, 2015. (Journal of Laws of March 6, 2015, item 315) regarding the recognition as a historical monument „Łódź – wielokulturowy krajobraz miasta przemysłowego", Resolution No. XXI / 483/15 of the City Council in Łódź of 09/12/2015. on the creation of the Culture Park of Piotrkowska Street, Resolution No. XVI / 671/19 of the City Council in Łódź of November 20, 2019. on the party „Gminnego Programu Opieki nad Zabytkami Miasta Łodzi na lata 2019-2022".
10. Pierre-Andre de Chalendar „Miasto wobec wyzwań", Stowarzyszenie Francja-Polska, 2021.
11. David Sim „Miasto Życzliwe", Wydawnictwo Wysoki Zamek, 2020.
12. Resolution No. XLIII / 824/12 of the City Council in Łódź of June 25, 2012. on the party „Strategia Zintegrowanego Rozwoju Łodzi 2020+".

13. Communication from the Commission to the European Parliament, the Council, the European Economic and Social Committee and the Committee of the Regions - A new EU Action Plan for a Circular Economy for a Cleaner and More Competitive Europe with Annex, Brussels, 2020.
14. Regulation of the Minister of Infrastructure of April 12, 2002. on the technical conditions to be met by buildings and their use.
15. Instrukcja ITB 376/2020 Ochrona zabudowy w sąsiedztwie głębokich wykopów.
16. Dominik Mączyński, „Drewniana, historyczna konstrukcja dachowa – ważnym źródłem informacji naukowej", Lubuskie Materiały Konserwatorskie 2017.

SECTION II
FAILURE OF GENERAL CONSTRUCTION BUILDINGS

PRE-FAILURE STATE OF THE SWIMMING HALLS' TIMBER ROOFS IN ONE OF THE OLDEST POLISH AQUAPARKS

JANUSZ BROL[1], *janusz.brol@polsl.pl*
JAN KUBICA[1]
KAROLINA KURTZ-ORECKA[2]
MAREK WĘGLORZ[1]

[1]Katedra Inżynierii Budowlanej Politechniki Śląskiej
[2]Katedra Fizyki Budowli i Materiałów Budowlanych ZUT w Szczecinie

Keywords: glued timber, straight girders, arch girders, wooden purlins, sandwich panels, thermo-humidity conditions

1. Introduction

Correct anchoring of roof structures is particularly important due to the significant increase in threats resulting from the impact of catastrophic winds in our climate zone [1]. One of the main types of damage caused by such winds is to roof structure elements, including the detachment of entire roof coverings, especially those that are poorly designed and manufactured.

The safety of the swimming pool roof structures in one of the oldest Polish water parks was endangered due to improper attachment of the purlins to the roof girders, in conjunction with long-term wind loads and thermal and humidity interactions. The pre-failure state of the structure was observed in the form of deformations in the roof purlins and roof panels. As a result of unsealing the roof joints and the subsequent thermal and humidity deformations of the roofing layer, numerous moisture stains appeared on the surface of the timber structure elements, causing their gradual degradation.

2. Description of the swimming pool halls' roof structure

The water park complex that is the subject of the research was built at the beginning of the 21st century. The roofs of the sports and recreational swimming pools are made of glued laminated timber, forming two independent but identical structures in the form of single-pitched roofs. The timber roof structure of the sports swimming pool hall, measuring 36.0 m × 25.0 m, was designed in the 8'-13'/A'-F' axes, while the timber roof structure of the recreational pool hall, measuring 50.4 m × 25.0 m, was designed in the B-K/1-4 axes (Fig. 1).

The main structure of the swimming pool halls consists of main hockey girders and rectilinear intermediate girders with a cross-section of 215 mm × 900 mm, except for girders in the D and E axes, where there are double girders with a cross-section of 2 × 140 mm × 900 mm.

The main girders, with a span between the support axes of 25.0 m and a height in the ridge of approximately 11.3 m, measured from the girder foundation level, were designed in the 9'-12' and C-J axes. They were made of two elements: rectilinear and arched, connected with pins and using steel sheets recessed into the cross-section.

Intermediate girders are located in the middle of the span between the 8'-13' and B-K axes.

The secondary structure of the roofing consists of purlins (continuous and at least two-span long) made of glued laminated timber with a cross-section of 90 mm × 166 mm and spaced 2.4 m apart, and single-span bracing purlins with a cross-section of 90 mm × 233 mm.

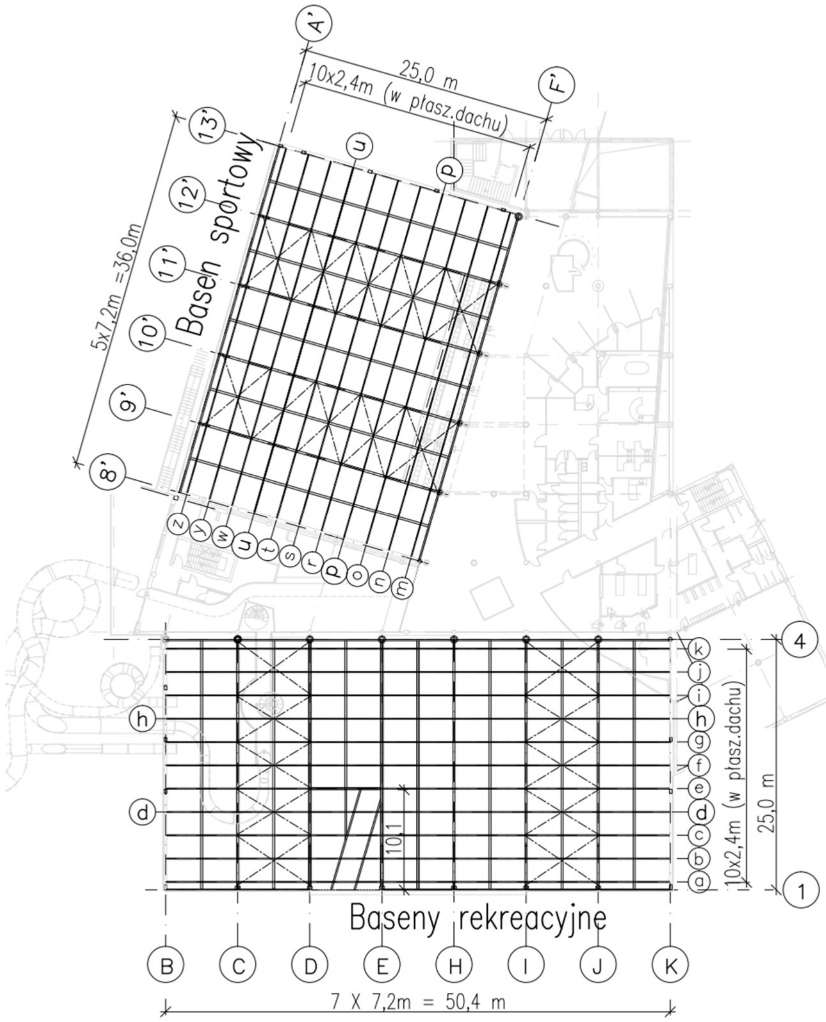

Fig. 1. Layout of the roof structure of the sports and recreational swimming pools

The timber structure of the roof of the recreational swimming pool hall is shown in Fig. 2. The purlins are covered with a roof made of Metalplast Isotherm 120 sandwich panels, 1.0 m wide, with a polyurethane core 80 mm thick and sheet metal cladding layers. The internal cladding has a thickness of 0.4 mm, while the external cladding has a thickness of 0.5 mm [2].

Fig. 2. View of the timber roof structure of the recreational swimming pool hall

The roof panels were joined lengthwise in two lines. The joints of the panels are located above the purlins located in the *p*, *u*, *d* and *h* axes.

3. Symptoms of the pre-failure condition of the swimming pool halls' timber structure

After 20 years of continuous use, the timber roof structures of the swimming pool halls exhibit numerous moisture stains on practically all elements. Deformations in the roof purlins and sandwich panels constituting the roofing have caused the moistening of the timber roof structure.

Water stains on the surfaces of the roof girders and purlins occurred particularly at the joints of the sandwich roof panels. The most intense moisture, covering almost the entire side of the purlins, was found on the roof purlins located in the p, u, d, and h axes, as marked in Fig. 1.

Fig. 3. Pulling out of the screw anchoring the roof purlin to the girder

Stains and moisture were accompanied by the exfoliation of the protective coatings on the wood, graying and blackening of the wood, and the appearance of algae on the surface of the timber purlins in areas with high moisture content. Localized biological corrosion (wood decay) was also found.

Lifting of the purlins in the *p, u, d*, and *h* axes by approximately 12-15 mm was observed at the joints with the main and intermediate girders. Additionally, loose wood fibers and a worn surface on the purlins indicated a permanent, cyclical situation of the purlins being pulled out. This suggested a lack of stabilization of the purlins by the fixing screw (lack of axial load capacity of the screw), as shown in Fig. 3. In many places, spacers were missing between the surfaces of the roof purlins and the girders. The improper fastening of the purlins to the main and intermediate girders could lead to the roof slope breaking under strong wind loads (wind suction on the roof plane), thereby directly threatening the safety of the structure.

4. Summary

The presented case study of the pre-failure state of the swimming pool halls' roof structure highlights the need to ensure the correct working conditions of the structure for its long-term use. Cyclic external influences, such as wind pressure and suction, along with the weakening of the purlin-girder joints, led to deformations of the purlins. Consequently, this resulted in the deformations of the roofing panels and the unsealing of their joints, significantly altering the hygrothermal working conditions at the joints of the roofing boards.

The emergence of a leak in the covering plane initiated deep condensation and the flow of condensate along the edges of the panel joints into the hall, causing the wooden structure to become damp. Additionally, increased heat losses, due to the opening of the roof panel joints, contributed to the melting of the snow cover on the swimming pool halls' roofs during winter periods. This led to the flow of meltwater towards the gutter strip, where it formed icicles, and further into the joints, and subsequently into the main timber structure of the swimming pool halls, causing its dampening. The prolonged process of permanent moistening of the structure resulted in further deterioration of structural elements, reducing their load-bearing capacity and that of the joints.

References

1. Żurański J., Gaczek M., Fiszer S.: Oddziaływanie wiatrów katastrofalnych na budynki w Polsce. Przegląd budowlany, nr 11/2009.
2. Katalog techniczny. Płyty warstwowe z rdzeniem z poliuretanu. Opis produktu. SIN, PLUS, SC, D. Ruukki Construction Polska Sp. z o.o., Oborniki 2006. http://wbiis.tu.koszalin.pl/kkm/rupwp.pdf, dostęp: 21.01.2022.
3. Kasperkiewicz K.: Obliczenia cieplne budynków. Poradnik. Instytut Techniki Budowlanej, Warszawa 2012.
4. Rozporządzenie Ministra Infrastruktury z dnia 12 kwietnia 2002 r. w sprawie warunków technicznych, jakim powinny odpowiadać budynki i ich usytuowanie. Dz.U.2002.75.690 z z późniejszymi zmianami.
5. PN-EN ISO 13788:2013-05: Cieplno-wilgotnościowe właściwości komponentów budowlanych i elementów budynku. Temperatura powierzchni wewnętrznej konieczna do uniknięcia krytycznej wilgotności powierzchni i kondensacja międzywarstwowa. Metody obliczania. PKN, Warszawa, 2013.
6. Europejska Aprobata Techniczna ETA-07/0285. SIMPSON Strong-Tie Hold Downs & Post Bases. ETA-Danemark A/S, Nordhavn, Kopenhaga 2021.
7. Katalog produktów. Oferta Simple. MARCOPOL Sp. z o.o., Producent Śrub. Chwaszczyno, 2021.

PROPOSAL FOR REPAIR AND REINFORCEMENT OF WOODEN STRUCTURES USING BASALT MATS

JANUSZ BROL[1], *janusz.brol@polsl.pl*
AGNIESZKA WDOWIAK-POSTULAK[2], *awdowiak@tu.kielce.pl*

[1]Katedra Inżynierii Budowlanej Politechniki Śląskiej
[2]Katedra Wytrzymałości Materiałów i Analiz Konstrukcji Budowlanych Politechniki Świętokrzyskiej

Abstract: The use of fiber composites to repair and strengthen timber structural members is proving to be an effective and efficient method. This paper presents a method of strengthening flexural beams using basalt fiber mats (BFRP). The paper includes completed experimental tests for engineered scale wooden beams reinforced with unidirectional basalt fiber mats (BFRP) and proposes a calculation algorithm based on the American standards PCF-5100 and PCF-6046.

Keywords: wood, glued laminated beams, reinforcement, basalt mats, flexural strength, ductility, theoretical analysis

1. Introduction

When repairing or reinforcing wooden structures, it is essential to remember that natural defects in wood can reduce the material's strength, particularly if located in the tension zone of the beams. To improve the mechanical properties of timber beams, artificial or natural fibre reinforcement may be used. Over time, structural members are subjected to constant and varying loads, chemical and biological agents, and sometimes increased design loads. Consequently, the structure may no longer maintain its initial design strength, necessitating repair or reinforcement. One method of improving the load-bearing capacity of damaged timber structural elements is to replace the damaged sections or use reinforcement, including composite reinforcement, which enhances the mechanical properties of these structural elements. Unfortunately, various restrictions may be encountered when replacing these elements due to high costs, environmental impact, or the incompatibility of the required timber species. These factors necessitate the use of alternative methods, such as FRP (Fibre Reinforced Polymers) materials [1, 2].

It should be noted that glued laminated timber beams may have natural defects, such as knots or slanting fibres, which reduce mechanical properties [1, 3]. Fibre composites are increasingly being used in the repair of structural beams due to their high corrosion resistance, strength, and straightforward application technique [4]. In recent years, considerable research has been conducted using carbon, aramid, or glass fibres to reinforce wooden or glued beams. However, the use of basalt fibres to reinforce timber structural elements is not very popular.

Bonding mats to the side of the element is also a solution, based on analogous methods commonly used in reinforced concrete structures. For such reinforced concrete structures, many proven algorithms exist for determining the effectiveness of the reinforcement. However, in the case of wooden structures, this issue is rarely addressed and is rather poorly described in European literature. Therefore, this article proposes a calculation method based on American standards PCF-5100 and PCF-6046, which are the only standards addressing the issue of strengthening wooden (glued) structures with fibre composites. These standards present methods for determining load capacity and stiffness for elements reinforced during production, such as wooden beams of glued laminated timber with reinforcement in the tensile fibres zone or in both the tensile and compressive fibres zones. This paper additionally proposes a shortened calculation algorithm for determining the load capacity of timber beams reinforced with fibre composites, including basalt mats.

2. Description of the test, the reinforcement method and the materials used

Tests were carried out using reinforcement made from BFRP mats glued to the underside of the beam along its entire length. The glued beams were from Pinus Sylvestris coniferous timber, strength sorted using the visual method [5]. The lumber with the highest mechanical properties was placed at the top and bottom of the glued beam (KS - medium quality grade), where the bending stresses (both compressive and tensile) are the highest, while the lumber with the lowest mechanical properties (KG - lower quality grade) was placed in the middle layers. In contrast, the basalt mats provided surface reinforcement on the underside of the beam along its entire length.

The epoxy adhesive for bonding the reinforcement to the wood was mixed by hand at a ratio of 100:35 (LG 815 epoxy resin and HG 353 hardener). After curing, the mixture achieved a flexural strength of 110 ÷ 120 MPa and a modulus of elasticity of 2700 ÷ 3300 MPa. The values of the elastic modulus and final deformation of the BFRP mats used were E = 55 GPa and εu = 28%, respectively. There were nine beams tested without reinforcement; the remaining beams were reinforced with unidirectional BFRP mats. The beams were reinforced with unidirectional basalt fibres arranged in two layers of 380±25 g/m^2 (BT11/1) glued to the bottom of the timber beams. The BFRP fibre was bonded to an epoxy resin matrix.

The tests were carried out on beam elements with a length of 3.65 m, a cross section of approximately 82x162 mm, and a support span of 3.0 m. The mechanical properties of the reinforced glulam beams were determined in accordance with PN-EN 408+A1:2012 [6]. In the study, 18 beams were tested, nine of which were unreinforced.

3. Experimental results

Glued laminated timber beams often deteriorate in the tension zone in places where there are knots, defects, or glued joints. Therefore, glulam is mainly reinforced in the tension zone to increase bending strength and stiffness.

Based on the obtained results, it was found that for five glued laminated beams reinforced with BFRP mats, there was an increase of 5 to 8% in displacements compared to unreinforced beams. Additionally, the experimental study showed that beams strengthened with BFRP mats exhibited an increase in ultimate load of up to 19%. The unreinforced beams primarily failed in the elastic region due to defects in the tension zone of the lower lamellas. In contrast, the glued laminated timber beams reinforced with basalt mats demonstrated significant ductility. This ductility in the reinforced beams depends on the quality of the lower timber layers.

Table 1 shows the obtained results of failure forces and bending moments for the given groups of specimens.

Table 1: Destructive force value and corresponding bending moment.

Model	$F_{max,(mean)}$ [kN]	M_{max} [kNm]	Model	$F_{max,(mean)}$ [kN]	M_{max} [kNm]
NWZ1	38.04	15.21	WZB1	48.53	19.25
NWZ2	36.21	14.38	WZB2	50.78	23.35
NWZ3	44.52	19.55	WZB3	55.56	26.13
Mean	39.59	16.38	Mean	51.62	22.91
Standard deviation	4.37	2.78	Standard deviation	3.59	3.46

4. Computational analysis

The design analysis was performed using the standards PCF-5100 [7] and PCF-6046 [8], which provide guidelines for the use of glass, aramid, or carbon fibre. These standards stipulate that the minimum percentage of reinforcement should be no less than 0.25%, while the maximum percentage of reinforcement should be no more than 2% for single reinforcement and 4% for double reinforcement.

For comparative verification, the mean values of the maximum bending moments M_{max} and the tensile stresses of the basalt mat obtained in the tests for the given models of unreinforced (NWZ) and reinforced (WZB) beams were compared with the value of the maximum mean moments M_a and the tensile stresses of the basalt mat obtained in the theoretical analysis. A satisfactory convergence of the results was obtained.

Table 2 compares the experimental and theoretical results, demonstrating the alignment between the observed performance of the reinforced beams and the predictions made using the design standards.

Table 2. Values of bending moments, tensile stresses of basalt mat obtained from experimental and theoretical analysis.

Model	M_{max} [kNm]	M_a [kNm]	σ_{BFRP} [MPa]	σ_a [MPa]
NWZ (Mean)	16.38	19.21	_	_
WZB (Mean)	22.91	26.48	61.35	69.22

5. Conclusions

This paper presents the results of experimental tests on glued laminated timber beams reinforced with BFRP basalt mats, alongside a theoretical analysis. Based on the analysis of the experimental and theoretical bending test results, the following conclusions are drawn:

- Basalt fibre mats applied to timber elements with low mechanical properties are an effective reinforcement method.
- They can be used as a reinforcing material in wooden beams, particularly in the tensile zones of beams with defects. This was confirmed in experimental studies, where reinforced glued beams were found to behave more uniformly than unreinforced beams, improving design properties.
- The tests revealed a significant increase in load-bearing capacity (approximately several percent), while stiffness values were slightly higher.
- The ease of implementation means that the use of basalt mats allows for simple restoration of structures, enabling higher permissible loads or restoring original strengths.
- The theoretical analysis has shown that using Uniform Building Code 6046 is justified when reinforcing flexural wooden beams with basalt mats. Comparative verification has resulted in satisfactory convergence in both experimental and theoretical studies.

The article presents the results of research on strengthening glued laminated timber beams with basalt fibre mats. However, the conclusions of the research are also applicable to strengthening solid wood elements.

References

1. Mascia N.T., Donadon B. F., Vilela R.: Glued Laminated Timber Beams Reinforced With Sisal Fibres, International Journal of Structural and Civil Engineering Research Vol. 8, No. 4, November 2019.
2. Fiorelli J., Dias A. A.: Fiberglass-reinforced glulam beams: mechanical properties and theoretical model, Materials Research, São Carlos-SP, vol. 9, no. 3, pp. 263-269, 2006.
3. Bodig J., Jayne B. A.: Mechanics of Wood and Wood Composites, Van Nostrand, New York, 1982.
4. Marques F. A. Z., Silva C. E. G., Christoforo A. L., Lahr F. A. R., Panzera T. H., Canto R. B.: Influence of Portland cement addition in the physical and mechanical properties of epoxy resin, Advanced Materials Research, Zurich, v. 1088, p. 411-414, 2015.
5. Softwood Structural Sawn Timber Sorted Using Strength Methods, PN-D-94021:2013-10, Polish Committee for Standardization: Warsaw, Poland, 2013.
6. Timber Structures—Structural Timber and Glued Laminated Timber—Determination of Some Physical and Mechanical Properties, PN-EN 408+A1:2012, Polish Committee for Standardization: Warsaw, Poland, 2012.
7. US standard ICBO/Uniform Building Code 5100.
8. US standard ICBO/Uniform Building Code 6046.

ANALYSIS OF CONSTRUCTION DISASTER IN POLAND, IN THE YEARS 2004 - 2019

WOJCIECH DROZD[1], *wojciech.drozd@pk.edu.pl*

[1]Politechnika Krakowska, Wydział Inżynierii Lądowej, Katedra Zarządzania w Budownictwie

Keywords: construction disasters, analysis, Poland

Abstract: The article is an attempt to analyze the construction disasters that took place in Poland, in the years 2004 - 2019. Using a comparative analysis, they were juxtaposed causes, places, scale and consequences of disasters. Certain regularities were observed, thanks to which conclusions were drawn, allowing to minimize the risk of construction disasters in the future.

1. Introduction

The reliability and operational safety of building structures are influenced by a large number of factors, as the processes of designing, constructing, and operating a building are very complex. Given the multitude of factors that directly affect the safety of a building, it can be stated with certainty that it is impossible to completely eliminate the possibility of a construction disaster. While the risk of such occurrences can be minimized, full reliability can never be achieved.

Collecting information about past construction disasters is highly useful. Analyzing these data allows for a better assessment of building conditions and verification of the quality of solutions used in construction. This, in turn, increases the safety of structures by avoiding previously committed mistakes in the future. Similar statistics and analyses are conducted in many countries. Thanks to such research, it is possible to improve the processes of designing, executing, and operating buildings. The collected data allows for improvements and amendments to building codes, design standards, and rules for construction and acceptance of construction works.

2. Basic information about construction disasters

The construction disaster, in accordance with Article 73 of the Construction Law [1], is defined as "unintentional, violent destruction of a building object or its part, as well as structural elements of scaffolding, elements of forming devices, sheet piling, and excavation lining." Thus, a construction disaster should be understood as the total or partial destruction of a permanent or temporary building, an engineering or industrial building, or a technical device.

Between 2004 and 2019, 6,627 construction disaster cases were recorded in Poland. Events that are not considered construction disasters according to Article 73 of the Construction Law include:

- Damage to elements built into the structure that are suitable for repair or replacement;
- Damage or destruction of construction equipment related to buildings;
- Installation failures.

It is important to emphasize that a construction disaster must be violent, meaning sudden and unexpected. Gradual destruction of a construction site, occurring over time due to long-term neglect, cannot be classified as a construction disaster.

The investigation into the causes of disasters is conducted by the locally competent construction supervision authority. Initially, this is always the authority of the first instance, i.e., the Poviat Building Supervision Inspectorate [1] (Art. 76 section 1 point 1 in connection with Art. 74 of the Building Law). The proceedings may later be taken over by a higher authority, such as the Voivodship Inspectorate of Construction Supervision and the Chief Supervisory Office of Construction (Art. 77 of the Act).

3. Analysis of construction disasters in Poland in the years 2004-2019

Figure 1 shows the number of construction disasters in Poland from 2004 to 2019, as provided by the General Office of Construction Supervision.

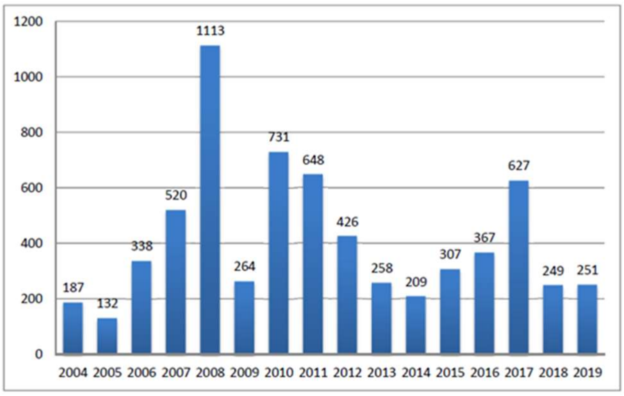

Fig. 1. The number of disasters in Poland. Source: own study based on [2]

Looking only at the statistical data on the number of disasters, as shown in Fig. 1, it is difficult to draw clear conclusions because there is no evident downward, upward, or stabilization trend. The years 2004 and 2005 mark the beginning of Poland's membership in the European Union. During these years, foreign capital began flowing into Poland, which had a significant impact on the economy, particularly the construction sector. Funding for entrepreneurs, municipalities, and farmers led to a rapid increase in the number of industrial facilities, roads, agricultural, and residential structures being erected. The increased amount of construction work is associated with a higher risk of construction disasters.

References

1. Ustawa z dnia 7 lipca 1994 r. - Prawo budowlane (Dz.U.2020.1333 t.j.).
2. Główny Urząd Nadzoru budowlanego: Katastrofy budowlane w 2004 - 2019 roku, Warszawa, 2005 – 2020.
3. https: // dziennikpolski24.pl/zerwane-dachy-na-domach-i-kaplicy-cmentamej-wichura-szalała-w-powiecie-krakowskim/ar/13952431.
4. Referat Ochrony Przed Powodzią w Wydziale Bezpieczeństwa i Zarządzania Kryzysowego Urzędu Miasta Krakowa: Raport po powodzi z maja i czerwca 2010 r. Kraków, 2010.

THE CAUSES OF PARTITION WALLS DAMAGE IN RECENTLY COMPLETED BUILDING

PIOTR DYBEŁ[1], *dybel@agh.edu.pl*
MILENA KUCHARSKA[1]

[1]AGH Akademia Górniczo-Hutnicza

Keywords: cracks, partition walls, non-load-bearing walls, active deflections, laboratory and office building, excessive slab deflections, design errors

1. Introduction

Cracking of partition walls is one of the most common defects in buildings and can be caused by design, execution, and exploitation factors. Statistically [1], approximately 60-70% of non-load-bearing wall cracks in central and eastern Europe occur due to the deformation of structural support members. This issue has often been neglected in structural analyses and calculations of load-bearing systems of designed structures [1-3].

One approach to protecting non-structural and finishing elements is to limit the active deflection of flexural members, i.e., the difference between the total deflection and the deflection determined directly after the completion of the support installation and the incorporation of the non-load-bearing element, such as partition walls. EN 1992:2008 [3] states that the deflection of the structure should not exceed the limits that can be accommodated by other connected elements, and that this limitation may be required to ensure the proper functioning of machinery or apparatus supported by the structure.

In this extended abstract, an example of a laboratory and office building is presented, in which insufficient deflection limits and design simplifications led to extensive cracks in the partition walls of passageways and rooms.

2. Building description

The object under analysis is a five-storey building constructed between 2010 and 2012 using monolithic post-and-beam construction technology. The structure is situated on a rectangular plan with added avant-corps on the southern and eastern sides. The basic load-bearing structure consists of three-nave reinforced concrete frames on which reinforced concrete slabs are placed.

All reinforced concrete structural elements of the building (floor slabs, beams, columns, foundations) were made of C25/30 concrete. The main reinforcement was provided by AIIIN (B500 SP) steel. The masonry walls were made of Porotherm blocks, while the partition walls on the 2nd and 3rd floors were made of 18 cm thick autoclaved aerated concrete blocks.

3. Damage description

Damage to the partition walls in the building under investigation was observed shortly after the facility was commissioned. The cracks occurred only within the second and third floors of the building. Regarding the main structural elements of the building, no alarming phenomena were found that could indicate improper functioning.

The survey of the partition wall cracking indicated that most of the cracks had a typical pattern related to the excessive deflection of the wall-supporting structure (Figure 1). The course of cracks in the partition walls was heterogeneous, with both vertical cracks and cracks with distinct horizontal and diagonal courses observed. The horizontal cracks usually passed through the bracket welds, whereas the diagonal cracks ran along the bracket and butt welds or through the masonry elements.

The most pronounced cracks were observed in the partition walls of the rooms and the hallway located above the lecture hall (Figure 2). The crack development in this area ranged from 0.9 to 2.4 mm. The remaining observed crack widths reached 0.3 to 0.6 mm.

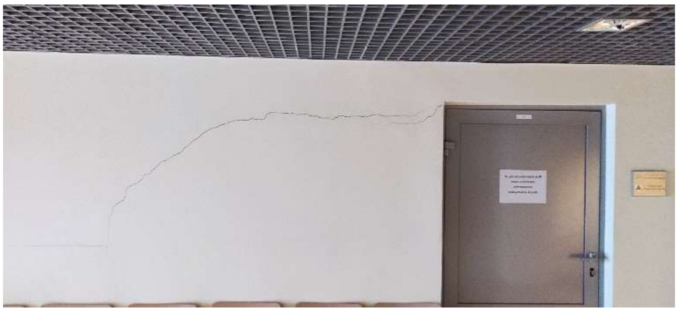

Fig. 1. A typical course of partition wall cracking

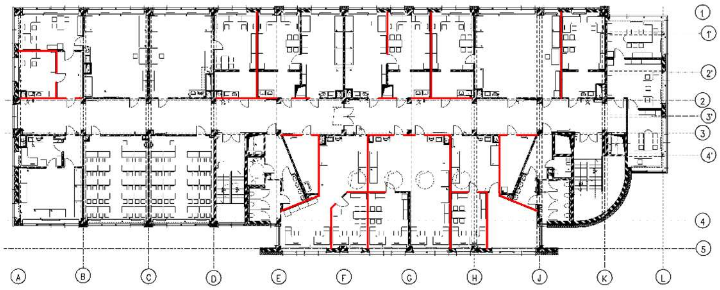

Fig. 2. Second-floor plan with an indication of cracked walls

A certain regularity in the location of partition wall cracks can be distinguished within the examined floors of the building:

- The most extensive cracking occurred in the area of axes F, G, and H, directly above the lecture hall. The load-bearing system in this part of the building is characterized by the longest spans of construction elements.
- Cracks in transverse partition walls (parallel to the load-bearing frames) appeared when they rested directly on the slabs. Cracking is practically eliminated when transverse walls are supported on beams.
- Cracking of corridor walls was observed in segments connected with transverse partition walls supported on slabs.

In addition, deflection measurements were conducted on selected structural elements that provided support for the cracked partition walls and were easily accessible. The deflection of the bottom surface of unfinished structural elements of the second floor was recorded. The results showed that at that time, the deflections of structural elements had not exceeded the limit value of 1/250 of the span relative to the supports, according to PN-EN 1992:2008 [3]. Nevertheless, it should be noted that in the case of the unidirectional reinforced concrete slabs, the value of the maximum deflection relative to supports was close to the limit value. Deflection values in the range of 1/255 to 1/290 of the span were registered.

The measurements of deflection of structural elements also revealed the occurrence of displacement of columns in the F and H axes relative to the column in the G axis at the level of the 2nd-floor ceiling. The frames in the F and H axes at the level of the ground floor and 1st floor do not contain the columns on axis 3, due to the location of the lecture hall at these levels. The columns in question are supported by joists located in the ceiling above the first floor. Consequently, the measurements indicated the influence of deflection of these joists on the deformation of the 2nd- and 3rd-floor structures within the lecture hall.

4. Structural analysis of the building

A spatial calculation model for structural and deformation analysis was developed in Autodesk Robot Structural Analysis 2013. The structure was modeled using beam and shell elements forming the spatial frame and floor systems. The load specification was adopted according to the structural design. The calculations included interaction with partition walls in the form of a linear load where they occur.

The structural analysis indicated that the ultimate limit states were not exceeded in the main structural elements of the building. Based on the calculations, it can be estimated that the values of active deflection for the ceilings of the 1st and 2nd floors in relation to non-deformable supports range from 1.2 to 2.3 cm. Therefore, the obtained values exceed the permissible active deflections determined based on EN 1992:2008 [3] and ISO 4356 [4]. The distributions and values of total deflections from long-term loads received in the numerical calculations are consistent with the measurements of actual deflections of structural members, as well as with control analytical calculations of selected structural elements.

5. The cause analysis of partition walls cracking

The direct cause of the partition walls' cracking on the 2nd and 3rd floors was the increment of deflection of floors supporting the partition walls, which occurred after the structure's completion. The values of the active deflection obtained for the ceilings of the 1st and 2nd floors significantly exceeded the permissible shape deformation angle for walls made of autoclaved aerated concrete. It should also be noted that the adopted static system within the lecture hall additionally intensified the described reason for partition wall cracking. The increase in deflection of the lecture hall ceiling joists in the F and H axes, due to rheological phenomena, resulted in the displacement of the structural elements of the 2nd and 3rd floors.

Moreover, other design errors were found, such as the application of a substitute impact of load from partition walls despite their arrangement perpendicular to the ceiling span, or the underestimation of load from suspended installations.

Additional factors affecting the cracking of the partition walls include the lack of appropriate technological guidelines in the design documentation for the execution of partition walls on ceilings with considerable spans, and the use of a crack-prone material - autoclaved aerated concrete - for partition walls. The influence of further factors related to the construction process is also not excluded.

6. Summary

Damage to partition walls commonly occurs in newly erected buildings during the initial period of their use. This cracking is mostly related to the deformation of structural elements supporting these walls. The standards concerning the structures on which the partition walls are placed provide various permissible values for their deflection. Moreover, the standard guidelines do not take into account the influence of the location of openings in relation to the length of the walls, the conditions of the ceiling support, and the conditions of the wall connection with surrounding structures on their resistance to cracking. Therefore, it is advisable to conduct research on the behavior of partition walls located on vulnerable ceilings and to specify standard guidelines for this issue. Doing so will make it possible to eliminate damage to partition walls in newly designed buildings.

The results of the investigations in this analysis have led to recommendations for the repair of cracks in partition walls. However, it should be emphasized that no repair technology provides a full guarantee that cracks in damaged walls will not reappear.

References

1. Kania T, Derkach V, Nowak R.: Testing crack resistance of non-load-bearing ceramic walls with door openings. Materials, nr 14/2021.
2. Wesołowski M.: Building failures due to faulty design solutions. Przegląd Budowlany, nr 6/2017. (in Polish)
3. Szulc J.: Active deflections of RC slabs and damage to adjacent elements. Materiały budowlane, nr 4/2013. (in Polish)
4. EN 1992-1-1. Design of concrete structures - Part 1-1: General rules and rules for buildings., Belgium 2016.

ISO 4356: Bases for the design of structures. Deformations of buildings at the serviceability limit states, 1977.

CONSEQUENCES OF LACK OF APPROPRIATE PROTECTION OF HISTORICAL BUILDINGS DURING THE OPERATING SHUTDOWN

LESŁAW HEBDA[1]
MICHAŁ CZESZYŃSKI[2]
DAMIAN NIKODEM[3], *damian.nikodem@barg.pl*

[1]Doradca Techniczny Dorota Hebda, ul. Albatrosów 15f/11, 05-500 Piaseczno, Poland
[2]BARG Centrum Sp. z o.o., ul. Kazimierza Kamińskiego 28, 05-850 Ożarów Mazowiecki, Poland
[3]BARG Zachód Sp. z o.o., ul. Kazimierza Drewnowskiego 2B, 61-248 Poznań, Poland

Keywords: historic buildings, biological corrosion, diagnostics of building objects, humidity tests, construction mycology, structure degradation, masonry structures, strength tests

Abstract: The article presents the most common damage to the structure of historic buildings caused by natural factors. The authors of the text indicate how important it is to properly maintain and protect historic buildings in order to limit the degradation of the structure. On the example of two objects entered in the register of monuments, an analysis of their technical condition was carried out, along with an indication of the causes of the damage. On this basis, the authors show how large losses were incurred in the historic matter in a relatively short time.

1. Introduction

In Poland, at the turn of the 20th and 21st centuries and the early years of this century, many buildings and structures appeared that, as a result of ongoing economic processes, lost their owners, or the owners did not have the financial resources to maintain them or ideas for their development. Often, these buildings and facilities have been or are still left without proper protection. They are devastated by human activity as well as atmospheric factors. In the technical assessments of their condition, tests for moisture, salinity, and the strength of the materials from which they were made are usually conducted. The degree of freeze corrosion and other chemical degradation is also assessed. Damage caused by nature, especially vegetation, is treated marginally, as if in retaliation against humans for the invasion and brutal occupation of its territory.

2. New Weaving Mill-Nowa Tkalnia

The first example analyzed in the article is the former Uniotex plant in Łódź, Poland -"New Weaving Mill-Nowa Tkalnia." The complex of industrial facilities was established in 1898 and was part of Charles Scheibler's cotton empire. The author of the design of the complex was Paweł Rubensahm. At that time, the Nowa Tkalnia facility occupied an area of 3 hectares.

Fig. 1. Archival plan of an industrial complex in Łódź [1]

The complex of buildings in Nowa Tkalnia comprised mainly rows of one-story buildings. The exceptions were buildings located on the north and south sides, which were erected as two-story structures. The weaving building has a characteristic raised central part. In this zone, various transformed forms taken from the early Renaissance can be found. Over the years, some of the buildings have been rebuilt, with an additional story added [1].

After World War II, the Nowa Tkalnia complex changed its name several times, a fact that the inhabitants of Łódź undoubtedly remember, giving this place a certain symbolic status. Following the Pope's visit, the complex operated under the local name of "papal weaving mill."

Since 1989, the building has changed owners several times, and its detailed history is not well documented. It is known that by the end of the first decade of this century, the building was empty. During this time, the roof collapsed. In 2012, there was a large fire in the Engine Room building, during which the roof and the historic ceiling were completely destroyed.

It seemed that including the entire building complex in the register of monuments in 2012 would improve its technical well-being, but this did not happen. It was not until 2017, after the property was taken over by a new owner, that conceptual work on the development of this area began.

3. Palace near Poznań

The second example analyzed in the article is a palace located in a village near Poznań, Poland. The facility is situated in the central part of a historic manor park. The construction of the building dates back to the early 20th century, utilizing the walls of an older building from the 17th century.

The palace was expanded and renovated many times. In the 1960s, it housed a student center. The last changes in appearance took place at the turn of the 20th and 21st centuries, when improperly carried out renovations resulted in the destruction of the architectural decoration of the facade. The last user of the facility was the management of the State Farm. The building has not been used since 2009.

Fig. 2. General view of the palace - photo taken in 2021

During the diagnostic work on these two building complexes, it was found that the brick walls did not contain a high concentration of harmful building salts. Their dampness varies but does not exceed the limit of a "moderately moist wall" according to the WTA classification. Harmful building salts are present at most in average concentrations. The strength of the brick in the walls turned out to be very diversified, influenced not only by corrosion processes but also likely by the variability in quality during the construction stage.

The biggest surprise was the attack of vegetation on the abandoned and devastated walls of the former industrial buildings. Initial examination revealed a typical wall covering with vegetation. However, what was surprising was the scale of damage caused by the root systems. In some places, the wall was delaminated and detached due to the roots (see Figures 3 and 4).

a)

b)

Fig. 3. Example of demages: a) the root system of plants inside the building, b) degradation of the wall of the brick weaving mill in Łódź

Fig 4. Example of demages – The plants existed in the roof of the palace building near to Poznań

4. Summary

The examples shown above demonstrate that the enemy of buildings erected by humans and left unattended is not only the devastation and destructive impact of weather conditions but also the "retaliatory" action of animate nature. This occurs both in rural areas, where nature is dominant, and in the centers of large urban agglomerations. This impact of nature must be taken into account when planning the renovation of old buildings that have gone through a period of abandonment. Sometimes, a small investment in appropriate protection of the building against extended breaks in its operation can save future owners and investors a significant amount and extend the longevity of the renovation.

References

1. Technical opinion on the condition of the existing buildings of the Nowa Tkalnia building complex in Łódź at ul. Tymienieckiego 3-7 and Milionowa 2/4. WIP Projekt Sp. z o.o., November 2018
2. Concept for the construction project "Nowa Tkalnia building complex, Łódź" Biuro Projektowe - Architektura - BroadwayMalyanBM, 21/05/2019.
3. Documentation of conservation research on the construction team of the "new weaving plant" of the joint-stock company near Scheibler. Katarzyna Przesmycka - restorer of architectural details and elements, Łódź 2018.

4. Conservator's opinion on the concept of land development and development of Nowa Tkalnia - decision WUOZ-ZN.5183.1133.2018.AWJ, Łódź Provincial Conservator of Monuments, Łódź, 5 July 2019.
5. Construction project for renovation, reconstruction and extension of a residential building - palace in Przylepki, commune of Brodnica, plot No. 8/3. Design unit: Pracownia Architektury "GANDALF" Przemysław Matysiak, ul. Szewska 5, 60-401 Poznań, Poznań, September 2009
6. Manor house in Przylepki near Mosina. Construction inventory along with the technical opinion of the building, LT SERVICE Sp. z o.o., 5 Andersa Square, 61-894 Poznań, 2009.
7. Collective work edited by J. Poszny and J. Krysia, Protection of buildings against biological corrosion, Arkady, Warsaw, 2001.
8. Skowroński W., Piotrowska M., Matkowski Z., Magott C., Kania T., Aspects of protecting buildings against biological corrosion and fire, Series: PSMB Monographs, Wrocław, 2019
9. Diagnostics of buildings. Principles of performing experiments, edited by Leonard Runkiewicz, Wydawnictwo Naukowe PWN SA, Warsaw 2020.

CAUSES OF DAMAGES OF CANTILEVER BALCONIES AND GALLERIES – ANALYSIS OF CASES WITH SAFETY RISK

PIOTR MATYSEK[1], *piotr.matysek@pk.edu.pl*
KRZYSZTOF KOZIŃSKI[2]

[1,2]Cracow University of Technology

Keywords: cantilever balconies, damages, design faults, poor workmanship

1. Introduction

Damage to cantilever balconies and galleries occurs in buildings erected several decades or even more than a hundred years ago, as well as in modern facilities [1-5]. These damages are of various natures and depend on many factors. The basic factors influencing the condition of balconies and galleries include the period and degree of exposure to the adverse effects of the external environment, the type of materials and technologies used in their construction, the quality of workmanship, and the frequency and manner of past renovation works.

This paper presents examples of balconies and galleries where the technical condition posed a safety risk and required immediate intervention for repair and renovation. The presented examples constitute a small part of expert studies carried out by the authors, which concerned the assessment of the technical condition of balconies and galleries. The examples were selected to illustrate the problems as widely as possible, including balconies and galleries in a tenement house, prefabricated concrete buildings, as well as buildings with a monolithic reinforced concrete structure and masonry structure, which are currently dominant in construction.

In addition to analyzing the causes of damage to balconies and galleries, the paper also provides suggested methods of repair.

2. Research on balconies and galleries - case report

The balconies and galleries presented in this chapter are located in five buildings. In all cases, the technical conditions of the balconies and galleries required protective and repair measures.

The galleries with a steel and timber structure in a building erected at the beginning of the 20th century were in the worst technical condition (gallery G1 in Fig. 1). Due to the poor technical condition of the timber elements (beams and balustrades), it was recommended to exclude them from use and proceed with immediate repairs. A new structural system was proposed. For conservation reasons, some original elements of the balconies, such as steel cantilever beams and steel elements of balustrades, have been preserved.

a)

b)

Fig. 1. Technical condition of galleries with a) steel and b) timber structure (G1)

Many damages were also found in galleries with a steel and concrete structure located in a service and commercial building (gallery G2 in Fig. 2). The pavilion was erected in the late 1970s. The damages affected both the balcony structure and the top layers. Based on in-situ tests and control calculations, it was recommended to reduce the service loads and ultimately perform a general renovation of the galleries. The proposed solution included strengthening the balcony structure and replacing the balcony layers.

a) b)

Fig. 2. Damages to galleries with a) steel and b) concrete structures (G2)

The cantilever balconies in residential buildings that had been in use for over 40 years were also in poor technical condition (balconies B1 in Fig. 3). These balconies were made as prefabricated reinforced concrete elements. In in-situ tests, no waterproofing layers were found. The temporary renovation of balconies carried out in the past was limited to the implementation of new top layers on the existing layers, which led to an additional load on the structure. It was recommended to remove all existing top layers and install new ones in accordance with modern materials and technological systems. Repair of the reinforced concrete slabs of the balconies was also recommended. Until the renovation is carried out, the permissible service load on the balconies has been limited.

Fig. 3. View of the balconies in residential building with prefabricated structure (B1)

The prefabricated balcony slabs were also used in a building erected in the 1970s using the prefabricated construction system WUF-T/67. Tests of these balconies showed numerous damages to both the reinforced concrete balcony slabs and the layers on the balconies (balconies B2 in Fig. 4). The steel balustrades were also subject to corrosion. Based on the research, it was found that there was no waterproofing on the balconies. The lack of waterproofing and the poor condition of the flashings were the reasons for water stains and corrosion damage to the balconies.

Renovation was recommended, consisting of removing the balustrades and all layers above and below the prefabricated reinforced concrete slabs, and then installing new balustrades and layers.

Fig. 4. Damages to prefabricated balconies (B2)

Extensive damages also occurred in the balconies of a building that had been in use for only a few years. These balconies were constructed as monolithic reinforced concrete cantilever slabs. The damages included issues with the top layers, fronts of the balconies, and corrosion of the steel balustrades (balconies B3 in Fig. 5).

Leaks were visible on the underside of the balconies. During the tests, poor workmanship was identified. The balconies were not constructed in accordance with the design specifications. The waterproofing and flashings were improperly executed, which resulted in material deterioration and detachment of the top layers. Consequently, the balconies were qualified for renovation after only several years of use.

Fig. 5. Damages to balconies in building used for 6 years (B2)

3. Analysis of research results

The case review given in Chapter 2 shows that the problem of poor technical conditions of balconies and galleries affects not only buildings in use for several decades but also new facilities. In buildings that have been used for a long time, the poor technical condition of balconies and galleries is usually due to poor-quality materials and neglect of renovation. Damage to balconies and galleries mainly concerns the top layers. Strong deterioration of these layers and the lack of timely repairs ultimately lead to the destruction of structural elements as well.

In buildings used for a short time, the causes of damage are usually design faults and/or poor workmanship. Improperly installed waterproofing (or lack thereof) results in the dampness of the materials and stains visible on the underside of gallery and balcony slabs after a short time. The destruction processes of materials are also intensified by their strong moisture content.

Renovations of damaged balconies should be preceded by appropriate research and the development of a repair project. In-situ tests are of fundamental importance in assessing the technical condition of balconies. Minor destructive tests, supplemented by non-destructive tests and laboratory tests of materials collected from structures, enable the diagnosis of the causes of damage to balconies and galleries and the planning of their repair and strengthening.

The research on balconies should have a wide scope because the systems of the layers on balconies, even in the same building, may differ. This is due to the fact that apartment owners themselves carry out finishing work on the balconies. Many owners perform this type of work on their own, unaware of the phenomena and processes taking place on the balconies. The negative effects can be seen after a short time.

The cases presented in Chapter 2 show that damages to balconies can often result in the detachment of balcony top layers. Loose fragments of detached materials constitute a safety risk and should be immediately removed. Regular technical inspections and repairs are essential to limit the pre-failure conditions of balconies and galleries.

4. Summary

Cantilever balconies and galleries, due to their location in buildings, are particularly exposed to the adverse effects of environmental factors and the related processes of material destruction.

The cases presented in the paper show that the poor technical condition of balconies and galleries is most often caused by poor planning or workmanship. Additionally, improper use, lack of inspections, and lack of ongoing repairs contribute to their deterioration.

The pre-failure condition of balconies and galleries necessitates extensive renovation. It is often necessary to remove all top layers of the balcony or gallery and strengthen the structure. The costs of such works are very high, often exceeding the cost of constructing new elements.

References

1. Ślusarek J.: Ocena stanu materiałów, konstrukcji i izolacji tarasów i balkonów, XII Ogólnopolska Konferencja Warsztat Pracy Projektanta Konstrukcji. Ustroń 1999, tom I, cz. 2, s. 337-366.
2. Piekarczyk A., Starosolski W.: Uszkodzenia balkonów spowodowane wpływami termicznymi, XXIII Konferencja Naukowo-Techniczna Awarie Budowlane, Szczecin-Miedzyzdroje 2007, s.765-772.
3. Dębowski J., Radoń M.: Błędy projektowo-wykonawcze przyczyną uszkodzeń balkonów w budynkach systemowych, Czasopismo Techniczne 1/2011, str. 31-38.
4. Błaszczyński Z., Łowińska-Kluge A.: Trwałość balkonów i loggii - błędy projektowe i wykonawcze, Izolacje 7-8/2013.
5. Rokiel M.: Sposoby naprawy uszkodzeń okapu na tarasach i balkonach, Izolacje 4/2020.

SELECTED ASPECTS OF DIAGNOSTICS AND RENOVATION OF GREEN HISTORICAL OBJECTS

ELŻBIETA RADZISZEWSKA-ZIELINA[1], *elzbieta.radziszewska-zielina@pk.edu.pl*
MAŁGORZATA FEDORCZAK-CISAK[1], *malgorzata.fedorczak-cisak@pk.edu.pl*
TOMASZ STEIDL[2], *tomasz.steidl@polsl.pl*

[1]PolitechnikaKrakowska
[2]Politechnika Śląska

Abstract: The article presents selected aspects of diagnostics and renovation of historic sacred buildings, based on the example of two churches, one in the town of Rybna and the other in Skórc. Particular attention was paid to the damage caused by uncontrolled flow of heat and moisture through the building's partitions. The necessity to use modern computational methods in the analysis of design (possible) solutions in the field of heat-moisture issues has been demonstrated. It was also indicated that an indispensable element of the planning process of the renovation of sacred historic buildings has to take into account the opinion of the local community.

Keywords: sacred historic buildings, numerical analysis of design solutions, heat and humidity simulations, social aspect, survey research

1. Introduction

Renovation of elevations and insulation of walls in historic buildings requires the fulfillment of conservation requirements [1]. The problem of poor technical condition in historic buildings representing various construction solutions frequently affects their usability. This situation can only be improved by carrying out renovation and thermo-modernization works, tailored individually for each historic building. The algorithm for proper thermal diagnostics of historic buildings in the context of renovation activities is presented in [2].

There are few publications on specific renovation problems for historic sacred buildings, so it is worth expanding knowledge in this area through "in situ" research on sacred buildings, which should form the basis for selecting the scope of renovation works. An example of such a methodology is the research carried out in the 17th-century church in Sękowice [3]. In situ tests showed significant damage due to factors such as water and moisture. In sacred buildings, wall dampness causes many structural damages as well as the destruction of wall paintings [4].

Diagnostics of the condition and renovation of churches is an important and specific issue to ensure the comfort of the people staying inside. The aim of this article is to discuss selected aspects of diagnostics and renovation of historic sacred buildings, with a focus on scientific, technical, and social interests.

The research was carried out for two buildings, churches in Rybna and Skórzec.

2. Characteristics of selected sacred buildings

In order to discuss the characteristic damages that occur in sacred objects, two buildings were selected for analysis, representing a similar style of architecture (Fig.1). Both buildings are separated by a distance of approximately 400 km, and share a similar cubature, time of erection, and a style that can be described as classicist. Initially built as wooden churches, they have been rebuilt and are now brick buildings with a wooden roof truss.


a)


b)

Fig. 1. a) Church in Rybna, b) The parish church in Skórzec

3. Damage to sacred buildings

The list of damages to the above-ground parts of the structures in Rybna and Skórzec is presented in Table 1. These damages were classified as aging-related, due to the long-term impact of environmental factors.

Table 1 List of damage to elements in the objects in Rybna and Skórzec

No. / Element	**The parish church in Rybna** Description of the damage	**The parish church in Skórzec** Description of the damage
1. Wooden roof structure	No visible damage. 	No damage. The elements damaged by biological corrosion were replaced during the last renovation.
2. Wooden structure of the ceiling	The ceiling beams are reinforced with steel. Locally damaged fragments were replaced. 	Minor scratches in the aisles visible from the inside. 
3. External walls from the inside	Strong dirt in places of leaks and local freezing of walls. 	Strong dirt - the wall surface freezes. 
4. Floors	Old, cracked and uneven floor to be completely replaced 	The floor has been completely renovated – replacement 

Figure 2 shows exemplary thermograms for wall fragments in the analyzed objects, on the left is the church in Rybna, on the right in Skórzec (newly erected wall - 2012)

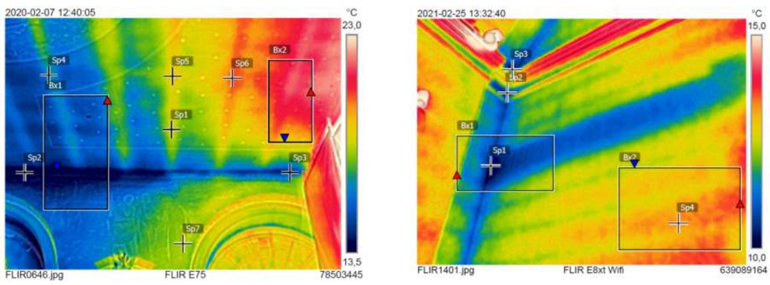

a) b)

Fig. 2. Thermograms of wall fragments with thermal damage

In the opinion of the authors, the thermal imaging analysis of sacred monuments should be supplemented with a numerical analysis of the damage to identify the cause of their occurrence. In both structures, there are clearly visible damages caused by the influence of groundwater and rainwater in the plinth band.

4. Selected aspects of the renovation process. Social participation

The authors propose that the social aspect, understood here as the participation of residents and believers in the process of making renovation decisions, should become a standard practice. This has not been common so far. Research in this area can be carried out in the form of a questionnaire or interview with the parish community.

As part of the research conducted, respondents were asked to rate the parameters related to the comfort of using the facility on a five-point scale from 1 (bad) to 5 (good). The worst assessment was for visual comfort (average rating 1.9), followed by respiratory comfort (average rating 2.7). In an open question further exploring their opinions, respondents pointed to observed problems such as feeling dampness and mold, walls requiring painting, and the need for renovations to the ceiling and chimney.

5. Recommended actions before renovation

The design of renovation activities should depend on several factors: the results of diagnostics and expert opinions on the condition of the structure; the results of historical and archaeological research carried out prior to the renovation decision; arrangements with the local conservator of monuments; the opinion of the local parish community; and the financial capacity of the investor.

6. Summary and conclusions

The number of sacred monuments in Poland, which are not necessarily class "0" monuments, can be estimated at least 5,000. The vast majority of them are in a technical condition that can be described as satisfactory, but requiring renovation measures on a larger or smaller scale. The factors that have a decisive impact on the destruction of structural and non-structural elements in these facilities include, primarily, the effect of water and moisture.

The use of modern computational methods in the selection of solutions, particularly regarding construction and thermal and humidity issues, is now an indispensable element of the renovation project for a historic sacred building. In the opinion of the authors, such a project should also take into account the opinions of parishioners regarding renovation activities, a practice which has not been widely adopted so far.

References

1. Nowogońska, B. Performance Characteristics of Buildings in the Assessment of Revitalization Needs. Civ. Environ. Eng. Reports 2019, 29, 119–127.
2. Orlik-Kożdoń B., Radziszewska-Zielina E., Fedorczak-Cisak M., Steidl T., Białkiewicz A., Żychowska M., Muzychak A., Historic Building Thermal Diagnostics Algorithm Presented for the Example of a Townhouse in Lviv, Energies 2020, 13, 5374.
3. Nowogońska, B. Consequences of improper renovation decisions in a 17th century half-timbered building. Sci. Rev. Eng. Environ. Sci. 2021, 29, 557–566.
4. Faella, G.; Frunzio, G.; Guadagnuolo, M.; Donadio, A.; Ferri, L. The Church of the Nativity in Bethlehem: Non-destructive tests for the structural knowledge. J. Cult. Herit. 2012, 13, e27–e41.

FAILURE AND CONSTRUCTION DISASTER IN TWO RENOVATED BUILDINGS

RADOSŁAW SEKUNDA[1], *r.sekunda@maz.piib.org.pl*
JACEK SZER[2],

[1]Mazovian District Chamber of Civil Engineers
[2]Lodz University of Technology, Faculty of Civil Engineering, Architecture and Environmental Engineering

Abstract: The article deals with the subject of construction failures occurring during renovation works and related to the reconstruction of construction structures. Two cases of construction failures resulting from faulty technology and organization of construction works have been described. The first case concerns a situation that occurred during renovation works of the roof panels in a used multi-family residential building. The second case is a construction disaster that occurred during construction works related to the reconstruction of a Leipzig type building. The study of both cases describes the situations and circumstances of the failure, shortened results of the research and recommended recovery proceedings.

Keywords: construction failure, construction disaster, renovation buildings, organization of works

1. Introduction

Construction failures occur both during the construction stage of buildings and throughout their use. A special case of construction failures (sometimes also disasters) is when they occur not because of improper use of the facilities, but because of the construction works carried out in them, such as renovation or reconstruction. In these cases, they are usually the result of the lack (or defect) of design documentation, faulty technology, and organization of construction works, or they result from sudden and random situations that are impossible to predict at the design and execution stage.

This article addresses the issue of building failures occurring in renovated and reconstructed construction structures. It will present cases where construction failures arose due to technological and organizational errors in connection with the execution of construction works (renovation, reconstruction).

In both cases, one of the authors of this publication was involved in expert work related to the described failures.

2. Construction failure resulting from a roof fire

The article presents a case of a fire of the roof covering on a multi-family residential building in Warsaw.

The aim of the expertise was to assess the technical condition of the building structure in the area affected by the fire and determine its impact on the technical condition of the entire facility. Additionally, the expertise aimed to assess the scope of works necessary to restore the building's condition in compliance with the law.

The part of the roof structure that caught fire was made of wood and reinforced concrete. The wooden roof truss, which includes purlins with a 14x14 cm cross-section, 8x18 cm rafters, and 14x14 cm wall plates, transfers the loads to a reinforced concrete frame structure consisting of purlins (binders) with a 25x30 cm cross-section and reinforced concrete columns supporting it. The roof load-bearing structure was based on the reinforced concrete ceiling of the highest storey of the building and its external walls. The roof was covered with tar paper.

The planned scope of the roof renovation works included detailed guidelines, the most important of which, from the point of view of the conducted analyses, were:

- Installing the OSB board covering with increased water resistance.
- Priming.
- Installing the base layer of SBS roofing felt mechanically attached to the substrate.
- Heat-welded SBS on the flat part of the roof, attics, and chimneys with asphalt roofing flashings.

On May 7, 2018, during renovation works related to the replacement of the roof covering of the building, a fire started, resulting in the destruction of the roof structure above the attic premises.

As a result of a visual inspection and own research in the period following the fire, the following were observed:

- There was significant damage to the roof covering and the wooden roof structure.
- Rooms of residential premises located at the level of the usable attic were heavily contaminated by elements of the structure and roofing, which ended up inside the building as a result of the fire.
- **Most importantly, construction works were performed inconsistently with the building permit design**. A significant deviation influencing the occurrence of the fire was the arbitrary change of the mechanical fastening of the base asphalt roofing (permit design solution) to welding of the base asphalt roofing to the OSB boards (Fig. 1).

Fig. 1. View of the weldable asphalt roofing on the primed OSB board (private photo)

Based on the conducted local inspections and the excavations made, it was decided that the roof truss, along with the entire roof covering, needed to be replaced.

Regarding the impact of the fire on the global structure of the building, since no damage was found indicating a threat to the safety of the structure or its use, only protective and maintenance works were recommended.

3. Construction disaster during the reconstruction of the Lepzig type building

The catastrophe took place in 2017 during the construction works related to the reconstruction of a Leipzig-type office building for the needs of one of the ZUS (Social Insurance Institution) branches in Warsaw. In connection with the disaster and the emergency condition of the structure, a technical expertise was commissioned to determine the method of securing the stability of the damaged rafters of the structural frames and temporarily protecting the entire structure of the building.

Fig. 2. View of the broken nod at the ceiling level of the 5th storey (axis 3 and front axis A)

The building was a six-storey office structure with six above-ground storeys and a total height of 26.6 meters. The building's development area was 930 square meters, and the usable area was 5,483 square meters.

On July 17, 2017, during construction works related to the removal of floor slabs, the steel structure of the building was damaged. The site manager assessed the degree of damage to the structure, classified the event as a construction disaster, and took actions in accordance with the law.

Tearing of the nodes (rafter-column) in the longitudinal direction along the A axis and in the axis 3 at the +5, +4, and +3 levels was found during the structural inspection. The joint was broken at the welded connection (the bolted joint showed no deformation) due to a vertical seam cut in the joint plate girder, with deformation and tearing off of the horizontal brace stabilizing the fastening of the plate girder of the node to the web of the column. From level +2 downwards in the discussed field, the joints appeared visually in good condition.

For the purposes of securing the stability of the damaged rafters in the structure's frames and enabling further diagnostics of the building structure, it was recommended to

- Assemble a cap on columns 2 and 3 in the A axis.
- Use hangers (C160) to support the roof rafters.
- Weld "stools" (L100) to secure the ceiling rafters above storeys +4 and +3.
- Use 20 mm diameter tie rods welded to the columns in axes 2, 3, 9, and 10. Ties should be adjustable with turnbuckles.
- Brace the structure in the transverse axes 2, 3, 9, and 10 using braces made of round pipes RO82.5x5.
- Dismantle floor slabs above level +5 in the discussed field.

The above recommendations were followed, enabling further and comprehensive diagnostics of the building structure's condition (including scanning of nodal welds) and other laboratory material tests. Finally, the building structure was completely dismantled.

4. Conclusions

Two cases of construction failures (catastrophes) described in this publication relate to situations where the permit design guidelines for technological and material solutions were ignored (the first case) or the organization of works, which has a significant impact on their implementation and safety, was not analyzed and thus not included in the design (second case). This clearly indicates the importance of planning and compliance with appropriate technology and organization of works. This factor is often underestimated, especially in renovation and construction. A lack of analysis in this area or ignoring permit design guidelines, combined with the lack of proper supervision, may lead to far-reaching consequences, or even a construction disaster. In the construction process, an important factor is compliance with construction technologies and procedures as well as reliable performance of works.

References

1. Sekunda R., Machnikowski M.: Ekspertyza techniczna dotycząca dachu budynku mieszkalnego wielorodzinnego zlokalizowanego przy ul. Kochanowskiego 31 w Warszawie, uszkodzonego w wyniku pożaru, z uwzględnieniem jego wpływu na stan techniczny całego obiektu, zgodnie z Postanowieniem PINB dla m.st. Warszawy nr III, Warszawa, 21.05.2018.
2. Tyczyński Z., Sekunda R., Machnikowski M., Szymczyk D.: Ekspertyza techniczna dotycząca sposobu zabezpieczenia stateczności uszkodzonych rygli ram konstrukcji oraz tymczasowego zabezpieczenia całej konstrukcji budynku typu Lipsk przy ul. Czerniakowskiej 16 w Warszawie, Warszawa, 02.08.2017.

POSSIBLE CAUSES OF CHAMPLAIN TOWER SOUTH CONDOMINIUM COLLAPSE IN SURFSIDE TOWN, FLORIDA

TOMASZ WAŚNIEWSKI[1], *tomasz.wasniewski@p.lodz.pl*
EWELINA KOŁODZIEJCZYK[1]

[1]Katedra Budownictwa Betonowego Politechniki Łódzkiej

Abstract: The article presents the course of the failure and partial disaster of the Champlain Towers South condominium located in Surfside, Florida. It introduces the function of the building and characterizes its main structural system. Based on available materials, it also discusses the technical condition of the building in the years leading up to the disaster. The main causes of the floor's failure can be attributed to insufficient punch-through resistance and severe corrosion of the reinforcement caused by years of water penetration deep into the floor structure due to leaky waterproof insulation. Weak reinforcement bonds at the plate-column floor nodes and connections between columns, as well as long-term structural weakening due to temperature changes, were reasons why a local failure triggered a progressive disaster.

Keywords: Progressive disaster, Surfside, Champlain Tower South, corrosion, punching shear

1. Introduction

Damage to a single structural element can lead to an extensive disaster and, consequently, even complete destruction of a building. The spread of a local failure to the entire structure is known as a progressive disaster and most often occurs in structures characterized by low ductility and a low level of ability to redistribute internal forces [1]. The type of construction and attention to details such as proper reinforcement overlaps and appropriately designed beams are crucial here.

The article presents the course of the partial progressive disaster of the Champlain Towers South condominium located in Surfside, Florida. Based on the analysis of technical documentation and photographic materials, an attempt was made to determine the possible causes of the disaster.

2. The course of disaster

On June 24, 2021, at 1:25 AM local time, a partial collapse occurred at the 12-story Champlain Towers South (CTS) condominium in Surfside, Florida. Figure 1 shows a photo of the building in use from 2015 and shortly after the tragedy. The destruction occurred at night, while residents were sleeping, resulting in a tragic death toll of 98 victims. The catastrophe was survived only by those who lived in the western part of the building and those from the eastern part who were awake before the disaster and managed to evacuate.

a) b)

Fig. 1. General view of the building a) in 2015. Source: [2] b) the day after the disaster. Source: [3]

Based on this footage from surveillance cameras, the course of the progressive disaster affecting the eastern part of the building can be traced. It can be divided into three stages, which are schematically illustrated in Figure 2.

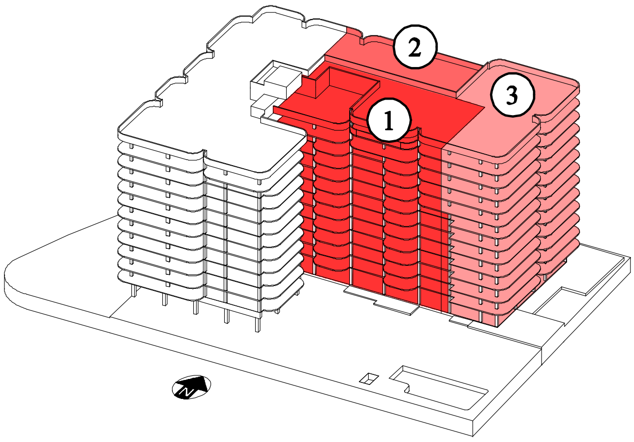

Fig. 2. Axonometric view of the building with the stages of the disaster marked

In the first stage, the central (southern) part of the eastern wing of the building collapsed. All floors above the ground level began to slide down together. There was no observed avalanche effect of the higher floors collapsing onto the lower ones, as was seen in the World Trade Center disaster, which would suggest a failure in the upper parts of the building. After a fraction of a second, the northern part of the building collapsed in the same manner (stage 2). Both parts—the central and northern—separated from the western wing and the remaining eastern section of the building. This was due to the building's design—the division occurred along the edges of the reinforced concrete shear walls. Unfortunately, the remaining eastern part of the building lost stability and collapsed shortly thereafter (stage 3). Similar to the central and northern parts, this section collapsed due to a failure in the lower part of the structure.

The central and northern parts of the western wing collapsed vertically. Additionally, the western section of the building tilted towards the south.

3. Building's function

The Champlain Towers South (CTS) condominium was constructed at the turn of the 1970s and 1980s [4]. It was located in the town of Surfside, situated on a peninsula in the Biscayne Bay area of Florida. The building was part of a series of attractive condominiums built along the coastal strip of the Atlantic Ocean.

The building had 13 stories—1 underground and 12 above ground. The underground portion entirely comprised a garage. Its layout was trapezoidal, directly resulting from the geometry of the plot. The length of the underground part of the building was 95 meters, and its width was 60 meters. An axonometric view of this level is shown in Figure 3. There was one two-way entrance to the underground garage from the north side.

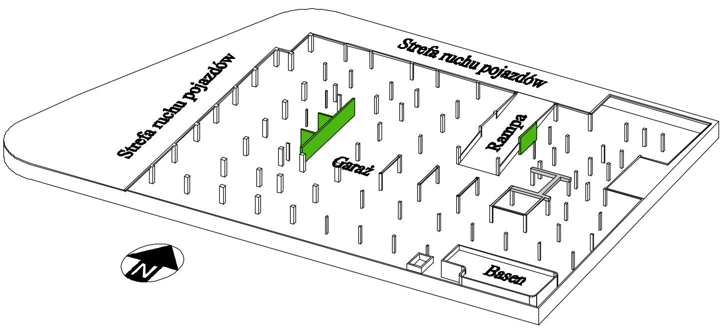

Fig. 3. Axonometric view of the underground part

The floor plan of the above-ground levels of the building was shaped like an "L". The building was 65 meters long and 50 meters wide. It had 12 above-ground floors, with 9 of them being repetitive. The ground floor housed a driveway, an open parking area, reception, technical rooms, a gym, and apartments. Also, on the ground level, but outside the outline of the above-ground part, there was a pool area with a pool located in the southeast corner.

Figure 4 presents an axonometric view of this level, and Figure 5 shows the view of the repetitive floors, from the second to the ninth floor. Each of these floors contained 12 apartments. The subsequent floors mainly differed in the geometry of the balconies and a slightly altered apartment layout. The last, twelfth floor was incomplete and was designated for a luxury penthouse. The above-ground part of the building was 37 meters high.

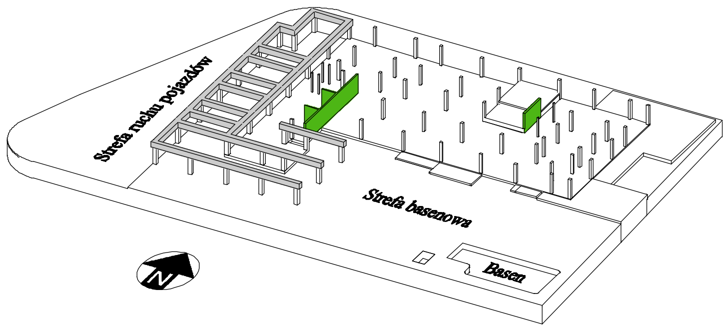

Fig. 4. Axonometric view of the ground level (lobby)

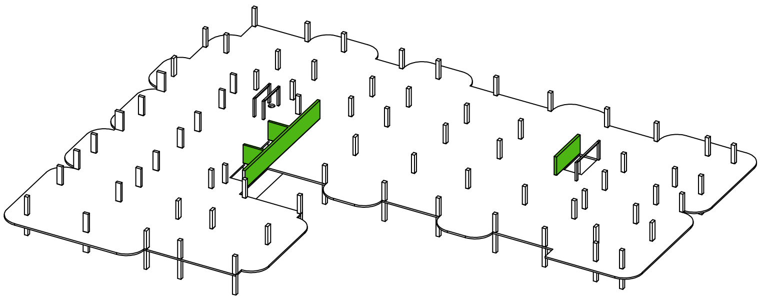

Fig. 5. Axonometric view of above ground levels

4. Description of the building structure

The main load-bearing structure of the building was a plate-column skeletal system [5]. This design allowed for flexible space configuration within the building.

Foundations: The building was indirectly supported on Franki-type reinforced piles with a capacity of 150 tons. Under the columns, 2 to 4 of these piles were grouped together and connected by a reinforced concrete ring beam. A greater number of piles were used under the shear walls, and the ring beams were shaped like the letter "I". Under the external bearing walls of the garage, piles were evenly distributed along the perimeter of the building.

The foundation slab, which also served as the garage floor slab, rested on these ring beams. It had a thickness of 230 mm. The primary lower reinforcement of this slab was Ø13 at 300 mm intervals, laid in both directions. The upper reinforcement above the columns was made with Ø16 bars at 200 mm intervals.

Columns: The spacing between columns in the building was irregular, ranging from 3.8 m to over 8.0 m, adjusted to meet architectural functions. In the eastern wing of the building, the grid of columns was consistent in height across all floors. In contrast, in the western part of the building, the spacing of the columns on the garage and ground floor differed from that of the upper floors.

Columns throughout the building had a rectangular cross-section. Single-story columns in the vehicle traffic area and pool area had a cross-section of 300×400 mm. In the garage and ground floor level under the western wing, columns with a cross-section of 610×610 mm were used. From the first floor upwards, columns with a cross-section of 300×400 mm were used. In the eastern wing of the building, columns of 300×400 mm and 400×400 mm were used throughout the height of the building.

Floors: The garage ceiling had a thickness of 240 mm. Due to the variation in finishing layers of the ground floor, several stepped level changes were made in the floor—most often at the axes of the main columns. At these step changes, beams were introduced with a height corresponding to the height difference and a width equal to the thickness of the floor. Additionally, under the pool area and patio, support beams of 300 mm width and 380 mm height were added. The garage ceiling was reinforced with a lower mesh of Ø13 at 300 mm intervals. Above the columns, a mesh of Ø16 bars spaced 200 mm apart was used in both directions. The inter-columnar bands were reinforced unidirectionally with Ø12 bars at varied spacing. Figure 6 shows the principle of floor reinforcement [5].

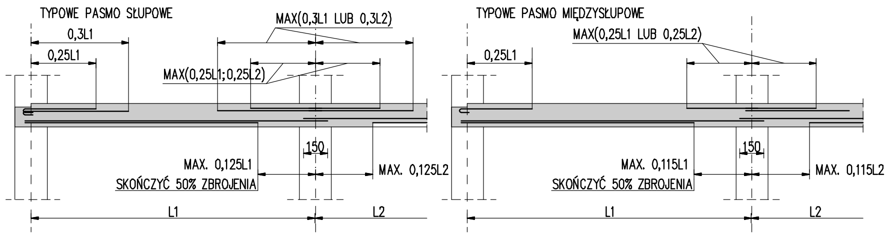

Fig. 6. Guidelines for reinforcing a typical columnar band and inter-columnar band [5]

The floor above the first level had a thickness of 200 mm. Due to the change in the spacing of the columns from the first floor level of the western part, to transfer the reaction from higher floors, a reinforced concrete grid at the level of the floor above the ground floor was used (see Fig. 4). The tie beams had a height of 1220 cm and a width ranging from 760 to 920 cm. The floors of the remaining higher levels also had a thickness of 200 mm and did not require the use of tie beams. The primary reinforcement for these floors was Ø13 every 330 mm. Above the columns, reinforcement of Ø16 every 200 mm was applied. No transverse reinforcement for punching, rigid inserts, or capitals were used in any of the floors.

Building Stiffening and Circulation: The overall stability of the building was provided by two communication cores (marked in green on Figs. 3-5). In the western part, a core was located, consisting of a longitudinal wall 300 mm thick and two perpendicular reinforced concrete walls defining the elevator shaft. In the eastern part of the building, a single stiffening wall of the same thickness was used. An emergency staircase was located next to each of these walls. The staircases were made of prefabricated steel.

Masonry Walls: External and internal partition walls were made from two-chamber concrete blocks with dimensions of 20×20×40 cm. These walls did not serve a load-bearing function. It is important to note that the project [5] specified that masonry walls should only be constructed after the main structure of the building had been erected.

5. Materials

Different strengths of structural concrete were used in the construction of the building. The foundation slab and the floors up to the sixth floor inclusive were designed using concrete with a characteristic compressive strength f_{ck} = 27,6 MPa. For the floors of the higher levels, concrete with a strength of f_{ck} = 20,7 MPa was specified. The columns of the underground garage and the first three floors were designed with concrete having a compressive strength of f_{ck} = 42 MPa. From the third to the sixth floor inclusive, the columns were made from concrete with a strength of 34.5 MPa, and the columns of the higher floors were made from concrete with f_{ck} = 27,6 MPa.

All reinforced concrete elements were reinforced with deformed steel. According to the design, GRADE 60 steel as per ASTM A615 standard [6] was used. This is a hot-rolled structural steel with a distinct yield point f_y = 420 MPa. The ductility class for this grade of steel according to [7] is Class B.

6. Technical condition of the building

The more significant damages found were related to the elements of the facade and balconies: blistering of plasters at the edges along with deeper erosion on the underside of the slabs, cracked ceramic tiles, cracks, and blistering of the facade plaster.

While the facades and above-ground part of the building did not raise concerns during the inspection, the underground part did. Numerous multi-directional cracks were found on the lower surface of the ceiling above the garage. The width of the cracks ranged from 0.1 mm to 2 mm. Most of the cracks were located in the area of the pool zone and patio. Visible were rust stains indicating rebar corrosion and gravitational stains of leached calcium carbonate, meaning the cracks in the ceiling were through-and-through. During the inspection, there were also failed attempts to seal the cracks with resin (leftover packers were found).

Besides ceiling damage, numerous defects were found on the edges of the columns and severe degradation of the ramp descending to the garage. Examples of these damages are shown in Figure 7.

The numerous, still active leaks through the ceiling cracks led the review author to conclude that the insulation on the ceiling was not watertight. Moreover, it was observed that the slopes on the ceiling were either not made or were too small, leading to the formation of water stagnation.

Fig. 7. Damage to the structure in the underground garage Source: [8,9] a) cracks and rust stains on the lower surface of the ceiling, b) column damage, c) defects in the ramp plate

The author of the studies [8,9] stated that the corrosion spots on the reinforced concrete structure present at that time were local and did not pose a threat to the overall safety of the building, but they required prompt repairs using appropriate techniques such as injection, reprofiling, or filling of voids.

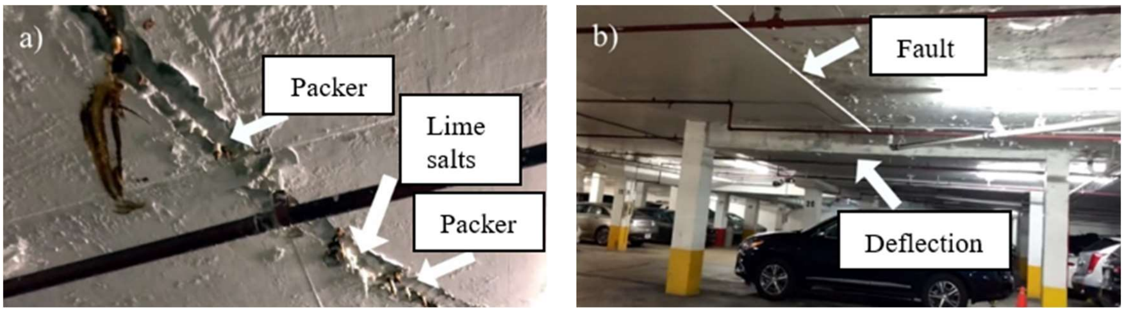

Fig. 8. Ceiling damage. Source: [11] a) close-up of a crack, b) view of the ceiling in the failure zone

The condition of the ceiling above the underground garage is confirmed by a video [11] made in 2020. The video shows numerous cracks and efflorescence on the lower surface of the ceiling in the area of the driveway as well as the pool and patio areas (Fig. 8a). One of the shots filmed the area of potential failure (Fig. 8b). There is a clear difference in the condition of the ceiling surface at the junction of the patio and the residential part of the building. The supporting beam was visibly deflected, estimated from the photo to reach about 30-40 mm.

Fig. 9. Views of core samples taken from the garage ceiling. Source: [9]

For the purposes of this study, core samples were taken from the garage ceiling (Fig. 9). Cores were collected from the patio area, the ceiling within the building outline, and the driveway. The condition of the concrete can be considered satisfactory. No rust was found in the samples, but concerns arise from the concrete voids around the reinforcement and the ease with which the rebar can be detached from the concrete. This may indicate reduced adhesion between the reinforcement and the concrete. Based on the recommendations from the reviews [8,9], a comprehensive repair project for the building was developed [10].

7. Causes of the ceiling failure

As previously mentioned, just before the collapse of the eastern part, witnesses reported the ceiling above the garage caving in. Figure 10 schematically shows the area of the ceiling failure, and Figure 11 presents photos of the damaged ceiling. It cannot be ruled out that the initial area of failure covered a smaller area (marked in red), and further destruction of the ceiling was caused by the collapse of the above-ground floors of the eastern part of the building.

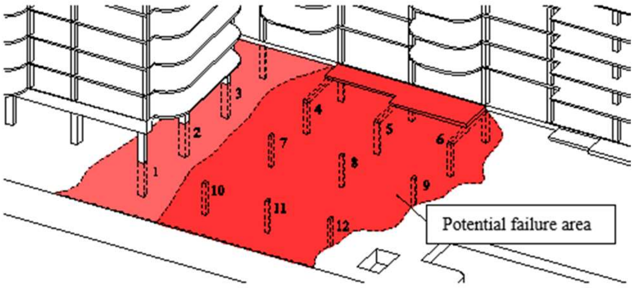

Fig. 10. Hypothetical area of the ceiling failure above the garage

Fig. 11. Collapsed ceiling above the garage - visible effects of the punch-through. Source: [12]

As seen in Fig. 11, in the area of the failure, the ceiling underwent a punch-through on all visible columns regardless of their size. Most of the joints were essentially completely destroyed—this applies to columns with a cross-section of 300×400 mm. In columns with a cross-section of 610×610 mm, which supported the part of the building that survived, partial punch-through cones can be seen, characteristic of eccentric load effects.

To confirm the hypothesis that the ceiling was destroyed by punch-through, a numerical computational analysis of the ceiling above the garage was conducted. Internal forces in the ceiling were determined using a spatial model. It included floors and vertically cooperating elements—columns and walls (Fig. 12). A finite element mesh (FEM) of 50 cm size was used, with local densification over the columns. The lower columns and walls were anchored in the foundation. The ends of the upper columns and walls were also anchored, with only the vertical axis sliding allowed.

The ceiling was subjected to a uniformly distributed load based on the existing finishing layers. For the pool area, a load of 2.0 kN/m^2 was applied. Additionally, planters placed on the patio with shrubs and palms were considered (5.0 kN/m^2). In the lobby part, a load of 1.0 kN/m^2 was assumed. Since there was no live load on the ceiling at the time of the failure, it was omitted from the calculations.

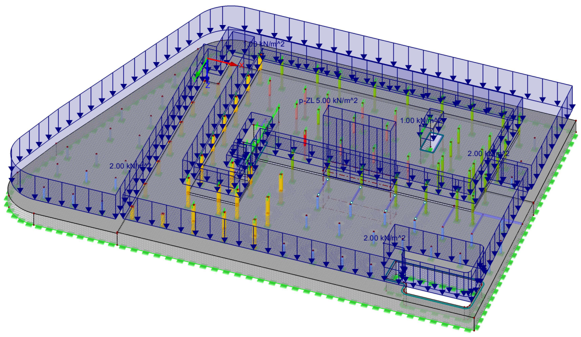

Fig. 12. Computational model of the ceiling above the garage

The calculations of the ceiling's capacity for eccentric punch-through were conducted according to Eurocode 2 [7] and the American standard ACI 318-77 [13] that was current at the time the building was designed. Both cases considered the designed material data and geometrical specifications.

The calculations confirmed that the capacity for punch-through was exceeded even for the permanent load alone, regardless of the standard used. In the case of calculations according to EC2 [7], deficiencies in capacity occur in all zones of column punch-through with a cross-section of 300×400 mm, ranging from 27% to as much as 102%. The areas around columns with a cross-section of 610×610 mm are an exception, where there is a small margin. In the case of calculations according to the ACI 318-77 standard [13], there are also deficiencies in capacity, though they are less severe.

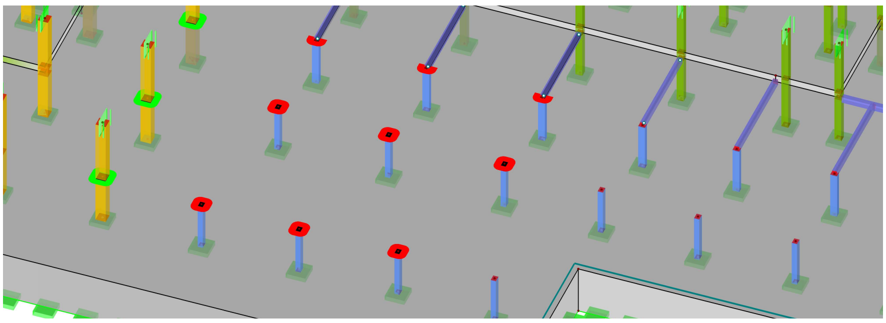

Fig. 13. Graphical presentation of control perimeters according to EC2 [7]. Red color indicates exceeding shear capacity.

We must ask why the failure did not manifest earlier. This can be explained by the fact that the structure had an additional reserve capacity due to the actual properties of the materials—concrete and steel. Additionally, membrane forces from the interaction with retaining walls might have provided some increase in punch-through capacity. It is also likely that the nominal design load was not fully applied in the failure area. This slight reserve capacity was gradually reduced by external factors. The lack of watertight insulation on the ceiling and the inaction in undertaking appropriate repair work in this area allowed moisture and chloride ions from the marine environment to penetrate the structure over many years. This caused severe corrosion of the reinforcement, often hidden under finishing layers.

According to the authors, corrosion was one of the causes of the disaster, gradually weakening the structure by reducing the effective reinforcement area and causing progressive cracking, leading to the redistribution of internal forces. It is possible that the punch-through failure was preceded by a local exhaustion of bending capacity (e.g., in the beams supporting the ceiling—see Fig. 8b).

8. Conclusions

Based on the analysis of the collected materials, the following conclusions can be drawn:

- From the moment of its construction, the building faced inevitable failure due to deficiencies in punch-through capacity in the ceiling above the garage.
- The probable cause of the ceiling failure was punch-through. This was confirmed by the computational analysis of the ceiling, revealing severe capacity deficiencies.
- The lack of repairs and years of neglecting leaks through the ceiling allowed for the unrestricted development of reinforcement corrosion in the ceiling, which was an additional cause of the disaster.
- The lack of continuity of the lower reinforcement of the ceilings above the columns and in the inter-column bands, low degree of reinforcement, and short reinforcement overlaps were factors conducive to the development of the progressive disaster in the eastern wing.
- Variable thermal effects may have contributed to the weakening of the structure.

The CTS building disaster caused a significant stir, as there are many similarly constructed and aged residential buildings in Florida. It turned out that the technical condition of many of them is similar and will require costly repairs. Undoubtedly, the CTS tragedy will lead to a reform of the regulations in the USA regarding building inspections and maintenance.

References

1. Derkowski W., Ślaga Ł.: Czy i jak projektować budynki zabezpieczone przed katastrofą postępującą?, Materiały Budowlane, nr 11/2013,
2. Microsoft streetside, https://en.wikipedia.org/wiki/Surfside condominium collapse#/ media /File:Champlain_Towers_South.png (dostęp:01.01.2022),
3. Miami-Dade Fire Rescue Department, https://twitter.com/MiamiDadeFire/status/ 1408021153415892992, 25.07.2021, (dostęp:01.01.2022),
4. Friedman W.M & Associates Architects Inc., Champlain Towers South 135 Unit Condominium Architecture design, 1979,
5. Breiterman, Jurado & Associates Consulting Engineers, Champlain Towers South 135 Unit Condominium, Structural design, 1979,
6. A615 Standard Specification for Deformed and Plain Carbon-Steel Bars for Concrete Reinforcement, ASTM, 1979,
7. European Committee for Standardization. EN 1992-1-1 Eurocode 2: Design of concrete structures Part 1-1: General rules and rules for buildings. CEN, Brussels, 2004
8. Morabito. F.P.: Inspection Report of CTS Condominium, Surfside 2018,
9. Morabito. F.P.: CTS Condominium Structural Field Survey Report, Surfside 2018,
10. Morabito Consultants: 40 Year Building Repair and Restoration, Champlain Tower South Condominium, 8777 Collins Avenue, Surfside 2021,
11. Terenzi F.: Champlain Tower South underground garage parking video of JULY 17 2020, https://www.youtube.com/watch?v=cAiIte8i2oM (dostęp:01.01.2022),
12. Pizzo J., https://twitter.com/senpizzo/status/1417657635709636613 (dostęp: 01.01.2022),
13. ACI 318-77 Building Code Requirements for Structural Concrete, ACI 1977.

SECTION III
DIAGNOSTICS IN STRUCTURAL SAFETY ASSESSMENT

ANALYSIS OF THE CAUSES OF CRACKING OF STONE SLABS IN LARGE-AREA FLOORS

JERZY HOŁA[1], *jerzy.hola@pwr.edu.pl*
ŁUKASZ SADOWSKI[1]

[1]Politechnika Wrocławska

Keywords: large-area floors; top layer; stone slabs; executive irregularities; cracking; non-destructive testing methods

1. Introduction

Large-area floors in prominent commercial and public facilities often have a top layer made of stone slabs, most commonly marble. The dimensions of these slabs typically measure 500x500 mm, 500x1000 mm, and 1000x1000 mm, with a minimum thickness of 30 mm. These floors endure not only pedestrian traffic but also the load from electric trolleys transporting construction materials and goods to retail outlets, carts of mechanical washers, scaffolding used during repair and maintenance works, etc.

Besides high aesthetic value, large-area floors with a stone top layer are expected to have high durability and ensure safe use [1-3]. However, these expectations are not always met. Construction practice shows that in some buildings, stone slabs crack after a short period of use. Individual slabs or assemblies consisting of several slabs often break, and typically, the number of these damages increases over time.

Based on several cases diagnosed by the authors, some recurring causes and irregularities at the execution stage responsible for this state of affairs have been identified. Considering the above, the aim of this work is to share this knowledge and draw attention to non-destructive methods useful in testing such floors, both before use and during operation.

2. The technology of making the top layer of stone slabs in large-area floors

The technology used for making the top layer of stone slabs in large-area floors is generally straightforward. This process involves laying the slabs on a concrete base, which may rest on the ground or on a reinforced concrete ceiling, through a substrate that consists of a cement mortar layer several centimeters thick with a moist consistency. Immediately after laying the cementitious mixture and leveling the fresh layer, a cement laitance is evenly distributed on its surface to serve as the bonding layer between the substrate and the slabs. On this successively prepared cement substrate, the stone slabs are then laid in succession.

3. Description and analysis of the causes of cracking of the slabs

Stone slabs in large-area floors often crack after short-term use, and over time, the occurrence of these damages increases. Cracks typically appear in individual slabs in different areas of the floor, but sometimes several adjacent slabs break. These cracks can be described as "typical" and manifest in the following forms:

- Fractures parallel to the sides or along the diagonals of the slabs
- Broken slab corners
- Large local nicks, dents, and edge chippings

Crack lines are usually imperfect, featuring small nicks and chips. Broken corners often "collapse" and, over time, create oblique surfaces that are especially dangerous for pedestrian traffic, similar to edge chipping. The vast majority of slabs damaged in this manner cannot be repaired and must be replaced with new ones.

During the diagnosis of several large-area floors by the authors, it was found that cracks in the stone slabs are primarily caused by significant irregularities at the execution stage, specifically regarding the incorrect method of preparing the substrate. These irregularities include:

- Streaked deficiencies of the cement mortar under the slabs and lack of alignment
- Local shortages of cement mortar, especially in the corners and around the edges of the slabs

Additionally, other causes include:

- Embedding stone slabs with a thickness less than the designed specification
- Lack of effective technical supervision in the field of substrate preparation and slab laying

The streaked shortages of cement mortar under the slabs and the lack of leveling are technological irregularities that result in cracking when heavy loads, such as the wheels of an electric trolley loaded with building materials during the finishing stage or goods during operation, drive over these slabs. The mechanism of slab cracking in such situations is illustrated in Fig. 1.

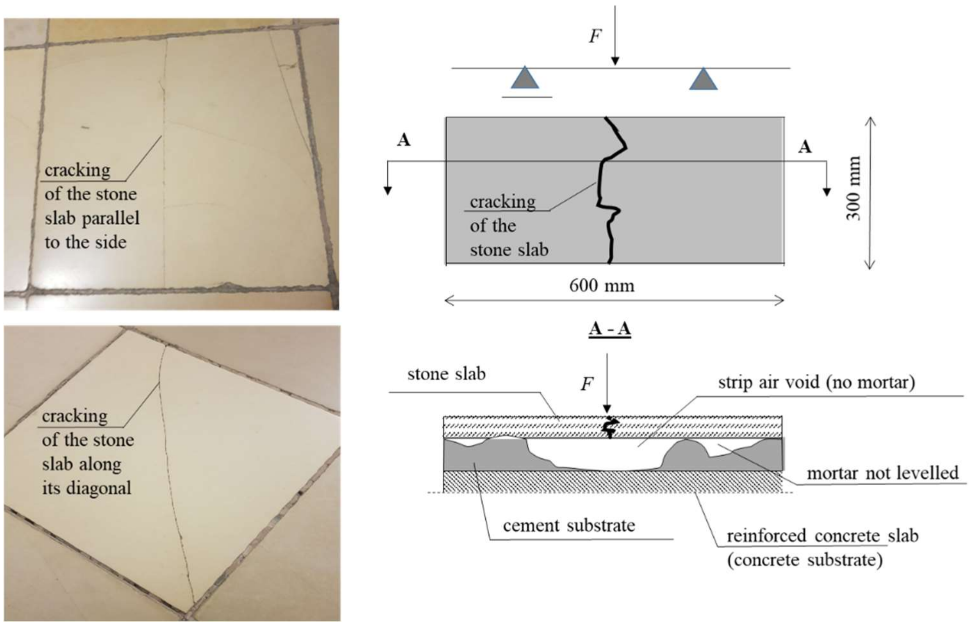

Fig. 1. The mechanism of cracking of stone slabs in exploited floors

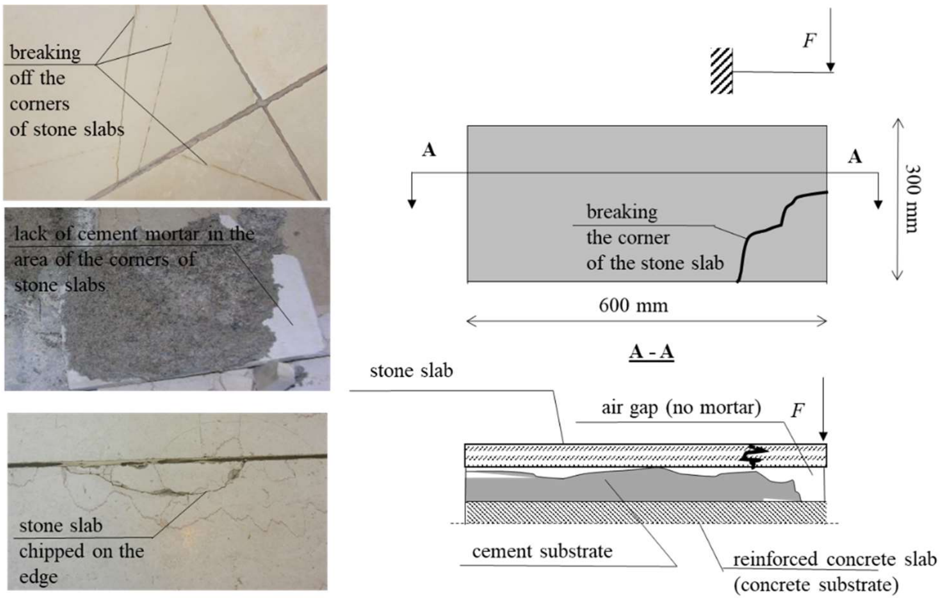

Fig. 2. The mechanism of cracking of stone slabs in exploited large-area floors when there are local deficiencies of cement mortar in the area of corners or edges

The lack of cement mortar in the area of the corners or edges of the slab is another technological irregularity that occurs when the slabs are placed on "spots" of cement mortar. In such cases, the corners become supports that are susceptible to breaking off not only when the wheel of a loaded trolley runs over them but also when they are loaded by scaffolding used for repair and maintenance works. The mechanism of slab corner cracking in these situations is illustrated in Fig. 2.

In the event of the above-mentioned performance irregularities, a cumulative cause that increases the susceptibility of stone slabs to cracking may be their thickness being too small compared to the designed specifications. An example of this situation is a large-surface floor with a top layer made of marble slabs, where the design specified a thickness of 30 mm, but this was changed to 20 mm at the execution stage [4]. The results of measuring the thickness of the slabs in this floor are shown in Fig. 3.

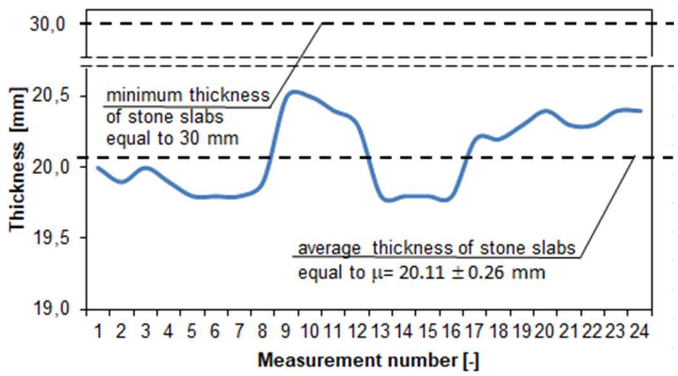

Fig. 3. Results of measurement of the thickness of samples of marble stone slabs cut from the floor (own elaboration based on the results of the research published in [4])

The fact that significant irregularities occur in the preparation of the concrete substrate for stone slabs during the execution stage, along with changes in the slab thickness to less than what was designed, indicates a lack of effective technical supervision or negligence. It should be noted that detecting irregularities in the preparation of the substrate for stone slabs at the stage of final qualitative acceptance of the floor is challenging. The focus is primarily on the general aesthetics of the workmanship, and control tests to assess the bonding of stone slabs to the ground using non-destructive testing equipment are rare. Typically, control consists of randomly tapping the floor surface with a wooden element and making a subjective diagnosis based on the presence or absence of the so-called "dead noise." In this context, it is highly recommended to use non-destructive research methods such as impulse response and impact-echo testing [5, 6].

4. Summary

The extended abstract analyzes the causes of cracking in stone slabs used in large-surface floors in prominent commercial and public buildings. This analysis is based on our own diagnostic cases and relates to the technology of laying these slabs used in construction practice. It has been shown that cracking is primarily caused by significant irregularities committed during the execution stage, specifically in the preparation of the cement substrate for the slabs. The problem of non-destructive control tests for such floors before they are handed over for use, which allows for the detection and location of potential irregularities, has been highlighted. Useful non-destructive testing methods have been identified for this purpose.

References

1. Drozd W., Kowalik M.: Współczesne posadzki przemysłowe. Przegląd Budowlany, nr 7-8/2014, s. 34-39.
2. Nowobilski T., Hoła B.: Bardziej i mniej znane posadzki dla budownictwa mieszkaniowego. Builder, nr 21 (3)/ 2017, s. 84-87.
3. Chmielewska B., Czarnecki L.: Wymagania norm dotyczące posadzek przemysłowych. Materiały Budowlane, nr 2/2012, s. 5-9.
4. Hoła J., Sadowski Ł., Nowacki A.: Analysis of the causes of cracks in marble slabs in a large-surface floor of a representative commercial facility. Engineering Failure Analysis, nr 97/2019, s. 1-9.
5. Sadowski Ł., Hoła A., Hoła J.: Methodology for controlling the technological process of executing floors made of cement-based materials. Materials, nr. 13(4)/ 2020.
6. Runkiewicz L.: Diagnostyka obiektów budowlanych. Cz. 2. Badania i oceny elementów i obiektów budowlanych / red., Wydawnictwo Naukowe PWN SA., Warszawa 2021

SAFETY OF GLASS BARRIERS IN THE LIGHT OF STANDARDS AND OWN EXPERIMENTS

MARCIN KOZŁOWSKI[1], *marcin.kozlowski@polsl.pl*

[1]Silesian University of Technology, Faculty of Civil Engineering

Keywords: glass barriers, dynamic load, soft body impact, experiments, numerical simulations

1. Introduction

In recent decades, there has been a significant increase in the use of structural glass in contemporary architecture [1]. This trend applies to building elements that play a crucial role in ensuring the safety of building users [2]. The primary purpose of using barriers in buildings is to protect users from falling from a height. These elements are installed in places where there is a significant difference in levels between the surfaces on both sides of the barrier [3]. To fulfill their function, barriers must meet several requirements. The first requirement concerns the minimum height of the barrier, which depends on the functional purpose of the element and its location in the building. Another requirement is sufficient load-bearing capacity, meaning safe behavior under static and dynamic loads. The last requirement concerns minimum stiffness, which relates to limiting excessive deformation and thus ensures the functionality of the barrier and the comfort of building users.

The loads acting on barriers are directly related to the actions of building users. These include static loads related to crowd pressure and wind loads, if the barrier is installed outside the building. The crowd load, depending on the category of use of the surface, is usually applied as a linear, horizontal load along the upper edge of the barrier, at a height of not more than 1.2 m from the floor surface. In addition to static loads, the barrier should also safely carry dynamic loads that may occur during its service life. There are two types of dynamic loads: soft body impact associated with human impact and hard body impact. Dynamic loads are crucial for ensuring the safety of building users and should be a fundamental element of static and strength calculations for such elements [4].

Glass barriers should fulfill their function in both the elastic state and the postcritical phase [3]. The glass may fracture for many reasons, including overloading, acts of vandalism, accidental impact with a hard object, or spontaneous breakage of tempered glass caused by the inclusion of nickel sulphide [5]. Due to the brittle behavior of glass, it is important in the design process to consider not only the ultimate limit state (ULS), which ensures safety in use, and the serviceability limit state (SLS), related to the aesthetics and comfort of use, but also additional limit states. These additional states refer to the post-breakage phase, i.e., from the moment the pane fractures [6, 7].

The first of these, the so-called fracture limit state, directly relates to the moment and manner in which an element fails. To meet this limit state, it must be ensured that the fracture of a single pane or the entire element will not pose a threat to people in its immediate vicinity and that the impactor will not penetrate the element. When analyzing this limit state, particular attention should be paid to dynamic issues, such as impacts with soft and hard bodies. The second of these new states, the so-called destruction limit state, applies to the phase from the moment of fracture for a defined time, allowing for the evacuation of building users or replacement of the element.

So far, no uniform standards and regulations containing the methods and principles of designing structures made of building glass have been developed in Europe [2]. Since 1999, the European Committee for Standardization within the Technical Committee CEN / TC 129 "Glass in Building" has been working on drafts of documents for the design of elements made of glass [8], which in 2020 resulted in the publication of the PN-EN 16612 standard [9]. However, this standard applies only to secondary (non-structural) glass elements whose task is to transfer loads to the load-bearing structure, which significantly limits its applicability. It should be noted that the CEN / TC 250 / SC 11 "Structural Glass" commission is currently working on the development of a common standard for glass design for all member countries [10].

2. Classification of glass barriers and dynamic loads generated by building users

The most common classification of glass barriers was originally included in the German regulations [11] and later adapted in the DIN 18008-4 standard for glass barriers [12]. This classification depends on the geometric parameters of the barrier, the method of fixing, and the load transfer function (whether the element is structural or non-structural). The standard [12] defines three main classes of glass barriers:

- **Class A**: Full-height barriers;
- **Class B**: Free-standing glass barriers;
- **Class C**: Glass infill elements.

Correct classification of the barrier is a key task in the examination of the structure and is decisive for determining the value of the dynamic load.

In the past, studies with volunteers have been conducted to estimate the maximum impact energy that can be generated by a moving human [13-18]. In Europe, experimental and numerical research on the simulation of a human impacting a barrier is carried out using a soft body—a two-tire pendulum model adapted from the standard for the classification of flat glass products [19]. The pendulum, with a total weight of 50 kg, is made of two pneumatic tires and a steel cylinder. During laboratory tests and computer simulations, the impact energy is controlled by the drop height of the pendulum, determined by the difference in the height of the center of gravity of the pendulum in its resting state (before being released) and at the moment it impacts the element.

3. Selected results of own experiments

The article presents selected results of research on a free-standing glass balustrade, which is part of the research project "Structural Safety of Glass Components" (grant no. 18-510), financed by the ÅForsk Foundation and carried out in the Division of Structural Mechanics, Faculty of Engineering LTH, Lund University in Sweden, during 2017-2018 [21, 22].

Fig. 1a shows the test rig for testing a free-standing glass balustrade subjected to a soft body impact with a two-tire pendulum according to [19]. A test element with dimensions of 1000 mm × 1200 mm, made of laminated glass (two panes, each 10 mm thick, with a 1.52 mm PVB interlayer), was mounted in a steel bracket to a depth of 100 mm. Two strain gauges measuring vertical strains in the glass on both sides of the balustrade were mounted to the lower part of the glass pane.

During the tests, the pendulum was released from a height of 300 mm, corresponding to an impact energy of 147.1 J. This impact energy value is close to the average impact energy determined in experimental studies with volunteers running and hitting the barrier [4, 18]. Additionally, the element was tested in a post-fracture state (with one sheet fractured on the side of the pendulum) with the pendulum released from a reduced height of 100 mm.

As part of the research project, a numerical model was developed in the ABAQUS environment to simulate the impact of a soft body against a glass barrier (Fig. 1b). The simulations were conducted using the Implicit Dynamic [23] solver.

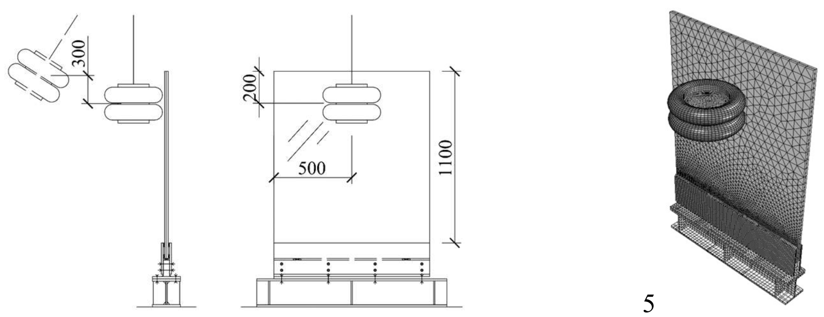

a) b)

Fig. 1. Research on free-standing glass balustrade: a) experimental test setup, b) numerical model

Fig. 2 shows a comparison of the results obtained from laboratory tests (average result for five repetitions) and computer simulations for the impact of a pendulum against a glass barrier from a height of 300 mm, measured at the strain gauge mounting points. The stresses were calculated based on the standard value of the Young's modulus of glass, equal to 70 GPa [9]. In the numerical analyses, very good agreement was obtained regarding the maximum values of stresses in the glass; for tensile and compressive stresses, the difference was not greater than 5%. It should be emphasized that the obtained stresses relate to the strain gauge location. The global principal stresses obtained in simulations occur at the edge of the steel fastening and are about 80% higher.

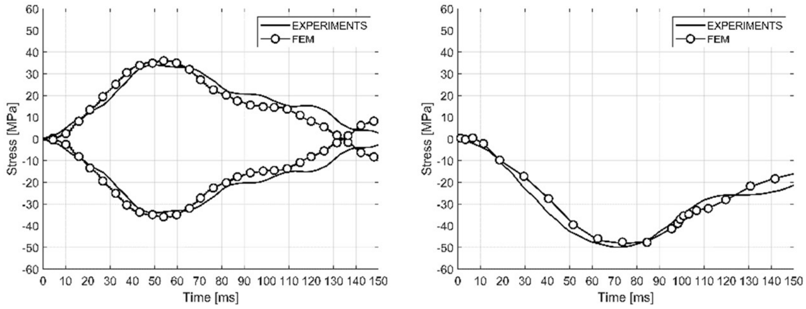

a) b)

Fig. 2. Comparison of results obtained from numerical analyses and experiments: a) elastic state, b) post critical state

This paper was funded by the ongoing research project "Innovative Solution for Point Fixed Laminated Glass with Improved Capacity After Glass Fracture" (LIDER/34/0125/L-11/19/NCBR/2020), financed by the National Centre for Research and Development (NCBR) within the LIDER XI Program.

References

1. Belis J., Louter C., Nielsen J.H., Schneider J.: Springer Handbook of Glass, Springer 2019.
2. Kozłowski M.: Glass balustrades. Experimental and computational analyzes, the basics of design, Silesian University of Technology, Gliwice 2019.
3. Pinto A., Reis L.: Barrier for buildings: analysis of mechanical resistance requirements, Procedia Structural Integrity 1, 2016, s. 281–288.
4. Schneider J.: Impact Loading on Glass Panes by Soft Body Impact – Theoretical Analysis and Experimental Verification, Proceedings of Glass Processing Days, Tampere, 2001, s. 682-687.
5. Karlsson S.: Spontaneous fracture in thermally strengthened glass – a review and outlook, Ceramics-Silikáty 61(3), 2017, s. 188-201
6. Honfi D., Reith A., Gergely Vigh L., Stocker G.: Why glass structures fail? – Learning from failures of glass structures, Proceedings of Challenging Glass 4 & COST Action TU0905 Final Conference, 2014.
7. Lenk P., Honfi D.: Resilience, Damage Tolerance & Risk Analysis of a Structure Comprising Structural Glass, Proceedings of Engineered Transparency, International Conference at Glasstec, Düsseldorf, 2016.
8. Feldmann M., Kasper R., Di Biase P.: European Structural Design of Glass Components – Information on European standardization, Stahlbau 85, 2016, s. 219-229.
9. PN-EN 16612:2020-03 Glass in building. Determination of the lateral load resistance of glass panes by calculation, Polish Committee for Standardization
10. Feldmann M., Di Biase P.: The CEN-TS Structuralal Glass – Design and Construction Rules as pre-standard for the Eurocode, Proceedings of Engineering Transparency, Duesseldorf, 2018, s. 90-98.
11. TRAV: Technische Regeln für die Verwendung von absturzsichernden Verglasungen, DIBt Communication 2/2003.
12. DIN 18008 – 4: 2013 Glass in Building - Design and construction rules - Part 4: Additional requirements for barrier glazing, DIN.
13. Nilsson L.: Impact Loads Produced by Human Motion, Part 1: Background and experimental investigation, Lund University, Lund, 1976.
14. Nilsson L.: Impact loads produced by human motion, Lund University, Lund 1982.
15. Huber K.: Entwicklung eines Stoßkörpers für Pendelschlagversuche, IFT Rosenheim Institut für Fenstertechnik Fenstertage 34867, 1995.
16. Wörner J., Schneider J.: Zwischenbericht zur Durchführung von Versuchen zum weichen Stoß mit dem Pendel nach DIN EN 12600, Institut für Statik, Darmstadt (2000).
17. Bucak Ö.: Bauteilversuche zur Ermittlung der Schultersteifigkeit beim Anprall an Glas, Fachhochschule München, 2004.

18. Schuler C., Koch S., Binder M., Bucak Ö.: Comparative studies to shock loads during the construction project Zoo Wuppertal, University of Applied Sciences Munich, 2005.
19. PN-EN 12600:2004 Szkło w budownictwie - Badanie wahadłem - Udarowa metoda badania i klasyfikacja szkła płaskiego, Polski Komitet Normalizacyjny.
20. Kozłowski M.: Structural safety of glass components, Lund University, 2020.
21. Kozłowski M.: Experimental and numerical assessment of structural behaviour of laminated glass balustrade subjected to soft body impact, Composite Structures 111380, 2019.
22. Simulia ABAQUS v. 6.14, Computer Software and Online Documentation, Dassault Systems: Providence, RI, USA, 2018.

PUFJ AND FRPU SYSTEMS AS EARTHQUAKE PROTECTION OF REINFORCED CONCRETE STRUCTURES WITH INFILLS

ARKADIUSZ KWIECIEŃ[1], *akwiecie@pk.edu.pl*

[1]Cracow University of Technology, Faculty of Civil Engineering

Keywords: RC frames with infills, polymer flexible joints, PUFJ, FRPU, dynamic tests on shake table, cyclic and resonance loading, antiseismic protection

1. Introduction

Earthquakes are among the most catastrophic events beyond human control, often leading to the failure and deterioration of building structures, which can contribute to a higher number of casualties. Engineers are tasked with designing structures according to current standards to ensure resistance to exceptional loads, such as those caused by earthquakes. Unfortunately, many buildings constructed in recent centuries lack sufficient anti-seismic protection, particularly brick structures. The inertial forces generated by ground movement during an earthquake can lead to various damage mechanisms in buildings, which have been extensively described in the world literature in recent decades.

The last major earthquakes in Europe occurred in the Balkans in 2020. Damage to the masonry structures of many buildings in Petrinja was characteristic of seismic areas, featuring in-plane and out-of-plane damage modes. Croatian engineers proposed solutions for reconstructing damaged gable walls using a technology popular in seismic areas—reinforced concrete frames with infills. These structures are based on a reinforced concrete skeleton as a load-bearing structure, with the infill wall serving as a non-structural element.

Post-earthquake inspections reveal that the damage pattern of infills is usually characterized by oblique fractures from in-plane shear or out-of-plane collapse, slippage of joints at the connection with the reinforced concrete frame, or a combination of these issues [1], leading to the infills falling out of the frames. Generally, non-structural infill walls are more prone to damage and fail faster compared to reinforced concrete load-bearing elements. In some cases, the infills can cause harmful destruction of reinforced concrete columns, and even lead to the collapse of the building (the so-called soft-story). Additionally, even in moderate earthquakes, the cost of repairing infills is very high, which underscores the urgent need to consider the impact of non-structural filler walls on the overall behavior of the structure and to use innovative solutions to protect them from damage during repeated strong earthquakes [1]. The main cause of infill failure is the insufficient ability of the rigid elements to transmit forces due to the relatively large displacement imposed by the reinforced concrete columns. Stress concentrations at the contact points between reinforced concrete elements and filling walls cause damage even at very small horizontal drifts, below 0.5% [2].

2. Experimental study

Polyurethane Flexible Joints (PUFJ) and Fiber Reinforced Polyurethanes (FRPU) are designed to secure structures in seismic areas. They can simultaneously carry heavy loads and large deformations while dissipating energy due to their visco-elastic-plastic properties. Their high efficiency has been verified by experimental tests in cyclic push-over tests [2], tests on aseismic tables [3], and harmonic resonance tests [1]. The behavior of PUFJ and FRPU in protecting structures has also been analyzed using numerical models [4].

Cyclic push-over shear tests were conducted at the ZAG Laboratory in Ljubljana, Slovenia, on reinforced concrete frames filled with masonry made of ceramic blocks. Four types of systems shown in Fig. 1 were tested. The classic frame connected to the wall with a rigid mortar (Type A) was tested until the wall detached from the frame around the entire perimeter (risk of out-of-plane damage). The wall was then reinforced on both sides with FRPU (rescue reinforcement) and tested again to the maximum deflection. Type B involved cutting three furrows, 2 cm wide, on the top and side edges of the wall, which were then filled with injection PUFJ (simulation of wall protection in an existing building). In Type C, the inside of the frame was first lined with prefabricated PUFJ of 2 cm thickness, and then the wall was built (simulation of wall protection in a newly constructed building).

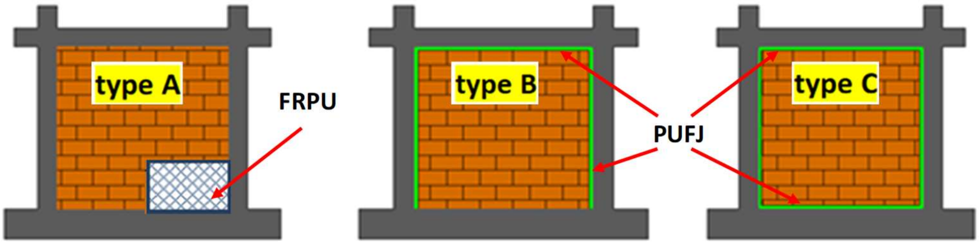

Rys. 1. Schemes of the tested reinforced concrete frames with infills: type A (rigid mortar connection) without and with FRPU reinforcement (left), type B with injection PUFJ on 3 edges (center), type C with prefabricated PUFJ on 4 edges (right)

Type B and C frames, with walls fixed using PUFJ joints, demonstrated very high resistance to cyclic loads with large horizontal displacements (up to 100 mm) and deflections (up to 4%). They retained the ability to transfer vertical and horizontal loads further (reaching the operating range limit of the actuator) without the risk of the infill falling out, and their behavior remained ductile. Damage to the corners (Fig. 2a, b) indicates that PUFJ helped redistribute stress concentrations. Out-of-plane tests of the damaged Type B and C frames, conducted on a seismic table and subjected to dynamic harmonic excitations in resonance (for 10 minutes), did not result in the infills falling out of the frame plane (Fig. 2c).

a) b) c)

Rys. 2. Damaged frames after in-plane cyclic shear tests: type A (a), type B (b) and the frame type B after the action of out-of-plane dynamic harmonic loads in resonance - for 10 minutes (c)

For comparison, the A-type wall completely detached from the frame at a deflection of 0.5%, with edge chipping occurring at 1.6%. There was a risk of the wall falling out of the frame plane. The test was stopped to install the FRPU reinforcement. The A-type frame, reinforced with FRPU, showed a significant increase in load capacity and ductility compared to the damaged A-type frame without FRPU. Moreover, even with significant deflection of the frame after FRPU reinforcement, there was no significant damage that could lead to the wall falling out of the frame plane. This was confirmed by visual inspection after a cyclic test, where attempts to remove the reinforced wall from the reinforced concrete frame were unsuccessful [8].

It should be noted that all filled frames equipped with PUFJ or FRPU systems were able to transfer significant amounts of shear forces (190-220 kN), even with very large deflections of the structure (3.5-4.0%) repeated cyclically, without losing the bond between the frame and the filling wall. This condition is a design requirement according to seismic standards, with Turkey specifying that the structure must be able to safely drift to a level of at least 2% [5]. PUFJ and FRPU technologies fulfill these conditions with a significant margin. Furthermore, they can dissipate considerable amounts of energy in each cycle while maintaining load capacity.

Dynamic tests of infills with PUFJ and FRPU were carried out in the laboratory at IZIIS Skopje in North Macedonia as part of the H2020 SERA project. A symmetrical building with B and C type walls was tested in four phases (Fig. 3). The phases of the test on the seismic table, along with the maximum values recorded during the tests, are presented in Table 1. The building was rotated by 90 degrees between Phases II and III. The recorded values indicate that the PUFJ joint kept a very badly damaged B-type wall in the plane of the frame with accelerations above 1.5 g and a building deflection of 3.7% (significantly above the standard requirements of 2%) in Phase I.

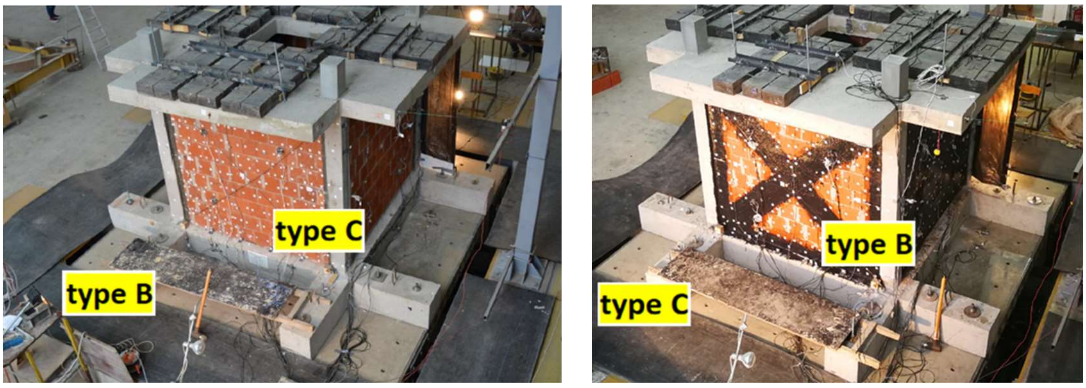

a) b)

Rys. 3. View of the infills building with PUFJ and FRPU on the seismic table: Phase I - B (in-plane) and C (out-of-plane) (a), Phase IV - B_FRPU (out-of-plane) and C_FRPU (in-plane) (b)

Table 1. Maximum values recorded during tests on a seismic table

Testing phase	Infill type (excitation direction)	Table acc. [g]	Slab acc. [g]	Slab displ. [mm]	Drift [%]
I	B (in-plane) C (out-of-plane)	1.64	1.52	88.9	3.7
II	B_FRPU (in-plane) C (out-of-plane)	0.39	0.89	38.9	1.6
III	B_FRPU (out-of-plane) C (in-plane)	0.35	0.48	16.0	0.7
IV	B_FRPU (out-of-plane) C_FRPU (in-plane)	0.95	1.25	21.0	0.9

In the same phase, the C-type wall resisted out-of-plane forces of the same level without any damage. The global stiffness of the tested building degraded to 6% of its initial stiffness, caused by resonance in the 2.5-4.0 Hz band, which was dominant during the given scaled Kefallonia 2014 seismic excitation. At the end of Phase I, the heavily damaged B-type walls were reinforced with FRPU on both sides, and the Phase II test was repeated to a safe level for the building. After rotating the building by 90 degrees, the C-type in-plane walls were tested until the bonds in the joints between the blocks in the wall opened during Phase III. After reinforcing the C face with FRPU, the tests continued in Phase IV up to the maximum load capacity of the seismic table (limited by the actuator's failure).

After installing FRPU reinforcements and completing tests in all phases, the building maintained its global stiffness at 52% of its initial value, despite the presence of plastic hinges at the ends of the reinforced concrete columns. This performance was due to the cooperation between PUFJ and FRPU masonry walls. More details can be found in [3].

The building made with PUFJ and FRPU, which remained in good condition after tests on a seismic table, was subjected to dynamic resonance tests with harmonic forces [1]. Despite several minutes of continuous dynamic excitations (sweeps) at different set resonant frequencies (totaling over 2 hours of work in resonance) and the reduction of global stiffness to approximately 10-15%, the building retained its elastic nature and global stability without any signs of the infills falling out from the plane of the RC frames. The only significant damage was the cutting of glass fibers in the FRPU composite in the center of the C-type wall. The loss of symmetry in stiffness and its significant reduction did not negatively affect the building's seismic resistance. The PUFJ and FRPU systems helped maintain the building's integrity until the end of the study.

The presented research results concerning innovative PUFJ and FRPU systems for fastening infills to RC frames have confirmed their high efficiency as permanent anti-seismic protection. A one-time installation of these systems can protect property and human life during repeated earthquakes, as confirmed by experts in anti-seismic engineering [1, 4].

References

1. Kwiecień A., Rakicevic Z., Bogdanovic A., Manojlovski F., Poposka A., Shoklarovski A., Rousakis T., Ilki A., Gams M., Viskovic A.: PUFJ and FRPU earthquake protection of infills tested in resonance. 1st Croatian Conference on Earthquake Engineering 1CroCEE, 22-24 March 2021, Zagreb, Croatia, pp. 465-475.
2. Triller P., Kwiecień A., Bohinc U., Zając B., Rousakis T., Viskovic A.: Preliminary in-plain shear test of damaged infill strengthened by FRPU. 10th International Conference on FRP Composites in Civil Engineering (CICE 2020/2021), Istanbul 8-10 Dec. 2021.
3. RousakisT., Ilki A., Kwiecien A., ViskovicA., Gams M., Triller P., Ghiassi B., Benedetti A., Rakicevic Z., Colla C., Halici O.F., Zając B., Hojdys Ł., Krajewski P., Rizzo F., Vanian V., Sapalidis A., Papadouli E., Bogdanovic A.: Deformable polyurethane joints and fibre grids for resilient seismic performance of reinforced concrete frames with orthoblock brick infills. Polymers 2020, 12, 2869; doi:10.3390/polym12122869, pp. 1-20.
4. Rousakis T, Vanian V, Fanaradelli T, Anagnostou E.: 3D FEA of Infilled RC Framed Structures Protected by Seismic Joints and FRP Jackets. Applied Sciences. 2021; 11(14):6403.
5. Turkish Seismic Design Code 2018. Turkish Ministry of Interior, Disaster and Emergency Management Presidency.

PRE-FAILURE CONDITION AND THE METHOD OF REPAIRING GLUED TIMBER ROOF BEARS

MACIEJ NIEDOSTATKIEWICZ[1], *mniedost@pg.edu.pl*
TOMASZ MAJEWSKI[2]

[1]Department of Civil Engineering, Faculty of Civil and Environmental Engineering, Gdansk University of Technology
[2]Industrial Doctoral School, Gdansk University of Technology

Keywords: roof girders, glued timber, reinforcement, sports hall, renovation works

1. Introduction

Design documentation of glued-laminated timber roof girders is in many cases very general, does not contain details and design solutions, and the contractors do not have experience in the implementation of this type of structure [1-2]. Design and execution errors, including those related to glued laminated timber roof girders, not only affect the safety and durability of the structure of the facility in which they were built in, but also affect the safety of its use [3-4]. The aim of the article is to present the impact of the design and execution errors which cumulated after a short period of operation of the sports hall led to its exclusion from use. The article also presents the implemented method of strengthening the roof girders in question.

2. General information

The building of a sports hall at a secondary school with dimensions in the horizontal projection of ~ 20×30 m (construction axis spacing) was used to conduct physical education classes and extracurricular sports activities. The roof structure consisted of GL28h glued laminated timber roof girders, spaced every 6.00 m. Longitudinal purlins (12×32 cm) made of glued laminated timber were attached to the roof girders, at the level of the upper edge. The purlins are supported on the girders with the use of galvanized steel tables fastened with screws to the side surfaces of each girder. On the purlins, parallel to the roof girders, rafters with a cross-section of 6×12 cm with a spacing of ~100 cm were placed. From the bottom, directly to the rafters, with the help of additional battens, 1 cm thick soffit boards were fixed with nails (so-called upholstery nails), the direction of which was laid parallel to the roof girders. Along the purlins and along the roof girders, the edges of the soffit planks are masked with battens measuring ~ 1,0×1,5 cm (the so-called quarter round).

3. Description of the damage to the girders

The roof girders made of glued laminated timber exhibited cracks occurring both between the layers of glued lamellas (board delamination) and within their thickness (splitting of the wood along the fibers). Diagonal cracks in individual wooden lamellas were also visible on the side planes (on both sides). The extent of damage to all roof girders was very similar, effectively identical, for both girders loaded with the steel structure of basketball baskets and for unloaded ("clean") girders.

The steel elements of the fastening (gusset plates) of the basketball backboard support structure were deformed at the points of contact with the side surfaces of the roof girders, and there was no adhesion of the sheets to the girder planes (the so-called leverage effect was observed). Additionally, the snake plates used for attaching the roof braces to the girders were deformed. The soffit boards, across the entire projection area of the sports hall, showed loosening at the points of attachment with nails and had slid from the quarter-round slats onto the floor.

4. Analysis of the existing condition of roof girders

Influence of constructional and material solutions

The load lists in both the construction design and the detailed design do not account for the weight and impact of the fastening (in the form of concentrated forces, bending, and torsional moments) of mobile basketball backboards. The summary only includes the value of a uniformly distributed technological load of 0.20 kN/m², without any additional comments.

The verification calculations were made for two operational situations:

- Variant I - girder in an undamaged condition,
- Variant II - girder in a weakened state (with delamination).

The calculations for the roof girders were made for the "clean" girder, i.e., not loaded with the weight of the cage supporting structure (Case 1), and for the case when the girder is suspended from the supporting structure (Case 2).

During the inspection, attempts were made to lower and raise the baskets (basketball backboards). It took more than 1 minute to raise/lower the basket. The results of the observations led to the conclusion that the movement of the cage is slow and does not cause visible twisting of the roof girder. Both during the initiation and completion of lowering, as well as during the initiation and completion of lifting, there was no sudden jerk (impact) phenomenon transferred to the glued timber roof girders. Due to the relatively long time of lowering/lifting the plate, which was over 1 minute, dynamic effects were ignored, and a detailed analysis (the spar's dynamic response to impact) was not performed, treating it as insignificant.

Based on the analysis of the obtained calculation results, it was found that for Case 1, i.e., the intact girder (Variant I), it did not meet the Ultimate Limit State (ULS) conditions. In particular, attention should be paid to exceeding, in the middle of the span, the permissible tensile stresses perpendicular to the fibers by 180%. The girder also did not meet the Serviceability Limit State (SLS) condition due to permissible deflections being exceeded by over 200%.

In the weakened state (after delamination) (Variant II), the spar did not meet the load capacity (ULS) and deflection (SLS) conditions and required reinforcement due to bending and local pressure. In particular, attention should be paid to exceeding, in the middle of the span, the permissible tensile stresses perpendicular to the fibers by ~60% and the permissible deflections by over 330%.

Based on the analysis of the obtained calculation results, it was found that for Case 2, i.e., the intact girder (Variant I), it did not meet the Ultimate Limit State (ULS) conditions. In particular, attention should be paid to exceeding, in the middle of the span, the permissible tensile stresses perpendicular to the fibers by 185%. The girder also did not meet the Serviceability Limit State (SLS) condition due to permissible deflections being exceeded by ~220%.

In the weakened state (after delamination) (Variant II), the spar did not meet the load capacity (ULS) and deflection (SLS) conditions and required reinforcement due to bending and local pressure. In particular, attention should be paid to exceeding, in the middle of the span, the permissible tensile stresses perpendicular to the fibers by ~68% and the permissible deflections by ~350%.

Influence of soil and water conditions

There was no visible damage to the outer walls of the sports hall that could indicate overloading or uneven settlement of the foundations.

The influence of trees and vegetation

There were no grounds to conclude that the root system of the stand contributed to the damage of the glued timber roof girders and the wooden soffit by damaging the foundations of the sports hall. Additionally, there was no evidence that the roots of the stand contributed to the disturbance of soil and water conditions in the area adjacent to the sports hall.

Influence of communication interactions

No perceptible ground vibrations were found around the sports hall building, and no damage to the hall walls caused by ground vibrations was observed.

5. The method of repairing roof girders

Three conceptual solutions for the reinforcement of the girders were considered: using double-sided waterproof plywood overlays, vertical steel flat bars, and an additional brace at the level of the lower fibers of the roof girder.

Ultimately, considering the economic (cost of repair work) and organizational conditions (time, simplicity, ease of execution), the decision was made to reinforce the girders by introducing additional steel flat bars fixed on both sides of the roof girders. All roofing girders made of glued laminated timber, arranged in axes 2, 3, 4, 5, and 6, were reinforced. Each girder was reinforced with 80x3 mm steel flat bars, with lengths ranging from 1150 to 1850 mm. The flat bars were attached to the girders with steel wood screws, Ø10 mm and 140 mm long.

As part of the renovation works, the wooden soffit was rebuilt: the boards were attached with screws (Ø8 mm and 60 mm long) to the wooden battens and rafters. Loose upholstery nails were removed and replaced with screws; in other cases, a screw was installed next to the nail, ensuring a minimum distance from the free edges to prevent fiber splitting.

After completing the reinforcement of the roof girders and the repair of the soffit, the tension of the roof bar braces was checked and adjusted (clearances on turnbuckles were tightened). It was recommended to regularly clear the roof of residual snow, avoiding the unacceptable accumulation of snow in piles, known as snow bags, on the roof slope. Additionally, it was advised to check the ventilation system and constantly monitor the air humidity in the sports hall. The recommended air humidity level is between 50% and 60%, and it should not exceed 80%, at which point the exhaust fans should be activated.

6. Conclusions

The direct causes of damage, in the form of scratches and cracks visible on the vertical surfaces of roof girders made of glued wood and deformation of the plane of the wooden soffit, were design errors and manufacturing errors. The design errors included: omission of the weight of the hall equipment elements attached directly to the wooden girders and the method of their assembly, and the use of girders with insufficient load-bearing capacity. The manufacturing errors included: uncritical implementation of the project with significant deficiencies, the use of ceiling strips with dimensions too small for their transverse loads, and the use of round nails to attach the soffit boards to the grid of wooden laths.

References

1. Markiewicz P.: Detale projektowe dla architektów. Wydawnictwo Archiplus, Warszawa, 2009.
2. Beinhauer P.: Katalog standardowych rozwiązań projektowych detali dla projektów budowlanych. Państwowe Wydawnictwo Techniczne, Warszawa, 2010.
3. Szer J., Jeruzal J., Szer I., Filipowicz P.: Kontrole okresowe budynków – zalecenia, wymagania i problemy. Wydawnictwo Politechniki Łódzkiej, Łódź, 2020.
4. Baranowski W.: Zużycie obiektów budowlanych. Wydawnictwo Warszawskiego Centrum Postępu Techniczno-Organizacyjnego Budownictwa, Ośrodek Szkolenia WACETOB sp. z o.o., Warszawa, 2000.
5. Brol J., Ajdukiewicz A.: Zagrożenie awarią zadaszenia z drewna klejonego warstwowo nad obiektem rekreacyjnym. XXVIII Konferencja Naukowo-Techniczna Awarie Budowlane-2013, 261-272, Szczecin-Międzyzdroje, 2017.
6. Al Sabouni-Zawadzka A., Gilewski W., Pełczyński J.: Projektowanie belek z drewna klejonego warstwowo z uwagi na naprężenia prostopadłe do włókien. Inżynieria i Budownictwo, 1, Warszawa, 2019.

DIAGNOSIS OF THE TECHNICAL CONDITION OF AN SECESSION VILLA

BEATA NOWOGOŃSKA[1], *b.nowogonska@ib.uz.zgora.pl*

[1]Uniwersytet Zielonogórski, Instytut Budownictwa

Keywords: diagnostics, cracks and fissures, technical condition, historic building

1. Introduction

Scratches and cracks in building elements are a visible symptom of damage to the building structure, and the Analysis of the shape, direction, and course of scratches, along with their location and behavior over time, provides clues in determining the causes of deformation in the building structure [1-4]. Scratches may indicate excessive strain on the structure, resulting from masonry deformations caused by external or internal influences [5]. Often, the formation of scratches is related to foundation issues, such as heterogeneity of the substrate, uneven soil settlement, substrate instability, soil movements, high-grade soils, and changes in water conditions in the soil [6].

On the slope descending towards the river Nysa, in the town of Gubin, there is a free-standing, two-story building with a basement constructed using traditional techniques. Built at the beginning of the 20th century, the building originally served as a residence for the owner of one of the Gubin factories and is currently used as an office building [7]. The villa, featuring Art Nouveau ornamentation, is set on an irregular, elongated rectangle. The plan is further diversified with risalits in the front elevation (south-western) and the side elevation (south-eastern), as well as a veranda annex on the northern side.

The south-west and south-east elevations are richly decorated with architectural details. These elevations are divided with cordon cornices and segmented with a risalit topped with a triangular gable. The tympanum features floral decorations, fanciful heraldic shields, and an owl figure. The corners are accented with rusticated pilasters. In the lower part of the elevation, at the basement and ground floor levels, there is rustication. The ground floor window openings and the door portal are embellished with profiled frames with keystones richly decorated with floral motifs. The first-floor window openings are framed by pilasters and topped with segmented pediments filled with ornamental decoration [8].

The foundations of the building consist of brick footings measuring 55 x 150 cm with a 6 cm (1/4 brick) offset, made of solid brick class 7.5-10, set in lime mortar. The depth of the bench foundation ranges from approximately 2.7 m to 3.6 m below ground level.

External and internal walls are made of burnt solid brick of class 7.5-10, also set in lime mortar, and plastered on both sides. The thickness of the external walls is 43 cm (1.5 bricks with plaster), and the thickness of the internal walls varies from 43 cm (1.5 bricks with plaster) to 9 cm (1/2 brick with plaster).

The basement ceilings are constructed as fragmentary ceramic vaults of the Klein type light on steel beams: I 260, I 240, I 200, and I 160, with an average spacing of 1.5 m. The vault on the ground floor is a two-span cross vault supported on Ionic pilasters. Other ground floor rooms are covered with a wooden ceiling with a blind ceiling. The ceiling joists measure 18 x 26 cm in section and are spaced 80 cm apart. A fragment of the original floor made of colorful, textured terracotta tiles has been preserved in the hallway. The basement has a concrete floor, while the ground floor and other floors have wooden floors.

The internal staircase between the stories is made of wooden stringers, with broken steps and a wooden balustrade. The structure of the internal stairs between the basement and the ground floor is a brick arch supported on a steel substructure and foundation. The main entrance is preceded by a straight flight of concrete stairs framed by a stepped plaster wall.

The roof is of wooden construction, covered with tar paper, and features a purlin and plywood roof truss with two pine lumber walls. Thermal insulation consists of 10 cm thick mineral wool, and the attic is finished with 1.25 cm thick plasterboard. There is a skylight in the middle of the roof slope. Gutters and downpipes are made of galvanized steel sheet.

Lintels are constructed as segmental brick arches, basket arches (with a decorative keystone), and flat arches made of steel sections. On the ground floor and upper stories, there are double and tripartite box windows with fanlights, wooden and PVC joinery, and wooden window sills. In the basements, there are wooden single glazed frames. The building also features wooden panel doors.

Fig. 1. Secession villa in Gubin

2. Damage inventory

Two vertical cracks are visible on the north-west wall, with the cracks spreading up to 20 mm. The first crack runs approximately 4 meters from the north-west corner along the window axis, extending from the foundations up to the roof eaves. This crack spans the entire thickness of the wall and is also visible inside the building. The second vertical crack runs in the middle of the building from the foundations to the ridge. This crack is also structural, spanning the entire thickness of the wall [9].

Two vertical structural cracks are also visible on the south-east elevation. They run along both sides of the ground floor window opening in the risalit part of the building and continue upstairs along the windows. On the ground floor, the cracks run along the edges of the cellar windows.

a) b)

Fig. 3. Fragment of vertical cracks a) on both sides of the ground floor window opening ,b) to the eaves on the south-east elevation

Excavations of the foundations of the central part of the north-west wall have been carried out. There is a vertical structural crack in the foundation wall and subsequently in the foundation, which is an extension of the visible vertical crack in the wall running from ground level to the eaves. In addition, surface dampness from rainwater was found. It must be assumed that the foundation cracks extend along the same lines as the cracks on both the northwest and southeast walls.

3. Failure cause analysis

The building is situated on a slope descending from the north-east direction down towards the road. The cracks visible on the north-west and south-east walls are caused by parts of the building moving down the slope in the south-west direction.

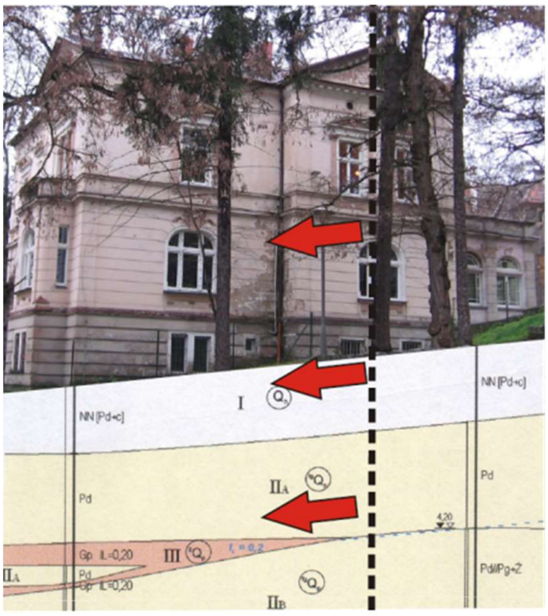

Fig. 5. Direction of building displacement

The analysis of geological cross-sections presented in the geotechnical documentation of the building shows that under the foundations, at a depth of approximately 4 meters below ground level, there is a thin (approximately 0.5 meters thick) layer of sandy clay [10]. This layer runs parallel to the slope of the ground in this location. Above it are fine sands, and below it are fine and coarse sands. This geological arrangement causes a slow sliding of the building along with the soil above the clay layer under the influence of the building's pressure in wet conditions. As a result of these movements, clear structural cracks and fissures have appeared on both façades parallel to the direction of the slope, providing evidence of the building's movement. The basement floors also show cracks across the building between the northwest and southeast walls.

Uneven displacement can lead to a building disaster. The brick structure of the walls and foundations, the lack of reinforcement rims, and the unstable ground result in the building having little rigidity. As the front part of the building slowly slides down along with the slope, the side walls and ceilings between these walls crack.

4. Summary

The technical condition of the walls and foundations is unsatisfactory and may lead to a building catastrophe in the future. The geotechnical conditions of the ground substrate are the cause of significant scratches on the building.

The scratches appearing in the north-western and south-eastern walls indicate progressing uneven horizontal displacements of the building. These movements are unstable over time due to the complex ground and water conditions. Sandy loams are present in the subsoil (in the southern and south-western part of the building) below the foundation level, lying parallel to the slope of the terrain. The cracking that develops over time may lead to a collapse of the floor beams, thus resulting in a building disaster.

References

1. Janowski Z.: Diagnostyka naprawy i rekonstrukcje obiektów murowanych. XX Konferencja Naukowo-Techniczna Awarie Budowlane, Szczecin-Międzyzdroje, 2001.
2. Runkiewicz L. i inni: Diagnostyka obiektów budowlanych. PWN, Warszawa 2020.
3. Zaleski S.: Remonty budynków mieszkalnych. Poradnik. Arkady, Warszawa, 1997.
4. Małyszko L., Orłowicz R.: Konstrukcje murowe. Zarysowania i naprawy. Wydawnictwo Uniwersytetu Warmińsko-Mazurskiego, Olsztyn, 2000.
5. Drobiec Ł.: Przyczyny uszkodzeń murów. XXII Ogólnopolska Konferencja Warsztat Pracy Projektanta Konstrukcji. Szczyrk 2007.
6. Linczowski Cz.: Naprawy, remonty i modernizacje budynków. Wydawnictwo Politechniki Świętokrzyskiej, Kielce 1997.
7. Grander K.: Geschichte der Stadt Guben, Guben 1925.
8. Karta Ewidencyjna Zabytków Architektury i Budownictwa Willa ul. Piastowska 18 Gubin, nr 2531 w Rejestrze Zabytków, archiwum Wojewódzkiego Urzędu Ochrony Zabytków w Zielonej Górze.
9. Nowogońska B., Eckert W.: Opinia techniczna budynku przy ul. Piastowskiej 18 w Gubinie, Zielona Góra 2017.
10. Gontaszewska A. Dokumentacja geotechniczna budynku przy ul. Piastowskiej 18 w Gubinie, pow. krośnieński, Zielona Góra 2017.

ANALYSIS OF CLIMATE CONDITIONS DURING ACCIDENTS ON CONSTRUCTION SCAFFOLDINGS ON THE EXAMPLE OF AIR TEMPERATURE

IWONA SZER[1], *iwona.szer@p.lodz.pl*
BOŻENA HOŁA[2]

[1]Lodz University of Technology
[2]Wroclaw University of Science and Technology

Keywords: accident, air temperature, scaffoldings, construction sites

1. Introduction

Based on the data provided by the Central Statistical Office in 2018, in Poland, construction accidents resulted in 5,247 people being injured, 48 fatalities, and 85 individuals sustaining grievous bodily injuries [1]. The subject of researching the causes and preventing accidents has been repeatedly mentioned in the literature both in Poland [2] and worldwide over the last few years [3]. Stricter occupational safety regulations have resulted in a reduction in the number of accidents in Poland, but the number of people injured in accidents is still high.

In most cases, construction scaffolding work is carried out outdoors, often in dynamically changing climates. Unfavorable environmental conditions—such as high or low air temperatures, precipitation, and strong winds-significantly hinder the execution of work and may contribute to accidents. Research has shown that accidents are influenced by air temperature and humidity [4]. Most accident reports lack information about the weather. Out of 47 analyzed protocols in the Lodz Voivodeship, only one report contained information about strong winds, and one mentioned snowfall. This may indicate a lack of awareness of the influence of external environmental conditions on the occurrence of accidents.

2. Materials and methods

The article analyzes 47 inspection reports made between 2011 and 2017 in the Lodz Voivodeship. These reports were provided by the National Labor Inspectorate for the research project [5]. All sensitive data (e.g., the name and surname of the victim, the name of the company where the accident took place, etc.) were deleted. A total of 51 people were injured in these accidents. For accidents in which more than one person was injured (4 accidents), calculations were done as if these were separate events. Four people had accidents inside the building; therefore, these accidents were not included.

Data from meteorological stations used in the article were obtained from the National Institute of Meteorology and Water Management - National Research Institute (IMWM-PIB). Data were collected from the synoptic station closest to the accident site. Based on the collected data, the air temperature was analyzed over the time corresponding to the time of the accident. Publicly available data are given with information on the hour and refer to average 10-minute values measured during the last 10 minutes of each hour. For accidents occurring on the hour, the air temperature at the time of the accident was taken from the weather station at the same time. For accidents occurring at other times, the temperature was calculated by linear interpolation. For the five cases in which data on the time of the accident were missing, it was assumed that the accident occurred at 12 p.m.

Table 1. Ranges of air temperatures and the corresponding types of days

Air temperature [ºC]	Types of days
> + 30	a very hot day
+ 25.0 – + 29.9	a hot day
+ 20.0 – + 24.9	a very warm day
+ 15.0 – + 19.9	a warm day
+ 10.0 – + 14.9	a chilly day
0.0 – + 9.9	a cold day
- 0.1 – - 10.0	a frosty day
< - 10.0	a very cold day

The approximate assessment of thermal conditions was determined based on the air temperature at the day and time of the accident. For an employee, working conditions are uncomfortable when there is very high or very low air temperature. The ranges of the maximum air temperature on a given day and the corresponding days are presented in Table 1 [6].

3. Results and discussion

Analyzing the obtained data, the lowest air temperature, -3.0 °C, was recorded during an accident in Lodz in February 2012. An employee fell from the scaffolding to the floor from a height of about 6 meters after tripping over a Euro-pallet lying on the scaffolding platform. As a result of the fall, the employee sustained serious bodily injury. There was no information about the weather during the accident in the accident report. The highest air temperature, 28.5 °C, was recorded during an accident in Ostrow in July 2015. A worker fell from the scaffolding to the ground from a height of approximately 3 meters after losing balance on an incomplete working platform. As a result of the fall, the employee suffered minor bodily injuries. There was no information about the weather during the accident in the accident report. Research has shown that the number of accidents depends both on the season and the consequences of the accident [7,8].

Table 2 presents the number of injured people in relation to the seasons and the consequences of the accidents. The lowest number of injured people was registered in autumn (4 accidents), while the highest numbers were in summer (19 accidents) and winter (13 accidents). This may suggest that air temperature may also have contributed to incidents resulting in accidents. Both high and low temperatures adversely affect the comfort of work, contributing to situations that could cause an accident. Minor bodily injuries most often occurred during accidents in spring and summer, grievous bodily injuries in summer, and fatalities in autumn and winter.

Table 2. Number of people injured, broken down by seasons and the result of the accident

Seasons	Consequence of the accident	Number of people injured
winter	minor bodily injury	2
	grievous bodily injury	9
	death of an employee	2
spring	minor bodily injury	5
	grievous bodily injury	6
	death of an employee	1
summer	minor bodily injury	6
	grievous bodily injury	12
	death of an employee	0
autumn	minor bodily injury	2
	grievous bodily injury	0
	death of an employee	2

Figure 1 shows the histograms of the volume of a given air temperature for all 47 events, broken down into temperature ranges corresponding to the days included in Table 1.

By analyzing the obtained histograms, one can notice differences in the number of accidents depending on the air temperature. Most accidents occur in the temperature range from 0 °C to 9.9 °C, which corresponds to a cold day, and in the range from 20 °C to 24.9 °C, which corresponds to a very warm day.

This data suggests that extreme temperatures, both cold and very warm, may contribute to an increased number of accidents. These conditions likely affect worker comfort and safety, leading to a higher likelihood of incidents.

Research has shown that the air temperature on scaffoldings, which are most often placed at the facade of buildings, may be higher than at the weather station [9]. In built-up areas of cities, "heat islands" are observed, where the air temperature is often higher, especially in the summer. Weather stations are typically located on the outskirts of cities, outside densely built-up areas, most often at airports.

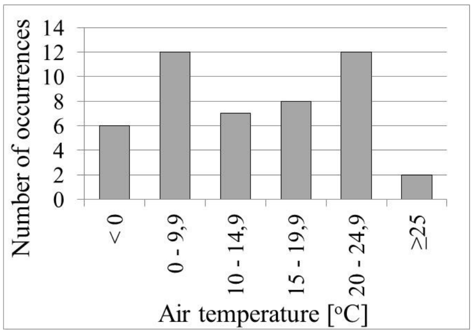

Fig. 1. Histogram of air temperature distribution during accidents, broken down by ranges of temperatures corresponding to the types of days

The dependence, calculated based on tests considering the difference between the air temperature at the meteorological station in Lodz and the temperature on scaffoldings tested in the Lodz Voivodeship, is defined by the equation:

$$y = 0.8706x - 16749 \tag{1}$$

Based on this equation, an air temperature of 20 °C at the weather station corresponds to a temperature of 24.9 °C on a scaffolding. Therefore, the thermal sensation of the worker on the scaffolding will be shifted one level up.

This information is crucial as it indicates that workers on scaffoldings experience higher temperatures than those recorded at weather stations, which may affect their comfort and safety, potentially leading to an increased number of accidents.

4. Conclusions

The analysis of 47 accidents on scaffolding showed that air temperature may contribute to the occurrence of accidents. The lowest number of accidents was recorded in autumn, while the highest number occurred in summer, with 18 people injured. The number of accidents in summer is 4.5 times higher than in autumn. Strenuous physical activity combined with high temperatures and insolation may cause a reduction in concentration, consequently contributing to situations that may result in accidents. Additionally, working at height means that accidents at higher temperatures can more often result in severe bodily injuries. A significant number of accidents were also observed in winter. Low air temperatures may, in extreme cases, cause icing on scaffolding platforms, contributing to accidents. As a result of global warming, we will record both higher air temperatures and an increasing number of days with high temperatures.

Therefore, when assessing the risk of accidents, we should pay attention to environmental conditions. It would be beneficial if accident reports included information on the environmental conditions in which the accident occurred, such as air temperature, humidity, pressure, wind speed, or the type of rainfall if any occurred.

The paper was prepared as part of the project supported by the National Centre for Research and Development within the Applied Research Programme (agreement No. PBS3/A2/19/2015 "Modelling of Risk Assessment of Construction Disasters. Accidents and Dangerous Incidents at Workplaces Using Scaffoldings").

References

1. Główny Urząd Statystyczny, https://stat.gov.pl
2. Nowobilski T., Hoła B.: The qualitative and quantitative structure of the causes of occupational accidents on construction scaffolding, Archives of Civil Engineering 65 (2), 2019, pp 121-131, DOI: 10.2478/ace-2019-0023
3. Ohdo K.: The Effect of Fall Prevention Methods for Construction Scaffolds in Accident Prevention. In: Arezes P. (eds) Advances in Safety Management and Human Factors. AHFE 2018. Advances in Intelligent Systems and Computing 791, Springer, Cham, 2019.
4. Koehn G. Brown, G.: Climatic effects on construction, Journal of Construction Engineering and Management 111(2), pp. 129-137, 1985.
5. Błazik-Borowa E, Szer J.: Podstawowe elementy modelu oceny ryzyka wystąpienia zdarzen niebezpiecznych na rusztowaniach, Przegląd Budowlany 10, 2016, pp. 24–9.
6. Błażejczyk K., Kunert A.: Bioklimatyczne uwarunkowania rekreacji i turystyki w Polsce, PAN, Instytut Geografii i Przestrzennego Zagospodarowania, 2011.
7. Hoła B., Topolski M., Szer I., Szer J., Blazik-Borowa E.: Prediction model of seasonality in the construction industry based on the accidentality phenomenon, Archives of Civil and Mechanical Engineering 22(1), 2022, DOI:10.1007/s43452-021-00348-7
8. Szer I., Lipecki T., Szer J., Czarnocki K.: Using meteorological data to estimate heat stress of construction workers on scaffolds for improved safety standards, Automation in Construction 134, 2022, https://doi.org/10.1007/s43452-021-00348-7

SECTION IV
GEOTECHNICAL CAUSES OF STRUCTURAL FAILURE

FAILURE OF THE STRUCTURE OF THE FLOOR IN A WAREHOUSING FACILITY CAUSED BY SETTLEMENT OF THE SUBSOIL

ŁUKASZ DROBIEC[1]
SŁAWOMIR KWIECIEŃ[2], *slawomir.kwiecien@polsl.pl*

[1]Silesian University of Technology, Civil Engineering Faculty, Department of Building Structures
[2]Silesian University of Technology, Civil Engineering Faculty, Department of Geotechnics and Roads

Keywords: differential settlement, ground improvement, micropiles, numerical analysis, FEM, organic soils

1. Introduction

The article discusses a case of damage to an atypical floor structure caused by the differential settlement of layers of organic and man-made fill soil accumulated in the ground to a depth of several meters, as well as the method for its repair.

2. Description of the facility and floor structure

The hall in question, measuring approximately 31x43 meters and 14 meters in height, is a single-story building without a basement. The load-bearing pillars are made of reinforced concrete, and the roof structure comprises a lattice of steel trusses. The load-bearing structure of the facility has been founded on caps and large diameter piles. It is a single-zone facility built over with mobile racks (Fig. 1a) and stationary racks.

a)

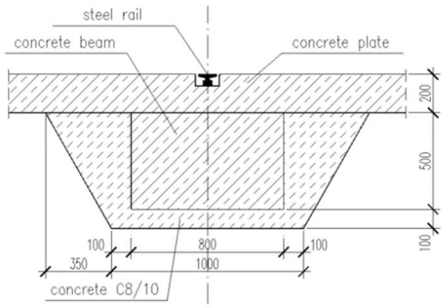

b)

Fig. 1. View of: a) mobile racks and cracks on the warehouse floor surface, b) cross-section of the floor structure

The floor structure was designed specifically for the use of mobile racks. Its top layer consists of a 20 cm thick reinforced concrete slab, reinforced at both the top and bottom, and supported on a reinforced concrete grid that is 50 cm high and 80 cm wide (Fig. 1b). The spacing of the main beams of the grid, corresponding to the width of the axles of the racks, is 2.8 m and 3.7 m. Transverse beams of the grid measure 50x50 cm and are spaced every 6 m. The entire structure is made of C25/30 concrete. Additional encasing made of low-resistance concrete (C8/10, Fig. 1b) was designed under the grid and on its sides. The racks move on steel rails measuring approximately 39.7 m in length. The loading with the rack bogeys is approximately 174 kN/mb for the middle rail and approximately 87 kN/mb for the side rail.

3. Damage of the structure of the floor

From the beginning of the facility's operation, differential settlement of the floor and rails of the mobile racks was observed. This resulted in floor cracking and self-movement of the racks. By 2019, cracking had occurred on the surface of almost the entire hall, with the distribution of cracks being irregular.

The analysis of the results of geodetic measurements shows that in the first two years of the floor's use (2008-2010), the greatest settlement values of 20 mm were recorded for rail no. 5 (blue graphs – Fig. 2). Over the next 9 years, these settlements increased by another 20 mm (red graphs – Fig. 2). Settlement for the remaining beams was similar, approximately 25–40 mm. The settlement distribution along the rails' length was irregular

(Fig. 2), resulting in rail inclinations of up to 8 mm/m. Additionally, local inclinations of the floor perpendicular to the rails measured up to 16 mm/m.

Excavation revealed that the floor slab lacked the intended top and bottom reinforcement, having only dispersed reinforcement instead. Furthermore, the main beam of the grid was not covered with concrete, and a 10 cm layer of concrete was placed under the slab. Analysis during the excavation further demonstrated that the bent main beam of the grid was not cracked and was in contact with the soil along its entire base.

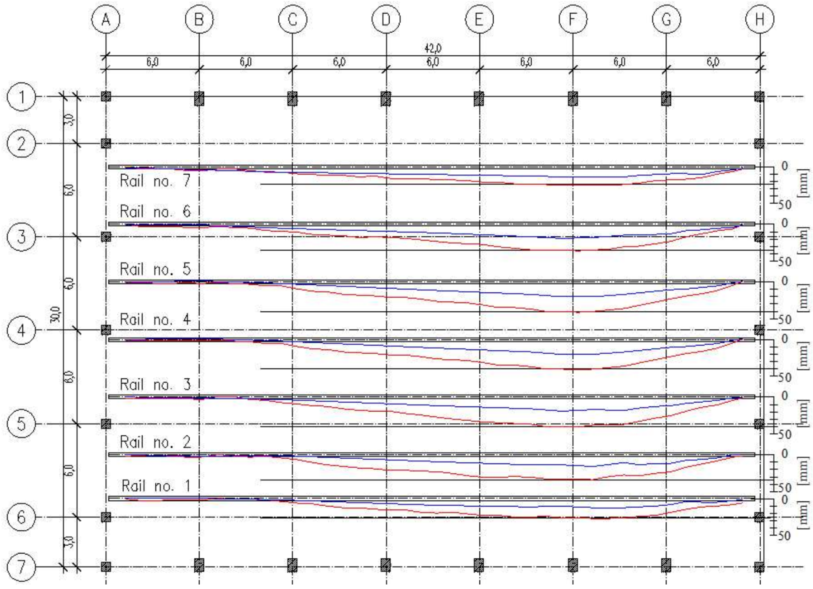

Fig. 2. Plots of warehouse floor (steel rails) settlement

4. Soil and water conditions

As a result of the conducted testing within the hall, it was determined that the substrate consisted of four main groups of soils characterized by different strengths and stiffness. The first group, identified from the ground level to a depth of 2.2–3.4 meters, consisted of compacted construction embankments and loose non-construction embankments of various granulations. The second group comprised fluvioglacial soils, including cohesive and organic soils, accumulated to a depth of approximately 4.4–5.7 meters below ground level. These included peats, firm alluvial silt, and stiff and firm clays with silt and humus additions. Below this layer, to a depth of approximately 11.2 meters BGL (below ground level), were medium dense gravels and sands with gravels, with the addition of cobbles and clay (third group), lined with soft rock in the form of clay shale (fourth group).

During drilling in the gravel and silt layers at a depth of approximately 4.4–5.4 meters BGL, the presence of groundwater with a confined water table was confirmed, stabilized at a depth of 2.7–3.3 meters BGL.

The geotechnical documentation proposed deep foundation (e.g., piles) on the gravel layers, or alternatively the replacement of the low resistance and rigidity soil accumulated to a depth of approximately 4.4–5.7 meters BGL. These recommendations were partially implemented. The structure of the building was founded on 8.0-meter-long piles based on medium dense gravels and sands with gravels, whereas the floor layers relied solely on the partial replacement of the soil.

5. Analysis of the causes for the damage

In order to confirm the influence of soil and water conditions on the observed settlement of the floor structure, a numerical spatial analysis was carried out using the finite element method in the Z_Soil software (Fig. 3a).

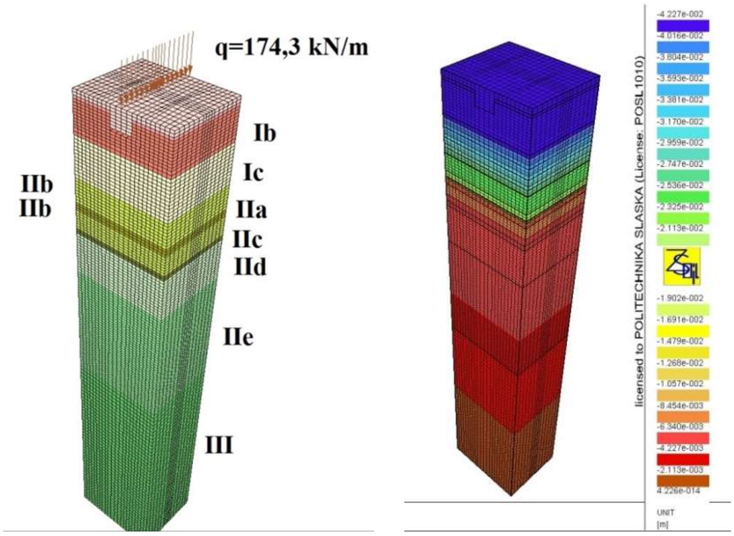

a) b)

Fig. 3. Numerical (FEM) model : a) main view, b) maps of vertical settlement

The analysis included all stages of construction. An elastic perfectly plastic model with a Coulomb-Mohr boundary surface and non-associated flow rule was adopted as a material model for the continuous elements, i.e., native soil layers and embankment layers. The reinforced concrete and concrete elements were modeled as linear elastic. The soil and water conditions, as well as some of the constitutive model parameters, were selected based on geotechnical documentation.

Since the documentation did not provide parameters for the layers of non-construction embankments as well as the layers of peats and silts, these parameters were determined through back analysis. The basis for this analysis was the observed floor settlement. The parameter selection criterion was to obtain calculated settlements similar to the actual settlement values. Numerical analysis showed that compliance with the settlement (Fig. 3b) was achieved for peat layers with a modulus of elasticity of approximately 1 MPa and for non-construction embankments with a modulus of elasticity of approximately 3 MPa. This analysis proved the influence of organic soil layers on the damage.

6. Repair and renovation

It was decided to improve the low rigidity layers by using drilled micropiles, due to the limited space available during repair work. The plan involved constructing perpendicular steel beams supported by a pair of micropiles (one at each end of the steel beam) under the reinforced concrete grid. These beams would be spaced along the length of the grid according to the grid loads, and actuators would be introduced between the beams and the grid to enable leveling of the structure. Subsequently, construction embankments and a floor slab would be executed.

Micropile calculations were conducted in two stages. Firstly, the micropile load-bearing capacity was determined in accordance with the guidelines provided in the Titan design guide book [2] and the PN-EN 1997-1 standard [3]. Secondly, the system settlement was checked using a calibrated, spatial numerical model in the Z-Soil software. The steel beam cross-section was determined in accordance with the PN-EN 1993 standard [4], and the verification of the reinforced concrete beam was conducted in accordance with the PN-EN 1992-1:2008 standard [5].

Calculations of the load-bearing capacity of the reinforcement showed that with micropiles 300 mm wide and 9 m long, the transverse spacing of the micropiles would be 1.5 m, and the longitudinal spacing would be 3.0 m for middle rails and 6 m for side rails. The micropile reinforcement would be provided in the form of single steel bars with a 40/16 mm cross-section. The steel beam would consist of two HEB220 H sections. Despite the change in the static scheme of the reinforced concrete grid, the original design of the cross-section with a new floor slab would transfer the stress forming within the grid.

References

1. Zimmermann Th., Truty A., Urbański A. i inni: Theory manual. Z_Soil.PC 2011, 2011.
2. Titan. Przewodnik Projektowy, 2018.
3. PN-EN 1997-1:2008/A1:2014-05. Eurokod 7: Projektowanie geotechniczne. Część 1: Zasady ogólne.
4. PN-EN 1993-1-1:2006/A1:2014-07. Eurokod 3: Projektowanie konstrukcji stalowych. Część 1-1: Reguły ogólne i reguły dla budynków.
5. PN-EN 1992-1-1:2008/NA:2016-11. Eurokod 2. Projektowanie konstrukcji z betonu. Część 1-1: Reguły ogólne i reguły dla budynków.

FROM LEGEND TO DISCOVERY – HISTORICAL AND GEOTECHNICAL CONDITIONS RELATED TO THE DISCOVERY OF TUNNELS UNDER THE CASTLE HILL IN SZCZECIN

TOMASZ GODLEWSKI[1,], *t.godlewski@itb.pl*
RADOSŁAW MIESZKOWSKI[2]
MACIEJ MAŚLAKOWSKI[3]

[1] Building Research Institute, 21 Ksawerów St., 02-656 Warsaw, Poland;
[2] Warsaw University, Geology Department, 93 Żwirki i Wigury St., 02-089 Warsaw, Poland
[3] Warsaw University of Technology, Faculty of Civil Engineering, 16 Armi Ludowej St., 00-637 Warsaw, Poland

Keywords: geotechnical research, geophysical methods, tunnels, historical object

Abstract: In the article, various geotechnical and geophysical surveys are described, which led to a discovery of potential causes of a structural failure at historical Castle of Dukes of Pemerania in Szczecin. The Castle became famous after the failure, which occured on 11th of May 2017. The failure was very sudden, lasting just few seconds. Its occurence was registered by the surveillance cameras, with a sudden collapse of a column. The rooms in which the failure occured are adjacent to a staircase (as well as the entrance B and C) of the northern wind of the Castle. In the central part of each room, i.e. in the basement, as well as at the ground, first and second floors, a massive column supporting the ceilling of a given level was located. Investigation conducted after the collapse indicated that the pillar has dropped down by one level, without rotating, while the basement part collapsed under the ground. Most of the rubble fallen down into the basement, which became partially buried and not accessible for a time. A significant inclination of the bottom of the cavity towards western direction and a niche inside, probably of antropogenic origin, were documented. Fortunately, besides the material losses, there were no casulties. However, this event started a three-year long investigation into the causes of the failure. It also aimed to answer a question whether the rest of the structure founded on the Castle hill is safe.

1. Methods of geophisical and geotechnical investigation

The described mode of failure (collapse of the columns at a significant depth) and the conclusions of experts suggested, despite a large number of tests conducted so far, the possibility of the existence of some structures or openings in the ground under the Castle [1], [2]. These speculations were based on the number of anomalies registered in geophysical tests, which were compared to maps of planned bunkers from wartime. Despite numerous boreholes, this hypothesis could not be confirmed directly. Additionally, historical conditions and numerous renovations of the Castle added erroneous clues.

To minimize the risk associated with conducting construction works related to renovation, the Castle administration decided to conduct additional geotechnical and geophysical investigations. The first tests (boreholes) were conducted in May 2020 to fulfill the recommendations of an expert opinion [1], which stated the need to verify the ground conditions along the line between the failure location and a collapsed cavity that occurred in the 1970s on the northern terrace. A cavity was found along the borehole, at a depth between 12.5 m to 16.0 m below ground level (b.g.l.) [3].

This discovery justified the need for conducting additional works related to the investigation of the conditions. Additional tests were conducted in July 2020 [3] and September 2020 [4]. These tests aimed to detect or exclude underground cavities that might have influenced the failure of the column in the northern wing of the Castle. As part of both stages of the investigation, a total of 30 boreholes and 30 dynamic soundings were executed, up to a maximum depth of 19.5 m b.g.l., with a total length of approximately 475 m for the boreholes and approximately 345 m for the dynamic soundings. The tests were planned in the locations of anomalies noticed in the geophysical investigation.

The scope of the geophysical investigation included 36 ERT profiles, with a total length of over 3000 m. The assumed methodology included spacing of 2 m, 1 m, and 5 m for the electrodes, using a measuring system of 4x21 and 2x21, which resulted in high accuracy and investigation up to 15-17 m b.g.l., depending on the length of the profile. In terms of SRT seismic profiling, a total of 44 profiles were conducted with a total length of approximately 2400 m, mostly in the area of the Castle's courtyard. The tests were conducted using a parallel system of profiles every 1 m, with geophones spaced every 2 m. This allowed for obtaining a prospection up to approximately 20 m b.g.l. [5].

2. Results

Geophysical (ERT and SRT profiles) and geotechnical (boreholes and soundings) tests executed methodically and comprehensively (successive ground profiling with verification of encountered anomalies) revealed the existence of previously unknown underground structures (tunnels, bunkers) from the times of German Szczecin, under the Castle hill. In several boreholes at depths of approximately 15.4-17.3 m b.g.l. (8.4-6.5 m a.s.l.), the presence of these structures was confirmed. Using an inspection camera, their type and state were documented through photos and videos.

The obtained distributions of electrical resistivity of the ground were highly disturbed due to the presence of technical infrastructure (electrical cables), a few meters thick fill layer, and underground structures (reinforced concrete tunnels constructed for shelter). In the ERT_3 profile, a noticeable vertical boundary between zones of low (<50 Ωm) and high (>200 Ωm) electrical resistivities at the distance of 70 m was present. This boundary resulted from the strong shielding of the tunnel structure—reinforced precast concrete. This was an important discovery (confirmed by the borehole) from the point of view of further research.

A borehole (9ITB) performed in this area showed a void in the ground at a depth of approximately 15.4-17.3 m b.g.l. After inserting the camera into the hole, it was found that the drilled cavern was a fragment of reinforced concrete tunnels—German shelters from the World War II period. Similar to the boundary described earlier, the boundary between the anomalies was also encountered in the ERT_3 profile along a length of 50 meters. A borehole (12ITB) made in this place showed the presence of a collapsed corridor of the shelter. This was also confirmed in the SRT profile (Fig. 1). A detailed description of these discoveries, along with the documentation of the identified tunnels, is included in the investigation reports [3], [4]. Most of the underground corridors were constructed using the mining method with prefabricated reinforced concrete slabs and beams, measuring approximately 1.9 m high and 1.5 m wide, with local widening and narrowing of the tunnels. By analyzing the type of structure and comparing it with known objects of this type in Szczecin, these tunnels were identified as German tunnels from World War II, serving as shelters (Fig. 2a).

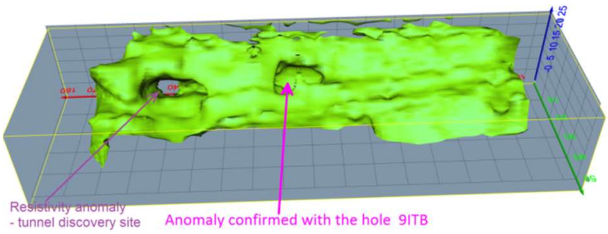

Fig. 1. An example of a 3D visualization of geophysical test results (spatial representation of resistance for a value of 140 m), a visible profile along the northern slope, which describes anomalies indicating the course of tunnels and one of the exits from the shelter on the east side of the slope [3].

At the site where the existence of the tunnel network was first confirmed (borehole 9 ITB - marked with an orange arrow in Fig. 2b), a detailed camera inspection revealed the presence of an intersection from which three corridors depart in mutually perpendicular directions (north, west, south). This discovery demonstrates that the previously discovered cavern in the area of the sinkhole from the 1970s (marked with a blue arrow in Fig. 2b) is closely related to the course in the vicinity of these tunnels. These objects, located at the base of the Castle hill, due to the nature of their structure (the use of a temporary casing made of bricks before the execution of the reinforced concrete structure—with the disturbed ground zone around) and the conditions related to their implementation (numerous leaks, especially at the unfinished stages, voids at the face), constitute drainage points and privileged groundwater flow directions. These conditions have led to the formation of local voids and erosive cavities along the tunnel structure, as confirmed by numerous inspections.


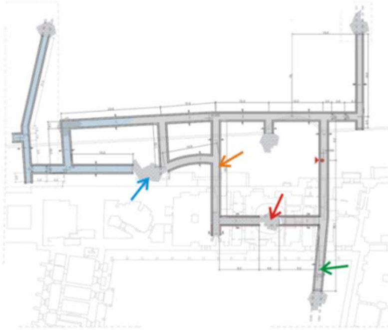

a) b)

Fig. 3 a) left: the view of the face of the unfinished tunnel under the courtyard (behind the green arrow according to Fig. 3b) – you can see the inflows, b) in the foreground next to (right) the established inventory of tunnels on the basis of direct exploration [7] – the red arrow indicates the site of the disaster and the collapse within the brick tunnel. The others are explained in the text.

The investigation conducted within the courtyard aimed to confirm or exclude the existence of the structure according to historical plans (an underground shelter for nearly 1500 people). Analysis of the results of the distribution of seismic wave velocities at a depth of approximately 16 m below ground level (the approximate depth of the detected tunnel location from earlier drillings) revealed two linear zones of reduced velocities, similar to the hypothetical tunnels depicted in the archival German plans. However, verification of these zones through drilling and dynamic probing (DPM, DPSH) indicated that these anomalies resulted from the lithological heterogeneity of the native soil, particularly the presence of highly water-bearing sandy layers of lower density. Thus, besides the fragment in the area of the 16ITB borehole (marked with a green arrow in Fig. 2), the existence of other underground structures in the ground under the courtyards was not confirmed. Additional studies in the courtyard also supported earlier findings, indicating the complex nature of the first groundwater level within the Castle Hill, characterized by sandy lenses at different depths, with confined water, which could influence the analysis of the causes of the disaster.

3. Summary

The historical background of a building significantly influences the variability of geotechnical conditions. Changes in structural systems, functions, or architectural elements over time can alter ground and water conditions. Cultural or historical layers, such as fill grounds around the structure, can accumulate and change rainwater flow patterns, leading to uneven subsidence. Additionally, historical events like fires, war devastation, and bombings can cause damage to monuments. In the case of the facility under discussion, military operations, including the construction of underground shelters, also negatively impacted the structure, contributing to structural failure. However, this facilitated the verification of legends and assumptions regarding the existence of underground structures, which could be confirmed through well-planned geophysical and geotechnical surveys.

References

1. Kamiński S. M., Nowaczyk S., Rzeźniczak J.: Ekspertyza techniczna dotycząca ustalenia przyczyn katastrofy budowlanej, jaka miała miejsce w dniu 11. maja 2017 r. w budynku Zamku Książąt Pomorskich w Szczecinie oraz jej oddziaływania na skrzydło północne Zamku Książąt Pomorskich, Szczecin 2019.
2. Lasocki M., Ostrowski Sz., Pacanowski G.: Sprawozdanie z badan geofizycznych w celu identyfikacji przyczyn katastrofy w NE skrzydle Zamku Książąt Pomorskich w Szczecinie, PIG-PIB, Warszawa 2018.
3. Godlewski T., Jaśkiewicz K., Niemyjska M., Mieszkowski R.: Sprawozdanie z badań geofizycznych i geotechnicznych podłoża skarp dotyczących kompleksowego zagospodarowania i modernizacji Tarasów Zamku Książąt Pomorskich w Szczecinie w kontekście geotechnicznych warunków posadowienia, ITB Warszawa, etap I, lipiec 2020.
4. Godlewski T., Jaśkiewicz K., Niemyjska M., Mieszkowski R.: Sprawozdanie z badań geofizycznych i geotechnicznych podłoża w celu realizacji zadania pn.: Modernizacja i remont dziedzińców Zamku Książąt Pomorskich w Szczecinie oraz zadania pn.: Kompleksowe zagospodarowanie tarasów Zamku Książąt Pomorskich w Szczecinie w kontekście geotechnicznych warunków posadowienia, ITB Warszawa, etap II, wrzesień 2020.

5. Kaczmarek Ł., Mieszkowski R., Kołpaczyński M., Pacanowski G.: Application of electrical resistivity tomography (ERT) In the investigation of Quaternary landslide zone, based on the selected regions of Płock slope, Studia Quaternaria, vol. 31, no. 2/2014.
6. Sokołowski D., Olbrychowski Sz.: Inwentaryzacja tunelu podziemnego Zamku Książąt Pomorskich, ARIKARA, Szczecin 2020.
7. Maślakowski M.: Analysis of foundation and structuras damages of the historic Oporów Castle, Inżynieria i Budownictwo, R 62, nr 6/2006, 313-314.

INFLUENCE OF MINING DEFORMATIONS ON THE EMERGENCY CONSTRUCTION OF A TENNIS COURTS COMPLEX

JAKUB KRUPA[1], *j.krupa@itb.pl*
LESZEK SŁOWIK[1]
MARIAN KAWULOK[1]
ARTUR PIEKARCZUK[1]

[1]Building Research Institute

Keywords: mining area, impact of mining exploitation, contionous surface deformation, mining damage, building damage

1. Introduction

Mining exploitation often leads to displacement of rock mass elements, resulting in continuous surface deformation. These deformations, such as subsidence troughs, can extend well beyond the exploited field [1]. The article discusses a case involving the impact of terrain deformation, specifically horizontal compressive strains, on a tennis courts complex.

The area where the complex is situated has undergone multiple mining exploitations. When assessing the cause-and-effect relationship between the damage to the complex and mining activities, it's crucial to consider the overlapping impacts from underground mining operations conducted before, during, and after its construction in 2016.

2. Mining conditions

The mining exploitation conducted from 2015 to 2019 resulted in continuous surface deformations, primarily in the form of mining depression troughs. Forecasted total values of indicators were generated to assess the extent of these deformations:

- resultant slope of the terrain: $T = 6.9‰$;
- horizontal deformation: $\varepsilon = 5.8‰$;
- terrain curvature radius: $R = 16.4$km.

The court complex area was classified as the 3rd category of mining area deformation [2] due to the terrain slope T and horizontal deformations ε. This classification indicated that the area was significantly affected by mining-induced deformations. The analysis revealed that the complex was unfavorably positioned, as it was subjected to continuous deformations caused by both ongoing and past mining activities [3]. Additionally, the presence of an exploitation edge under the plot further contributed to the adverse conditions.

Moreover, the mining exploitation also resulted in dynamic influences within the vicinity of the court complex [4]. Five high-energy tremors were recorded by the mining geophysics station within a radius of 1 km from the buildings of the courts. These tremors had a maximum energy of $E = 2\text{x}10^7$J and a maximum ground vibration acceleration of $a_{max} = 388\text{mm/s}^2$.

3. Technical characteristics of the court complex

The complex includes: a hall which is a roof for 4 tennis courts, 6 outdoor courts and elements of land development and utilities.

a) b)

Fig. 1. Buildings of the tennis court complex: a) the hall is located on the right side of the drawing, b) view of the interior of the hall

The construction design [5] and expertise [6] indicate that the hall was designed as a two-nave structure with a wooden arch system, supported by reinforced concrete footings interconnected with anchor and diagonal ties. The hall's projection measures 36.70m x 77.10m.

The foundation was placed at a depth of 1m below the ground level. To safeguard against mining exploitation, the foundation of the hall was divided into two segments with a 10cm wide expansion joint between them. However, no expansion joints were incorporated into the aboveground portion of the hall. The strip footings were reinforced to withstand additional forces resulting from horizontal soil deformations corresponding to the 3rd category of mining area. Additionally, a 10cm thick floor made of C20/25 concrete reinforced with polypropylene fibers was constructed above the foundation.

The ground floor structural elements of the hall consist of repeatable arched frames made of glued laminated timber. These frames are spaced at intervals of 5.14 meters and have a rectangular cross-section measuring 140mm in width and 520mm in height. Each frame is connected along the entire length of the hall with wooden purlins, which have a cross-section of 120mm x 120mm (200mm).

To provide additional structural support, steel S355JR round bars with a cross-section of 16mm are used as bracings. These bars are arranged in four fields within the hall.

4. Damage investigated

The mining exploitation caused damages and irregularities to the building elements and infrastructure (Fig. 2a, particularly affecting the tilt and deformation of the hall's load-bearing frames. Geodetic measurements [8] revealed significant deflections of the apex from the plane of the frame, with a maximum deflection of 161 mm.

While similar values of vertex displacements were observed based on geodetic measurements, the deviations of the northern segment differed significantly from those of the southern segment. These deflections and changes in the geometry of the braced fields resulted in excessive stress and damage to the bracings (Fig. 2b).

a) b)

Fig. 2. a) tilt of hall load-bearing frame, b) broken hall bracings

In addition to the damages to the load-bearing frames, other identified damages included: damages of concrete floor inside hall (Fig. 3b), deformation of the surface of the outdoor courts (Fig. 3c) and paving stones (Fig. 3a).

b

c

a

Fig. 3. a) deformation of paving stones, b) damage of concrete floor inside hall,
c) Deformation of the surface of the outdoor courts

5. Assessment of the causes of the damage

The structure was significantly affected by the pronounced deformation effects of the established concave mining trough, categorized as a 3rd mining category deformation. These effects manifested as horizontal deformations of the mining substrate, resulting in its compaction (ε). The expanded sections of the hall shifted with the terrain, causing displacement of the bases supporting the arched girders. The compressive deformations led to the sliding of foundations. As per the original design [5], the load-bearing transverse structures of the hall lacked full expansion joints along the entire height of the cross-section, contributing to the deformation of the load-bearing frames. The design flaw in this scenario was the absence of an expansion joint in accordance with guidelines [1, 7], from the foundation base to the roof slope. This oversight affected the interaction of the segments, resulting in deflection from the vertical and deformation of the hall's load-bearing frames.

Continued use of the court complex became feasible after implementing recommendations outlined in the study [6]. These recommendations focused on rectifying structural damage, which, if left unaddressed, could render the courts and infrastructure unusable in the event of further deformation.

6. Summary

Locating buildings in mining areas necessitates the implementation of various forms of construction prevention during the design and construction stages, aimed at mitigating damages and inconveniences resulting from additional impacts of mining exploitation. Design guidelines and technical requirements for buildings situated in mining areas are outlined in [1, 7].

In conclusion, it can be stated that there are two main causes of damage to the hall and related infrastructure:

- the effects of mining exploitation,
- improper adaptation of the structure or their complete omission in the elements of technical infrastructure.

References

1. Kawulok M. i inni: Wymagania techniczne dla obiektów budowlanych wznoszonych na terenach górniczych. Instrukcja ITB nr 364/2000. Warszawa 2007.
2. Kwiatek J. i inni: Ochrona obiektów budowlanych na terenach górniczych. Główny Instytut Górnictwa. Katowice 1997
3. Kawulok M.: Szkody górnicze w budownictwie. ITB. Warszawa 2015.
4. Mutke G. i inni: Zasady stosowania górniczej skali intensywności sejsmicznej GSIS-2017 […], seria: Instrukcje nr 23. Główny Instytut Górnictwa, Katowice 2018.
5. Projekt budowlano-wykonawczy zespołu hal rekreacyjno-sportowych wraz z budynkiem zaplecza. Tom I i II. Październik 2014.
6. Ekspertyza budowlana dotycząca stanu kompleksu kortów na okoliczność wpływów górniczych od prowadzonej eksploatacji. ITB. Katowice 2019.
7. Kawulok M.: Projektowanie budynków na terenach górniczych. Instrukcja ITB nr 416/2000. Warszawa 2006.
8. Operat pomiarowy – Pomiar kontrolny przemieszczeń. Katowice 2019.
9. Kawulok M.: Zasady stosowania na terenach górniczych nawierzchni utwardzonych drobnowymiarowymi elementami, na przykładzie kostki brukowej. Przegląd budowlany nr 2/2017.

MAINTENANCE AND INSPECTION OF RAILROAD TUNNELS IN THE USA

ANNA M. RAKOCZY[1,], *anna.rakoczy@pw.edu.pl*

[1]Zakład Geotechniki, Mostów i Budowli Podziemnych, Instytut Dróg i Mostów, Wydział Inżynierii Lądowej, Politechnika Warszawska

Keywords: Inspection Reports, Railway Tunnels, Tunnel Inspection, Tunnel Inventory, Tunnel Maintenance

Abstract: Maintenance of railway tunnels includes activities aimed at sustaining the safe use of the tunnel throughout its lifetime. An effective maintenance program helps reduce costs, reduce tunnel closures, increase public safety and ensure an adequate level of service. There are several publicly available standards and guides in the USA that provide detailed information and guidance about potential tunnel defects and damage, and how to maintain them. The AREMA Railway Manual, Chapter 1, Part 8, lists potential tunnel damage, and the AREMA Bridge Inspection Manual, Chapter 11 - Tunnel Inspection, provides information on the tunnel structure inspection protocol. Section 4.5 of the SRI TSI covers rules for the maintenance of railway tunnels, including identification of components that are subject to wear and degradation; definition of the limits of use of deteriorated elements, and description of measures to prevent this deterioration. The TOMIE Handbook provides detailed information on the operation, maintenance, inspection, and evaluation of tunnels. This article describes the practices and standards of tunnel inspection, monitoring, and maintenance in the USA.

1. Introduction

Railroad tunnels are integral to the rail transit industry and crucial for facilitating passenger movement across cities in the United States. They provide alternatives for crossing bodies of water or navigating through physical barriers such as mountains, existing roadways, railroads, or facilities. Additionally, tunnels offer a viable means to mitigate potential environmental impacts stemming from traffic congestion, including air quality deterioration, noise pollution, or visual intrusion. They also serve to provide alternatives for pedestrian movement and safeguard areas of special cultural or historical significance, such as conservation districts, buildings, or private properties. Furthermore, tunnels contribute to sustainability efforts by helping to preserve natural habitats and minimizing disturbances to surface land. However, the existing tunnel infrastructure in the USA inventory comprises many tunnels that are over 100 years old, posing potential chokepoints that could severely disrupt passenger mobility in the event of a fire or security incident [1].

Figure 1 illustrates the year of construction completion in the United States [2]. Approximately half of the tunnels were constructed over 50 years ago, with around 15% exceeding 100 years in age. This indicates a nearly equal distribution between newer tunnels (less than 50 years old) and older tunnels (over 50 years old).

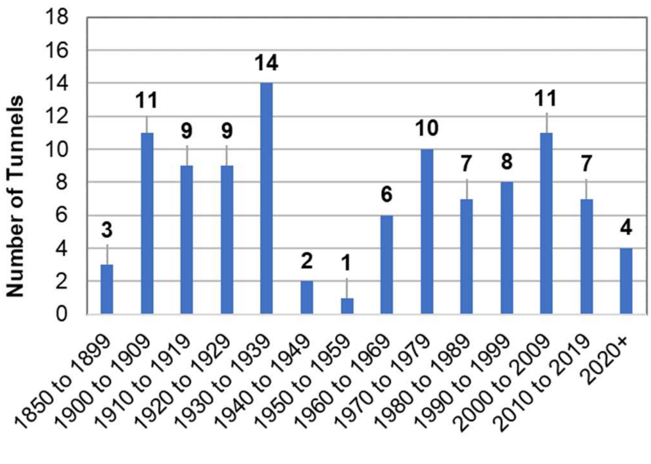

Fig. 1. Age of rail transit tunnels in the USA

The cost of maintaining and renovating tunnel systems must be balanced against available funds. Resources for repairs and improvements are limited, necessitating prioritization to make informed investment decisions. Expert opinions are typically sought upon receipt of inspection data. Sound engineering judgment is employed to assess the consequences of tunnel system or component failure in terms of overall safety, service level, and cost. In cases where design data is lacking, additional inspection and testing may be necessary. Risk assessment techniques should encompass strategies for deploying, operating, maintaining, upgrading, and disposing of tunnel system components in a cost-effective manner.

Several publicly available standards and guides in the USA offer information on tunnel maintenance, inspection, and rehabilitation, including:

- FHWA-NHI-10-034 [3] - A comprehensive document contains details on design and rehabilitation. The standard is dedicated to road tunnels. Most topics also cover railway tunnels, but some aspects of railway operation are missing.
- AREMA Bridge Inspection Handbook [4] - Provides general guidelines but lacks details.
- FHWA-HIF-15-005 (TOMIE Manual) [5] - A comprehensive document contains details about the design. The standard is dedicated to road and rail tunnels. However, some aspects of rails operation are missing.
- 23 CFR Part 650 (2015) [6] - Minimum requirements for highway tunnels. Most topics also cover railway tunnels, but some aspects of railway operation are missing.

The available documents are often dedicated to road tunnels, therefore, some agencies are developing their own standards to supplement the necessary information.

2. Maintenance of tunnels

Older tunnel infrastructure necessitates adequate maintenance, inspection, and rehabilitation measures to ensure continued safe operation. An effective maintenance program helps reduce costs, minimize tunnel closures, enhance public safety, and ensure an appropriate level of use. Maintenance activities span from simple tasks to complex undertakings, as indicated in the hierarchy below:

- Removing debris, snow, and ice
- Washing tunnel structures, flushing drains, tightening bolts, and changing light bulbs
- Servicing equipment, painting fixtures, and restoring pavement
- Tests, verifications, measurements, and calibrations
- Planned interventions
- Unplanned interventions
- Rehabilitation (large-scale repairs and upgrades are implemented).

Tunnel operation can be divided into two parts: normal operation and emergency response. Normal operating procedures include maintaining traffic flows, tunnel traffic closures, studying weather conditions, clearing roadway hazards, inspecting critical areas, checking functional systems, servicing equipment, clearing the tunnel facility, maintaining vehicles and equipment, completing daily logs and checklists, processing work orders, checking information, and evaluating sensors and meters. Emergency response includes:

- Impacts and collisions: remove vehicles, clear debris, repair pavement, inspect tunnel damage
- Fires: emergency ventilation measures, rapid detection
- Floods: pump systems
- Earthquakes: structural damage, leaks

An effective tunnel maintenance program reduces costs, decreases closures, and increases safety. Ideally, the maintenance strategies of a tunnel facility should strike a balance between preventative maintenance and on-demand maintenance. If safety or structural concerns are identified in the process of carrying out maintenance tasks, then the defects should be addressed promptly.

3. Inspection of tunnels

Tunnel inspection requires multidisciplinary personnel familiar with various functional aspects of a tunnel, including civil/structural, mechanical, electrical, drainage, and ventilation components, as well as operational aspects such as signals, communication, fire-life safety, and security components. The inspectors should be certified and knowledgeable about inspector responsibilities [5].

The FHWA has developed the National Tunnel Inspection Standards (NTIS) [7], TOMIE Manual [5], and Specifications for the National Tunnel Inventory (SNTI) [8] to help safeguard tunnels and ensure reliable levels of service on all public roads. The NTIS includes the legal requirements of the National Tunnel Inspection Program (NTIP); the TOMIE and SNTI manual have been incorporated by reference into the NTIS to expand upon the requirements. The TOMIE Manual is a resource to assist in the development of tunnel operations, maintenance, inspection, and evaluation programs; it provides uniform and consistent guidance. The SNTI provides instructions on how to transfer inventory and inspection data to FHWA, which will be maintained in the National Tunnel Inventory (NTI) database to track the condition of road tunnels throughout the United States.

Additionally, the SNTI is used to collect tunnel inventory items such as tunnel identification, age and level of service, classification, geometric data, inspection, load rating and postings, navigation, and structure type. The SNTI inventory items require the following information: the item name, specification, commentary, examples, format, and alphanumeric identification. The specification contains descriptions of each inventory item and provides a series of explanations in the commentary section.

4. Summary

The cost of maintaining and repairing tunnel systems must be balanced against available funds. Resources for repair and maintenance are limited; therefore, repairs must be assessed and prioritized to make informed investment decisions. A tool such as the SNTI (Specifications for National Tunnel Inventory), which provides instructions on how to transfer inventory and inspection data to FHWA, is a good example of how to operate with an extensive tunnel network. The National Tunnel Inventory (NTI) database collects and stores information to track the status of tunnels throughout the United States. This is the direction that should be implemented in Poland, where the number of tunnels is growing every year, and their maintenance will be a challenge for future generations of engineers.

References

1. Lipiński J.: Fundamenty pod maszyny, Arkady, Warszawa 1985.
2. Chvatal T.: Neuer schnell erhartender Zement. Zement Kalk Gips, nr 8/1973.
3. Kowalski J., Kowalski K., Kowalski M. i inni: Tytuł, Wydawnictwo, rok wydania.
4. Rakoczy, A.M, Wilk, S., Jones, MC., "Security and Safety of Rail Transit Tunnels", Transportation Research Record 2019, Vol. 2673(1) 92–101, National Academy of Sciences: Transportation Research Board 2019
5. Rakoczy, A., S. Wilk, and M. C. Jones, Review of Specifications and Guidelines for Rail Tunnel Design, Construction, Maintenance, and Rehabilitation. Report Prepared for FTA and CUTR, P-18-008. 2018.
6. Federal Highway Administration. FHWA-NHI-10-034, Technical Manual for Design and Construction of Road Tunnels – Civil Elements. December 2009.
7. American Railway Engineering Maintenance-of-Way Association. AREMA Bridge Inspection Handbook, Chapter 11 – Tunnel Inspection. 2010 Edition.
8. Federal Highway Administration. FHWA-HIF-15-005, Tunnel Operations, Maintenance, Inspection, and Evaluation TOMIE Manual, Washington D.C. 2015.
9. Code of Federal Regulations. 23 CFR Part 650 National Tunnel Inspection Standards, NTIS for highway tunnels. 2015.
10. Federal Highway Administration. FHWA, Rule: 80 FR 41349 "National Tunnel Inspection Standards," 2015.
11. Federal Highway Administration. FHWA-HIF-15-006, "Specifications for National Tunnel Inventory (SNTI)," 2015 edition, available in electronic format at http://www.fhwa.dot.gov/bridge/inspection/tunnel/.

EMERGENCY CONDITION OF A MULTI-FAMILY BUILDING IN THE INFLUENCE OF MINING EFFECTS

LESZEK SŁOWIK[1], *l.slowik@itb.pl*
JANUSZ RUSEK[2]
LESZEK CHOMACKI[1]

[1]Building Research Institute
[2]Department Of Engineering Surveying And Civil Engineering, AGH University Of Science And Technology

Keywords: discontinuous deformation of the mining area, flexure, field threshold, continuous deformation of the mining area, mining trough, structural failure, construction prevention, damage to the building

1. Introduction

In areas of active mining activity, which have been ongoing for several decades, there are numerous risks related to deformation, water, and dynamic factors such as paraseismic shocks [1].

This article discusses a case involving complex mining influences on a building located in one of the cities of Upper Silesia. This includes deformation excitations caused by discontinuous deformation, represented by a linear threshold (referred to as flexure) [2,3], as well as soil pressures on the foundation walls and building foundations within the concave part of the mining trough [1,4].

As a result of mining impacts, the building structure experienced numerous damages in the form of cracks and displacements, reaching a level of emergency that threatened the safety of its use according to its intended purpose. The paper presents an assessment of the causes of damage and the scope of preventive temporary construction works that enabled the safe and continuous use of the building.

2. Mining influences

Discontinuous deformations of the mining substrate are identified in both mining and post-mining areas [5]. Terrain thresholds on the ground surface were inventoried on the northwest side and directly under the building (Fig. 1a, b). They appeared on the ground surface as a result of intensive mining exploitation in this area, within the zone of overlapping edges of mining plots in the seams. This subject is discussed in detail in [6].

Continuous deformation of the terrain in the form of mining basins results from underground mining of minerals, including hard coal. In total, a deposit with a thickness of about 35.5 m was exploited, but up to 1965, to a total height of about 9.0 m, mainly with dry filling. After 1965, the total thickness of the selected 12 seams was about 25 m, primarily with roof collapses.

Data provided by the Mining Plant and documentation indicate that the ongoing mining operations, planned until 2027, will be conducted with roof collapse. Until November 2021, the longwall, with a thickness of 2.0 to 3.0 m, at a depth of about 750 m, was operated beneath the district where the building in question is located.

This exploitation resulted in the occurrence of continuous deformation indicators on the surface, classified into the III category of mining area. The building was within the impact range of the established mining trough, with the dominant influence of horizontal deformations of the mining subsoil, resulting in its compaction, not exceeding $\varepsilon- \leq 6$ mm/m

a) b)

Fig. 1. Terrain thresholds: a) under the pavement and the building on the north-west side of the building, b) in the road surface on the north-west side of the building

3. Characteristics of the building

The building subject to mining influence was erected at the beginning of the 20th century. In the horizontal projection, it has a shape similar to a rectangle with dimensions of 9.91 m x 15.24 m. The segment, built in semi-compact development, has a full basement and three above-ground storeys. The basic structural system consists of brick load-bearing walls. Brick vaults were made above the basement, and wooden-frame ceilings over the remaining floors. The foundation is made of brick foundation walls. The whole is crowned with a wooden gable roof structure covered with ceramic tiles. During the period of use, the building structure was strengthened against the negative effects of mining influences. Steel anchors were used, located in the ceiling levels, running along the longitudinal and transverse directions, fastened in the corners of the building to steel angles located along the edges of the vertical walls along their entire height.

a) b) c) d)

Fig. 2. Damages to the building: a) cross-cracks in the lintel, sill and inter-window strips of the northern wall, b) cross-cracks in the lintel, sill and inter-window strips of the southern wall, c) vertical and horizontal cracks and pushing into the building interior, the western gable wall on the basement floor, d) cracks in the longitudinal wall in the basement

Inventory of the state of damage to the building is carried out systematically as part of construction supervision. The first damage to the building structure was observed in September 2021 when the work front in the mining plot was located approximately 100 m from the building. The purpose of their systematization can be generally distinguished:

- damage visible on the outside of the building: cross-cracks in the lintel, sill and inter-window strips, occurring in the long external northern (Fig. 2a) and southern (Fig. 2b) walls; horizontal cut with displacement towards the interior of the building of the western gable wall, visible on the ground floor level;
- damage visible inside the building: horizontal and vertical cracks in the western gable wall visible on the basement (Fig. 2c); cracks in the walls on the basement (Fig. 2d); numerous cracks in the vaults in the basement; uplift of the basement floor; cracks in the walls of the staircase, cracks in the longitudinal stiffening wall on the ground, first and second floors; numerous cracks in the lintel strips of door openings and deformation of the floor in residential premises.

The observed damage was characterized by considerable intensity. The cracks in the transverse load-bearing walls on the basement storey had a width of up to 20 mm, while in the case of the western gable wall, it was moved from the plane towards the center of the building. Cracks in the external longitudinal walls and the internal stiffening wall and the staircase walls had a width of up to 25 mm. The cracks in the vaults above the basement were up to 3mm wide. It should be added that these damages intensified over time, more or less within 3 months from the time of their occurrence.

The building in question was subject to the simultaneous impact of discontinuous and continuous mining deformations that occurred on the surface as a result of mining exploitation. Maintaining the continuity of use of the building, in accordance with its intended use, required urgent ad hoc construction activities, which are generally discussed in point 4.

4. Construction works recommended for implementation

The significant intensity of damage to the building structure determined the need to undertake urgent, ad hoc construction activities. These works were recommended for implementation as a result of construction supervision carried out by employees of the Building Research Institute. In general, they concerned:

- re-bricking of through-cracks in the longitudinal walls shown in Fig. 2a and Fig. 2b, and the internal stiffening wall;
- hammering a concrete slab at the western gable wall, the stiffness of which intensified the pressure on this partition;
- support of the cracked western gable wall displaced inside the building (Fig. 3a);
- support of the ceiling above the basement in the south-west part of the building;
- support of the staircase wall in the attic level (Fig. 3b);
- hammering loose plaster, stairways and ceilings in living quarters.

a)

b)

Fig. 3. Temporary support: a) of the western gable wall, cracked and moved inside the building, b) of the staircase wall in the attic level

5. Summary

The chapter of the monograph discusses the case of an emergency condition in the structure of a residential building, which arose as a result of the disclosure of deformation influences on the surface of the area related to the effects of a mining operation carried out until November 2021. Simultaneously, the structure of the discussed segment was affected by discontinuous linear deformations in the form of terrain sills and a concave mining trough. The undertaken remedial actions and strengthening of the structure made it possible to continue its use. Ultimately, the possible renovation of the building will be determined by the technical and economic opinion commissioned by the mine responsible for causing the damage.

References

1. Kawulok M.: Szkody górnicze w budownictwie. Wydawnictwo Instytutu Techniki Budowlanej, 2015.
2. Kowalski A.: Deformacje powierzchni na terenach górniczych kopalń węgla kamiennego. Głowny Instytut Górnictwa, 2020.
3. Popiołek E.: Ochrona terenów górniczych. Wydawnictwo AGH, 2009.
4. Kwiatek J.: Obiekty budowlane na terenach górniczych. Główny Instytut Górnictwa, 2017
5. Kawulok M.: Ocena przydatności terenów górniczych do zabudowy. Wydawnictwo Instytutu Techniki Budowlanej, 2013.
6. Ignacy D.: Wymagania dotyczące opisu zagrożenia deformacjami nieciągłymi terenów górniczych w opiniach geologiczno-górniczych i dokumentacjach geologiczno-inżynierskich. Obiekty budowlane na terenach górniczych. Polski Związek Inżynierów i Techników Budownictwa, Katowice, 2018.

THE ANALYSIS OF THE BREAKDOWN OF A COMMERCIAL BUILDING DURING ITS RENOVATION

JÓZEF SZCZOTKA[1], *j.szczotka@outlook.com*

[1]F.U.I Józef Szczotka, adres: 43-426 Gumna, ul. Miodowa 31

Abstract: The following paper describes the breakdown of a commercial building located in Cieszyn, Silesia, Poland. The breakdown occurred during the construction works regarding drainage and the foundations of the building. The analysis of the breakdown was done indicating the protection works enabling the continuation of the renovation.

Keywords: building embedding, band drainage, foundation walls reinforcement, ground works, wall insulation, reinforced concrete band

1. Introduction

In order to elevate the standard of commercial spaces, investors undertake renovations. According to Polish construction law, several renovations do not require project documentation. Occasionally, documentation may be incomplete to reduce costs, or there may be inadequate supervision at renovation sites. In most cases, the construction company serves as the sole source of advice. The apparent savings during the preparation of renovation works often result in poor execution and increased costs.

When works involve anti-moisture isolation of the foundation, including drainage, in buildings lacking construction records, a supervisor with a suitable construction license should be present. Such supervision ensures proper ground isolation works. The lack of experience in the construction team may lead to building fractures and, in extreme cases, structural failure. Foundation-related works are specialized and should be carried out by companies with appropriate experience. Therefore, consideration should be given to introducing changes in construction law to eliminate such situations and mandate proper applications, including construction documentation and technology.

2. Building description

The building is located on Ladna Street, Cieszyn, Poland. This commercial building was erected between the two World Wars at the beginning of the last century. It consists of three stories: the basement, ground floor, and attic. The building was constructed using a traditional mixed-bearing system. The foundations are made of full brick and stone-concrete, while the walls are constructed of full brick. The basement ceiling is covered with a staple vault supported by steel beams, and the ground floor has a timber ceiling cover. The roof timberwork consists of purlins covered with ceramic tiles.

The building is directly embedded without horizontal isolation. At the embedding level, there is resilient and hard-resilient clay. The foundations are made of full brick laid with lime mortar, with stones also placed on lime mortar, matching the width of the construction walls of the building. The mixed-bearing system includes brick walls of various widths made of full brick.

The building was not in use during the renovation. Until the day of collapse, renovation works were ongoing, focusing on exposing the outer part of the foundations to reinforce and vertically isolate them.".

3. Renovation works till breakdown

In order to eliminate dampness of the outer walls, the owner of the building had undertaken the following actions:

- East and south foundation excavation was done to the depth below the embedding.
- The ground works were done manually and mechanically.
- The vertical covers of the foundations were cleaned and prepared for the horizontal isolation as well as the reinforcement made of a concrete holdfast wall.

4. Description of construction breakdown

Fig.1. The view of the building partly collapsed.

On the evening of November 9th, 2019, the southern part of the building leaned out, causing the collapse of the commercial section. The southern and eastern walls suffered partial damage, along with the ceiling cover over the ground floor and the roof timberwork with its covering (Fig. 1).

At the time of the collapse, there were no construction teams present on-site. Additionally, there had been torrential rain in the area for a few days leading up to the incident.

5. Analysis of breakdown causes

There were two main causes of the breakdown of the commercial building in Cieszyn, Poland:

- The excavation of the building foundations had been done below the level of the embedding of the building which resulted in surpassing the vertical bearing capacity of the ground below the level of embedding. The range of the excavation was shown of the existing foundations of the top wall in the south-east corner as well as the level of embedding, the depth of the excavation compared with the basis of the foundations on the ground.
- The direct cause was the loss of the ground bearing capacity at the level of the embedding of the building in the south-east corner. The ground clay at the level of embedding became ductile due to previous abundant precipitation.

6. Inaccuracies during the renovation

The basic inaccuracies during the renovation were:

- The excavation along the longitudinal (east) wall at its entire length as well the top (south) wall. In such cases the excavations should be done in sections;
- The most crucial inaccuracy was the excavation of the south-east corner of the building;
- The depth of the excavations which surpassed the depth of the embedding;
- The lack of proper supervision of the renovation works by an authorised person experienced in the field.

7. Description of protection works

The aims of the protection works are:

- Fencing off the danger zone permanently in order to eliminate trespassing as well as signing it with warning signs;
- Outsourcing of companies experienced in such works to do protection and demolition works;
- Outsourcing of an authorised person to supervise the works permanently;
- Demolition to be done mechanically by an excavator with a long arm to eliminate danger;

- The range of the demolition includes the roof timberwork together with the attic walls and chimneys, ceiling covers and south-east ground floor walls.

8. Round-up and repair solutions

Recommendations to reinforce the foundations of the collapsed part of the building:

- Placing a concrete mix with a waterproof and self-compacting additive in the excavations along the intact zones of the building, at a minimum height of 70 cm. This applies to the excavation along the east wall and partially along the top wall in the southeast corner. The concrete should be pumped in using a concrete pump to eliminate the risk of sending workers into the danger zone.
- Using a concrete mix of class C20/25.
- After the concrete has reached at least 70% of its guaranteed strength, commence work on breaking the roof timberwork and its covering, to avoid damaging the structure of the part of the building that should be preserved.
- The aforementioned work should be carried out from a crane positioned at least 8 meters away from the building to ensure worker safety.
- Upon completion of the aforementioned tasks, proceed with insulating the foundation walls, installing band drainage, and laying a gravel layer up to the height of the excavation.
- Prepare project documentation for the restoration of the collapsed part of the building.
- Conduct construction works related to the restoration of the building (see Fig. 2).

Considering all the material related to the breakdown of the commercial building, there is only one conclusion: every general renovation of a building should be prepared with proper documentation, the selection of a suitable building firm, and supervision by an authorized person. Attempts to cut costs on these actions often result in serious financial consequences and civil liability. The breakdown revealed significant gaps in Polish law as well as the incompetence of building firms in the market. While this incident only resulted in financial loss, the potential consequences could have been much worse if workers had been on-site. Therefore, the importance of proper planning before renovation works cannot be overstated.

Fig. 2. The view of the building under reconstruction

References

1. Z. Hyrnik, Ekspertyza techniczna określająca stan techniczny budynku w kontekście zaistniałej katastrofy budowlanej części obiektu w dniu 09.11.2019r. położonego w Cieszynie, zgodnie z Postanowieniem PINB (Świętoszówka, listopad 2019)
2. J. Szczotka, Opinia techniczna dotycząca stanu technicznego budynku po uszkodzonego w wyniku awarii położonego w Cieszynie, (Cieszyn, luty 2020)
3. E. Masłowski, D. Spiżewska, Wzmacnianie konstrukcji budowlanych, Arkady (Warszawa 2000)

SECTION V
FAILURES OF METAL STRUCTURES

PRE-FAILURE CONDITION OF THE INCLINED COAL CONVEYOR STRUCTURE

PAWEŁ A. KRÓL[1], *pawel.krol@pw.edu.pl*
AGATA GODLEWSKA[2]
RADOSŁAW JÓŹWIK[2]
KACPER WIŚNIEWSKI[2]

[1]Warsaw University of Technology, Faculty of Civil Engineering
[2]CONSTRUCTION Sp. z o.o., Warsaw

Keywords: inclined structure, coal conveyor, deformations, torsional deformations, transverse profile, longitudinal profile, wall truss, load bearing capacity assessment

1. Introduction and description of the structure

Inclined coal conveyors are key elements of process lines that feed coal to power units in power plants and combined heat and power plants that utilize solid fuels for energy production. They serve as supporting structures for belt conveyors that transport coal. The structure described in this case study is located within the premises of the Kozienice Power Station in Świerże Górne, in southern Mazovia. During the operation of the structure, technical inspection staff observed visually apparent deepening deflections of the conveyor spans and twisted bottom chord members of the longitudinal side trusses. Cyclical geodetic measurements confirmed these observations. The deformation measurements prompted a comprehensive assessment of the technical condition of the structure to ensure its continued safe operation and to determine the causes of the deformations.

The inclined coal conveyor discussed in this paper is a structure that measures 128.0 m in length, 8.0 m in width, and 4.6 m in height up to the roof ridge. It spans between the tunnel leading from the transfer station and the transfer tower situated next to the boiler house. Longitudinally, the structure is constructed as a three-span elevated steel conveyor, with spans measuring 43.7 m, 43.7 m, and 40.6 m in the axes of supports, respectively. The conveyor is inclined at an angle of 16° in relation to the ground level.

In terms of the transverse profile, the conveyor consists of closed frame structures spaced every 3.0 m along the length of each span and every 2.15 m in the support areas. These transverse frame structures are connected along the length of the conveyor with longitudinal connecting beams made of 2xUPN300 profiles. These beams are joined with rigid battens—one at the eaves joint level and one at the level of the bottom edge of the column. These connecting beams serve as the bottom chord and the upper chord of the side wall trusses, with the columns of the transverse frames acting as the posts of these trusses. At the bottom part, the transverse frame systems are connected using transverse floor beams, which support the concrete ceiling of the coal conveyor and the belt conveyors (see Fig. 1).

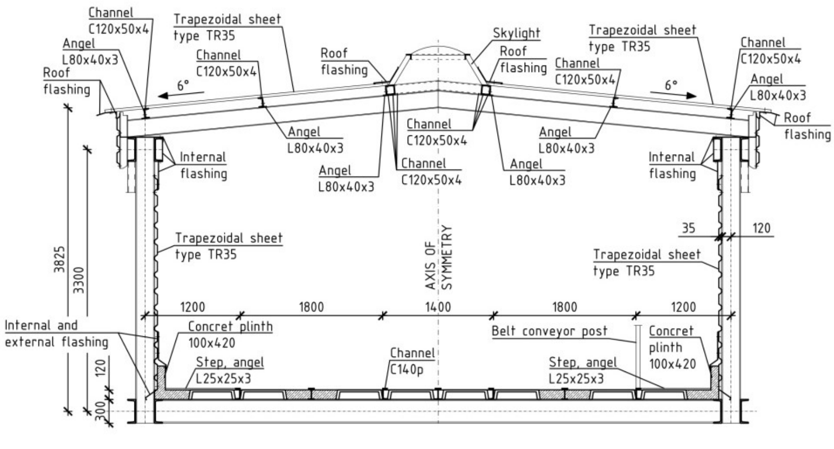

Fig. 1. View of the transverse profile of the structure in the current condition

2. History of the structure

The inclined coal conveyor described in this paper was constructed in 1977 based on design documentation developed in 1975 and was in continuous operation from 1977 to 1999. In 1999, due to its poor technical condition [1, 2], the structure underwent modernization that included updates to the walls, roof, and ceiling of the coal conveyor. Additionally, extensive renovation work was carried out, which involved updating the anti-corrosion protective coatings. The solutions applied during this modernization significantly impacted the subsequent method of loading and using the structure. Notably, the changes made to the ceiling edge were crucial in terms of the later operation of the structure and the deformations observed. The work involved, among other things, the dismantling of a jointless floor slab approximately 40 cm wide along the side trusses on both sides, and the construction of a reinforced concrete plinth 40 cm high, which also incorporated a portion of the adjacent floor slab. The differences in the method of constructing the floor slab according to the original design and after the 1999 modernization are illustrated in Fig. 2.

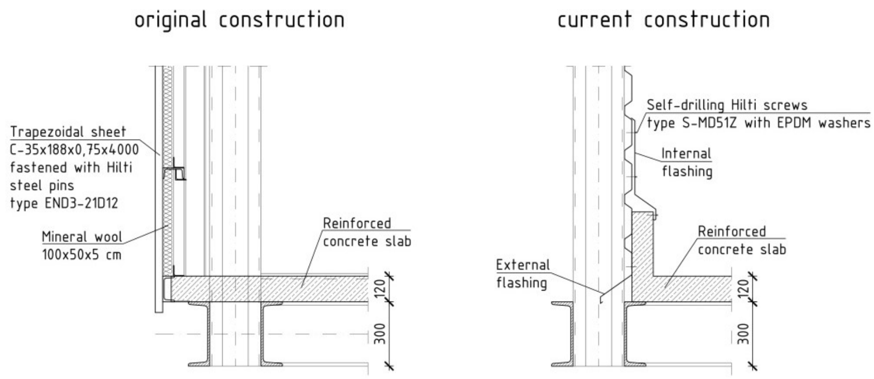

a) b)

Fig. 2. Differences in the method of making and supporting the floor slab according to: a) original design solutions, b) condition after the modernization in 1999

3. Structural deformations

An in-depth analysis of the cyclical archival geodetic measurements of the inclined coal conveyor's geometry confirmed that significant differences in structural deformation were observed between the measurements conducted in the years 1999-2000, coinciding with the period of structural system reconstruction. This period included modifications to the support method and the solution applied to the floor slab edge of the structure [3]. Measurements of the support subsidence did not reveal any irregularities in this regard [4], which, along with the geotechnical tests conducted [5], confirmed the high level of consolidation of the soil subbase below the foundation footing level of the intermediate supports. On-site inspections carried out in the summer of 2020, as well as supplementary geodetic measurements of deformations of the built-up bottom side chords of the longitudinal wall trusses, confirmed the earlier in-situ macroscopic observations, as shown in Fig. 3.

Fig. 3. Deflection of the bottom side chord of the longitudinal wall truss

4. Calculation analysis of the structure

To verify whether the structure meets the standard conditions of the ultimate limit state (ULS) and the serviceability limit state (SLS), four calculation models of the structure were developed using a computer program, each differing in terms of assumptions made, geometry, modeling methods of selected members, and support conditions:

- **Model 1**: Takes into account an ideal geometry of the structure, consistent with the original design documentation, with the bottom chord of the wall truss modeled as a built-up chord member with battens. This model provides for axial transfer of loads from the floor slab to the member.
- **Model 2:** Takes into account an ideal geometry of the structure as in Model 1, with the bottom chord of the wall truss modeled in the form of two parallel members, connected with tilting connectors imitating battens. This model allows for the transfer of loads from the floor slab only to one of the truss chords, as shown in Fig. 2b.
- **Model 3:** Considers structural assembly errors in the form of induced load on the supports and assumes that the truss bottom chord will be used as a built-up member (similar to Model 1). Instead of the columns—intermediate supports—the model accounts for elastic supports prone to movement in each direction.
- **Model 4:** At the client's request, a hypothetical situation was assumed, considering the implementation of measures to prevent a potential failure. Asymmetric variable loads were assumed, coming from only one working conveyor, and the coal conveyor structure was supported with additional temporary or permanent pin supports near the center line of each span.

Additionally, a buckling analysis of the bottom chords of trusses was performed for the cases presented in Models 1 and 3 (the 2xUPN 300 built-up member model) and in Model 2 (loading of a single UPN 300 member). For the individual C-shaped beams of the bottom chord from Model 2, an analysis of the buckling impact on the stress levels of these members was also conducted.

5. Summary

The results of the comprehensive stress and strength analyzes confirmed that the structure is in a pre-failure condition and specific interventions need to be made to improve operating conditions of the structure and prevent a potential collapse. Based on results of one of the analyzed computational models, a conceptual design and directions of the suggested modernization were developed. A complete design documentation was prepared, covering not only structural works, but also other renovation works. The adopted solutions enable carrying out the works in continuous operation, without the need to shut down the structure, which was one of Client's requirements that increased the difficulty of the design work. A first stage of the designed work was implemented in the summer of 2021, which involved construction of three additional intermediate supports and necessary reinforcements of selected structural members. The remaining work is planned for the next summer season.

References

1. Ocena stanu technicznego – obiekty nawęglania od wieży przesypowej budynku głównego do wywrotnicy wagonowej nr 3 (Assessment of the technical condition – coal feeding structures from the transfer tower of the main building to rail car dumper No. 3 – text in Polish), "Energoprojekt-Warszawa" S.A., Warsaw 1998.
2. Obiekty nawęglania bl. 500 MW. Most skośny nawęglania. Aktualizacja (*Coal feeding structures to the 500 MW unit. Inclined coal conveyor. Update* – text in Polish), "Energoprojekt-Warszawa" S.A., Warsaw 1999.
3. Pomiary geodezyjne elementów mostów skośnych nawęglania (*Geodetic measurements of inclined coal conveyor members* – text in Polish), "Geomap" Sp. z o.o., Kielce 2007.
4. Okresowy pomiar przemieszczeń obiektów elektrowni w latach 2017-2019 (*Cyclical measurement of displacements of power plant structures in 2017-2019* – text in Polish), "Geoplan" Zakład Usług Geodezyjnych, Warsaw 2019.
5. Dokumentacja geologiczno-inżynierska określająca warunki geologiczno-inżynierskie dla potrzeb budowy instalacji katalitycznego odazotowania spalin dla kotłów AP-1650 nr 9 i 10 oraz modernizacji elektrofiltrów na terenie ENEA Wytwarzanie Sp. z o.o. w Świerżach Górnych (*Geological and engineering documentation determining geological and engineering conditions for the construction of a flue gas catalytic denitrification system for AP-1650 boilers No. 9 and 10 and the modernization of electrostatic precipitators at ENEA Wytwarzanie Sp. z o.o. in Świerże Górne* – text in Polish), GEOTEKO Serwis Sp. z o.o., Warsaw 2016.

RUPTURE OF THE STEEL SHEET OF THE SILO WALL A CASE STUDY

JAKUB MARCINOWSKI[1], *j.marcinowski@ib.uz.zgora.pl*
VOLODYMYR SAKHAROV[1]

[1]University of Zielona Góra, Institute of Building Engineering

Keywords: steel silo, corrugated steel sheet, rupture of the steel sheet, material tests, analytical calculations, numerical simulations

1. Introduction

Steel grain silos have become a permanent fixture in the landscape of contemporary villages and are essential on farms specializing in cereal cultivation. Both relatively small silos for poultry feed, known as bins with capacities of several cubic meters, and real giants with capacities of up to 30,000 cubic meters are constructed. Unfortunately, silos are engineering structures that fail relatively frequently, which is why they are the subject of particular interest among many researchers (see, for example, [1], [2]).

Fig. 1. The view of the lower part of damaged silo

Modern steel silos are constructed as large cylindrical vessels for flat-bottom silos. In the case of silos with hoppers, the structure is a composition of a cylindrical part and a conical part (hopper), supported on peripheral columns. The cylindrical section is typically assembled from horizontally corrugated steel sheets, strengthened by external columns made of thin-walled, cold-formed sections. This type of silo, used for grain storage, became the subject of the author's interest after a wall rupture occurred in the third year of the silo's operation. The main purpose of the investigations presented in this paper was to determine the causes of the silo's failure.

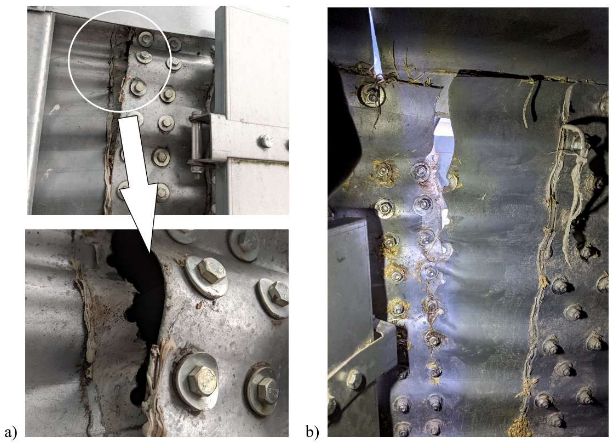

Fig. 2. Details of the wall rupture: a) view from outside b) view from the inside

The failure occurred when the silo was completely filled with wheat, and the discharging operation was initiated. Shortly after the start of the discharging operation, a wall rupture appeared, and a narrow stream of grain began to flow from the location indicated in Fig. 1. The discharging was immediately stopped, and the opening was provisionally blocked. Subsequently, the silo supplier installed strengthening rings (see Fig. 1) to prevent further progression of the rupture. Afterwards, the upper layers of grain were vacuumed out to reduce the silo's capacity to half. The remaining wheat was then discharged using the standard discharging devices installed in the silo. Details of the wall rupture are shown in Fig. 2.

The paper presents detailed considerations focused on determining the cause of the described silo failure. An analytical approach based on formulas available in the Eurocodes [3], [4], [5], and [6] was adopted to check the load-bearing capacity of the silo's wall at the level where the rupture occurred. Additionally, numerical simulations were performed, aiming to determine the stress distribution within the course where the rupture took place.

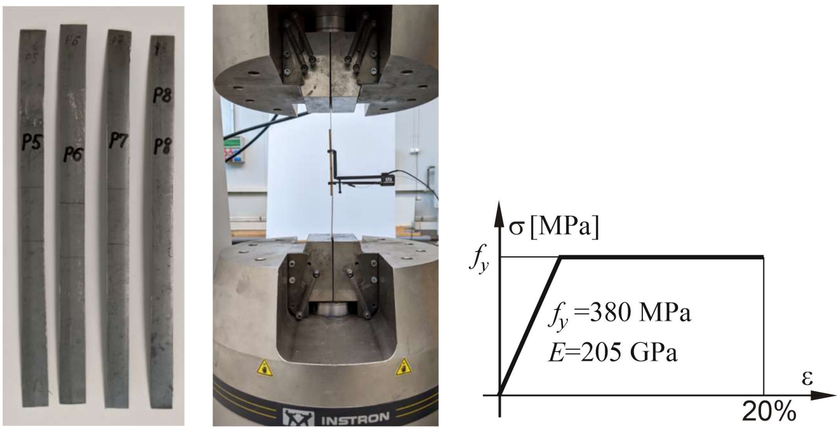

a) b) c)

Fig. 3. Coupons used in material tests a), the coupon during the test b) and the material model c)

2. Details of performed analyses

In the first step, material tests were conducted on coupons cut from the steel sheet remaining after the silo assembly. Figure 3a displays four coupons and the course of the material test. As a result, the following material parameters were obtained: yield strength f_y = 380 MPa, ultimate tensile strength f_u = 400 MPa, and modulus of elasticity E = 205 GPa. The simplified material model adopted for the numerical analyses is shown in Figure 3c.

Loads acting on the silo's wall were defined based on Eurocode [3] specifications for wheat. The silo, with a height of 16 m (cylindrical part) and a diameter of 8.16 m, was classified as slender (comp. [3]). The total capacity of the silo was 760 tons, placing it in Action Assessment Class 2 (comp. [3]). Both scenarios were considered: loads during filling and loads during discharging.

Resistances were checked according to rules given in Eurocodes [4], [5], and [6]. As a result of resistance verifications, it was revealed that some limit states had been surpassed. Specifically, the resistance of the net area of a cross-section along two sections weakened by holes for fasteners (bolts) was too low (measured at 249.09 kN) compared to the calculated axial (peripheral) force at the analyzed location (measured at 259.54 kN). This force also exceeded the bearing resistance of the bolt connection, which was determined to be 225.69 kN. The ratio of exertion was 1.04 (259.54/249.09) and 1.15 (259.54/225.69), respectively, indicating the degree to which the resistance was surpassed.

The considered segment of the silo's wall was also analyzed numerically. To this end, the corrugated wall was modelled along with all details like holes for fasteners, external pillars, and constructional details of the hatch door housing. Both components of wall pressure were adopted as determined based on [3]. The Abaqus system, based on the finite element method, was used, and the analyses were carried out within a materially nonlinear range. The finite element mesh was designed to detect all local effects suspected within the analyzed area of the silo wall. The total number of nodes of the used mesh was 487,307, and the total number of degrees of freedom of the discrete model was nearly 3 million. The materially nonlinear analysis (MNA) was carried out using the incremental Newton-Raphson approach with load control.

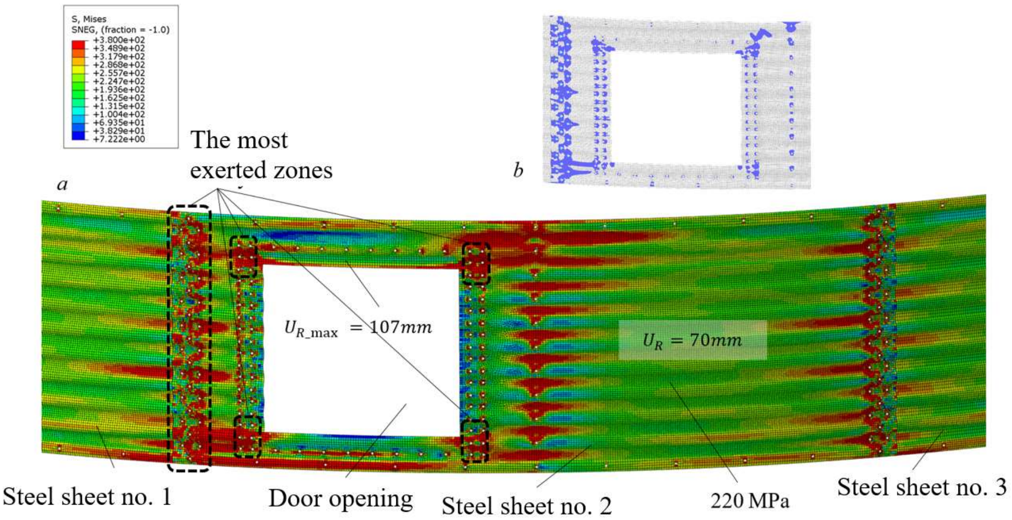

Fig. 4. Stress and strains distributions within steel sheets: *a* – equivalent stresses due to Huber-Mises-Hencky hypothesis in [MPa], *b* – effective plastic strains greater than 0.1%

The most significant results of the numerical simulations are presented in Fig. 4. Equivalent stresses, based on the Huber-Mises-Hencky stress criterion, are shown in Fig. 4a, where spots in dark red indicate zones where the yield state was achieved. Effective plastic strains greater than 0.1% are depicted in Fig. 4b as zones painted blue. "Ur," indicated in Fig. 4a, represents the radial displacement. The plots in Fig. 4 reveal that the most stressed zones occur within the lap connections between steel sheets and in the vicinity of the hatch door housing, precisely where the rupture occurred.

3. Conclusions

The primary objective of the analyses performed was to determine the cause of the rupture in the silo wall sheets at the border between the second and third courses, counting from the ring of the hopper. This overarching goal defined the scope of the analyses conducted. Both analytical calculations, based on detailed standard provisions, and numerical simulations were limited to the scope necessary to explain the observed mechanism of the silo rupture.

As a result of the analytical calculations, which utilized standard procedures, it was shown that when the silo is filled with wheat, the bolt bearing capacity is exceeded at the point where the sheets of the silo wall are joined, at the level of the second course. Another potential breakage point is the section weakened by holes for bolts that fix the manhole door frame to the shell sheet.

The identified mechanisms of failure of the sheet metal of the considered course were also confirmed in the performed numerical simulations. The most probable mechanism was the rupture of the sheet metal in the vicinity of the manhole door installation, and this is what occurred in the silo in question.

Summarizing the analyses carried out, it can be concluded that the main cause of the silo failure was the excessively thin corrugated sheet of the silo wall, which was only 1 mm thick, and the incorrect design of the lap joints between individual sheets and between the silo wall sheet and the hatch door housing.

References

1. Rejowski K., Iwicki P., Simplified stability analysis of steel cylindrical silos with corrugated walls and vertical columns. Recent Progress in Steel and Composite Structures – Giżejowski et. al. (Eds). Taylor & Francis Group,London 2016, s. 525–532.
2. Hotała E., Skotny Ł., Kuśnierek M., Boniecka J.: Experimental investigations on the resistance of vertical stiffeners of steel silos shells made of corrugated sheets. Recent Progress in Steel and Composite Structures – Giżejowski et. al. (Eds). Taylor&Francis Group, London 2016, s. 186 –187.EN 1991-4: 2006, Eurocode 1. Actions on structures. Part 4: Silos and tanks.
3. EN 1993-1-1: 2006, Eurocode 3. Design of steel structures - Part 1-1: General rules and rules for buildings.
4. EN 1993-1-3: 2006, Eurocode 3. Design of steel structures - Part 1-3: General rules - Supplementary rules for cold-formed members and sheeting.
5. EN 1993-1-8: 2006, Eurocode 3. Design of steel structures - Part 1-8: Design of joints.
6. EN 1993-4-1: 2009, Eurocode 3. Design of steel structures - Part 4-1: Silos.

REINFORCEMENT OF DAMAGED POWER PLANT STEEL STRUCTURE FOR ADDITIONAL LOADS

WIESŁAW PACZKOWSKI[1]
KRZYSZTOF KOZIEŁ[2]
SZYMON SKIBICKI[1], *szymon.skibicki@zut.edu.pl*
MARCIN MATYL[2]
MACIEJ WIŚNIOWSKI[3]
TOMASZ WRÓBLEWSKI[1]

[1]Faculty of Civil and Environmental Engineering, West Pomeranian University of Technology in Szczecin, al. Piastów 50a, 70-311 Szczecin, Poland
[2]Optimal Design of Structures Krzysztof Kozieł, ul. Na Piasku 12a, 44-122 Gliwice
[3]Silesian University of Technology, Faculty of Civil Engineering, ul. Akademicka 2A, 44-100 Gliwice

Keywords: steel structure, ground subsidence, coal power plant, laser scanning, LiDAR

1. Introduction

In Polish coal power plants, modernization works are being carried out with the main purpose of adapting combustion installations to national and EU environmental requirements. These modernizations often introduce new loads on existing, already extensively used power plant structures.

The problem described in the article emerged during the preparation of project documentation for the SCR (Selective Catalytic Reduction) reactor support structure. The introduction of the SCR system resulted in new horizontal forces acting on the support structure of the boiler room. As part of the analysis of the impact on the existing structure, the designer determined that the structure was overloaded due to non-uniform ground settlement and had already been partially reinforced. This situation necessitated a detailed analysis and design of reinforcement.

The analyzed object is a steel frame structure of a coal power plant boiler room, built in the 1970s. The analysis covered the area of four blocks (Fig. 1). The structure of the boiler room for the entire plant consists of four separate sections, each measuring 72 m x 36 m. Each section contains two blocks. The multi-storey frame structure of one section features rigid floor plates with a column grid of 12 m x 9 m. In each separate part, two boilers are suspended from a grid supported on the tops of the columns.

The analysis of the structure was performed not only due to the planned works described in Section 1 but also due to numerous existing structural damages. These damages were particularly evident in the diagonals of the vertical bracing systems, as shown in Fig. 2. The analysis of existing damages allowed for their categorization into three types: 1) local loss of stability of bars; 2) global loss of stability of bars; 3) local damage, for example, rupture of tension bars. Examples of these damages are presented in Fig. 2.

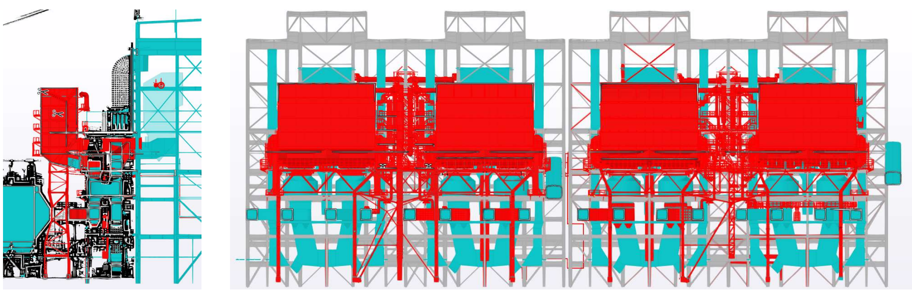

Fig. 1. View on blocks 5-8, red colour marks newly designed instalations and structures

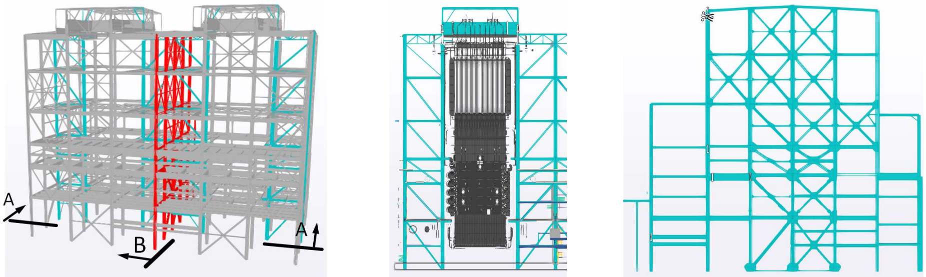

a) b) c)

Fig. 2. Construction of one of four boiler room sections with boilers hanging at +60m, a) view on a segment of blocks 5-6, b) cross-section A-A, c) cross-section B-B

The main cause of structural damage was the uneven settlement of the ground over years of operation. Structures as complex as the skeletal steel frames of the boiler room in a coal power plant are very sensitive to uneven ground settlement. This sensitivity is due to the high degree of static indeterminacy and an additional factor: the suspension of boilers, each with a mass of about 3600 tons, on a grid that rests on top of the supporting columns at a level of about 60 meters

a) b) c)

Fig. 3. Damages of the steel structure, a) buckling of gusset plate, b) buckling of a bracing bar, c) ruptured of bracing at the node

2. Laser scanning (LiDAR) as a tool for design

Laser scanning of structures, an engineering method, enables the measurement of even highly complex building structures [1]–[4]. This method facilitates the determination of detailed dimensions of a structure or its parts [2], its imperfections [1], or its global deformation state [3], [4].

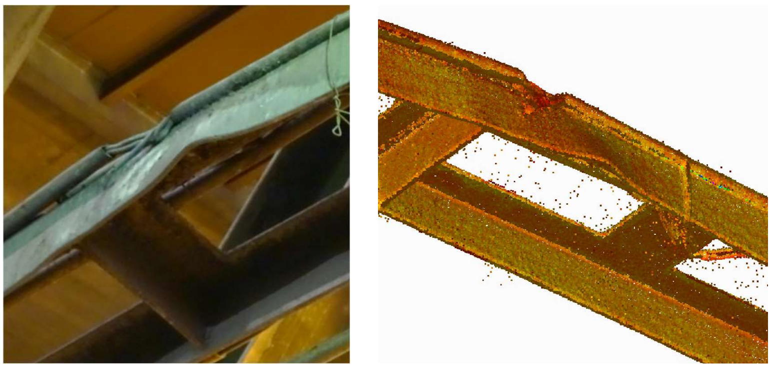

a) b)

Fig. 4. Comparison of a real-life photo of damaged member with a model from point cloud data

To obtain a detailed model of the structure and assess its global deformation state, laser scanning (LiDAR) was employed. The resulting point cloud, approximately 460 GB when compressed, provided detailed morphology of the structure, cross-sectional dimensions of the members, and enabled a detailed identification of the damage. In addition to obtaining detailed geometric data (Fig. 3), laser scanning was also used to determine the global deformation state of the structure.

By analyzing the point cloud data, the shape of column axes was identified, illustrating the displacement of the structure due to loads and settlements that occurred during the operation of the power plant. Data obtained from laser scanning confirmed that the standard requirements for columns' inclination imperfections are admissible.

3. Calculation model

Two types of analysis were applied: Linear Analysis (LA) and Geometrically and Materially Nonlinear Analysis with Imperfections (GMNIA). The results of the analysis using the linear elastic material model (LA) did not allow for an adequate evaluation of the structure's capacity. In many cases, the forces transmitted from the bracings to the columns—as a result of non-uniform settlement—exceeded the resistance of the bracing members. Consequently, the GMNIA model was employed, which considers the effects of stiffness degradation of the vertical bracing members, including buckling of compression members and yield/rupture of tension members, on the forces in the columns. GMNIA analyses of the structure were performed using two types of design models: 1) a global model comprising rod-shell 3D models of the boiler room, used to calculate internal forces and deformations of the structure, and 2) a local model using rod-shell detailed models of selected structural elements. Due to local stress concentrations in columns, particularly in the areas of connections with bolts, it was necessary to assess the amount of plastic reserve.

The results obtained from these calculations were used to evaluate the stress state of the columns and to analyze the global stability of the structure. Based on this analysis, the design of reinforcements was developed.

4. Reinforcement solution

Numerous analyses of global and local models led to the introduction of a structural reinforcement system consisting of local interventions that significantly improve the performance of the structure. This system enabled the restoration of the structure's safety with minimal intervention. This approach required complex numerical analyses, described in the paper, which were performed based on detailed data obtained from geodetic monitoring and point cloud.

5. Conclusions

The basic conclusions of this study can be presented as follows:

- Application of the linear analysis (LA) method would lead to an inadequate assessment of the technical condition; the obtained results of LA analysis showed in many cases the exceeding of the load capacity of bracing members.
- Proper calculation results were obtained based on advanced GMNIA nonlinear models, including the introduction of nonlinear hinges at failure member locations.
- The complexity of the object required the use of advanced measurement techniques in the form of laser scanning (LiDAR) to obtain data concerning the structure and its deformation. Obtaining this data using traditional methods would have been impossible.
- It was necessary to use geodetic monitoring data of the ground settlement in order to assess correctly the stress state of the structure.
- The use of local reinforcements of the structure allowed to restore its correct and safe operation.

Based on complex numerical analyses and using advanced measurement techniques, the existing structure was successfully strengthened and the SCR reactor support structure was designed and installed without compromising its operation and safety.

References

1. Feng, P.; Zou, Y.; Hu, L.; Liu, T. Use of 3D Laser Scanning on Evaluating Reduction of Initial Geometric Imperfection of Steel Column with Pre-Stressed CFRP. Engineering Structures 2019, 198, 109527, doi:10.1016/j.engstruct.2019.109527.
2. Leonov, A. v.; Anikushkin, M.N.; Ivanov, A. v.; Ovcharov, S. v.; Bobkov, A.E.; Baturin, Y.M. Laser Scanning and 3D Modeling of the Shukhov Hyperboloid Tower in Moscow. Journal of Cultural Heritage 2015, 16, 551–559, doi:10.1016/j.culher.2014.09.014.
3. Nowak, R.; Orłowicz, R.; Rutkowski, R. Use of TLS (LiDAR) for Building Diagnostics with the Example of a Historic Building in Karlino., doi:10.3390/buildings10020024.
4. Paczkowski, W.; Wróblewski, T.; Skibicki, S. Skanowanie Laserowe Stalowej Konstrukcji Elektrowni Węglowej. BUILDER 2020, 273, 22–25, doi:10.5604/01.3001.0013.8793.

ANALYSIS OF THE TECHNICAL CONDITION OF THE SOOT SILO BATTERIES

ZDZISŁAW PISAREK[1], *pisarzdz@prz.edu.pl*
ANDRZEJ WOJNAR[1]

[1]Rzeszow University of Technology

Keywords: metal structures, reinforced concrete structures, steel silos

1. Subject and scope of the paper

The paper presents the results of an expert opinion on the technical condition of steel silos located in an industrial plant. It includes selected results of measurements, calculation assumptions, methods of execution, and results of static-strength calculations. Recommendations concerning further exploitation of the silos are also provided.

The scope of the paper includes:

- A description of the structural inventory of the facility.
- An assessment of the technical condition of the steel structure of the silos and their reinforced concrete support structure.
- Preliminary verification of the technical condition of 12 silos and selection of 6 silos for further tests, including measurement of steel wall thickness, assessment of the technical condition of the walls, and the cone hopper of the silos.
- Checking the tightness of welded steel connections, technical condition of structural reinforcements, and joints.
- Checking the correctness of execution of the shaft with pneumatic transfer of soot.
- Analysis of damage causes and recommendations.


Fig. 1. View of the silo battery

2. Brief technical description of the silo battery

The silo battery consists of 12 silos, each with a capacity of 275 m³, and includes technical facilities for loading and unloading. The warehouse, a battery of silos, stores soot, silica, and chalk. The supporting structure of the silos is a monolithic reinforced concrete frame with plan dimensions of 36.70 x 12.80 meters and a height of 9.6 meters above the foundation slab level. The reinforced concrete columns of the frame are arranged in a grid of 6.0 x 6.0 meters and have cross-sections of 70 x 80 cm for edge columns and 70 x 120 cm for middle columns, with a height of 7.25 meters. The columns are interconnected at the top by a reinforced concrete grate consisting of beams with a cross-section of 70 x 120 cm. A 60 cm thick floor slab rests on these beams, filling the space in the corners of the grate from the silo hopper. The casing of the support structure is made from prefabricated reinforced concrete wall slabs attached to the columns of the reinforced concrete frame. The front wall features two rows of steel industrial windows.

a) b) c)

Fig. 2. View of a) reinforced concrete support structure and floor slab, b) cylindrical shell and c) cone hopper of the silo battery

The silo battery consists of twelve identical cylindrical silos, each with a height of 12.0 meters and a diameter of 5.40 meters. The silo shell is composed of eight segments, each 1.5 meters high. The segments are made from sheet metal, likely originally specified at thicknesses of 12 mm and 10 mm. The silo chamber shell is reinforced along its height with four clamps made of C240 steel channel. At the base of the silo chamber shell, there is a 730 mm high bottom ring, which consists of two horizontal sheets and is strengthened by 40 stiffeners made of 16 mm thick steel sheet. This ring is secured to the supporting structure with 12 M24 bolts. At the top of the silo shell, a 500 mm high horizontal top ring is present, stiffened with eight vertical plates and supports the steel grate of the filter hall floor. At a height of 6.67 meters, spanning the entire length of the silo battery, there is a gallery for silo service.

The staircase structure is supported by six steel columns made from HKS 700-11-300-30 welded I-beams. These columns are braced with transoms made of IPN240 I-beams and braces made of L150x15 and L100x8 angles. The steel columns of the staircase, in addition to the silos, also support the filter hall above.

The filter hall, situated above the silos and staircases, features a floor structure composed of a steel grate made from HKS 500-10-300-30 I-beams, IPN 300 I-beams, and IPN 160 I-beams, covered by a 20 cm thick reinforced concrete floor. The main load-bearing frames of the filter hall are also made of HKS 500x10x300x30 sections, with a span of 12.0 meters and a height of 5.0 meters, providing support for the wall casing bolts. The rafters are constructed from C120 channels, and the purlins from IPN 240 I-beams, spaced every 3.0 meters. The spacing between the wall enclosure transoms is 1.2 meters, and roof sheeting is attached to both the rafters and purlins.

Fig 3. View of staircase and filter hall (above silos battery)

3. Silo shell thickness measurements

Measurements of the silo shell thickness were conducted at four different levels: at the level of the reinforced concrete slab above the support structure, between the ribbing of the bottom ring, and above its top flange. Additional measurements were taken from the platform between the silos and of the thickness of the hopper sheets. It was observed that the measurement results were relatively consistent. The calculated average sheet thickness values ranged between 8 and 10 mm, while the measured values varied from 7.7 to 11.0 mm. This variance is likely attributable to the original thickness of the plates used for the shell rather than to corrosion or operational wear. The measurement results are summarized in a table. Notably, the plates used from level +7.50 to level +10.50 show a step change in thickness, indicating that a thinner plate was utilized in this section.

4. Verifying static-strength calculations

- A computational model of the silo battery structure was created using the Finite Element Method (FEM).
- The model employed beam-type and shell-type elements:
- Columns, beams, and bars of the framework were modelled using beam-type finite elements with six degrees of freedom at each node.
- Reinforced concrete slabs and the steel shell of the silos were modelled using shell-type finite elements.
- Wall cladding was modelled using flat panels, facilitating the separation of climatic loads such as snow loads and wind effects on the steel bar.
- Supports for the reinforced concrete columns were modelled as rigid supports (restraints).

Loads were adopted according to [1] and [2], with load combinations according to [3].

The load from the soot (stored material), including its own weight and the pressure of soot on the silo walls as well as friction against the walls, was determined in accordance with PN-EN 1991-4, following the guidelines and procedures outlined in Chapter 5 [2]. The specific weight of soot was assumed to be 18 kN/m³, based on information from Polsaros Sp. z o.o., a supplier of chemical raw materials primarily for the tire, rubber, and rubber industries [4]. Steel column supports were modeled as pinned, non-sliding supports.

The results of the calculations are presented as equivalent stress maps in the silo walls, with stress values determined according to the Mises stress hypothesis.

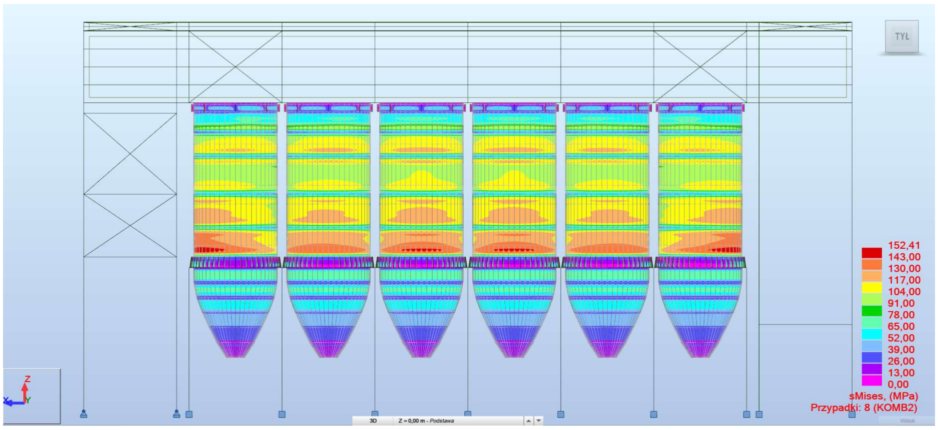

Fig. 4. Map of equivalent stresses in steel silo walls

5. Current technical condition of silo batteries

Based on the measurements and visual inspections conducted, the overall technical condition of the silo battery, along with the support structure and the filter hall in the carbon black warehouse, should be considered sufficient.

- The reinforced concrete support structure of the silos is in relatively good condition. No cracks or deformations that would indicate overloading were observed.

- Steel elements of the staircase support structure show no significant deformation or damage. Any local bending or damage observed does not affect the load-bearing capacity of the elements.
- The technical condition of the silos is satisfactory. There are no signs of damage or cracks on them, and no pitting corrosion was detected. However, damage to the paint coating was observed in many places on the surface.

References

1. EN 1991-1-3. Eurokode 1. Actions on structures. Part 1-3: General actions. Snow loads. CEN. 2002.
2. EN 1991-1-4. Eurokode 1. Actions on structures. Part 1-4: General actions. Wind actions. CEN. 2004.
3. EN 1990. Eurokode. Basis of structural design. CEN. 2001.
4. https://polsaros.com/pl/

UNIVERSAL MODULAR SUPPORT STRUCTURES AS AN ALTERNATIVE OF CURRENT TRANSMISSION IN EMERGENCY SITUATIONS

Grzegorz Kapłański[1]
Grzegorz Kowalczyk[2]
Leszek Szojda[3], *e-mail: leszek.szojda@polsl.pl*
Grzegorz Wandzik[4]
Kamil Włodarczyk[5]

[3,4] Department of Structural Engineering, Silesian University of Technology Gliwice
[1,2,5] Arinet sp. z o.o., Gliwice

Abstract: The System of the Universal Modular Support Structures (UMKW) has been detailed in this chapter for constructing high voltage steel towers that support temporary power lines with voltages of 110, 220, or 400 kV. This system is specifically designed for use in emergency situations, during renovation works, or when temporary conflicts arise with existing lines. The UMKW system offers two types of temporary support structures: single-shaft structures and portal frames. Both configurations consist of rectangular steel lattice modules, which serve as the fundamental components of the system. UMKW columns are versatile, able to accommodate various voltage lines and load requirements through the use of guy lines that adapt the structure to meet existing demands. Importantly, the system eschews traditional foundations, relying instead on the stability provided by connecting guy lines to the ground using screw anchors or employing ballast blocks. Preliminary analysis of hundreds of system variants, coupled with a dedicated computer application, facilitates rapid selection of appropriate structures in urgent scenarios. Several towers constructed using UMKW modules have successfully undergone real-scale field tests..

Keywords: emergency restoration system for power lines, power line support structures, steel structures, modular structures, overhead power lines

1. Introduction

Overhead power lines are influenced by cable loads and environmental factors such as wind, icing, and temperature changes. These interactions are dominant and, due to their random nature, forecasting the load states of the structure becomes challenging, increasing the likelihood of emergency situations. Additionally, exceptional circumstances such as cable breakage or excessive foundation settlement, possibly caused by flooding, further complicate stability and safety, necessitating quick removal or temporary solutions.

These considerations led to the development of the Universal Modular Support Structures (UMKW) system, designed for constructing temporary sections of power lines with voltages of 110, 220, and 400 kV. The system utilizes small-sized prefabricated lattice steel modules, allowing for the rapid construction of various support structures in diverse and often challenging locations. Adapted to meet Polish standards for power line design, both in terms of load and electrical requirements, the UMKW system has seen extensive research and development since its inception in 2018, supported by funding from project [1]. Since implementation, the system has been successfully deployed multiple times and was awarded a gold medal at Energetab, Poland’s largest energy fair, in 2020 [2].

2. Elements of the UMKW system

The Universal Modular Support Structures (UMKW) system primarily consists of two types of prefabricated spatial trusses with a cross-section of 0.5 x 0.5 meters and lengths of 1.5 and 3.0 meters, respectively. Additionally, the system includes a cubic element with each side measuring 0.50 meters. The walls of this cubic module are solid, except for two sides designed to attach line equipment. This module plays a crucial role in structuring system nodes, such as connecting the shaft with the transom or linking the transom to the lightning tower. Illustrations of the 1.5-meter-long truss module and the cubic element are provided in Figures 1a and 1b.

In addition to the larger modular elements, the UMKW system incorporates smaller overall elements of equipment, which are used, among other things, for connecting guy-ropes and insulators to the structure.

The foundation of the temporary structures within the UMKW system, designed for rapid assembly and relatively low vertical loads, utilizes a steel and wooden foundation grating laid directly on the ground surface. This setup effectively disperses vertical stresses to values not exceeding 100 kPa, enabling the placement of the grating structure on almost any type of terrain. Vertical stabilization of the structure is achieved through the use of guy-ropes, which are secured in the ground with screw anchors or supported by concrete ballast blocks to maintain stability.

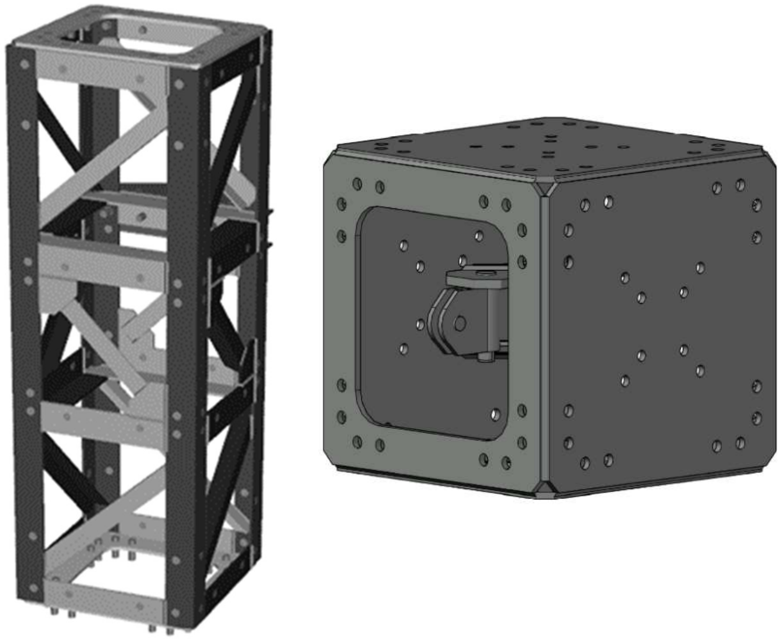

a) b)

Fig. 1. a) Basic truss module with a length of 1.5 m and base dimensions of 0.5 x 0.5 m,
b) cubic connection module for attaching lines accessories

3. Characteristics of the UMKW system

UMKW systems are classified within the power industry as part of the Emergency Restoration System (ERS) group. Each ERS system's concept, in addition to meeting technical requirements, also considers aspects related to transport, storage, assembly, and economics. Given the urgency of addressing failures promptly, UMKW system components must be readily available in sufficient quantities. Due to the wide variety of overhead power pole types, the UMKW must accommodate all configurations using repeatable modules.

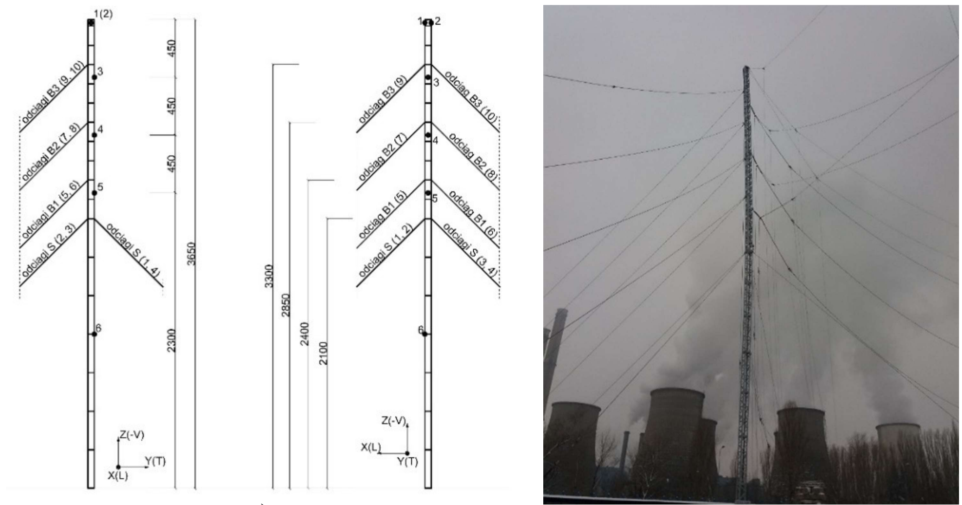

a) b)

Fig. 2. a) the silhouette of the UMKW single-shaft corner column for the vertical arrangement of 110 kV line conductors at the turn of the line route up to 90 ° (with load application points in field tests), b) photo of a single-shaft column of the UMKW during natural-scale field tests

To achieve this, comprehensive static and strength analyses were performed on over 500 structural systems. These systems varied by the function of the pole, span length, route angle, cable suspension height, and the rated voltage of the line, primarily focusing on 110 kV lines. The analyses involved determining forces according to code action systems as outlined in standards [3] and [4]. An example of a single-traverse column from the UMKW system is illustrated in Fig. 2a.

4. Research on the structure of UMKW on a natural scale

The requirement for all newly designed power line poles is to undergo real-scale testing, which is governed by the specifications of the European standard [5]. The modular supporting structures of the UMKW system have successfully passed these tests at the Elektromontaj SA Tower Testing Laboratory in Bucharest. The testing process included six poles representing all tension levels, differing in shape (single-shaft poles and portal frames) and the arrangement of stays. A photograph of one of the tested columns is featured in Fig. 2b, alongside the load pattern shown in Fig. 2a.

5. Summary

The UMKW system is designed to ensure the continuous transmission of electricity via power lines in emergency or repair situations. Developed for 110, 220, and 400 kV transmission and distribution lines, the main advantage of the system lies in its ability to rapidly assemble the necessary supporting structures. The design solutions adopted allow the UMKW poles to replace various types of poles, even in challenging terrain conditions. Several years of conceptual, design, and analytical work, alongside a range of field tests and software development efforts, have culminated in the creation of the first Polish comprehensive system of temporary support structures. With its broader implementation, the UMKW system is expected to significantly reduce the time required to restore the functionality of power lines during emergencies. The initial implementations and growing interest from the energy community suggest that the system's popularity is set to increase.

Acknowledgement

Development works of the UMKW system were financed by the grant no. POIR.01.01.01-00-0792 / 17 of the National Center for Research and Development, Intelligent Development Operational Program 2014 - 2020, action 1.1 / sub-action 1.1.1.

References

1. Pojekt POIR.01.01.01-00-0792/17 „Prace badawczo-rozwojowe nad kompleksowym systemem Emergency Restoration System na potrzeby krajowego rynku elektroenergetycznego w oparciu o technologię Uniwersalnych Modułowych Konstrukcji Wsporczych" ARINET Sp. z o.o., 2017,
2. Górecki P., Kapłański G., Kowalczyk G, Włodarczyk K.: Złoty Medal Targów Energetab 2020 dla polskiego systemu linii tymczasowych 110 kV, 220 kV i 400 kV. Wiadomości Energetyczne, Rok LXXXVIII 2020 nr 11, s. 35-38,
3. PN-EN 50341-1: 2013 – Elektroenergetyczne linie napowietrzne prądu przemiennego powyżej 1 kV. Część 1: Wymagania ogólne. Specyfikacje wspólne.
4. PN-EN 50341-3-22:2010: Elektroenergetyczne linie napowietrzne prądu przemiennego powyżej 45 kV, Część 3: Zbiór normatywnych warunków krajowych, PKN Warszawa 2010,
5. PN-EN 60652:2006: Badania obciążeniowe konstrukcji wsporczych elektroenergetycznych linii napowietrznych, PKN Warszawa 2006.

SECTION VI
FAILURES OF REINFORCED CONCRETE STRUCTURES

INFLUENCE OF THE TIE SYSTEM ON THE DEVELOPMENT OF A PROGRESSIVE COLLAPSE CAUSED BY THE FAILURE OF AN EDGE COLUMN IN THE RC FLAT SLAB

LIDIA BUDA-OŻÓG[1]
JOANNA ZIĘBA[1], *j.zieba@prz.edu.pl*
DAMIAN NYKIEL[1]
KATARZYNA SIEŃKOWSKA[1]

[1]Katedra Konstrukcji Budowlanych, Wydział Budownictwa Inżynierii Środowiska i Architektury, Politechnika Rzeszowska

Keywords: tie system, progressive collapse, column, RC flat slab, load capacity, strain

1. Introduction

RC flat slabs are one of the most popular and effective methods for shaping plates in buildings. They are favoured by architects for their flexibility in shaping the space within a building and are easier to manufacture compared to slabs with beams. However, flat slab systems are more susceptible to the development of progressive collapse because they lack beams to help redistribute loads in an accident situation [1].

2. Tying system in flat slabs

Methodologies for preventing accidental or unlikely structural failures are categorized into two approaches: direct and indirect. The direct approach involves recognizing potential hazards and ensuring that the structure is adequately fortified against their effects. It incorporates two primary strategies: one based on determining the value of exceptional impacts and another focused on limiting local failure. The indirect approach, on the other hand, simplifies design by overlooking the initiating actions and focuses only on their potential effects, such as the loss of a load-bearing member.

Two design methods that can mitigate the effects of possible structural failure are the key element method and the Alternate Load Path (ALP) method. The key element method involves designing a critical load-bearing element in such a way that its failure does not lead to disproportionate or extensive damage beyond a specified area, ensuring it can withstand the design exception load. The Alternate Load Path (ALP) method, conversely, accommodates the failure of a specific element by utilizing the additional strength and ductility of the materials and the enhanced load-bearing capacity afforded by the structural geometry, allowing it to support much greater loads than originally designed.

The effectiveness of the ALP method heavily relies on well-formed ties that connect the structural elements. Using formulas specified in standards [2] and [3], it is possible to calculate the force in the horizontal ties which helps redistribute vertical loads following the failure of supports. Generally, the force in the tendon between supports can be assumed as:

$$F = 0{,}8(g + p)l \text{ lub } 75 \text{ kN} \tag{1}$$

where:

g – permanent surface action applied on the considered floor;
q - variable surface action applied on the considered floor;
l - the span of the tie.

The research and numerical analysis presented in this paper aim to more precisely understand the phenomena occurring in the RC flat slab system and to assess the influence of the applied additional protection of the flat slabs against progressive collapse in the event of the failure of one of the supports.

3. Experimental design

The subject of the experimental investigations was a sixteen-field RC flat slab model, as depicted in Figure 1. The research focused on verifying the impact of reinforcement bars made of B600B steel on the potential development of progressive collapse following the removal of an edge support. The test model, designed at a 1:3 scale, accurately replicated the operation of the actual system.

In this model, the axial spacing of the supports was set at 2400 mm, resulting in a total slab dimension of 9900x9900 mm, taking into account the dimensions of the supports. The model was supported by 25 square precast columns, each measuring 300x300 mm and 1900 mm in height, and were articulated to the strength floor. The thickness of the plate was determined based on the condition of 1/30 of the floor span between supports, resulting in a thickness of 80 mm. The reinforced concrete columns were prefabricated, while the remaining part of the monolithic model was constructed at the Department of Structure Research at Rzeszow University of Technology.

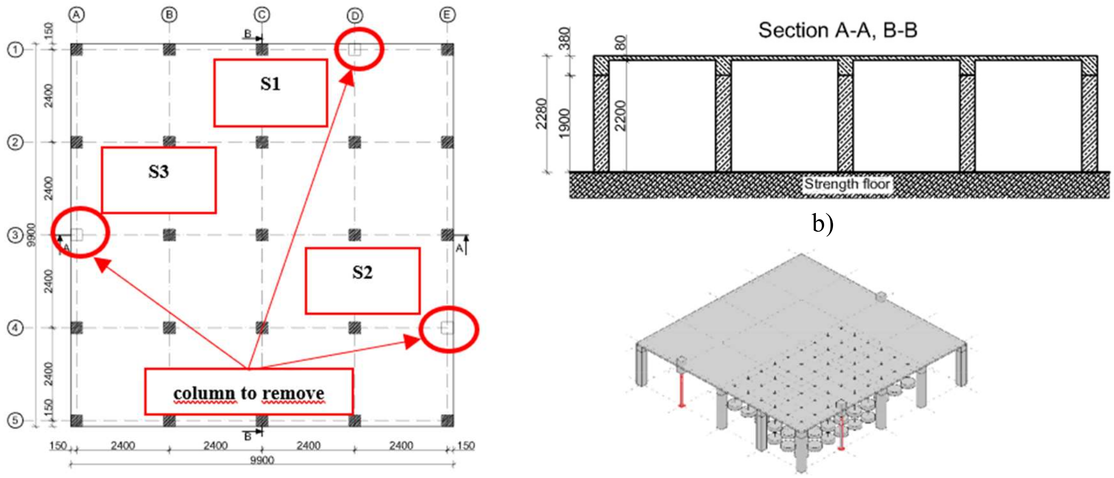

a) c)

Fig. 1. A simplified view of the model accepted for research: a) plan view, b) section A-A, B-B, c) perspective view

The large dimensions of the columns, relative to the plate thickness, were specifically chosen to prevent punching through over a significant portion of the anticipated load. Above the plate, where a column was removed, a segment of a higher-storey column was simulated to facilitate the transfer of loads from the actuator. In models 1, 2, and 3, the columns that were removed were simulated using easily dismantable slab props.

According to EN-1992-1-1 [3], structures that have not been specifically designed for exceptional actions should incorporate an adequate tie system. This system acts as a bridging mechanism after local failure to prevent progressive collapse. The bottom reinforcement configurations for the models were as follows:

- Model 1 (M1) utilized 2ϕ10 bars with an area of steel (As) of 157 mm²;
- Model 2 (M2) utilized 2ϕ12 bars with As = 226 mm²
- Model 3 (M3) utilized 3ϕ12 bars with As = 339 mm².

For slab reinforcement, bars with a diameter of 10 mm were used, while bars with diameters of 16 mm and 12 mm were employed to shape the slab-to-column joints and the tie system. The material parameters of the reinforcing steel used were determined during the tests and are detailed in Table 1. The concrete utilized in this study was of class C30/37, with a maximum aggregate size of 8 mm.

Table 1. Average values of reinforcing bars parameters obtained in tensile tests

Yield strength			Tensile strength			Modulus of elasticity			Strain		
f_{ym}	σ	ν	f_{tm}	σ	ν	E	σ	ν	ε_{uk}	σ	ν
MPa	MPa	%	MPa	MPa	%	GPa	GPa	%	%	%	%
658.1	67.0	10.2	743.2	66.5	8.9	200.5	9.7	4.8	8.7	1.6	18.8

where: σ – standard deviation of individual parameters, ν – coefficient of variation of individual parameters.

The loading of each separated research model was conducted in two main stages. In the first stage, gravity loading was progressively applied to represent the assumed permanent and variable actions on the plate. For this simulation, concrete elements weighing 200 kg and 100 kg were utilized, arranged in such a way to generate maximum values of internal forces in the slab at the area of the removed column. Depending on the model, the weights were suspended at 54 or 72 points on an 800 x 800 mm grid. Once all the assumed gravity loads were in place, the next step involved simulating a catastrophic event by removing the edge support. This was done under full gravity loading, where the support at the column location was removed, and the potential real-world forces at the damaged column location were simulated using a hydraulic actuator. The concentrated load was applied in increments of 5 kN until failure, utilizing an Instron-Schenck actuator.

To measure the displacements, inductive and draw-wire sensors were employed, mounted on a specially designed support structure in the area of the removed support. The arrangement of sensors was strategically planned within the two fields of the slab most affected by the failure. Additionally, the ARAMIS optical image correlation system, developed by the German company GOM, was used to measure the displacements of the plate. Displacements in the fields adjacent to the mainly loaded fields were measured using a conventional total station, with the measurement setup consisting of 8 prisms and a Leica total station.

During the tests, strain gauges and fiber optic strain sensors were used to measure strain. In the tested element, 76 electrofusion strain gauges TFs 5/120 were affixed to the reinforcing steel and 36 strain gauges TFs 60/120 to the concrete, with the distribution of strain gauges strategically designed in areas adjacent to the removed supports. Fiber optic strain sensors were also employed, allowing for quasi-continuous measurements along the length of a single fiber at 1 cm spacing. These sensors were placed along the reinforcing bars of the bottom rim reinforcement.

4. Results of experimental test

The key location for the analysis of the plate was at the point where the support was removed. Initially, the vertical displacement values of the plate at this location were plotted as a function of the applied loads, with the failure load specifically highlighted. This is illustrated in Figure 2.

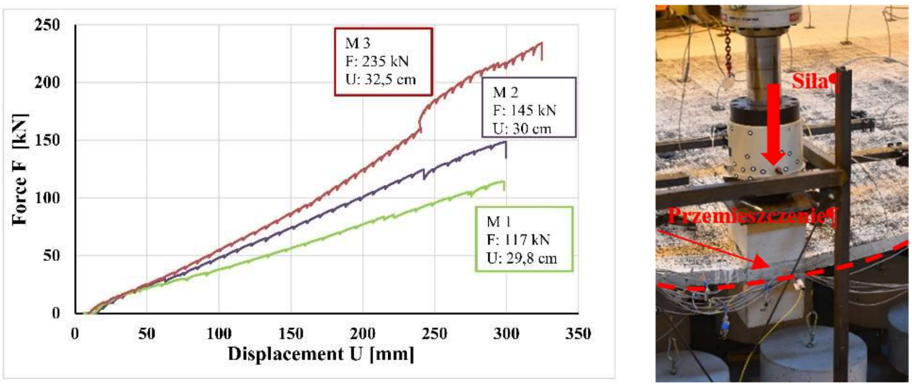

a) b)

Fig. 2. Diagram of vertical displacements in the place of removed support as a function of load

5. Conclusion

- The failure force obtained from the tests for model M1 was three times higher than the maximum design value of the axial force in the removed column, which was about 40 kN. Assuming the maximum measured angle of rotation of the plate over the support, which is 13.9°, we calculate that the force in the tendon formed after the failure of the column is about 500 kN. These results confirm that the structure achieved a much higher ultimate load than predicted by the design calculations.
- Comparing models M1 and M2, it can be seen that the main reinforcement of the slab significantly affects its post-failure capacity due to the failure of the support. The study showed that increasing the area of the tie reinforcement by 43% resulted in only a 23% increase in the failure load. However, considering the applied reinforcement in the tie of the potential tendon (i.e., half of the span between columns), the total increase in the area of the bottom reinforcement in the M2 model is only 11%.

- The study also showed that the location of the removed support is crucial for the post-failure performance of the structure. In the case of the M3 model, a 62% increase in load compared to the M2 model was observed, while the area of the tie reinforcement was increased by 50%.

References

1. Foraboschi P.: Structural layout that takes full advantage of the capabilities and opportunities afforded by two-way RC floors, coupled with the selection of the best technique, to avoid serviceability failures. Engineering Failure Anal. 70 (2016) 387–418.
2. EN-1991-1-7 (2006), Eurocode 1: Actions on structures – Part 1-7: General actions – Accidental actions.
3. EN-1992-1-1. Eurocode 2: Design of concrete structures – Part 1-1: Genereal rules and rules for buildings. 2004 CEN.

BEHAVIOR OF CONCRETE STRUCTURES IN A CRITICAL STRESS-STRAIN STATE

ŁUKASZ DROBIEC[1], *lukasz.drobiec@polsl.pl*
KRZYSZTOF GRZYB[1]
JAKUB ZAJĄC[1]

[1]Department of Building Structures, Faculty of Civil Engineering, Silesian University of Technology

Keywords: reinforced concrete structures, slab, column head failure, excessive deflection, parking

1. Introduction

Properly designed reinforced concrete structures are characterized by a significant degree of safety. Their stiffness, resulting from the massive cross-sections of the elements, limits deformation, and the concrete constituting the reinforcement matrix ensures high fire resistance and corrosion protection. The reliability of the structure is guaranteed by standardized design principles that ensure an appropriate level of safety both on the load side and on the material strength side. Even in cases of design, execution, or operational errors, reinforced concrete structures typically do not undergo a sudden collapse; instead, problems are usually indicated by excessive deformation [1] or cracking [2].

This paper presents a study of two separate construction cases in a critical stress-strain state. In the first case, despite a significant lack of reinforcement, the structure did not collapse. In the second case, a coincidence revealed internal construction problems that were not visible before the failure but posed a threat to the facility's users.

2. The building under conservation protection in Warsaw

The building complex was constructed around 1920 [3] for the Mechanical Shoe Factory "Polus" S.A. In recent years, the facility has served as the headquarters for various social initiatives, including theaters, and has provided a space for creative work and an aid point for charity organizations (Fig. 1a). During an inspection of the part of the building that was excluded from use, significant deflections of the slabs were observed (Fig. 1b). Upon removing the plaster from the slab above the second floor, cracks on the concrete surfaces were found. These cracks had openings exceeding 1.0 mm (Fig. 2).

a) b)

Fig. 1. a) view of the building from the south-east b) visible deflection of the slab above the second floor

a) b)

Fig. 2. Measurement of the crack width in the slab above the second a) crack width 1.0 mm b) crack width 1.2 mm.

Leveling measurements of the deflection of the slabs above the ground floor, first floor, and second floor were conducted. Abnormalities were observed in the ceiling above the second floor, with the deflection of the slab in the front part of the building measured at 102 mm, and the deflection over the central outbuilding at 141 mm. According to [4], deflections exceeding l/250 (where l is the span of the slab) may deteriorate the appearance and functionality of the structure, while deflections greater than l/500 may damage adjoining elements such as partition walls, which are present on the analyzed slabs. Significantly greater deformations directly compromise structural safety. In this context, the measured deflections of the slab did not meet the Serviceability Limit Conditions.

Numerical calculations revealed that the ultimate limit state (ULS) of the reinforced concrete floors above the ground floor, first floor, and second floor is not met. The load capacity is exceeded threefold in the longitudinal direction for the assumed loads. The slabs did not collapse, likely because they were never fully loaded and were partially restrained by the masonry walls. Calculations indicated that the floor requires reinforcement due to punching shear, which is currently not present in the structure. The exceedances of the punching shear resistance are 58%, 47%, and 61% for the slabs of the ground floor, first floor, and second floor, respectively. The analyses show that the ceilings, in their current state, are not suitable for further use. Strengthening the floor slab above the second floor is particularly challenging due to the severely deformed surface of the structure, with visible deformations both from the bottom and top of the slab. For the ceilings above the ground floor and first floor, it is possible to add a concrete thickness of about 10 cm and use composite mats on the bottom of the slabs.

3. Underground garage in Warsaw

On November 22, 2019, approximately 200 kg of a concrete head fragment detached from the slab of the underground garage in Warsaw and collapsed onto a car parked at the pole (Fig. 3a). The damaged column head measured 0.22 x 0.7 x 2.8 m. The detachment occurred across the entire width of the head and half of its length, resulting in a damage shape similar to a pyramid. Small detachments of concrete were also observed on the adjacent head at the expansion joint.

A visual inspection revealed no longitudinal or transverse structural reinforcement in the damaged zone at the height of the head. The bars shown in Fig. 3b represent the bottom reinforcement of the floor slab. The remaining column heads in the adjacent underground garages did not exhibit any scratches or other damage. According to facility users, the column head was damaged while driving the floor of a truck adapted for municipal waste collection (the garage ceiling also served as a patio between a group of residential buildings).

In theory, only compression should occur in the column heads. To explain the cause of the concrete fragment's detachment, static calculations were performed. A spatial shell-bar model of the structure was prepared (Fig. 4), along with a shell model of the roof strip in the axis of the column with the damaged head. The calculations considered the actual constant and variable loads (snow and vehicle), and the live load caused by a truck in the spatial model was analyzed according to the standard [5].

a)

b)

Fig. 3 View of the damage site a) front view b) side view, the arrow marks the bottom reinforcement of the slab

The calculations yielded tensile stress values of 3.3 MPa at the head joint with the ceiling and 9.5 MPa at the edge of the head with the column. These values exceed the tensile strength of concrete. The calculation results also showed that the floor met the Ultimate Limit State conditions, except for the heads of columns at the expansion joints.

The Serviceability Limit State in deflections was met for the entire floor slab. The maximum calculated deflection was 73% of the permissible value, and the measured displacements were also smaller than the calculated and allowable values.

An analysis of publications [7, 8, 9] on reinforced concrete structures, issued before the design and construction of the object, indicates that they recommend the use of structural reinforcement in the column heads in the form of a horizontal mesh made of 8 to 10 mm rods with a spacing of 10 to 15 cm. In addition to the structural reinforcement in the head, appropriate reinforcement for punching shear should be used if necessary. It is unclear whether the lack of reinforcement was due to a design or execution stage oversight. The available design documentation did not include detailed plans for the ceiling above the garage halls.

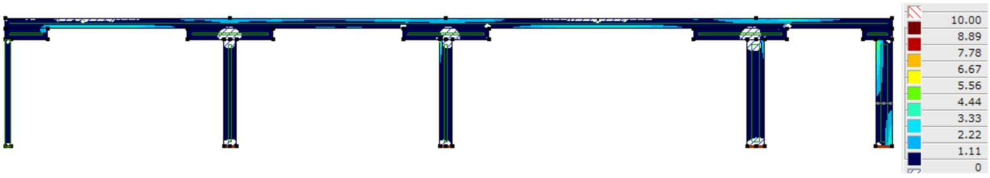

Fig. 4 Tensile stress areas (MPa) in the shell-bar numerical model

4. Summary

The described cases are representative examples of the behavior of reinforced concrete structures under pre-failure and critical stress-strain conditions. In the first analyzed building, despite the lack of reinforcement in the floor slabs and deformations exceeding the allowable deflection values for serviceability limit states, there has been no structural disaster over the 100-year history of the building. This can be attributed to the non-occurrence of maximum possible loads and the phenomenon of internal force redistribution.

In the second case, a sudden failure contributed to the verification of the load capacity of the structure. Despite the absence of visible cracks and deflections, the structure still posed a threat to its users. The load caused by the passage of a heavy car exceeded the tensile strength of the unreinforced structure, revealing internal defects of the slab. The primary issue was the absence of structural reinforcement, which is crucial for ensuring the reliability of the structure. Applying the principles of technical knowledge in each of these cases would undoubtedly ensure safety of use and extend the life cycle of each structure.

References

1. Drobiec Ł., Grzyb K., Zając J.: Analysis of reasons for the structural collapse of historic buildings. Sustainability 2021, 13 (18). https://doi.org/10.3390/su131810058
2. Drobiec Ł., Jasiński R., Piekarczyk A.: Diagnostyka konstrukcji budowlanych. Tom 1. Metodologia, badania polowe, badania laboratoryjne betonu i stali. Wydawnictwo naukowe PWN SA, Warszawa 2014
3. Krasucki M.: Katalog warszawskiego dziedzictwa postindustrialnego, Fundacja Hereditas, Warszawa 2009.
4. PN-EN 1992-1-1. Eurocode 2 – Design of concrete structures – Część 1-1: General rules and rules for buildings, PKN.
5. PN-EN 1991-1-1 Eurocode 1 – Actions on structures, PKN.
6. PN-EN 206. Concrete – Specification, performance, production and conformity, PKN.
7. Dąbrowski K., Stachurski W., Zieliński J.L.: Konstrukcje betonowe. Arkady, Warszawa 1982.
8. Kobiak J., Stachurski W.: Konstrukcje żelbetowe. Tom 2. Arkady, Warszawa 1987, Wydanie piąte zmienione i rozszerzone (oraz wydania wcześniejsze)
9. Starosolski W.: Konstrukcje żelbetowe. Tom 2. Wydawnictwo Naukowe PWN, Warszawa 1995 (oraz wydania późniejsze)

NATURAL DRAFT COOLING TOWERS: TYPICAL DEFECTS AND DAMAGE AFTER LONG-TERM OPERATION

JACEK HULIMKA[1], *jacek.hulimka@polsl.pl*

[1]Silesian University of Technology

Keywords: cooling tower, reinforced concrete structure, corrosion, chemical testing of concrete, repairs

1. Introduction

Industrial water cooling is an indispensable element of many technological processes. When cold water from sufficiently large reservoirs or rivers is not available, cooling towers are used to exchange heat with the atmosphere. The two main types of cooling towers are mechanical draft and natural draft. Natural draft cooling towers are most commonly constructed from reinforced concrete, though steel or wood may also be used.

This work presents the most common defects and damage found in typical cooling tower structures, including their causes and, where relevant, comments on the repair technologies applied.

2. Construction of a typical reinforced concrete cooling tower: an overview

The structure of a typical reinforced concrete natural draft cooling tower consists of the following components, from bottom to top: an annular foundation, a collecting basin with a surrounding drip zone, a system of diagonal or upright columns, and a hyperbolic shell topped with a stiffening beam that also serves as a walkway. Except for the columns, which were made as prefabricated units in some towers, all these components are monolithic concrete elements. The internal structural elements are also made of reinforced concrete.

Additionally, the structural elements of cooling towers include auxiliary steel structures, such as access ladders and guardrails.

3. Typical defects of and damage to the structural elements

A significant number of reinforced concrete natural draft cooling towers in Poland have been in operation for several decades under challenging environmental conditions. This prolonged exposure has led to various types of damage, some of which have already been repaired in certain cases. Additionally, some cooling towers had original defects that were impossible to rectify. While the types of damage and defects are extensive and typical of structures subjected to long-term operation, certain issues are particularly characteristic of cooling towers. The following text provides brief descriptions and photographs of these problems.

Specific conditions in which cooling towers operate include:

- Continuous submersion or exposure to water for their lower elements.
- Permanent contact with water vapor inside the shell.
- External exposure to water vapor from adjacent structures and flue gas.
- Direct impact from atmospheric conditions and significant temperature variations.

For many years, the acidification of process water was used to prevent algae growth, but this method accelerated corrosion-related phenomena in concrete and steel.

Damage and Defects of the Collecting Basin and Drip Zone

The basin bottom and walls are monolithic structures typically made of low-grade concrete, leading to freeze-thaw damage in zones of variable moistness. This damage is compounded by original defects such as concrete segregation in areas with increased reinforcement density. The drip zones often exhibit shrinkage cracks and are incorrectly joined with the basin walls (Fig. 1).

a) b)

Fig. 1. Typical damage to: a) the basin wall, b) the drip zone

Damage to and defects of the shell supporting columns

Columns supporting the shell were made as prefabricated units in most of the cooling towers in question. The main defect is insufficient cover thickness resulting in reinforcement bar corrosion, sometimes intensified by very poor quality of the concrete used to make the columns (Fig. 2). In rare cases, the columns are incorrectly seated, have geometrical defects or display damage stemming from the mounted steel brackets. In principle, the columns should not come into contact with process water, but they are often partially flooded for long periods due to air flow disturbances, which causes their icing in winter (Fig. 2).

a) b)

Fig. 2. a) column made of poor-quality concrete, b) iced columns

Damage to and defects of the tower shell

The shells of numerous cooling towers suffer from corrosion, causing the concrete cover to loosen and fall off (Fig. 3). This damage results from the use of low-grade concrete, careless placement of reinforcement, and workmanship defects in the concrete. Water leaks are frequently visible, indicating structural defects in the concrete (Fig. 3). The inner surfaces of the shells show signs of protective layer loosening and calcium salt leaching.

a) b)

Fig. 3. A) reinforcement corrosion and falling-off cover, b) water leaks

Damage to and defects of the upper beam (the walkway)

The damage observed within the upper stiffening beam is similar to that noticed in the shell but is intensified by greater exposure to high moisture and freeze-thaw cycles (Fig. 4).

Damage and Defects of the Internal Load-Bearing Elements

The prefabricated internal support elements, such as columns and beams, were made of relatively high-grade concrete, which has enhanced their durability. A typical defect in these areas is the corrosion of reinforcement due to an insufficiently thick concrete cover. Additionally, severe mechanical damage from the structure assembly period is observed in some areas (Fig. 4).

a) b)

Fig. 4. a) corrosion of the walkway, b) damage to internal elements

Damage to and defects of the auxiliary steel structures

The primary damage to the steel structures (ladders and guardrails) is corrosion of varying degrees, including complete destruction in extreme cases (Fig. 5). This damage is usually more severe on higher towers. Original defects include numerous geometrical inaccuracies and, less frequently, the absence of screws fixing the support elements of the ladders to the reinforced concrete structure.

4. Selected typical methods of repair

Repairs of damaged or worn-out reinforced concrete structures are standard practices and are covered by relevant standards. Materials used during repairs, such as Polymer Cement Concrete (PCC) and Engineered Cementitious Composites (ECC), are also typical. Cooling towers frequently undergo extensive surface repairs with shotcrete. Unfortunately, some of these repairs have proven to be ineffective or even harmful, hence they are discussed in greater detail below.

A key factor in repairs is achieving good bonding between the new concrete and the original material. Thin layers without reinforcement usually bond well, although exceptions do occur (Fig. 6). However, applying a thick layer of shotcrete with typical reinforcement can pose problems, as it tends to separate from the original shell during the repair process. This separation results in further damage, characterized by clearly visible water leaks (Fig. 6).

a) b)

Fig. 5. Corrosion of the ladder (left), and removal of a corroded guardrail (right)

a) b)

Fig. 6. Shotcrete coming off (left), and water leaks from underneath the concrete (right)

It must be mentioned that the repair technology depends on the chemical condition and durability of the concrete. Additionally, the repair scope must be adjusted to the anticipated operational period of the cooling tower.

5. Summary

A significant part of the cooling towers operated in Poland was built in the 1960s and 1970s, meaning they have been used for several decades under difficult conditions. Additionally, some structures were made of low-grade concrete and exhibit numerous original defects. Consequently, their technical condition varies from good to breakdown-inducing or even disastrous. Most of the existing cooling towers have already undergone overhauls, which were usually performed correctly; however, certain repairs were inappropriate, further deteriorating the technical condition of the structures.

This work lists the most common defects and types of damage in cooling towers, describing their causes. Only certain kinds of repairs are mentioned, as most of them are typical.

Despite the similarity of structural and material solutions, each cooling tower requires an individual approach. Numerous original defects and greatly varying operating conditions have resulted in diverse technical states of the towers after long-term use, even in the case of identical cooling towers situated next to each other. Still, these facilities demonstrate how durable reinforced concrete structures can be, even when operated in extremely unfavourable conditions.

DESIGN ERRORS CAUSE AN EMERGENCY OF THE REINFORCED CONCRETE TANK FOR COKE

TOMASZ MAJEWSKI[1], *tomimaj@pg.edu.pl*
MACIEJ NIEDOSTATKIEWICZ[2]

[1]Industrial Doctoral School, Gdansk University of Technology
[2]Department of Civil Engineering, Faculty of Civil and Environmental Engineering, Gdansk University of Technology

Keywords: reinforced concrete tank, design errors, scratches, cracks, repair, reinforcement, injection

1. Introduction

The quality of the developed design documentation and adherence to the technological regime during construction work have a decisive impact on the subsequent safety of the structure and the safety of building use [1-2]. This paper describes the defects and damages of an open, rectangular reinforced concrete tank for hot process water, which failed during a short period of operation [3-11]. The article also presents the proposed solution to address the existing damage to the tank structure.

2. General information

The analyzed tank was a single-chamber tank with a reinforced concrete structure, set on a foundation slab supported by piles. The external dimensions of the tank were as follows: width (B) = 8.2 m, length (L) = 20.7 m, maximum depth (H1) = 7.25 m, and total height (H2) = 8.1 m (height of the walls from the floor to the upper edge). The outer walls of the tank were made of reinforced concrete, monolithic, poured on-site, with a constant thickness of 35 cm, constructed from C30/37 class concrete, and reinforced with A-III N class bars. The tank also included a drainage chute along its length for drainage pumps. On the inner surfaces of the walls and chute ramps, cladding made of basalt slabs was installed to protect the concrete against abrasion.

3. Description of faults and damage to the tank

During the inspection and diagnostic measurements, the following issues were found: numerous scratches and cracks in the walls, intense cracking at the corners, active water leaks through existing scratches and cracks, and extensive changes in the concrete structure, including insufficient vibration and visible traces of previously performed repairs (injections). In the repaired areas (filled cracks), active water leaks were still visible.

4. Analysis of the condition of the existing tank

Based on the initial analysis of the crack morphology, the negative impact of the temperature gradient was identified as a potential source of the problems. During site visits, temperature measurements were taken on the outer surface of the tank walls using two methods: point-by-point measurements with a pyrometer calibrated with a classic thermometer applied to the tank surface, and using a thermal imaging camera.

During the operation of the installation, cool water was stored in the tank, into which hot coke was discharged twice a day. During the discharge period, there was a sudden, uncontrolled increase in water temperature by several dozen degrees Celsius. The water temperature varied throughout the year, depending on the weather conditions, as the reservoir was not heated. Consequently, the water was warmer in summer and cooler in winter, although it did not freeze.

Temperature measurement

Control measurements of the temperature of the outer surfaces of the tank walls were conducted during the winter period (February), one day before and immediately after the coke discharge, with a two-hour interval between the measurements.

Reinforcement scanning

The non-destructive test, which involved scanning the reinforcement, was carried out using a ferromagnetic detector. The number, spacing, and diameter of the reinforcement bars embedded in the tank walls (at the outer plane of the tank wall) were generally in line with the design specifications. The average cover thickness of the reinforcement bars ranged from 7 to 8 cm, which was greater than the 4 cm assumed in the design.

Concrete tests

To determine the actual class of concrete used in the tank walls, concrete samples were collected in the form of core boreholes. The concrete met the requirements for strength class C40/50, while the design documentation assumed the use of concrete class C30/37. The bulk density of the concrete in the collected cores ranged from 2.33 g/cm^3 to 2.38 g/cm^3, with an average of 2.37 g/cm^3. The water absorption of the concrete ranged from 4.3% to 4.9%, with an average of 4.5%. The ion content relative to the cement mass was as follows: Cl- ranged from 0.020% to 0.026%, and SO_4^{2}- ranged from 0.033% to 0.039%. The pH of the concrete samples ranged from 11.8 to 12.1, indicating that the concrete maintained its natural ability to protect the reinforcement against corrosion. The homogeneity of the concrete, determined by the sclerometric method using a Schmidt N-type hammer, was assessed as sufficient.

Checking static and strength calculations

Based on the static and strength analysis of the tanks, it was found that:

- in the existing state, for the water test, without taking into account the influence of temperature, the tank complied with the Ultimate Limit State (ULS) standard requirements. The built-in amount of reinforcement was sufficient to safely fill the tank with cool tap water (~ 10^{0}C);
- in the existing state, in the summer period, for the standard value of air temperature, the tank complied with the ULS and SLS standard requirements;
- in the existing state, in winter, for the standard value of air temperature, the tank did not meet the ULS and SLS standard requirements;
- in the existing condition, in winter, for the actual air temperature measured during the local inspection, the tank did not meet the ULS and SLS standard requirements;
- after the final repair and insulation, in the winter period, for the standard value of air temperature, the tank will meet the ULS and SLS standards.

5. The method of repairing the tank

Following the technological limitations as well as organizational and economic conditions, it was proposed to repair the reservoir in two stages:

Stage I (temporary)

The scope of work included sealing the leaking tank walls by:

- Flushing the existing scratches and cracks.
- Filling the scratches with a flexible, polymeric sealing material.
- Priming the entire surface of the walls (from the outside) with a primer.
- Applying a highly flexible polymer-epoxy membrane to the entire surface of the walls.
- Insulating the walls along their entire height with 15 cm thick thermal insulation material (extruded polystyrene (styrodur)) [12].
- Temporarily protecting the thermal insulation surface with a mineral coating against mechanical damage, with thin-layer mineral plaster recommended.
- During the repair work, particular attention was paid to the necessity of installing flashing at the top of the tank walls to limit the possibility of flooding (dampening) the thermal insulation material in the event of water overflowing through the upper edge of the tank.
- The proposed repair method should be treated as temporary, as it does not eliminate the causes of failures and damages, but only partially limits the negative impact (gradient) of temperature and slows down destructive processes.

- Until the completion of Stage II works, and after the completion of Stage I works, it was recommended to constantly monitor the tightness of the tank.

Stage II (final)

To reduce (eliminate) the negative influence of temperature, it was recommended to install thermal insulation inside the tank. This will require:

- Temporarily shutting down the tank (during the planned maintenance shutdown).
- Emptying the tank of water.
- Dismantling the inner lining of basalt plates.
- Installing a new layer of thermal insulation.
- Constructing an internal tank made of stainless steel.
- Putting the tank back into service.

The proposed method aims to limit (eliminate) the negative influence of temperature on the reinforced concrete walls of the existing tank. During the assembly of the internal metal tank, special attention must be paid to the method of fixing the designed thermal insulation to the reinforced concrete walls and ensuring the cooperation of the internal (steel) tank with the external (reinforced concrete) tank, with particular emphasis on the influence of temperature changes on the connectors.

6. Conclusions

The analyzed tank was incorrectly designed. The reinforced concrete structure of the tank did not meet the requirements of the Ultimate Limit State (ULS) and Serviceability Limit State (SLS) due to the permissible crack opening. The direct cause of water leaks through the walls of the reservoir was a design error that involved underestimating (or omitting in the calculations) the influence of temperature changes during operation on the wall strain. As a result of this error, all walls of the tank developed cracks, and almost the entire surface became unsealed.

References

1. Substyk M.: Utrzymanie i kontrola okresowa obiektów budowlanych. Wydawnictwo ODDK, Warszawa, 2012.
2. Baryłka A., Baryłka J.: Diagnostyka techniczna obiektu budowlanego. Budownictwo i Prawo, Warszawa, 19-22, 4, 2015.
3. Zybura A., Jaśniok M., Jaśniok T.: Diagnostyka konstrukcji żelbetowych. Badania korozji zbrojenia i właściwości ochronnych betonu. Wydawnictwo Naukowe PWN, Warszawa, 2011.
4. Drobiec Ł., Jasiński R., Piekarczyk A.: Diagnostyka konstrukcji żelbetowych. Metodologia, badania polowe, badania laboratoryjne betonu i stali. Wydawnictwo Naukowe PWN, Warszawa, 2010.
5. Kledyński Z., Ostromęcki R.: Uwarunkowania projektowe i technologiczne stanu zarysowania żelbetowego zbiornika wydzielonej komory fermentacyjnej. XXIV Konferencja Naukowo-Techniczna Awarie Budowlane-2009, Szczecin-Międzyzdroje, 2009.
6. Łukacz M., Płachecki M.: Awaria dwukomorowego żelbetowego zbiornika spowodowana oddziaływaniami termicznymi. XXV Konferencja Naukowo-Techniczna Awarie Budowlane-2011, Szczecin-Międzyzdroje, 2011.
7. Godycki-Ćwirko T., Piotrowski P.: Żelbetowe zbiorniki oczyszczalni ścieków po 20 latach eksploatacji. XXV Konferencja Naukowo-Techniczna Awarie Budowlane-2011, Szczecin-Międzyzdroje, 2011.
8. Dyczkowski J., Kaźmierowski M.: Analiza odkształceń ścian prostokątnych żelbetowych zbiorników na ciecze z uwzględnieniem zbrojenia przeciwskurczowego. Materiały Budowlane, 9 (517), Warszawa, 2015.
9. Flaga K.: Skurcz betonu i jego wpływ na nośność, użytkowalność i trwałość konstrukcji żelbetowych i sprężonych. Zeszyty Naukowe Politechniki Krakowskiej, seria Inżynieria Lądowa, 73, Kraków, 2002.
10. Kiernożycki W.: Betonowe konstrukcje masywne. Teoria, wymiarowaniem, realizacja. Wydawnictwo Polski Cement, Kraków, 2003.
11. Godycki-Ćwirko T.: Morfologia rys w konstrukcjach z betonu. Wydawnictwo Politechniki Białostockiej, Białystok, 1982.
12. Instrukcja ITB nr 447/2009: Złożone systemy ocieplania ścian zewnętrznych budynków (ETICS). Zasady projektowania i wykonywania. Wydawnictwo Instytutu Techniki Budowlanej, Warszawa, 2009.

BALCONY SAFETY ASSESSMENT ON SELECTED EXAMPLES OF BUILDINGS OF PREFABRICATED ELEMENTS

ANNA OSTAŃSKA[1], *e-mail: a.ostanska@pollub.pl*

[1]Lublin University of Technology

Abstract: It is the responsibility of the owner or manager to ensure the safe use of a building [1]. In Poland, the share of multi-family housing constructed with large-panel systems from 1946 to 1992 was about 50%, and for large-block systems (up to the present) about 30% [2]. This accounts for approximately 60,000 buildings made with large-panel systems [3]. This paper examines the technical condition of small prefabricated cantilever balconies in buildings constructed using the WBLŻ and OWT-67 systems in the Lublin region, along with an analysis of selected repair measures and their effects. Examples of good practices in replacing balconies with larger ones, both foreign and domestic, are also provided. Considering that there are more than 6.5 million balconies and loggias in the Polish industrialized construction industry, a checklist of factors related to cantilevered balconies has been developed. This checklist should be assessed as part of the periodic evaluation of prefabricated buildings. The proposed checklist will contribute to the prevention of balcony failures and ensure the continued safe use of precast buildings.

Keywords: prefabricated construction, emergency condition, occupant safety

1. Introduction

For several years (1962-2018), the study of the impact of design, construction, and operation quality on building hazards, failures, and disasters was conducted by the Building Research Institute [4]. It must be remembered that the technical condition of balconies affects the adjacent structural elements, such as ceilings and perimeter walls. Despite the large scale of the problem, there is still a lack of systematic research or evaluation of these failures. Additionally, there is a lack of effective and durable solutions to improve the condition of balconies implemented in specific systems.

The problems and issues associated with assessing the technical condition of balconies and loggias and designing modernization of large-panel buildings in this regard can be summarized as follows:

- There is a lack of commonly available technical drawings detailing how balconies are supported in some systems (e.g., the big-block system used in the Lublin region).
- Multiple renovations of balconies and loggias were carried out individually and often unprofessionally.
- Existing building modernizations, such as insulation, did not always include comprehensive balcony renovations and often interfered with their space and elements.

This paper attempts to address the extent to which small prefabricated cantilevered balconies have worn out technically [5] and functionally after 40 years of use. It also examines how past renovations have affected the safety of these balconies.

Drawings reconstructing the support of balconies in prefabrication systems found in the Lublin region are presented, based on literature, own research, and discoveries. Cases of balcony damage, both those present originally and those resulting from inadequate renovations, are described. A checklist of places and factors related to balconies that should be checked during periodic inspections of prefabricated buildings is proposed. Moreover, the paper attempts to indicate possible directions for effective balcony renovation, focusing on both durability and quality of use.

2. Selected examples of prefabricated cantilevered balconies

Despite the fact that the current repair has been repeated twice (2002, 2006) and a major overhaul was conducted (2012-2014) with the finishing layer of the balcony slab covered with ceramic cladding (Fig. 1a), the problem of leakage through the slab and the renewed flaking of the slab's bottom layer have not been resolved (Fig. 1b). So far, the manager has not made a decision on another major repair or replacement of the balconies.

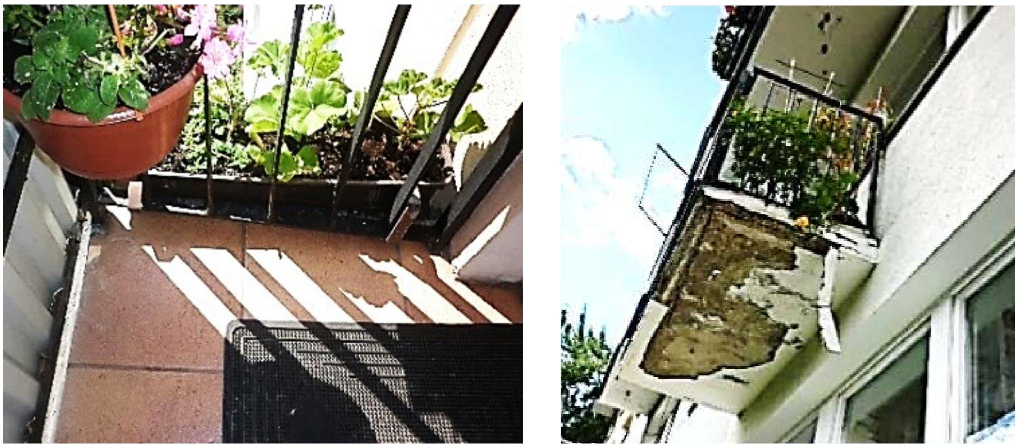

a) b)

Fig. 1. Balconies in a large-panel building in OWT-67 system: a) general view of balcony after two current repairs and one major repair with ceramic cladding, b) balcony - bottom of the balcony slab, peeling and losses after the third repair (major repair), despite the execution of the ceramic cladding from above.

3. Check-list for evaluating prefabricated cantilevered balconies

A checklist for a structured balcony inspection assessment has been developed based on many years of observations, supported by sociological surveys of residents' urgent needs conducted three times, every five years [6], and the ITB instruction from 2002 [7]. It has also been noted that the guidelines for assessing the technical condition of prefabricated balconies developed by ITB [7] 20 years ago need to be updated and supplemented. Below is an updated checklist for the periodic assessment of small prefabricated cantilevered balconies. The list of damages, the absence or presence of which must be ascertained, and other factors to be identified is as follows:

- Deflection of the ends of the balcony supports.
- Scratching of the reinforced concrete elements of the balcony, especially cracks on the upper surface of the balcony along the contact with the external wall.
- Cracking or cavities on the lower surface and the edges of the balcony structure.
- Corrosion damage to the steel components of the balcony structure (reinforcement bars, brands or caps).
- The balcony's lower surface or its edges are wet, discoloured or peeling.
- Salts on the lower surface of the balcony or the balcony edges.
- Overgrowth of vegetation on the upper surface of the balcony.
- Cracking, blowing out, and loss of the finishing layer on the balcony slab.
- Lack of proper slopes, stagnation of water on the slab surface.
- Cracking or spalling around balustrade post seating areas.
- Corrosion or loss of steel balustrade elements.
- Cracking or loss of elements filling the railing framework (panels of: reinforced concrete, reinforced glass, plastic, ligno-cement, etc.).
- Loosening of railings in the external wall or cut off from the wall during their insulating the building.
- Missing, deformed, or corroded flashings.
- Dampness of the exterior walls at the perimeter or along the contact with the balcony slab.
- Dampness of floor layers in the apartment at the balcony door threshold.
- Wetting of the corners of external walls and the ceiling below the balcony slab.
- Additional top layers, such as secondary ceramic tiles with slope levelling.
- Enclosure of the balcony with curtain walls.
- Excessive loads on the balcony slab, exceeding the standard value.
- Proper installation of additional equipment such as steel grilles, satellite dishes, air conditioners, etc.

4. Suggestions for corrective action

Replacing balconies with larger ones, such as additional ones (Fig. 2), eliminates the problems of technical wear and tear for the next 20-30 years and addresses functional wear and tear.

Fig. 2. Poland, Kozienice 2020, fragment of prefabricated building facade. During the insulation of the walls, a major renovation of some of the small balconies was carried out and the remaining ones were replaced to additional balconies of steel construction with PVC panels. Also balconies were added on the first floor

5. Conclusion

- The analysis of small prefabricated cantilever balconies has confirmed that after 40 years of use, irrespective of the realization system—big-block (WBLŻ) or big-panel (OWT-67)—the repair problems, especially concerning the balconies, and their technical and functional wear are similar.
- The most frequent damages of balconies in buildings of the WBLŻ and OWT-67 systems in the Lubelskie voivodeship are: edge losses of concrete, local dampness, discoloration, flaking and salting on the lower surface and edges of the balcony structure, lack of proper slopes, water stagnation on the surface of the slab, dampness of the floor layers in the apartment, lack of flashings or their deformations, dampness of external walls at the contact with the balcony slab, and cutting off the balustrade from the wall during wall insulation.
- The aforementioned damages have occurred either as a result of original errors or as a result of not removing the original defects during renovation. Generally, many renovations proved to be ineffective or caused secondary damage.
- Good practices from abroad and in Poland (Fig. 2) confirm that the replacement of balconies is the right course of action because it is more economically viable and effective than repeated repairs.

References

1. Ustawa *Prawo budowlane* 2021 z późn. zm. art. 1.
2. Ostańska A., *Podstawy metodologii tworzenia programów rewitalizacji dużych osiedli mieszkaniowych wzniesionych w technologii uprzemysłowionej na przykładzie osiedla im. St. Moniuszki w Lublinie*, Politechnika Lubelska, Monografie Wydziału Inżynierii Budowlanej i Sanitarnej Vol. 1, Wydawnictwa Uczelniane Lublin 2009, ss.1-173.
3. Soboń A., *Wielka płyta jest bezpieczna*, 30 stycznia br. wiceminister ogłosił plany Ministerstwa Inwestycji i Rozwoju (MIiR).
4. Runkiewicz L., *Uszkodzenia i zagrożenia budynków wielkopłytowych a potrzeby ich modernizacji i wzmacniania*. W: Poradnik inspektora nadzoru, kierownika budowy i inwestora. WACETOB nr 3/2013.
5. Szymański J., *Balkony i loggie w budynkach wielkopłytowych.* w: Bezpieczeństwo konstrukcji. Budynki wielkopłytowe – wymagania podstawowe zeszyt 5. Seria: instrukcje, wytyczne, poradniki nr 375/2002, ITB, Wa-wa 2002.
6. Wacław Baranowski, *Zasady ustalania zużycia obiektów budowlanych: podstawowe nazewnictwo budowlane*, wyd. Wydanie poprawione i uzupełnione, Warszawa: Warszawskie Centrum WACETOB, 1997, ISBN 83-7165-029-9, OCLC 1022801659.
7. Ostańska A., *Programowanie rewitalizacji osiedli mieszkaniowych z zastosowaniem modelu PEARS*. Lublin: Polska Akademia Nauk, 2018. 169 s. ISBN 978-83-939534-4-8.

DESIGN AND EXECUTION ERRORS AS A CAUSE OF DAMAGE TO ANTI-ELECTROSTATIC FLOORING

SYLWIA ŚWIĄTEK-ŻOŁYŃSKA[1], *sylwia.zolynska@pg.edu.pl*
MACIEJ NIEDOSTATKIEWICZ[2]
WŁADYSŁAW RYŻYŃSKI[3]

[1]Industrial Doctoral School, Gdansk University of Technology
[2]Department of Civil Engineering, Faculty of Civil and Environmental Engineering, Gdansk University of Technology
[3]Polytechnic Faculty, State Vocational University in Suwałki

Keywords: industrial floors, antistatic, static electricity, floor diagnostics

1. Introduction

Apart from technological lines, industrial floors are a key element in maintaining the continuity of work in both production plants and logistics centers [1,2]. The constantly developing industry of industrial flooring encompasses both classic design and technological flooring solutions, as well as specialized solutions used in facilities where technological processes or storage require system protection against static electricity [3]. Essential design and implementation activities, beyond the use of earthing systems for the elements of the supporting structure of the facility, include the execution of anti-electrostatic floors with parameters and functional features adapted to the facility's function [4,5].

2. Characteristics and classification of antistatic floors

The basic criterion for the classification of antistatic floors is electrical conductivity. Table 1 shows the division of floors according to [6].

Table 1. Division of antistatic floors according to [6]

Floors conductive	 dissipating electrostatic charge	 insulating
$R_u < 1 \cdot 10^5\ \Omega$	$1 \cdot 10^5\ \Omega \leq R_u < 1 \cdot 10^8\ \Omega$	$R_u \geq 1 \cdot 10^8\ \Omega$

Table 2. Classification of materials according to [7]

Floors antistatic conductive	 antistatic partially conductive	 having no properties anti-electrostatic
$\rho_v \leq 1 \cdot 10^4\ \Omega \cdot$ m i/lub $\rho_s \leq 1 \cdot 10^7\ \Omega$	$1 \cdot 10^4\ \Omega \cdot \mathrm{m} < \rho_v \leq 1 \cdot 10^7\ \Omega \cdot$ m i/lub $1 \cdot 10^7\ \Omega < \rho_s \leq 1 \cdot 10^{10}\ \Omega$	$\rho_v > 1 \cdot 10^8\ \Omega \cdot$ m i/lub $\rho_s > 1 \cdot 10^{10}\ \Omega$

Materials used on floors are also classified, based on the criterion of volume electrical resistivity (ρ_v) and surface (ρ_{rs}). Their division is presented in Table 2.

The most commonly used solutions for anti-electrostatic floors in industrial facilities involve the use of floor slab finishes in the form of ESD (Electrostatic Discharge) floor coverings based on PVC (polyvinyl chloride), resin coatings, and surface-hardened concrete monolithic floors with DST (Dry Shake Topping).

3. Methodology of tests and measurements of antistatic floors

Measurements of antistatic floors are made after the seasoning of the finishing coatings. For lining and resin flooring systems, the recommended minimum time from the implementation of the floor is 7 days, whereas for concrete floors, this period is 28 days.

The assessment covers the measurement of electrical resistance (R_u) and the equivalent resistance measured between the floor surface and the earthing mains (R_{gp}).

In order to classify the material the floor is made of in terms of its anti-electrostatic properties, the surface electrical resistance (R_s) is measured and the surface electrical resistivity (ρ_s) is determined.

The report on measurements should specify:

- The number of measurement points.
- The ratio of % measurement points to m² of free floor area.
- The ratio of % measurement points to the floor area in the tested area.
- The percentage share of the surface resistance (R_s) measurement points.

Additionally, the report should include:

- The date on which the floor was made.
- Important construction and material data.
- The date of measurements.

4. Examples of errors in concrete floors in the DST technology in terms of their anti-electrostatic properties

Example 1

The floating floor, 22 cm thick, was designed using C25/30 XC2 concrete with an upper substructure stabilized at R_m = 2.5 MPa and a thickness of 20 cm. The floor was designed to be steel fiber reinforced with local reinforcements. The design documentation specified the implementation of an anti-electrostatic monolithic concrete floor using Bautech Antistatic DST System technology, along with the installation of the earthing system within the construction plate.

During the implementation stage, the earthing system was installed directly on the layers of the upper foundation, in front of the sliding layer made of PE foil, similar to the building's lightning protection systems. The sliding layer acts as an effective separation layer between the conductive structure of the slab and the earthing installation, preventing the charge from being fully discharged from the slab structure.

To resolve the problem, it was proposed to dismantle the installation, align the foundation, lay a sliding layer, and then correctly install the load discharge installation at a height of approximately 1/3 from the bottom of the floor.

Example 2

The 20 cm thick floor was designed using C25/30 concrete, reinforced with dispersed reinforcement, and finished with the Bautech Antistatic DST System. It is a floating floor laid on a sliding layer of PE foil and a 10 cm thick substructure made of C8/10 class concrete.

The design documentation specified the implementation of floor markings, including those for separate traffic zones and parking zones, using conductive paints with appropriate parameters and approvals. The area intended for paint coatings was to be no more than 5% of the total usable area.

However, the floor marking was carried out using non-conductive coatings on approximately 8% of the surface. After the completion of the works, verification measurements regarding the discharge of charges from the floor showed that in the zones where the floor marking was performed, there was a local phenomenon of charge accumulation on the floor surface. It was found that the materials used for the coatings did not have the appropriate conductive parameters and approvals.

As a solution to the existing problem, it was proposed to remove the defective paint coatings and apply new markings with the correct conductive materials.

Example 3

The 18 cm thick floor was designed using C25/30 concrete, laid on a 10 cm thick substructure of C8/10 class concrete. The design documentation specified the implementation of an anti-electrostatic concrete floor with a hardening layer in the form of a DST hardening dry sprinkle.

Due to an error in the preparation of the concrete mix, defects appeared across the entire surface of the ~3000 m² floor, including numerous superficial and cross scratches and detachment of the top hardening layer. Although the compressive strength of the concrete met the average required results, there were samples where the minimum strength was not achieved. Pull-off adhesion tests showed that the peel strength in the series of tests did not exceed 1.0 MPa, with the required value being 1.5 MPa. The breakage of the samples occurred both in the hardened layer and in the subsurface concrete layer of the floor slab. This situation rendered the floor unfit for acceptance and operation, completely compromising its anti-electrostatic properties.

As a solution to the existing problem, it was proposed to remove the degraded surface layers and conduct further diagnostics to assess the strength and operating parameters of the construction plate. Given the deadlines for putting the facility into operation, it was decided to saturate the concrete base with deep penetration resin, and then apply the top finishing layers in the form of resin.

5. Conclusions

A properly selected antistatic floor is an important element of any system designed to protect against static electricity. The input data for designing antistatic protection should include an analysis of the technology and conditions of the production process, assessment of the electrification capacity of the media involved in the production process, consideration of the materials from which the apparatus and technological devices are made, identification of the locations where electrostatic charges are likely to form, possible measurement results of the degree of material electrification and electrostatic field strength in the production installations, and determination of current or expected disturbances.

The most popular floors, whose technological solutions enable their use for protection against static electricity, include concrete floors with a wear layer in the form of ESD floor coverings, synthetic epoxy resins, and hardened top surfaces with DST dry sprinkle.

In the case of DST floors, the most common design errors include the omission of important technological aspects and differences between standard DST solutions and anti-electrostatic DST systems. The most common execution errors include improper preparation of the substrate, primer, and foundation, incorrectly designed concrete mix recipes, and inadequate floor care.

References

1. Chmielewska B., Czarnecki L.: Materiały i wymagania dotyczące posadzek. XXVI OgólnopolskieWarsztaty Pracy Projektanta Konstrukcji, tom I: 239 – 279, 2011.
2. Czarnecki L., Mierzwa J.: Wybrane przyczyny materiałowe uszkodzeń posadzek betonowych". Materiały Budowlane 385 (9): 32 ÷ 34, 2004.
3. Kowalski J. M.: Ocena materiałów podłogowych w aspekcie ochrony przed elektrycznością statyczną. Podłoga, 3, 10-, Warszawa, 2000.
4. Ryżyński W., Świątek-Żołyńska S.: Posadzki antyelektrostatyczne w obiektach przemysłowych, Materiały Budowlane 10/2021
5. Świątek-Żołyńska, S., Majewski, T., Niedostatkiewicz, M.: Posadzki antyelektrostatyczne kluczowym elementem ochrony przed elektrycznością statyczną -
6. PN-EN 61340-5-1:2017 Elektryczność statyczna. Część 5 - 1: Ochrona przyrządów elektronicznych przed elektrycznością statyczną. Wymagania ogólne.
7. PN-EN 13318:2002 Podkłady podłogowe oraz materiały do ich wykonania.

STRENGTHENING OF FLOOR SLAB ON PUNCHING SHEAR – A CASE STUDY

TADEUSZ URBAN[1]
MICHAŁ GOŁDYN[1], *michal.goldyn@p.lodz.pl*
ŁUKASZ KRAWCZYK[1]

[1]Lodz University of Technology, Department of Concrete Structures

Keywords: flat slab, composite floor, support zone, punching shear, strengthening with flat bars, cracks

1. Introduction

The subject of this chapter is a reinforced concrete composite floor with a thickness of 0.28 m, serving as an intermediate building partition in a two-story production building with dimensions of 55 × 64 m (see Fig. 1). The floor is designed as a flat slab supported by columns with a cross section of 0.40 × 0.40 m and external walls with a thickness of 0.24 m, made of silicate blocks. The building features an almost regular grid of columns with an axial spacing of 6.0 / 7.7 m × 8.0 m. There is a construction joint in the building.

During the structure inspection, numerous cracks were found on the upper surface of the ceiling. These cracks, with a width of 0.3 to 0.4 mm, occurred mainly near the columns and within the span parts of the ceiling, where their width was up to 1.5 mm. The location of cracks in the span parts coincided with the anti-shrinkage reinforcement, which has a mesh size of 15 × 15 cm. Based on the recommendations of experts, who conducted technical inspections of the facility, most of the cracks were injected with resin.

2. Description of the problem

As a result of the performed inspections, the owner of the facility became concerned about the revealed cracks, despite the lack of the total design load. After about 9 years of facility operation, the authors were asked to evaluate the situation. Until then, the floor slab was only slightly loaded, with a surface load not exceeding 1 kN/m², and part of the ceiling was without any external loading. The design assumed a live load of 5 kN/m² and, additionally, the weight of a flooring with a thickness of 10 cm.

While analyzing the investment process documents, significant changes were found in the detailed design compared to the construction design. The construction design provided for a flat monolithic ceiling with a thickness of 0.35 m. During the construction stage, the ceiling was changed to a composite "filigree" type with a total thickness of 0.28 m. The monolithic concrete overlay was designed using C25/30 concrete, except for small parts hatched in Fig. 1, which were designed with C35/45 concrete. The design specified a nominal cover of the reinforcement equal to 2.5 cm (from the bottom) and 2.0 cm (from the top). Concrete cores taken from the structure showed the actual position of the top reinforcement in the floor slab, as shown in Fig. 2. It was found that the cover of the top reinforcement was exceeded by up to four times.

According to the principles of the PN-B-03264:2002 code [1], the punching reinforcement "should consist of vertical or diagonal stirrups, closed or otherwise well anchored at both surfaces of the slab." According to the design documentation, the ceiling's reinforcement consisted of C-shaped filigree inserts, made of Ø12 or Ø14 bars, embedded in the slab. The detailed drawings do not contain any cross-sections through the prefabricated slabs. In the described situation, the authors suspect that the transverse reinforcement may not be adequately anchored in both the tension and compression zones.

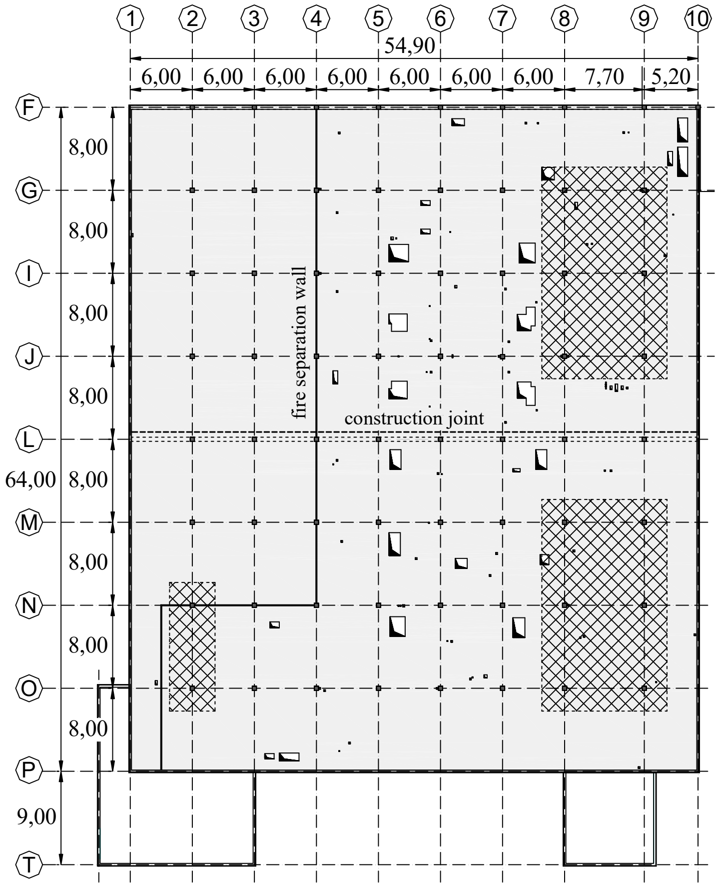

Fig. 1. Floor plan (hatched areas are designed of C35/45 concrete, the rest of C25/30)

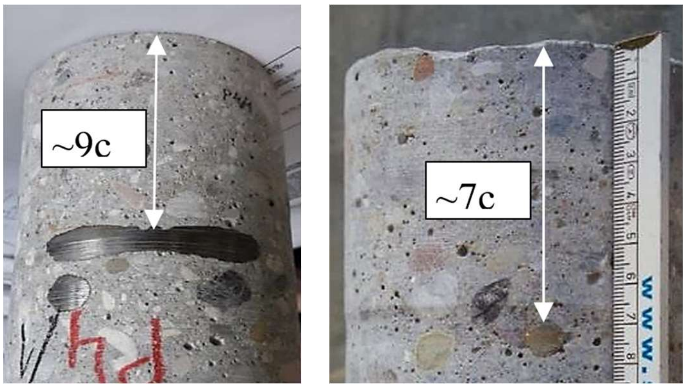

Fig. 2. View of the cores and cut main bars of the top reinforcement

3. Assessment of load-carrying capacity and design of strengthening

The checking calculations were made, adopting the assumptions made by the original designers of the structure, but including the actual location of the main reinforcement determined through tests (cores and scans). This resulted in a reduction of the effective depth in the support zones by more than 25%.

The ABC Płyta software was used for the design calculations. A computational model was prepared, taking into account the division into precast filigree elements. The reinforcement was calculated with respect to the ultimate limit state (ULS) as well as the serviceability limit state (SLS). Deficiencies in reinforcement were found across the entire surface of the floor, ranging from 2% to about 30% for bottom reinforcement, and even over 60% with respect to top reinforcement. The average deficit of top reinforcement in the support zones was 25% and 20%

in the x and y directions, respectively. Due to the significant identified deficits in load-carrying capacity, it was necessary to determine the safety of further use of the floor.

An additional analysis was carried out, taking into account the actual loads, which were about 60% of the loads assumed in the structural design. With these assumptions, the flexural reinforcement turned out to be sufficient with respect to ULS and SLS.

The downward shift of the reinforcement led to a reduction in the effective depth, which significantly influenced the results of calculations related to the punching shear resistance. At the designed loads, the deficit of the punching shear resistance was at the level of about 70% to 170% (see Fig. 3). The analysis carried out under the assumption of the actual loads acting on the slab showed a lower deficit, reaching a maximum of 40%.

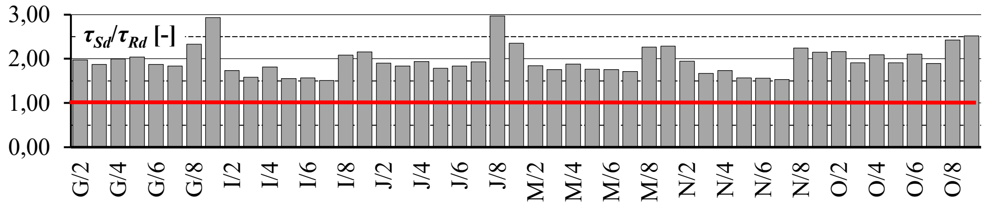

Fig. 3. Comparison between shear stress and punching shear resistance for design loads

Considering the technological and functional premises (the owner rejected the possibility of temporary exclusion from use), strengthening from the bottom was excluded. Analyses were conducted to determine the maximum permissible live load, assuming that strengthening could only be performed from the top in selected support zones. Strengthening in the form of external reinforcement consisting of steel flat bars was designed. The effectiveness of strengthening for punching shear with this type of reinforcement has been previously demonstrated [1, 2]. The use of CFRP strips was also considered as an alternative, but practical reasons argued against this solution.

Calculations of the punching shear resistance were performed using two methods: the Urban approach [1] and the principles of Eurocode 2. Both methods included the increase in the longitudinal reinforcement ratio and the effective depth resulting from the use of the steel flat bars.

It was planned to install additional reinforcement as close to the columns as possible, considering the openings in the floor slab. All of the flat bars were perforated with twice as many holes as the number of anchor bolts. The decision to increase the perforation was due to concerns about the possibility of correctly installing the anchor bolts in all intended locations. Due to the high density of reinforcement in the support zone and the potential for assembly deviations, it was necessary to anticipate the possibility of encountering a reinforcing bar. In such cases, drilling had to be stopped and the adjacent hole in the flat bar used for anchoring.

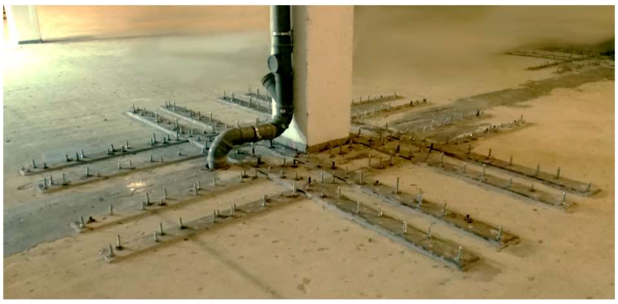

Fig. 4. View of the support zone strengthened with steel flat bars

To verify the technical feasibility of the designed solution, a trial strengthening of two support zones was conducted (see Fig. 4). The work, carried out over three days, was divided into stages, including: preparation of the floor surface by removing bleed water, cleaning, and degreasing the glued surfaces; gluing the first layer of flat bars to the concrete; pressing the flat bars with weights during adhesive setting (24 hours); drilling holes in the slab and installing screws; gluing the second layer of flat bars; drilling holes and installing new anchors; tightening the nuts and shortening excessively protruding screws.

Based on the experience from the trial strengthening, the owner of the facility decided to strengthen the ceiling in stages, depending on current needs. Office and technical areas are planned to be formed on the floor. To ensure an even surface in the offices, it was proposed to build a raised (technical) floor, supported on the existing ceiling.

4. Summary

The presented example demonstrated how far-reaching effects can result from the imprecise preparation of design documentation and insufficient supervision combined with execution errors during the construction stage. These errors led to a significant reduction in the flexural and punching shear resistance of the floor slab.

A strengthening method was proposed, consisting of increasing the longitudinal reinforcement by means of steel flat bars. The effectiveness of this solution has been confirmed in previous experimental investigations. The main advantage lies in the possibility of flexible selection of the cross-section of flat bars, and the fact that the work is limited only to the top surface of the ceiling. In the described case, it allowed for the avoidance of costly interference with the production carried out on the lower floor of the building.

The trial confirmed the technical feasibility of efficiently implementing the proposed strengthening method. Ensuring appropriate anchoring required increasing the perforation of the flat bars due to collisions with the existing reinforcement encountered during drilling, which necessitated additional holes in the floor slab.

References

1. PN-B-03264: 2002 Concrete, reinforced and prestressed concrete structures. Static calculations and design.
2. Urban T., Tarka J.: Strengthening of slab-column connections with CFRP strip. Archives of Civil Engineering, nr 2/2010, s. 193÷212.
3. Urban T., Gołdyn M.: How to Strengthen Flat Slabs On Punching Shear – Traditionally With Steel or Innovative, by Using Fiber Composite Materials? Engineering Structures and Technologies, nr 2/2019, s. 57÷65.

SECTION VII
FAILURES OF BRIDGE AND ROAD STRUCTURES

DAMAGE OF CONCRETE ROAD PAVEMENT - CASE STUDY

ARTUR JUSZCZYK[1], *a.juszczyk@ib.uz.zgora.pl*

[1]Institute of Civil Engineering, University of Zielona Góra

Keywords: concrete pavements, pavement damage, concrete pavement repair

1. Introduction

The first concrete pavement was laid in 1888 in Wroclaw. Many roads with surfaces from the 1930s-1960s are still in use today. At the beginning of the 21st century, there was a renewed interest in the construction of rigid pavements. Concrete pavements are increasingly being constructed in Poland, not only on national roads but also on communal and internal roads. Properly constructed concrete pavement is characterized by resistance to deformation and intensive traffic, which usually allows for longer use than initially assumed during the design stage.

Due to their constant exposure to degrading factors, concrete pavements are very sensitive to mistakes made during the design and construction phases. Each failure reduces durability and deteriorates traffic safety conditions. The risk of errors and their consequences, can be significantly reduced by contracting a road construction company experienced in concrete pavements. Despite careful design and construction, damage may occur during the operational phase. Maintenance measures, such as the replacement of expansion joint seals, are essential during this phase. The main causes of damage during operation include changing water conditions, increased traffic volume, and unforeseen factors such as high temperatures from a vehicle fire on the roadway.

Surface damage can be repaired or leveled by surface methods, depending on the scale and extent of the damage. By using suitable repair materials with good adhesion, low shrinkage, and adequate strength, it is possible to extend the service life by several years. Issues such as lack of roughness in concrete pavements can be addressed by sandblasting, shotblasting, grinding with water or diamond discs, and grooving with diamond discs. For slab keystoning, cement grout injections or dowelling can be performed. Structural damage may necessitate the complete replacement of the slab or the entire surface.

A private investor, attracted by the advantages of concrete pavement, decided to build internal roads with a rigid surface. The road renovation was contracted to a construction company, which carried out the work in June and July. The scope of work was relatively small, consisting of a new surface layer using the existing structure as a sub-base. The renovation involved two road sections with a total length of 223 m and a total surface area of 1039 m². The performed pavements were divided into slabs with joints filled with a pouring compound. These internal roads provide access to multi-family buildings and service and commercial facilities located nearby.

After a few weeks, the developer noticed numerous damages to the pavement. In December, it was decided to take samples and carry out destructive tests. It should be noted that the pavement had not yet been subjected to winter conditions. Tests carried out in section 1 by Laboratorium Budowlane Sp. z o.o. in Zielona Góra, after about 6 months of pavement usage, showed that the compressive strength of concrete was 5.2 MPa. Additionally, large air voids were found in the concrete, resulting from insufficient compaction of the layer.

The next control tests were carried out after more than 1.5 years of use. In section 1, the compressive strength of the pavement was only 3.5 MPa, while in section 2, it was recorded at 5.3 MPa. It is worth noting that in section 1, there were places where the level of degradation made it impossible to perform the tests.

Concrete pavement should increase its strength over time, but in this case, the opposite happened. After one year of use, a decrease of 32% in the compressive strength of the concrete was recorded.

During the field inspection, a preliminary visual assessment of the technical condition of the road surface was made. Numerous defects were found, mainly in the first section, significantly reducing the usable value of the road. However, the second section was not without execution defects either.

Acoustic tests showed incomplete support of the pavement slabs, which resulted in pressing of the pavement.

During the on-site inspection of section 1 the following pavement defects were found:

- lack of continuity of support of the surface layer;
- occurrence of localised areas with no drainage;
- deterioration of the pavement texture;
- transverse and diagonal cracks;
- irregular shapes of technological connections of the pavement.
- significant losses of the pavement up to the steel mesh laid on the substructure before the new surface layer was made;
- irregular shapes of technological connections of the pavement.

The view of selected pavement damages of section 1 is presented in Figures 1a-d.

a) b)

c) d)

Fig. 1. Pavement damage: a) pavement degradation, b) damaged to pavement texture, c) exposed steel mesh, d) 6 cm undersized manhole cover

Section 2 exhibited similar damage, but with lesser intensity. The better condition of this section was due to negligible vehicle traffic, as it was a no-passing road with a parking ban.

Cracks in the concrete slabs were caused by insufficient concrete strength, improper composition of the concrete mixture, errors in the execution of joints, defects in the pavement construction, and improper care of the concrete during the setting and hardening process.

The surface layer did not meet the basic requirements for improved hard pavement, such as evenness and dustlessness. The resulting defects reduced the aesthetics and usable value of the pavement, road safety, and its service life. Based on the test results, progressive degradation of the concrete pavement of the analyzed roads was observed. Continued operation was unsafe due to protruding bars, necessitating a remedial action program.

Due to the fundamental problem of low compressive strength of the concrete and its decline over time, it was not possible to reinforce the existing pavements with surface measures. It was proposed to replace the concrete surface layer. For technological reasons, an alternative solution of paving with concrete cobblestones was also accepted. This solution limits the execution time and the need for extensive equipment mobilization.

Ultimately, the alternative proposed was implemented and the view before and after pavement repair is shown in Figure 2a and b.

a) b)

Fig. 2a) view of the damaged concrete pavement, b) pavement after the repair

National experience in the implementation of rigid pavements has made it possible to popularize this type of solution in the Polish road construction industry. Unfortunately, the requirements of this technology are not always observed in engineering practice, and concrete pavements are very sensitive to deviations from these requirements. The reasons for this situation may include the pressure of realization deadlines or a desire to limit costs. However, it is important to remember the responsibility that rests on individuals performing independent technical functions in construction. As a civil engineer exercising a profession of public trust, one is obliged to exercise due diligence in carrying out construction works in accordance with technical knowledge. Numerous workmanship errors led to the concrete pavement being in such a state that it was difficult to determine whether it was a pavement or a dirt road. A lack of experience cannot always be compensated for by ambition and diligence.

The implementation of the concrete pavement has resulted in unnecessary losses in various areas. Financial costs were incurred without achieving the intended effect. Socially, the local community was exposed to prolonged construction works. There were also image costs concerning the industry and the pavement technology.

Based on the case presented, two main conclusions can be drawn

- The contractor must comply with the requirements of the cement concrete pavement technology, otherwise it increases the risk of incurring additional costs resulting from the implementation of the repair works programme.
- The developer should commission people with relevant experience to supervise and manage the works.

UNIVERSITY BRIDGE IN BYDGOSZCZ: DISTRIBUTED FIBRE OPTIC MEASUREMENTS (DFOS) OF STEEL ANCHORAGES DURING THEIR RENOVATION

RAFAŁ SIEŃKO[1]
ŁUKASZ BEDNARSKI[2]
TOMASZ HOWIACKI[1,3], *th@shmsystem.pl*
MAREK GOTOWSKI[4]
PAWEŁ PIETRASZAK[4]
DAMIAN WILUŚ[4]

[1]Faculty of Civil Engineering, Cracow University of Technology
[2]Faculty of Mechanical Engineering and Robotics, AGH University of Science and Technology in Krakow
[3]SHM System Sp. z o.o., Sp. kom., www.shmsystem.pl, www.nerve-sensors.com
[4]Kormost S.A., www.kormost.pl

Keywords: bridge, steel, anchorage, cable, yielding, renovation, DFOS measurement, optical fibre, strain, temperature

1. DFOS measurements - introduction

Safety-critical structures, especially innovative bridges, are nowadays equipped with systems enabling data acquisition on their technical condition over time. Based on the information provided by monitoring, decisions are often made directly related to structural safety (e.g., renovation, strengthening, traffic restriction, decommissioning). Therefore, it is reasonable to seek newer and better diagnostic tools (measurement techniques, sensors, recorders) that provide more helpful information. Work in this field is carried out worldwide, both in scientific and commercial units.

Distributed fibre optic sensing (DFOS) is one of the most promising technologies [1] as it allows for the direct detection of local events or damages like cracks in concrete or yielding areas within steel. This is impossible with conventional spot gauges located only at selected points of the structure. The DFOS-based system consists of a data logger and sensors, which are the most important components. Once installed within the structure, they should operate over the years. Therefore, particular attention should be paid to their strength, flexibility, and elastic operation range. Their design and installation method must provide a reliable strain transfer mechanism for the correct structural condition assessment.

This article describes the successful application of the DFOS-based measurement system within the famous steel Polish University Bridge in Bydgoszcz. The optical data logger based on Rayleigh scattering [2] was used, enabling an extremely high spatial resolution equal to 5 mm (200 measurement points per meter of the sensor). Thanks to the unique capabilities of distributed fibre optic sensing, a significant increase in its application has been observed over the last few years, both in laboratory and in situ applications.

2. Example applications in bridge engineering

More than 10 bridges in Poland are equipped with distributed fibre optic sensors. This section provides a brief overview to better understand their possible applications and benefits.

The first example is related to a new structure where composite and monolithic strain sensors, called EpsilonRebars [3], were installed over the deck length (80 m) of the footbridge in Nowy Sącz [4]. It is worth noting that the entire reinforcement was done as a composite (Fig. 1a). EpsilonRebars serve a dual function: both reinforcing and sensing simultaneously. Based on the data from 12 sensors, it is possible to analyze strains, cracks, displacements, stress, and temperatures.

Fig. 1b shows one of the largest concrete bridges in Poland: the Rędziński Bridge in Wrocław. Due to cracks in the horizontal beam of the pylon, EpsilonRebars were installed inside near-to-surface grooves at each corner of the beam. Both short- and long-term measurements allowed for detecting and precisely analyzing crack width changes over time.

a) b)

Fig. 1. a) Footbridge with composite reinforcement and DFOS sensors [4]; b) one of the largest concrete bridges in Poland with distributed fibre optic strain sensors in the pylons' beam

Another project was conducted on an existing steel bridge in Przemyśl, Poland (Fig. 2a). Measurement DFOS fibers were glued to the steel girders using two-component epoxy. The analysis focused particularly on the anchorage zone and local effects influencing the strain profiles within this area.

Example results over a 20 m section (Fig. 2b) indicate that the maximum strain values in the girder, caused by the anchorage, are much greater than those registered in the pure area between the anchorages. This localized strain information is crucial for understanding the structural behavior and integrity of the bridge under various loading conditions.

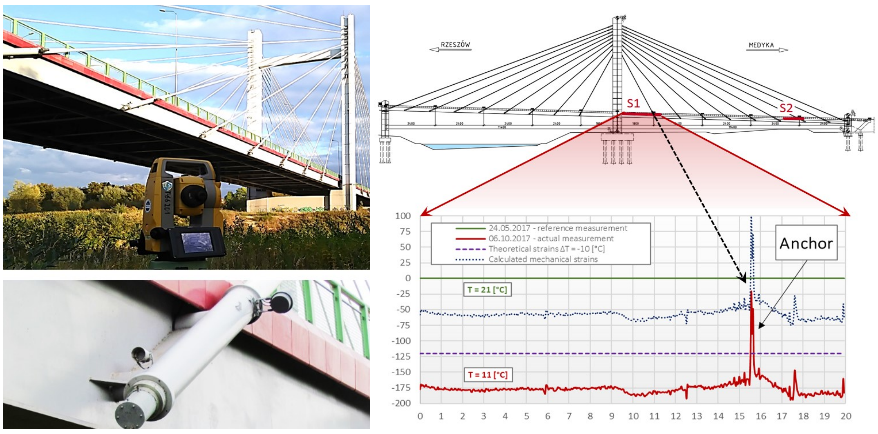

a) b)

Fig. 2. „Brama Przemyska" Bridge: a) general view and close-up to the anchorages; b) example results

3. University Bridge in Bydgoszcz and example DFOS results

The University Bridge in Bydgoszcz is one of the most famous bridges in Poland, mainly due to its unusual geometry (Fig. 4b). The pylon consists of two intersecting parts in the shape of Greek capital letters: alpha (A) and omega (Ω). The steel deck is suspended using 16 multi-strand steel cables. The bridge was placed in service in 2014; however, after only 7 years of operation, it experienced a failure. A technical inspection identified permanent (plastic) deformation of the steel plates within the cable anchorages. This caused the bridge to be taken out of service, sparking widespread discussion in the scientific and engineering community. Eventually, a strengthening solution for the anchorage zones was designed, which involved relieving the cables, welding additional structural plates, and re-stressing the cables. The strengthening was performed by Kormost S.A.

Measurement fibres with a 250 µm diameter were installed within the anchorages before the cable relieving and annealing. Spatial numerical simulations determined the detailed route. The setup consisted of two sections, each 50 cm long (Fig. 3a). Considering the loop connecting the two sections, the length of the optical fibre at each anchorage was 115 cm. This setup provided 3680 measurement points on 16 anchorages (with a spatial resolution of 5 mm). An important aspect was ensuring the correct strain transfer mechanism through appropriate installation. The sensors were bonded directly to a clean and degreased steel surface (Fig. 3b) after removing the protective coatings, which were restored after installation. A two-component epoxy resin with verified flexibility was used to utilize the entire strain range of the optical fibre, allowing for correct measurements even in the plastic range.

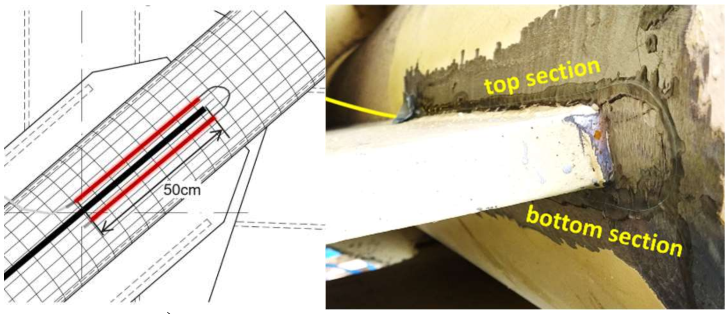

a) b)

Fig. 3. Measurement sections formed using DFOS optical fibres: a) scheme; b) actual view

Measurements were performed in periodic sessions. The zero (reference) readings were taken before relieving the cables, and the next session was conducted after relieving. Therefore, the obtained strain (stress) results should be treated as increments rather than absolute values. Temperature measurements using a pyrometer were done to compensate for the strain results.

For clarity, the measurement results are presented for the top sections only, for all anchorages. The calculated stress (based on compensated strains and according to Hooke's law) is shown in Fig. 4a. A significant increase in tensile stress was observed on some anchorages (mainly the external ones), while the values were close to zero on the remaining ones. The unique measurement data allowed for identifying the most stressed zones within the anchorage (local analysis) and the most stressed anchorages within the bridge (global analysis). To facilitate graphical interpretation, the maximum stress values recorded in each anchorage are presented in a spatial visualization (Fig. 4a). The red color indicates the cables at which significant deformations were observed at the anchorages.

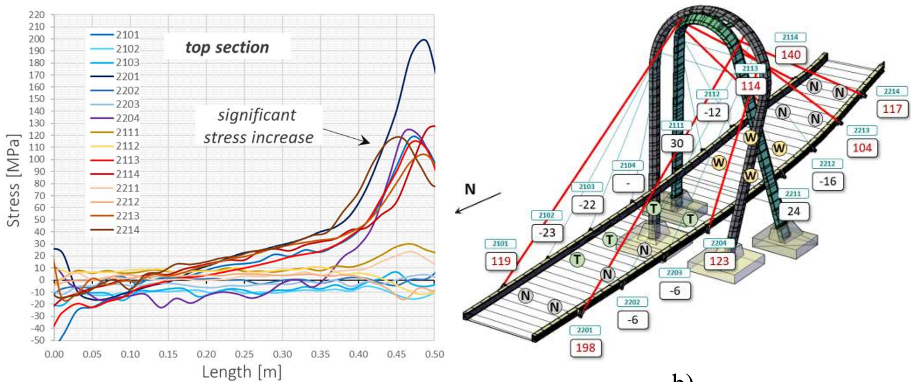

a) b)

Rys. 4. Example stress results: a) distributions over the length of the top section;
b) spatial visualisation with maximum stress values [MPa]

4. Summary

The extraordinary capabilities of DFOS technology have led to a significant increase in its applications in recent years, not only in laboratories but primarily within actual engineering structures [5], including bridges. The extensive strain range of fiber optic sensors enables their safe operation and correct measurements even in cases of extremely large strains caused, for example, by steel yielding. This paper presents an example of a successful application within the University Bridge in Bydgoszcz, Poland. Despite the system involving only 115 cm long measuring routes, the total number of measuring points amounted to 3680 (including 16 anchorages and 5 mm spatial resolution). Installing such a large number of conventional spot gauges is neither technically possible nor economically justified.

Due to the negligible cost of DFOS sensors relative to the cost of the structure itself or its potential failure, it is recommended to install them on all safety-critical structures (including bridges, stadiums, industrial facilities, gas pipelines, earth embankments, and others). The system, analogous to the human nervous system, can inform about all potential threats regardless of their location. Moreover, the optical infrastructure integrated with the structure will be ready for future use, regardless of the direction of the development of DFOS-based techniques and optical data loggers.

References

1. Howiacki T.: Światłowody – przełom w pomiarach, Builder, wrzesień 2019, 78 – 80.
2. Palmieri L., Schenato L.: Distributed Optical Fiber Sensing Based on Rayleigh
3. Scattering, The Open Optics Journal, 2013, 7, (Suppl-1, M7) 104-127.
4. www.nerve-sensors.com
5. Sieńko R., Bednarski Ł., Howiacki T.: Smart Composite Rebars Based on DFOS Technology as Nervous System of Hybrid Footbridge Deck: A Case Study, European Workshop on Structural Health Monitoring, Special Collection of 2020 Papers, Volume 2, Springer, 2021, 340 – 350.
6. Bado M. F., Casas J. R.: A Review of Recent Distributed Optical Fiber Sensors
7. Applications for Civil Engineering Structural Health Monitoring. Sensors 2021, 21, 1818.

THE THREAT OF A CONSTRUCTION DISASTER OF THE UNIVERSITY BRIDGE IN BYDGOSZCZ. ANALYZES AND RESEARCH

KRZYSZTOF ŻÓŁTOWSKI[1], *k.zoltowski@pg.edu.pl*
MIKOŁAJ BINCZYK[1]
PRZEMYSŁAW KALITOWSKI[1]

[1]The Faculty of Civil and Environmental Engineering, Gdansk University of Technology

Abstract: The University Bridge was closed 7 years after construction. The reason was the design fault revealed in the 2020 inspection, confirmed by theoretical load capacity analyses. The high risk of a construction disaster was the main reason for closing the crossing. In 2021, following the recommendation and expert concept, critical elements of the bridge structure were strengthened. In January 2022, the bridge was brought back into service. Despite the successful completion of the repair process, the taken discussion about the measures has not been completed. Opinions and studies have appeared that contest the closure of the bridge to traffic and propose a different scenario. The paper presents the issues of the load-bearing capacity assessment of the University Bridge in Bydgoszcz. Conclusions from the carried out work have been included. Additionally, new analyses of the load-bearing capacity of the overloaded steel nodes of the cable anchoring in the deck are presented.

Keywords: cable-stayed bridge, steel structure, load-bearing capacity, safety, FEM analysis, tests

1. Superstructure of the bridge

The University Route is a key element of the communication system of the city of Bydgoszcz (Fig. 1,2).

Fig. 1. University Bridge in Bydgoszcz (source: Gotowski.pl)

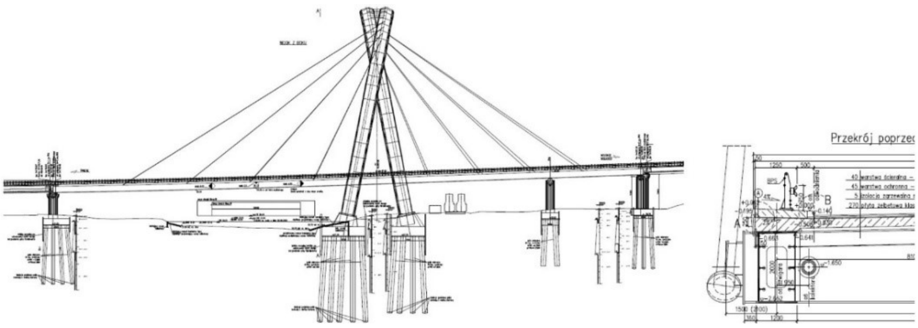

Fig. 2. University Bridge - suspended part, side view and cross-section [1]

The designer of the route is Transprojekt Gdański [1], and the contractor is a consortium of companies Mosty Łódź SA and Gotowski Sp. z o.o. The construction process was supported by an advisory consulting team [2]. Before opening, the bridge underwent a load test process [3,4]. The route was opened on November 30, 2013. The static scheme of the bridge is a continuous beam suspended to a pylon with spans of 110 + 90 m (Fig. 2).

2. Inspection

In July 2020, at the request of the bridge administrator, measurements of the forces in the suspension lines of the University Bridge were carried out [4]. The tests were performed using the vibration method. Additionally, the bridge administrator requested an assessment of the cables and suspension anchors. During the inspection, significant deformations of the plates in the anchorage structure were observed (Fig. 3).

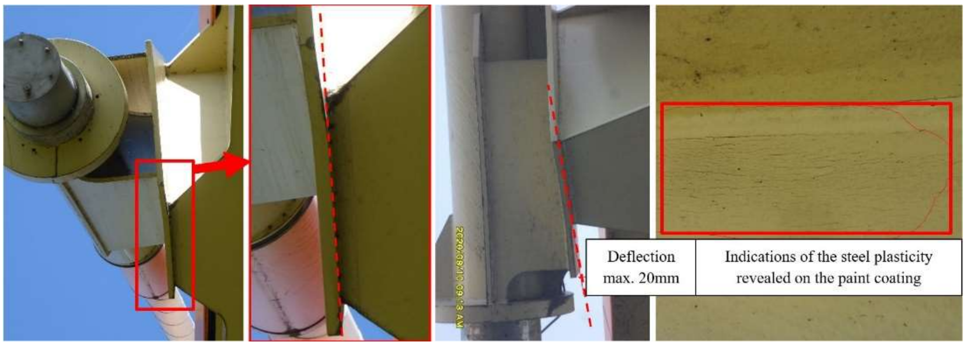

Fig. 3. Examples of deformed plates of cable anchorages and signs of overload

The preliminary estimated values of deformation indicated significant plasticization of the steel in the anchors. Signs of the steel plasticity were noted as a striped structure on paint coatings (Fig. 3).

3. Numerical analysis of the load capacity

As part of the theoretical analysis [5, 6], a global FEM model of the bridge structure was developed. The next step involved creating detailed models of the anchor details. These models were constructed entirely as shell models, using the QUAD 4 element in the SOFiSTiK FEM environment (Fig. 4).

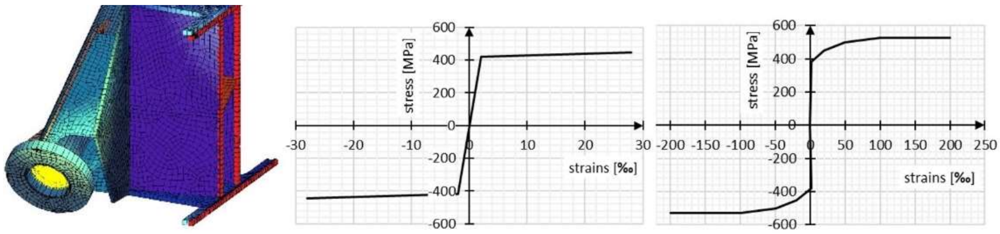

Fig. 4. FEM model of the anchorage with a typical boundary conditions system, material law no. 1 and no. 2 applied in the analyses

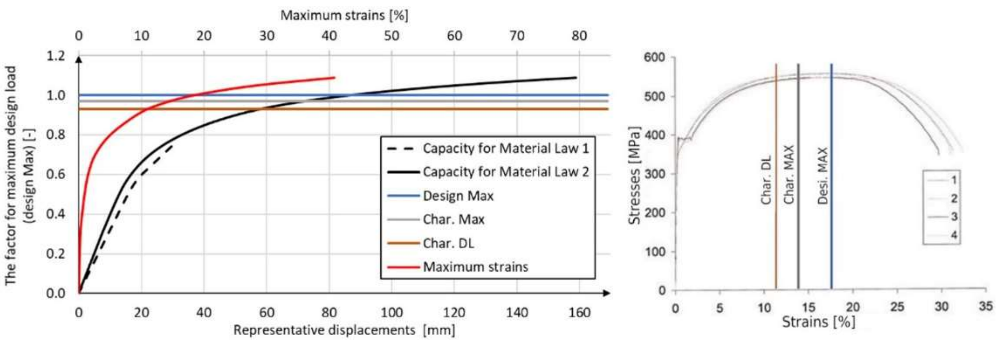

Fig. 5. Result of the nonlinear computation (left side) and material low no. 3 (right side)

Fig. 5 presents a summary of the nonlinear analyses of the element capacity. Material law no. 1 was used for the engineering analysis, limited by the maximum strain value of 5%. Law no. 2 was defined based on experimental research [7] (law no. 3) and used to analyze the full range of strain. The diagram (Fig. 5–law no. 3) shows the result of the uniaxial tension test. The vertical lines indicate strain values at the characteristic load levels of the structure. The analysis shows that under the characteristic dead load (Char. DL), the material reaches full plasticity, and the strain in steel exceeds approximately 10%. Similar results were obtained in [8, 9]. However, the authors of these works presented a different opinion on the safety of the structure, considering the closure of the bridge as an unjustified action.

Additional proof of the validity of the decision to close the bridge may be the analysis of the variability of the force in the critical suspension cable, which is influenced by daily temperature changes.

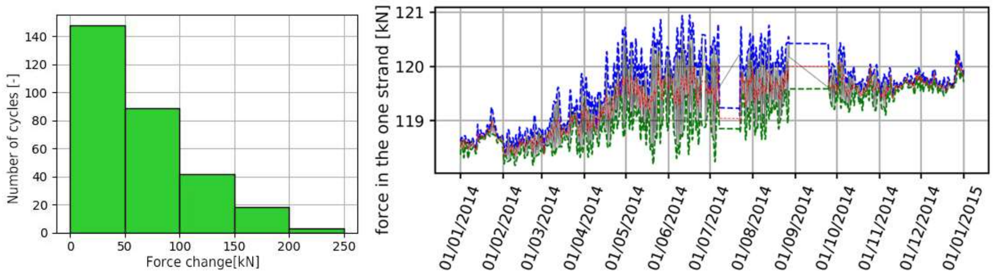

Fig. 6. Annual histogram of the daily force variation in the suspension cable and variation of the force in the only one strand of the critical suspension cable

Fig. 6 shows the distribution of daily force changes in the cable based on the SHM (Structural Health Monitoring) system installed on the bridge. This phenomenon contributes to the problem of low-cycle fatigue strength, with a constant strain of 10% and the one-year load variation presented in Fig. 6.

4. Conclusions

In the case of the University Bridge, the decision to close traffic was made based on theoretically advanced, yet practical engineering analyses. Further research of a scientific nature, presented in [6,8,9] and in this paper, despite significant differences in result interpretation, in the authors' opinion, confirm the correctness of the decision. Ultimately, everything was conducted according to the prepared scenario. The bridge was closed to traffic, secured, and repaired according to the expert concept [10,11]. After a one-year break, during which the structure was strengthened, the University Bridge in Bydgoszcz was reopened following a positive load test on January 26, 2022.

References

1. Detailed Design - Construction of ul. Ogiński in – Cable-stayed Bridge M-2 - Transprojekt Gdański Sp. z o. o. (in polish)
2. Sokołowski W., Sochacki J., Gotowski M., Chróścielewski J., Miśkiewicz M., Pyrzowski Ł., & Wilde, K.: Constructing of the University Bridge in Bydgoszcz. Mosty, 5, 43-47, 2015 (in polish)
3. University Bridge over the Brda River in Bydgoszcz. Final report on the static and dynamic test load. Aspekt Sp. z o.o. December 2013 (in polish)
4. Żółtowski K., Binczyk M., Kalitowski P .: Measurements of the tension forces of the cables on the University Bridge (M2 suspension bridge) together with the technical assessment. Expertise, Kormost, 2020 (in polish)
5. Żółtowski K., Pełka D., Nowak A.: Technical report on the analysis of the load capacity of the anchorage nodes in the University Bridge in Bydgoszcz. KBP Żółtowski, 2020 (in polish)
6. Żółtowski K., Binczyk M., Kalitowski P.: University Bridge in Bydgoszcz. Theoretical basis for the decision to exclude the bridge from traffic. Technical Confference Wroclaw Bridge Days. Wroclaw, 2021 (in polish)
7. Test report no. 01/2021. Strength test of samples taken from the steel structure. Laboratory of Materials and Structures Testing. Bydgoszcz University of Technology, 2021. (in polish)

8. Wilde K., Chróścielewski J., Miśkiewicz M., Pyrzowski Ł., Sobczyk B .: Technical expertise: Preparation of a co-report to reports on the University Bridge in Bydgoszcz prepared by the KBP Krzysztof Żółtowski, 2021 (in polish)
9. Wilde K., Chróścielewski J., Miśkiewicz M., Pyrzowski Ł., Sobczyk B.: University Bridge in Bydgoszcz - advanced study of the suspension system anchoring zones in the bridge. Wroclaw Bridge Days. Wroclaw, 2021 (in polish)
10. Żółtowski K.: Conceptual design of strengthening the anchorage nodes in the bridge deck across the Brda River along the University Route in Bydgoszcz. KBP Żółtowski, 2021 (in polish)
11. Biliszczuk J., Kożuch M., Lorenc W., Onysyk J., Skrętkowicz Ł., Sułkowski M., Teichgraeber M.: Strengthening of the anchoring nodes of the cables in the University Bridge in Bydgoszcz. Wroclaw Bridge Days, Wroclaw 2021, (in polish)

AUTHOR INDEX